

**CHEMICAL CONSTITUENTS AND BIOLOGICAL  
ACTIVITIES FROM *Artocarpus heterophyllus*  
AND *Artocarpus lakoocha* Roxb.**



**SIRADA BOONYAKETGOSON**

**DOCTOR OF PHILOSOPHY**

**IN CHEMISTRY**

ลิขสิทธิ์มหาวิทยาลัยเชียงใหม่  
Copyright© by Chiang Mai University  
All rights reserved

**GRADUATE SCHOOL  
CHIANG MAI UNIVERSITY  
JULY 2019**

**CHEMICAL CONSTITUENTS AND BIOLOGICAL  
ACTIVITIES FROM *Artocarpus heterophyllus*  
AND *Artocarpus lakoocha* Roxb.**

**SIRADA BOONYAKETGOSON**

**A THESIS SUBMITTED TO CHIANG MAI UNIVERSITY IN PARTIAL  
FULFILLMENT OF THE REQUIREMENTS FOR THE DEGREE OF  
DOCTOR OF PHILOSOPHY  
IN CHEMISTRY**

ลิขสิทธิ์มหาวิทยาลัยเชียงใหม่  
Copyright© by Chiang Mai University  
All rights reserved

**GRADUATE SCHOOL, CHIANG MAI UNIVERSITY**

**JULY 2019**

**CHEMICAL CONSTITUENTS AND BIOLOGICAL  
ACTIVITIES FROM *Artocarpus heterophyllus*  
AND *Artocarpus lakoocha* Roxb.**

SIRADA BOONYAKETGOSON


THIS THESIS HAS BEEN APPROVED TO BE A PARTIAL FULFILLMENT OF  
THE REQUIREMENTS FOR THE DEGREE OF  
DOCTOR OF PHILOSOPHY  
IN CHEMISTRY


**Examination Committee:**

.......... Chairman  
(Asst. Prof. Dr. Sarot Cheenpracha)

.......... Member  
(Asst. Prof. Dr. Napapha Promsawan)


.......... Member  
(Asst. Prof. Dr. Kongkiat Trisuwan)

.......... Member  
(Asst. Prof. Dr. Thunwadee Limtharakul)

.......... Member  
(Assoc. Prof. Dr. Lalida Shank)

**Advisory Committee:**

.......... Advisor  
(Asst. Prof. Dr. Kongkiat Trisuwan)

.......... Co-advisor  
(Asst. Prof. Dr. Thunwadee Limtharakul)

.......... Co-advisor  
(Assoc. Prof. Dr. Lalida Shank)

12 July 2019

Copyright © by Chiang Mai University

## ACKNOWLEDGEMENT

I would like to express my deepest gratitude and sincere appreciation to my supervisor, Assistant Professor Dr. Kongkiat Trisuwan, for his thesis inspiration, valuable knowledge, helpful guidance and good encouragement throughout my thesis and program of study. Everything will always keep in my mind.

I am very grateful to Assistant Professor Dr. Sarot Cheenpracha, Assistant Professor Dr. Napapha Promsawan, Assistant Professor Dr. Thunwadee Limtharakul and Associated Professor Dr. Lalida Shank for their kindness, suggestion and guidance on thesis writing.

I am very grateful to Professor Dr. David Kingston, the Department of Chemistry, College of Science, Virginia Polytechnic Institute and State University, United States of America for offering good opportunity, helpful advices and nice experience for doing oversea research in his laboratory.

I appreciate the Science Achievement Scholarship of Thailand for financial support on my oversea research and I am thankful to Graduate school, Chiang Mai University and the Department of Chemistry, Faculty of Science, Chiang Mai University for the partial financial support.

I would like to thank the staff of the Department of Chemistry, Faculty of Science, Chiang Mai University for instruments and assistance. I would like to thank Dr. Yongle Du, postdoctoral associate, for kind assistance in extraction and HPLC technique. I also thank Dr. Narasimha Murthy Shinaiah for helpful guidance about structural elucidation by nuclear magnetic resonance techniques.

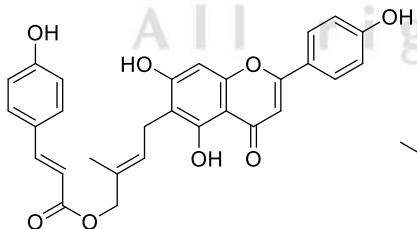
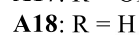
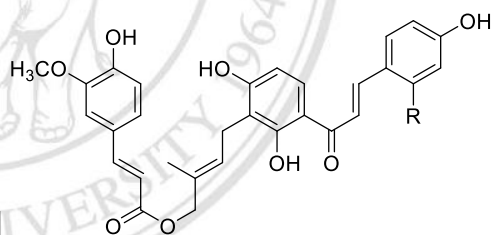
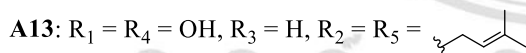
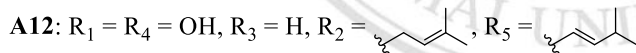
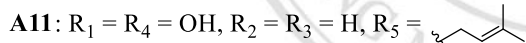
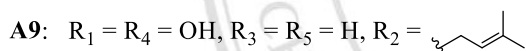
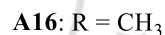
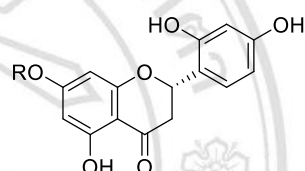
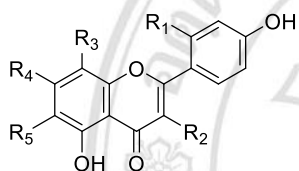
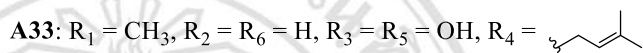
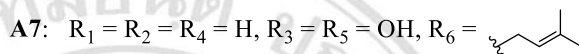
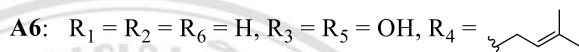
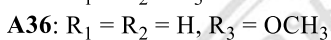
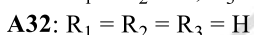
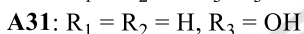
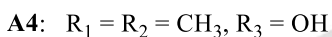
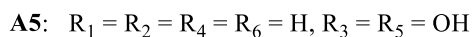
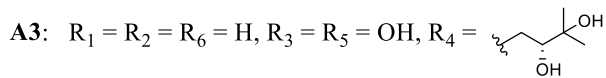
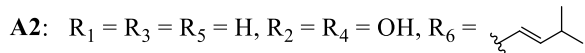
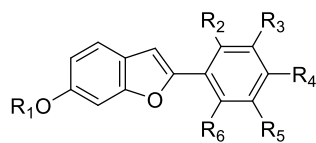
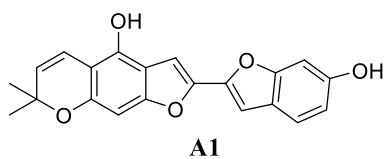
Finally, none of this would have been possible without love and encouragement of my family, colleagues and friends. I thank them all for their kindness and valuable advice.

Sirada Boonyaketgoson

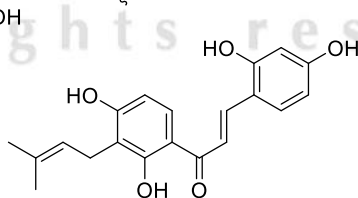
หัวข้อคุณสมบัติ	องค์ประกอบทางเคมีและฤทธิ์ทางชีวภาพจากขนุนและขนุนป่า	
ผู้เขียน	นางสาวศิริดา บุญญเขตกร โกศล	
ปริญญา	ปรัชญาดุษฎีบัณฑิต (เคมี)	
คณะกรรมการที่ปรึกษา	ผู้ช่วยศาสตราจารย์ ดร. ก้องเกียรติ ไตรสุวรรณ	อาจารย์ที่ปรึกษาหลัก
	ผู้ช่วยศาสตราจารย์ ดร. ธัญวดี ลิ้มธรากุล	อาจารย์ที่ปรึกษาร่วม
	รองศาสตราจารย์ ดร. ลลิตา แสงค์	อาจารย์ที่ปรึกษาร่วม

### บทคัดย่อ

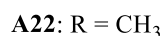
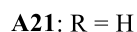
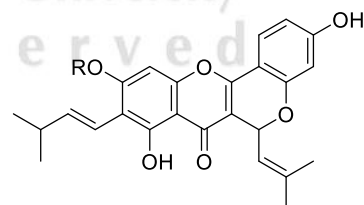
การศึกษาองค์ประกอบทางเคมีในส่วนสกัดหยาบเมทานอลของกิ่งขนุนและส่วนสกัดหยาบอะซิโตนของกิ่งและเปลือกขนุนป่าด้วยเทคนิคทางโครมาโทกราฟีแบบต่าง ๆ สามารถแยกสารบริสุทธิ์ได้ทั้งหมด 36 สาร (A1-A36) โดยส่วนกิ่งขนุนสามารถแยกสารใหม่ 4 สาร (A1-A4) และสารที่มีการรายงานโครงสร้างแล้วจำนวน 21 สาร (A5-A25) ส่วนกิ่งขนุนป่าสามารถแยกสารใหม่ 2 สาร (A26 และ A27) และสารที่มีการรายงานโครงสร้างแล้วจำนวน 17 สาร (A2, A4-A7, A9, A11-A12, A16, A18, A21-A22, A28-A32) และส่วนเปลือกขนุนป่าสามารถแยกสารบริสุทธิ์ได้ 8 สาร (A6, A28, A30-A31, A33-A36) ซึ่งสารทั้งหมดเป็นสารที่มีการรายงานโครงสร้างแล้ว วิเคราะห์โครงสร้างของสารบริสุทธิ์ด้วยเทคนิคทางสเปกโทรสโกปีโดยเฉพาะข้อมูล 1D และ 2D NMR สาร A3 มีฤทธิ์ในการต้านเซลล์มะเร็งทรวงอก (MCF-7) ด้วยค่า  $IC_{50}$  เท่ากับ  $12.6 \pm 1.5 \mu M$  สาร A12 และ A14 มีฤทธิ์ในการต้านเซลล์มะเร็งช่องปาก (KB) ด้วยค่า  $IC_{50}$  เท่ากับ  $18.5 \pm 3.8 \mu M$  และ  $13.6 \pm 0.1 \mu M$  ตามลำดับ เซลล์มะเร็งทรวงอก (MCF-7) ด้วยค่า  $IC_{50}$  เท่ากับ  $10.0 \pm 1.0 \mu M$  และ  $17.6 \pm 0.03 \mu M$  ตามลำดับ และเซลล์มะเร็งปอด (NCI-H187) ด้วยค่า  $IC_{50}$  เท่ากับ  $14.8 \pm 3.2 \mu M$  และ  $14.2 \pm 2.4 \mu M$  ตามลำดับ สาร A22 มีฤทธิ์ในการต้านเชื้อแบคทีเรีย *Staphylococcus aureus* และเชื้อรา *Cryptococcus neoformans* ด้วยค่า MIC เท่ากับ 2 และ  $4 \mu g/mL$  ตามลำดับ อีกทั้งสาร A27 มีฤทธิ์ในการต้านเชื้อมาลาเรีย *Plasmodium falciparum* K1 ด้วยค่า  $IC_{50}$  เท่ากับ  $2.8 \mu M$  นอกจากนั้นสาร A31 แสดงฤทธิ์ในการยับยั้งเอนไซม์อะซิetyl โคลิเนสเตอเรสด้วยค่าเปอร์เซ็นต์การยับยั้งเท่ากับ  $43.1 \pm 2.7$  ที่ความเข้มข้น  $100 \mu M$

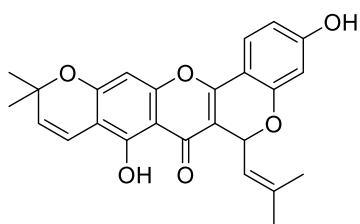


**A19**

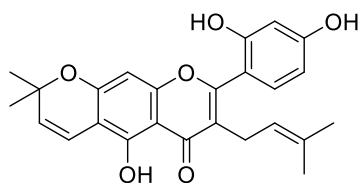


**A20**

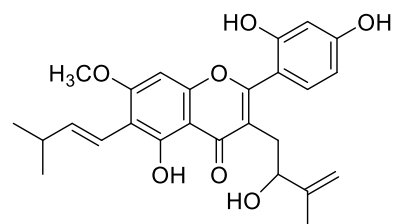




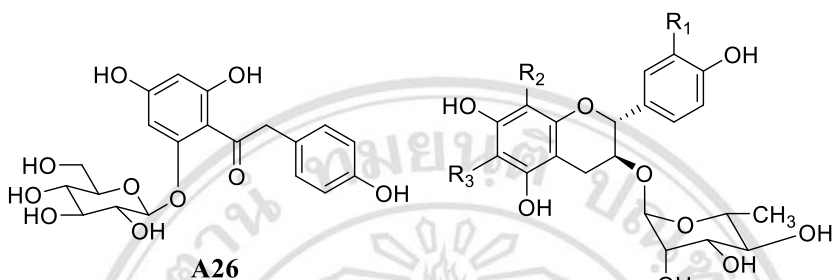
**A23**



**A24**



**A25**

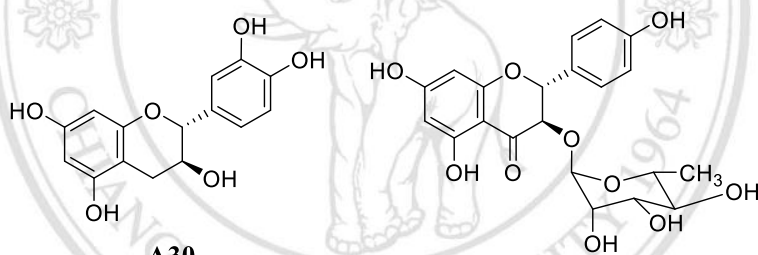


**A26**

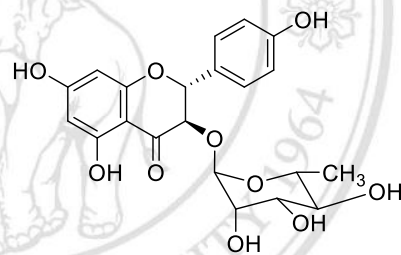
**A27:**  $R_1 = H, R_2 = R_3 = OH$

**A28:**  $R_1 = R_2 = R_3 = H$

**A29:**  $R_1 = OH, R_2 = R_3 = H$



**A30**



**A35**

ลิขสิทธิ์มหาวิทยาลัยเชียงใหม่

Copyright© by Chiang Mai University

All rights reserved

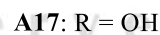
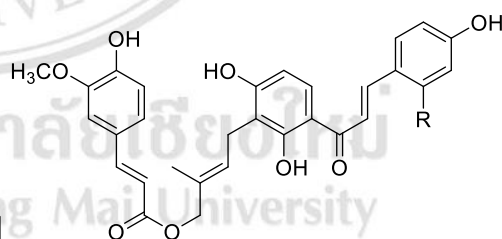
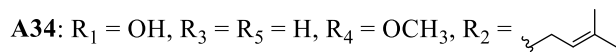
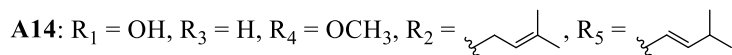
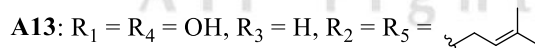
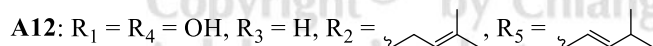
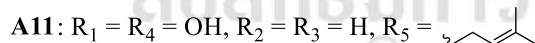
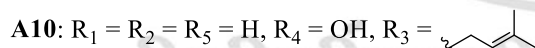
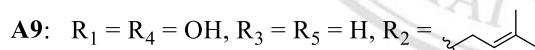
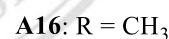
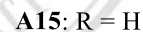
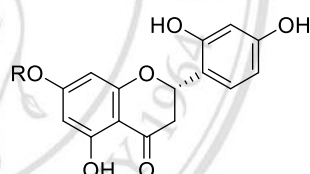
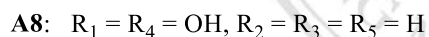
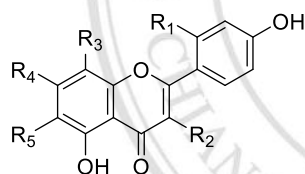
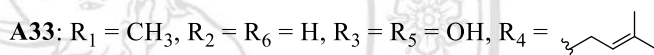
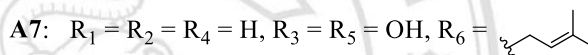
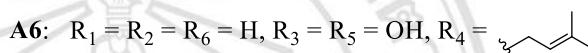
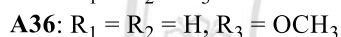
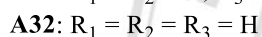
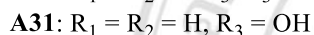
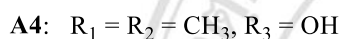
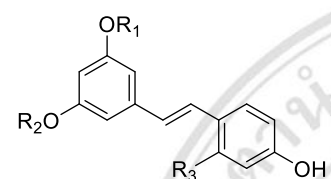
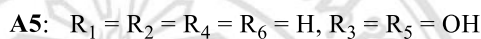
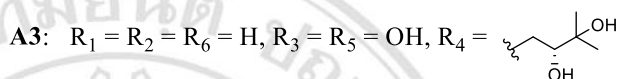
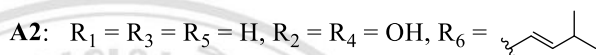
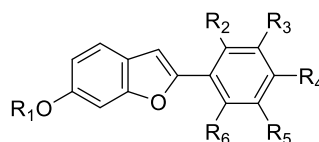
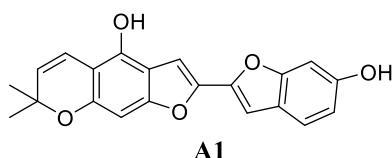
<b>Dissertation Title</b>	Chemical Constituents and Biological Activities from <i>Artocarpus heterophyllus</i> and <i>Artocarpus lakoocha</i> Roxb.	
<b>Author</b>	Ms. Sirada Boonyaketgoson	
<b>Degree</b>	Doctor of Philosophy (Chemistry)	
<b>Advisory Committee</b>	Assistant Professor Dr. Kongkiat Trisuwan	Advisor
	Assistant Professor Dr. Thunwadee Limtharakul	Co-advisor
	Associate Professor Dr. Lalida Shank	Co-advisor

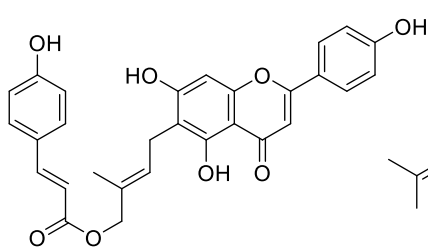
## ABSTRACT

Chromatographic separation of methanolic extract of twigs of *Artocarpus heterophyllus* and acetone extracts of the twigs and barks of *Artocarpus lakoocha* led to isolation of 36 compounds (**A1-A36**). The methanolic extract of the twigs of *A. heterophyllus* was isolated and gave four new compounds (**A1-A4**) together with 21 known compounds (**A5-A25**). The acetone extract of the twigs of *A. lakoocha* was purified and gave two new compounds (**A26** and **A27**) and 17 known compounds (**A2, A4-A7, A9, A11-A12, A16, A18, A21-A22, A28-A32**). The acetone extract of the barks of *A. lakoocha* was separated and provided eight known compounds (**A6, A28, A30-A31, A33-A36**). Their structures were elucidated by analysis of spectroscopic data, especially 1D and 2D NMR data. Compound **A3** showed cytotoxicity against human breast cancer cells (MCF-7) with the IC<sub>50</sub> value of  $12.6 \pm 1.5 \mu\text{M}$ , while compounds **A12** and **A14** exhibited cytotoxic activities against oral human carcinoma (KB) with the IC<sub>50</sub> values of  $18.5 \pm 3.8$  and  $13.6 \pm 0.1 \mu\text{M}$ , respectively, human breast cancer (MCF-7) with the IC<sub>50</sub> values of  $10.0 \pm 1.0$  and  $17.6 \pm 0.03 \mu\text{M}$ , respectively, and human small lung cancer (NCI-H187) cell lines with the IC<sub>50</sub> values of  $14.8 \pm 3.2$  and  $14.2 \pm 2.2 \mu\text{M}$ , respectively. Compound **A22** displayed antibacterial activity against *Staphylococcus aureus* and antifungal activity against *Cryptococcus neoformans* with the MIC values of 2 and 4  $\mu\text{g/mL}$ , respectively. Compound **A27** showed antimalarial activity against *Plasmodium*

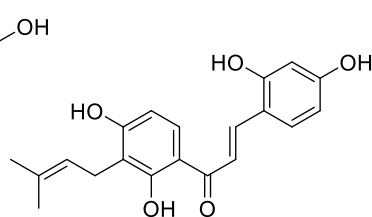


*falciparum* K1 with the IC<sub>50</sub> value of 2.8 μM and compound **A31** exhibited acetylcholinesterase inhibitory activity with % inhibition at 43.1 ± 2.7 (concentration 100 μM).

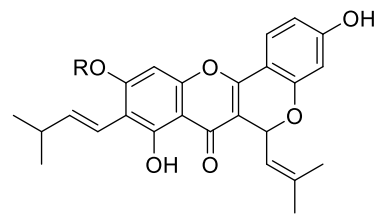




**A19**

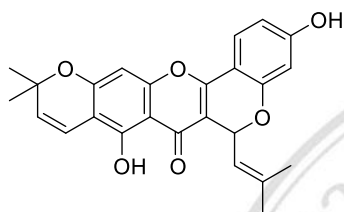


**A20**

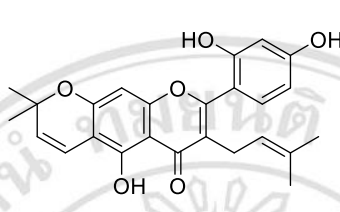


**A21: R = H**

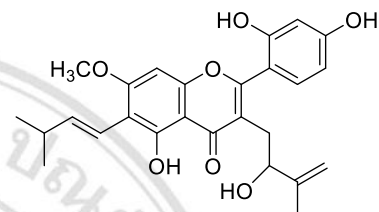
**A22: R = CH<sub>3</sub>**



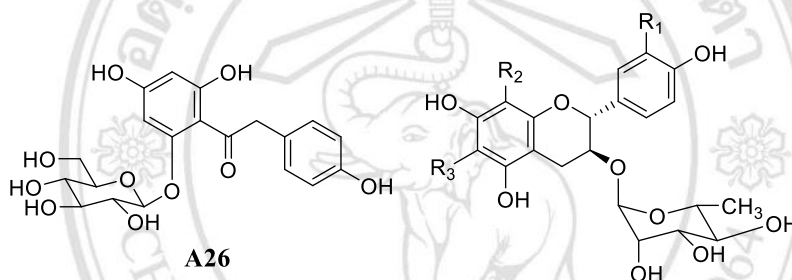
**A23**



**A24**



**A25**

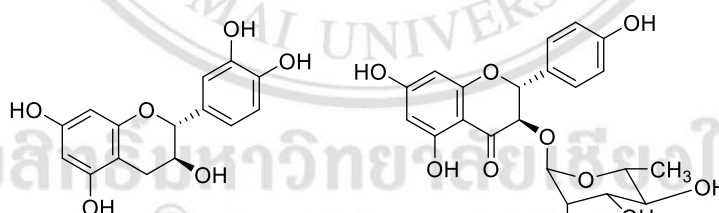


**A26**

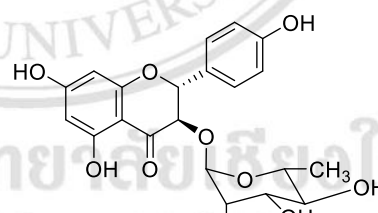
**A27: R<sub>1</sub> = H, R<sub>2</sub> = R<sub>3</sub> = OH**

**A28: R<sub>1</sub> = R<sub>2</sub> = R<sub>3</sub> = H**

**A29: R<sub>1</sub> = OH, R<sub>2</sub> = R<sub>3</sub> = H**



**A30**



**A35**

# CONTENTS

	Page
Acknowledgement	c
Abstract in Thai	d
Abstract in English	g
List of Tables	m
List of Figures	p
List of Abbreviations and Symbols	u
Statements of Originality in Thai	x
Statements of Originality in English	y
Chapter 1 Introduction	1
1.1 <i>Artocarpus</i> plants	1
1.2 <i>Artocarpus heterophyllus</i>	1
1.3 <i>Artocarpus lakoocha</i>	21
1.4 Objectives	27
Chapter 2 Experimental	29
2.1 Chemicals and general experimental procedures	29
2.2 Twigs of <i>Artocarpus heterophyllus</i>	30
2.2.1 Plant materials and extraction	30
2.2.2 Purification of methanolic extract of the twigs of <i>A. heterophyllus</i>	30

## CONTENTS (Continued)

	Page
2.3 Twigs of <i>Artocarpus lakoocha</i>	37
2.3.1 Plant materials and extraction	37
2.3.2 Purification of acetone extract of the twigs of <i>A. lakoocha</i>	37
2.3.3 Acid hydrolysis of compound <b>A26</b>	43
2.4 Barks of <i>Artocarpus lakoocha</i>	44
2.4.1 Plant materials and extraction	44
2.4.2 Purification of acetone extract of the barks of <i>A. lakoocha</i>	45
Chapter 3 Results and Discussion	58
3.1 Isolated compounds of the twigs of <i>Artocarpus heterophyllus</i>	58
3.1.1 Compound <b>A1</b>	58
3.1.2 Compound <b>A2</b>	60
3.1.3 Compound <b>A3</b>	62
3.1.4 Compound <b>A4</b>	64
3.1.5 Compounds <b>A5-A7</b>	66
3.1.6 Compounds <b>A8-A14</b>	69
3.1.7 Compounds <b>A15</b> and <b>A16</b>	75
3.1.8 Compounds <b>A17</b> and <b>A18</b>	76
3.1.9 Compound <b>A19</b>	78
3.1.10 Compound <b>A20</b>	81
3.1.11 Compounds <b>A21-A24</b>	82
3.1.12 Compound <b>A25</b>	85

## CONTENTS (Continued)

	Page
3.2 Isolated compounds from the twigs of <i>A. lakoocha</i>	88
3.2.1 Compound <b>A26</b>	88
3.2.2 Compounds <b>A27</b> and <b>A28</b>	91
3.2.3 Compounds <b>A29</b> and <b>A30</b>	97
3.2.4 Compounds <b>A31</b> and <b>A32</b>	101
3.3 Isolated compounds from the barks of <i>A. lakoocha</i>	102
3.3.1 Compound <b>A33</b>	102
3.3.2 Compound <b>A34</b>	103
3.3.3 Compound <b>A35</b>	105
3.3.4 Compound <b>A36</b>	106
3.4 Biological activities of some isolated compounds from <i>A. heterophyllus</i> and <i>A. lakoocha</i>	108
 Chapter 4 Conclusions	 113
 References	 117
 Appendix	 124
 Curriculum Vitae	 151

ลิขสิทธิ์มหาวิทยาลัยเชียงใหม่  
Copyright© by Chiang Mai University  
All rights reserved

## LIST OF TABLES

	Page
Table 1.1 Isolated compounds with biological activities from <i>A. heterophyllum</i>	3
Table 1.2 Isolated compounds with biological activities from <i>A. lakoocha</i>	22
Table 1.3 Biological activities of the extracts from the twigs of <i>A. heterophyllum</i> and <i>A. lakoocha</i>	27
Table 3.1 The NMR data (400 MHz, CDCl <sub>3</sub> ) of heterophyllene A ( <b>A1</b> )	59
Table 3.2 The NMR data (400 MHz, acetone- <i>d</i> <sub>6</sub> ) of heterophyllene B ( <b>A2</b> )	61
Table 3.3 The NMR data (400 MHz, acetone- <i>d</i> <sub>6</sub> ) of heterophyllene C ( <b>A3</b> )	63
Table 3.4 The NMR data (400 MHz, acetone- <i>d</i> <sub>6</sub> ) of heterophyllene D ( <b>A4</b> )	65
Table 3.5 The <sup>1</sup> H-NMR data of compounds <b>A5-A7</b> (400 MHz, acetone- <i>d</i> <sub>6</sub> ), moracin M (400 MHz, acetone- <i>d</i> <sub>6</sub> ), moracin C (300 MHz, acetone- <i>d</i> <sub>6</sub> ) and demethylmoracin I (500 MHz, acetone- <i>d</i> <sub>6</sub> )	68
Table 3.6 The <sup>1</sup> H-NMR data of compounds <b>A8-A10</b> (400 MHz, acetone- <i>d</i> <sub>6</sub> ), norartocarpetin (300 MHz, DMSO- <i>d</i> <sub>6</sub> ), albanin A (400 MHz, DMSO- <i>d</i> <sub>6</sub> ), and licoflavone C (400 MHz, acetone- <i>d</i> <sub>6</sub> )	71
Table 3.7 The <sup>1</sup> H-NMR data of compounds <b>A11</b> (400 MHz, DMSO- <i>d</i> <sub>6</sub> ), <b>A12</b> (400 MHz, acetone- <i>d</i> <sub>6</sub> ), <b>A13</b> (400 MHz, acetone- <i>d</i> <sub>6</sub> ), artocarpesin (300 MHz, DMSO- <i>d</i> <sub>6</sub> ), norartocarpin (400 MHz, acetone- <i>d</i> <sub>6</sub> ) and cudraflavone C (400 MHz, acetone- <i>d</i> <sub>6</sub> )	72
Table 3.8 The NMR data of compounds <b>A14</b> (400 MHz, CDCl <sub>3</sub> ) and artocarpin (500 MHz, CDCl <sub>3</sub> )	74
Table 3.9 The <sup>1</sup> H-NMR data of compounds <b>A15</b> and <b>A16</b> (400 MHz, acetone- <i>d</i> <sub>6</sub> ), steppogenin (500 MHz, acetone- <i>d</i> <sub>6</sub> ) and artocarpanone (400 MHz, acetone- <i>d</i> <sub>6</sub> )	76
Table 3.10 The <sup>1</sup> H-NMR data of compounds <b>A17</b> and <b>A18</b> (400 MHz, acetone- <i>d</i> <sub>6</sub> ), isogemichalcone C and artocarmitin B (500 MHz, acetone- <i>d</i> <sub>6</sub> )	77

## LIST OF TABLES (Continued)

	Page
Table 3.11 The NMR data of compound <b>A19</b> (400 MHz, acetone- <i>d</i> <sub>6</sub> ) and artocarmin B (500 MHz, DMSO- <i>d</i> <sub>6</sub> )	79
Table 3.12 The <sup>1</sup> H-NMR data of compound <b>A20</b> (400 MHz, acetone- <i>d</i> <sub>6</sub> ) and morachalcone A (500 MHz, acetone- <i>d</i> <sub>6</sub> )	81
Table 3.13 The <sup>1</sup> H-NMR data of compounds <b>A21</b> and <b>A22</b> (400 MHz, CDCl <sub>3</sub> ) brosimone I (300 MHz, CDCl <sub>3</sub> ) and cycloartocarpin (500 MHz, CDCl <sub>3</sub> )	83
Table 3.14 The <sup>1</sup> H-NMR data of compounds <b>A23</b> (400 MHz, CDCl <sub>3</sub> ), <b>A24</b> (400 MHz, acetone- <i>d</i> <sub>6</sub> ), cudraflavone A (400 MHz, CDCl <sub>3</sub> ) and cudraflavone B (300 MHz, DMSO- <i>d</i> <sub>6</sub> )	84
Table 3.15 The NMR data of compound <b>A25</b> (400 MHz, acetone- <i>d</i> <sub>6</sub> ) and artogomezianone (500 MHz, acetone- <i>d</i> <sub>6</sub> )	86
Table 3.16 The HMBC and COSY correlations of compound <b>A25</b>	88
Table 3.17 The NMR data (400 MHz, MeOD- <i>d</i> <sub>4</sub> ) of lakoochanoside A ( <b>A26</b> )	90
Table 3.18 The NMR data (400 MHz, MeOD- <i>d</i> <sub>4</sub> ) of lakoochanoside B ( <b>A27</b> )	93
Table 3.19 The NMR data (400 MHz, MeOD- <i>d</i> <sub>4</sub> ) of compounds <b>A27</b> and <b>A28</b> and (+)-afzelechin-3- <i>O</i> -α-L-rhamnopyranoside (500 MHz, MeOD- <i>d</i> <sub>4</sub> )	95
Table 3.20 The HMBC and COSY correlations of compound <b>A28</b>	97
Table 3.21 The <sup>1</sup> H-NMR data of compounds <b>A29</b> (400 MHz, MeOD- <i>d</i> <sub>4</sub> ), <b>A30</b> (400 MHz, acetone- <i>d</i> <sub>6</sub> ), (+)-catechin-3- <i>O</i> -α-L-rhamnopyranoside (400 MHz, MeOD- <i>d</i> <sub>4</sub> ) and (+)-catechin (400 MHz, acetone- <i>d</i> <sub>6</sub> )	98
Table 3.22 The <sup>13</sup> C-NMR data of compounds <b>A29</b> (100 MHz, MeOD- <i>d</i> <sub>4</sub> ), <b>A30</b> (100 MHz, acetone- <i>d</i> <sub>6</sub> ), (+)-catechin-3- <i>O</i> -α-L-rhamnopyranoside (100 MHz, MeOD- <i>d</i> <sub>4</sub> ) and (+)-catechin (100 MHz, DMSO- <i>d</i> <sub>6</sub> )	100

## LIST OF TABLES (Continued)

	Page
Table 3.23 The $^1\text{H}$ -NMR data (400 MHz, acetone- $d_6$ ) of compounds <b>A31</b> and <b>A32</b> , oxyresveratrol (400 MHz, MeOD- $d_4$ ) and resveratrol (400 MHz, MeOD- $d_4$ )	102
Table 3.24 The $^1\text{H}$ -NMR data of compound <b>A33</b> (500 MHz, acetone- $d_6$ ) and sanggenofuran B (500 MHz, $\text{CDCl}_3$ )	103
Table 3.25 The $^1\text{H}$ -NMR data (500 MHz, acetone- $d_6$ ) of compound <b>A34</b> and integrin	104
Table 3.26 The $^1\text{H}$ -NMR data of compound <b>A35</b> (500 MHz, acetone- $d_6$ ) and engeletin (400 MHz, MeOD- $d_4$ )	106
Table 3.27 The $^1\text{H}$ -NMR data of compound <b>A36</b> (500 MHz, acetone- $d_6$ ) and <i>trans</i> -2-methoxy-4,3',5'-trihydroxystilbene (300 MHz, acetone- $d_6$ )	107
Table 3.28 Cytotoxic activities of some isolated compounds	110
Table 3.29 Antimicrobial activities of some isolated compounds	111
Table 3.30 Acetylcholinesterase inhibitory and antimalarial activities of some isolated compounds	111



## LIST OF FIGURES

	Page
Figure 1.1 The parts of <i>A. heterophyllus</i>	2
Figure 1.2 The structures of isolated compounds from <i>A. heterophyllus</i>	17
Figure 1.3 The parts of <i>A. lakoocha</i>	21
Figure 1.4 The structures of isolated compounds from <i>A. lakoocha</i>	25
Figure 2.1 The isolation of the methanolic extract of the twigs of <i>A. heterophyllus</i>	30
Figure 2.2 The isolation of fraction AHT-2	31
Figure 2.3 The isolation of fraction AHT-4	32
Figure 2.4 The isolation of fraction AHT-5	33
Figure 2.5 The isolation of fraction AHT-6	34
Figure 2.6 The isolation of subfraction AHT-65	35
Figure 2.7 The isolation of fraction AHT-7	36
Figure 2.8 The isolation of subfraction AHT-73	36
Figure 2.9 The isolation of the acetone extract of the twigs of <i>A. lakoocha</i>	37
Figure 2.10 The isolation of fraction ALT-3	38
Figure 2.11 The isolation of fraction ALT-4	39
Figure 2.12 The isolation of fraction ALT-5	40
Figure 2.13 The isolation of fraction ALT-6	41
Figure 2.14 The isolation of subfraction ALT-65	42
Figure 2.15 The isolation of fraction ALT-7	43
Figure 2.16 The extraction of the barks of <i>A. lakoocha</i>	44
Figure 2.17 The isolation of the dichloromethane fraction of the barks of <i>A. lakoocha</i>	45
Figure 2.18 The isolation of fraction BLD-5	46
Figure 2.19 The isolation of fraction BLD-6	47

## LIST OF FIGURES (Continued)

	Page
Figure 2.20 The isolation of the aqueous fraction of the barks of <i>A. lakoocha</i>	47
Figure 2.21 The isolation of fraction BLM-2	48
Figure 2.22 The isolation of fraction BLM-4	48
Figure 3.1 The structure of heterophyllene A ( <b>A1</b> )	59
Figure 3.2 The structure of heterophyllene B ( <b>A2</b> )	61
Figure 3.3 The structure of heterophyllene C ( <b>A3</b> )	63
Figure 3.4 The structure of heterophyllene D ( <b>A4</b> )	65
Figure 3.5 The structure of compounds <b>A5-A7</b>	67
Figure 3.6 The structure of compounds <b>A8-A14</b>	70
Figure 3.7 The structure of compounds <b>A15</b> and <b>A16</b>	75
Figure 3.8 The structure of compounds <b>A17</b> and <b>A18</b>	77
Figure 3.9 The structure of artocarmin B ( <b>A19</b> )	79
Figure 3.10 The structure of morachalcone A ( <b>A20</b> )	81
Figure 3.11 The structure of compounds <b>A21-A24</b>	83
Figure 3.12 The structure of artogomezianone ( <b>A25</b> )	86
Figure 3.13 The structure of lakoochanoside A ( <b>A26</b> )	90
Figure 3.14 The structure of compounds <b>A27</b> and <b>A28</b>	93
Figure 3.15 The structure of compounds <b>A29</b> and <b>A30</b>	98
Figure 3.16 The structure of compounds <b>A31</b> and <b>A32</b>	101
Figure 3.17 The structure of sanggenofuran B ( <b>A33</b> )	103
Figure 3.18 The structure of integrin ( <b>A34</b> )	104
Figure 3.19 The structure of engeletin ( <b>A35</b> )	105
Figure 3.20 The structure of <i>trans</i> -2-methoxy-4,3',5'-trihydroxystilbene ( <b>A36</b> )	107

## LIST OF FIGURES (Continued)

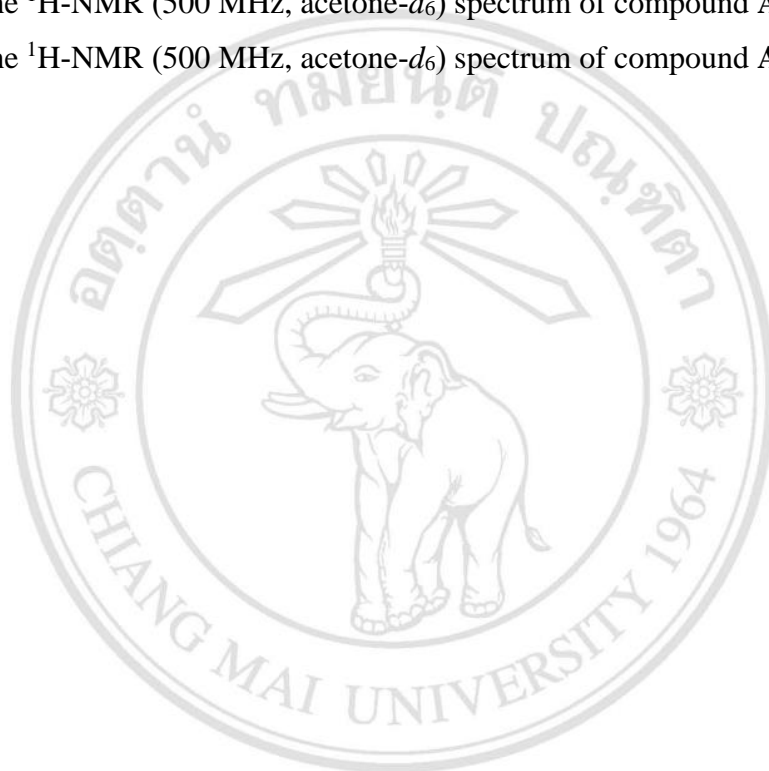
	Page
Figure 4.1 The structures of isolated compounds from <i>A. heterophyllus</i> and <i>A. lakoocha</i>	115
Figure 1 HPLC chromatogram of subfraction BLD-51	125
Figure 2 HPLC chromatogram of subfraction BLD-52	125
Figure 3 HPLC chromatogram of subfraction BLD-61	125
Figure 4 HPLC chromatogram of subfraction BLD-62	126
Figure 5 The $^1\text{H}$ -NMR (400 MHz, $\text{CDCl}_3$ ) spectrum of compound <b>A1</b>	126
Figure 6 The $^{13}\text{C}$ -NMR (100 MHz, $\text{CDCl}_3$ ) spectrum of compound <b>A1</b>	127
Figure 7 The $^1\text{H}$ -NMR (400 MHz, acetone- $d_6$ ) spectrum of compound <b>A2</b>	127
Figure 8 The $^{13}\text{C}$ -NMR (100 MHz, acetone- $d_6$ ) spectrum of compound <b>A2</b>	128
Figure 9 The $^1\text{H}$ -NMR (400 MHz, acetone- $d_6$ ) spectrum of compound <b>A3</b>	128
Figure 10 The $^{13}\text{C}$ -NMR (100 MHz, acetone- $d_6$ ) spectrum of compound <b>A3</b>	129
Figure 11 The $^1\text{H}$ -NMR (400 MHz, acetone- $d_6$ ) spectrum of compound <b>A4</b>	129
Figure 12 The $^{13}\text{C}$ -NMR (100 MHz, acetone- $d_6$ ) spectrum of compound <b>A4</b>	130
Figure 13 The $^1\text{H}$ -NMR (400 MHz, acetone- $d_6$ ) spectrum of compound <b>A5</b>	130
Figure 14 The $^1\text{H}$ -NMR (400 MHz, acetone- $d_6$ ) spectrum of compound <b>A6</b>	131
Figure 15 The $^1\text{H}$ -NMR (400 MHz, acetone- $d_6$ ) spectrum of compound <b>A7</b>	131
Figure 16 The $^1\text{H}$ -NMR (400 MHz, acetone- $d_6$ ) spectrum of compound <b>A8</b>	132
Figure 17 The $^1\text{H}$ -NMR (400 MHz, acetone- $d_6$ ) spectrum of compound <b>A9</b>	132
Figure 18 The $^1\text{H}$ -NMR (400 MHz, acetone- $d_6$ ) spectrum of compound <b>A10</b>	133
Figure 19 The $^1\text{H}$ -NMR (400 MHz, $\text{DMSO}-d_6$ ) spectrum of compound <b>A11</b>	133
Figure 20 The $^1\text{H}$ -NMR (400 MHz, acetone- $d_6$ ) spectrum of compound <b>A12</b>	134
Figure 21 The $^1\text{H}$ -NMR (400 MHz, acetone- $d_6$ ) spectrum of compound <b>A13</b>	134
Figure 22 The $^1\text{H}$ -NMR (400 MHz, $\text{CDCl}_3$ ) spectrum of compound <b>A14</b>	135
Figure 23 The $^{13}\text{C}$ -NMR (400 MHz, $\text{CDCl}_3$ ) spectrum of compound <b>A14</b>	135

## LIST OF FIGURES (Continued)

	Page
Figure 24 The $^1\text{H}$ -NMR (400 MHz, acetone- $d_6$ ) spectrum of compound <b>A15</b>	136
Figure 25 The $^1\text{H}$ -NMR (400 MHz, acetone- $d_6$ ) spectrum of compound <b>A16</b>	136
Figure 26 The $^1\text{H}$ -NMR (400 MHz, acetone- $d_6$ ) spectrum of compound <b>A17</b>	137
Figure 27 The $^1\text{H}$ -NMR (400 MHz, acetone- $d_6$ ) spectrum of compound <b>A18</b>	137
Figure 28 The $^1\text{H}$ -NMR (400 MHz, acetone- $d_6$ ) spectrum of compound <b>A19</b>	138
Figure 29 The $^{13}\text{C}$ -NMR (100 MHz, acetone- $d_6$ ) spectrum of compound <b>A19</b>	138
Figure 30 The $^1\text{H}$ -NMR (400 MHz, acetone- $d_6$ ) spectrum of compound <b>A20</b>	139
Figure 31 The $^1\text{H}$ -NMR (400 MHz, $\text{CDCl}_3$ ) spectrum of compound <b>A21</b>	139
Figure 32 The $^1\text{H}$ -NMR (400 MHz, $\text{CDCl}_3$ ) spectrum of compound <b>A22</b>	140
Figure 33 The $^1\text{H}$ -NMR (400 MHz, $\text{CDCl}_3$ ) spectrum of compound <b>A23</b>	140
Figure 34 The $^1\text{H}$ -NMR (400 MHz, acetone- $d_6$ ) spectrum of compound <b>A24</b>	141
Figure 35 The $^1\text{H}$ -NMR (400 MHz, acetone- $d_6$ ) spectrum of compound <b>A25</b>	141
Figure 36 The $^{13}\text{C}$ -NMR (100 MHz, acetone- $d_6$ ) spectrum of compound <b>A25</b>	142
Figure 37 The $^1\text{H}$ -NMR (400 MHz, $\text{MeOD-}d_4$ ) spectrum of compound <b>A26</b>	142
Figure 38 The $^{13}\text{C}$ -NMR (100 MHz, $\text{MeOD-}d_4$ ) spectrum of compound <b>A26</b>	143
Figure 39 The $^1\text{H}$ -NMR (400 MHz, $\text{MeOD-}d_4$ ) spectrum of compound <b>A27</b>	143
Figure 40 The $^{13}\text{C}$ -NMR (100 MHz, $\text{MeOD-}d_4$ ) spectrum of compound <b>A27</b>	144
Figure 41 The $^1\text{H}$ -NMR (400 MHz, $\text{MeOD-}d_4$ ) spectrum of compound <b>A28</b>	144
Figure 42 The $^{13}\text{C}$ -NMR (100 MHz, $\text{MeOD-}d_4$ ) spectrum of compound <b>A28</b>	145
Figure 43 The $^1\text{H}$ -NMR (400 MHz, $\text{MeOD-}d_4$ ) spectrum of compound <b>A29</b>	145
Figure 44 The $^{13}\text{C}$ -NMR (100 MHz, $\text{MeOD-}d_4$ ) spectrum of compound <b>A29</b>	146
Figure 45 The $^1\text{H}$ -NMR (400 MHz, acetone- $d_6$ ) spectrum of compound <b>A30</b>	146
Figure 46 The $^{13}\text{C}$ -NMR (100 MHz, acetone- $d_6$ ) spectrum of compound <b>A30</b>	147
Figure 47 The $^1\text{H}$ -NMR (400 MHz, acetone- $d_6$ ) spectrum of compound <b>A31</b>	147
Figure 48 The $^1\text{H}$ -NMR (400 MHz, acetone- $d_6$ ) spectrum of compound <b>A32</b>	148

## LIST OF FIGURES (Continued)

	Page
Figure 49 The $^1\text{H}$ -NMR (500 MHz, acetone- $d_6$ ) spectrum of compound <b>A33</b>	148
Figure 50 The $^1\text{H}$ -NMR (500 MHz, acetone- $d_6$ ) spectrum of compound <b>A34</b>	149
Figure 51 The $^1\text{H}$ -NMR (500 MHz, acetone- $d_6$ ) spectrum of compound <b>A35</b>	149
Figure 52 The $^1\text{H}$ -NMR (500 MHz, acetone- $d_6$ ) spectrum of compound <b>A36</b>	150



ลิขสิทธิ์มหาวิทยาลัยเชียงใหม่  
 Copyright© by Chiang Mai University  
 All rights reserved

## LIST OF ABBREVIATIONS AND SYMBOLS

$m/z$	a value of mass divided by charge
AcOH	acetic acid
Vero	african green monkey kidney cell
brs	broad singlet
$\delta$	chemical shift relative to TMS
CHCl <sub>3</sub>	chloroform
CC	column chromatography
c	concentration
COSY	correlation spectroscopy
$J$	coupling constant
CDCl <sub>3</sub>	deuteriochloroform
CH <sub>2</sub> Cl <sub>2</sub>	dichloromethane
diol CC	diol column chromatography
DEPT	distortionless enhancement by polarization transfer
d	doublet
dd	doublet of doublet
ddd	doublet of doublet of doublet
EtOAc	ethyl acetate
FT-IR	frontier Infrared spectroscopy
g	gram
HPLC	high-performance liquid chromatography
Hz	Hertz
HMBC	heteronuclear multiple bond correlation
HMQC	heteronuclear multiple quantum correlation
acetone- <i>d</i> <sub>6</sub>	hexadeuteroacetone
DMSO- <i>d</i> <sub>6</sub>	hexadeuterodimethyl sulfoxide
HSV	herpes simplex virus
MCF-7	human breast cancer cell

## LIST OF ABBREVIATIONS AND SYMBOLS (Continued)

SMMC-7721	human hepatocarcinoma cell line
A549	human lung carcinoma cell line
H460	human lung cancer cell line
NCI-H460	human lung cancer cell line
A2780	human ovarian cancer cell
PC-3	human prostate cancer cell lines
NCI-H187	human small lung cancer cell
kg	kilogram
Petrol	light petroleum ether
L	liter
MS	mass spectroscopy
$\lambda_{\max}$	maximum wavelength
$\nu_{\max}$	maximum wavelength number
MHz	MegaHertz
MeOH	methanol
$\mu\text{g/mL}$	microgram per milliliter
$\mu\text{L}$	microliter
mg	milligram
mL	milliliter
MIC	minimum inhibitory concentration
min	minute
$\epsilon$	molar extinction coefficient
m	multiplet
nm	nanometer
N	normality
NMR	nuclear magnetic resonance
1D NMR	one dimensional nuclear magnetic resonance

## LIST OF ABBREVIATIONS AND SYMBOLS (Continued)

KB	oral cavity cancer cell
QCC	quick column chromatography
$\text{cm}^{-1}$	reciprocal centimeter (wavenumber)
$t_R$	retention time
RPCC	reverse phase column chromatography
s	singlet
NaOH	sodium hydroxide
$[\alpha]_D$	specific rotation
$\text{MeOD-}d_4$	tetraduteromethanol
TMS	tetramethylsilane
TLC	thin-layer chromatography
TBARS	thiobarbirturic acid-reactive substance
t	triplet
2D NMR	two dimentional nuclear magnetic resonance
UV	ultraviolet spectroscopy
$\text{H}_2\text{O}$	water
DPPH	1,1-diphenyl-2-picrylhydrazyl
$\text{IC}_{50}$	50% inhibitory concentration

ลิขสิทธิ์มหาวิทยาลัยเชียงใหม่  
Copyright© by Chiang Mai University  
All rights reserved



## ข้อความแห่งการริเริ่ม

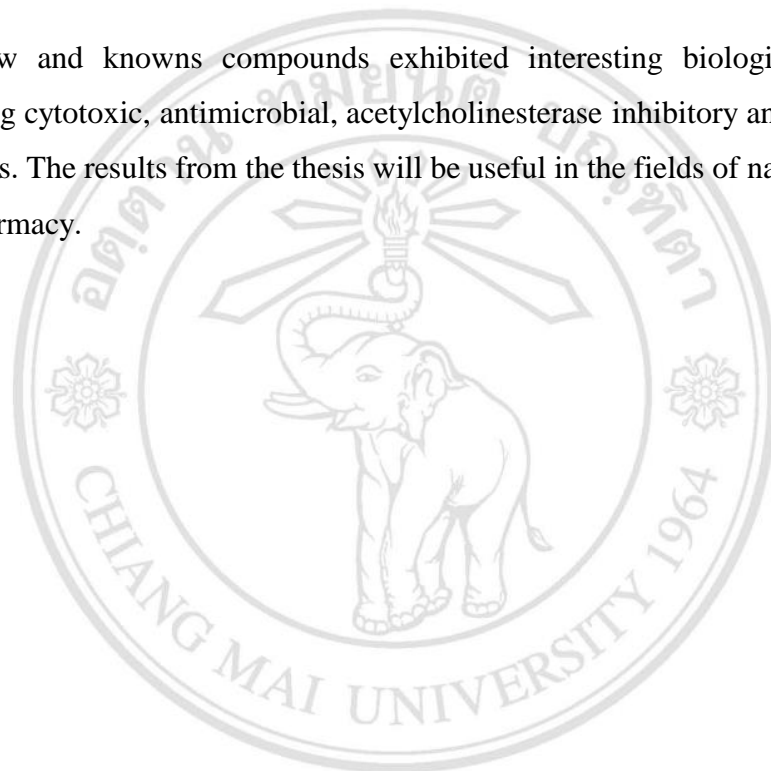
- 1) วิทยานิพนธ์นี้ได้นำเสนอการแยกและการวิเคราะห์โครงสร้างของสารจากสารสกัดเมทานอลจากกิ่งขนุน (*Artocarpus heterophyllus*) และสารสกัดอะซิโตนจากกิ่งและเปลือกขนุนป่า (*A. lakoocha*) โดยใช้วิธีทางโครมาโทกราฟีและวิธีทางสเปกโทรสโกปีแบบต่าง ๆ
- 2) สารใหม่และสารที่มีการรายงานโครงสร้างแล้วบางส่วนมีฤทธิ์ทางชีวภาพ ได้แก่ ฤทธิ์ต้านเซลล์มะเร็งชนิดต่างๆ ฤทธิ์ต้านจุลินทรีย์ ฤทธิ์ยับยั้งเอนไซม์อะซิติลโคลีนเอสเตอเรส และฤทธิ์ต้านเชื้อมาลาเรีย วิทยานิพนธ์นี้มีประโยชน์ในด้านผลิตภัณฑ์ธรรมชาติและทางเภสัชกรรม



ลิขสิทธิ์มหาวิทยาลัยเชียงใหม่  
Copyright© by Chiang Mai University  
All rights reserved

## STATEMENT OF ORIGINALITY

- 1) This thesis explained the isolation and structural elucidation from methanolic extract of the twigs of jackfruit (*Artocarpus heterophyllus*) and acetone extracts of the twigs and barks of monkey jack (*A. lakoocha*) by various chromatographic and spectroscopic techniques.
- 2) The new and known compounds exhibited interesting biological activities, including cytotoxic, antimicrobial, acetylcholinesterase inhibitory and antimalarial activities. The results from the thesis will be useful in the fields of natural products and pharmacy.



ลิขสิทธิ์มหาวิทยาลัยเชียงใหม่  
Copyright© by Chiang Mai University  
All rights reserved

# CHAPTER 1

## Introduction

### 1.1 *Artocarpus* plants

The genus *Artocarpus* belonging to the family Moraceae comprises approximately fifty species (Jagtap *et al.*, 2010). They are distributed widely in the many tropical and subtropical regions especially Asia including Thailand, Vietnam, Indonesia and India. Some species are used for edible fruit, furniture, vehicle, dye in industry and traditional folk medicine such as treating diabetes (*Artocarpus altilis*), diarrhea (*A. chempeden*), killing tapeworm (*A. lakoocha*), whitening lotion (*A. lakoocha*), activating milk production (*A. heterophyllus*) and healing wounds (*A. heterophyllus*) (Baliga *et al.*, 2011 and Jagtap *et al.*, 2010). Previously phytochemical investigations showed many types of compounds were isolated from *Artocarpus* plants including flavonoids (Zheng *et al.*, 2008), stilbenoids (Zheng *et al.*, 2014), benzofurans (Sritularak *et al.*, 2010) and chalcones (Fang *et al.*, 2008) with anticancer against PC-3 (human prostate cancer cell), NCI-H460 (human lung cancer cell) and A549 (human lung cancer cell) cell lines (Wang *et al.*, 2017), antimycobacterial (Puntumchai *et al.*, 2004), glucosidase inhibitory (Mai *et al.*, 2012) and tyrosinase inhibitory activities (Nguyen *et al.*, 2016). Therefore, this research focused on the isolation and structural elucidation of the compounds isolated from *Artocarpus* plants.

### 1.2 *Artocarpus heterophyllus*

*Artocarpus heterophyllus* or jackfruit belongs to family Moraceae. Thai common names are Ka-Noon, Ba-Nun and Mak-Mi. It is distributed in many tropical and subtropical areas in Asia such as Thailand, Vietnam, Indonesia and India. It is around 30-40 meters height. The stems and branches of jackfruit tree have latex like milk. The leaves

are oval thick green and the male and female green flower are in the same tree. It is the 30-40 centimeters cylindrical fruit and it is reaching as much as 25 kilograms. The parts of jackfruit tree are shown in **Figure 1.1**. The sweet pulps and seeds of fruit are edible for animals and the ingredient of curry, pickles, flour, dessert and liquor. The yellow timber heartwood is used for furniture, vehicles, music instruments and dye in industry. Moreover, the many parts of jackfruit tree are used as a folk traditional medicine. The roots are useful for skin diseases, asthma and diarrhea as well as the barks are used for dysentery. The leaves of jackfruit tree can be used for healing wounds, cooling tonic and activating milk for females. The ripen fruits can be treated cooling tonic and preventing excess bile (Baliga *et al.*, 2011).

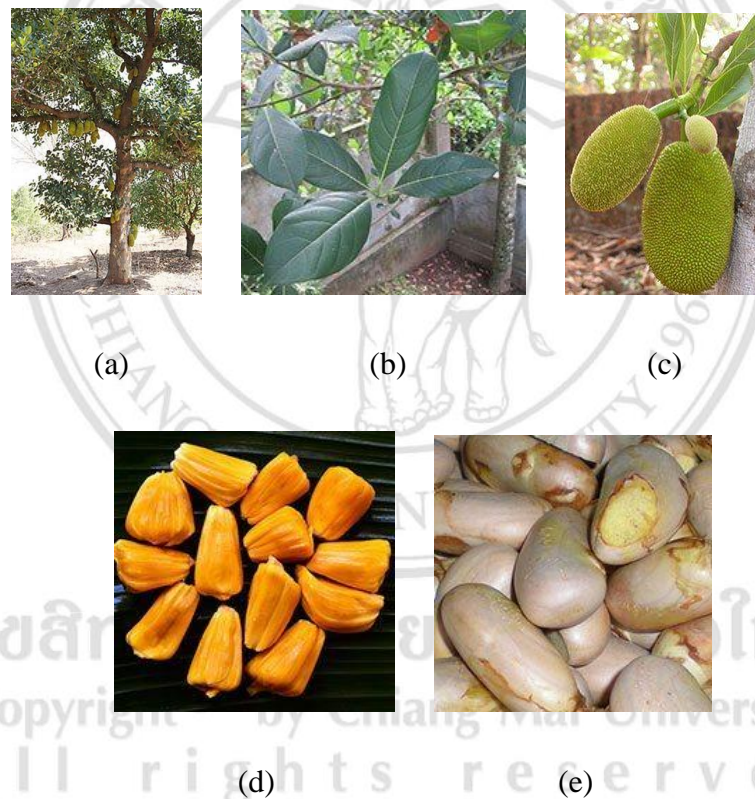


**Figure 1.1** The parts of *A. heterophyllus* (a) stems, (b) leaves, (c) fruits (d) pulps and (e) seeds (MedThai, 2017, <https://medthai.com/> ขนุน, accessed on 15 February, 2019)

On August 2010 - February 2017, many research groups investigated the bioactive compounds from many parts of *A. heterophyllum*. On the SciFinder Scholar Database, the isolated compounds isolated from *A. heterophyllum* were summarized in the **Table 1.1**, and the structures are shown in **Figure 1.2**.

**Table 1.1** Isolated compounds with biological activities from *A. heterophyllum*

Part of Plant	Compounds	Biological activity	References
Roots	Artoindonesianin F ( <b>1</b> )	Tyrosinase inhibition, IC <sub>50</sub> = 0.20 µg/mL	Rao <i>et al.</i> , 2010
	Artoheterone A ( <b>2</b> )	Anti-respiratory burst, IC <sub>50</sub> = 1.67 ± 0.58 µM	Ren <i>et al.</i> , 2015
	Artoheterone B ( <b>3</b> )	Anti-respiratory burst, IC <sub>50</sub> = 0.19 ± 0.05 µM	
	2,3-Dihydro-5,7-dihydroxy- 2-(2-hydroxy-4- methoxyphenyl)-4 <i>H</i> -1- benzopyran-4-one ( <b>4</b> )	Anti-respiratory burst, IC <sub>50</sub> = 87.00 ± 4.21 µM	
	Artocarpanone ( <b>5</b> )	Anti-respiratory burst, IC <sub>50</sub> = 106.90 ± 3.95 µM	
	Artoheteroid A ( <b>6</b> )	Cathepsin K inhibition, IC <sub>50</sub> = 93.9 µM	Yuan <i>et al.</i> , 2017
	Artoheteroid B ( <b>7</b> )	Cathepsin K inhibition, IC <sub>50</sub> = 76.4 µM	
	Artoheteroid C ( <b>8</b> )	-	
	Artoheteroid D ( <b>9</b> )	Cathepsin K inhibition, IC <sub>50</sub> = 8.5 µM	
	Morin ( <b>10</b> )	Cathepsin K inhibition, IC <sub>50</sub> = 18.6 µM	
	Artocarmin A ( <b>11</b> )	Cathepsin K inhibition, IC <sub>50</sub> = 61.0 µM	

**Table 1.1** (Continued)

<b>Part of Plant</b>	<b>Compounds</b>	<b>Biological activity</b>	<b>References</b>
Roots	Albanin A ( <b>12</b> )	-	Yuan <i>et al.</i> , 2017
	Euchrenone a7 ( <b>13</b> )	-	
	Steppogenin ( <b>14</b> )	Cathepsin K inhibition, IC <sub>50</sub> = 1.4 µM	
	Norartocarpanone ( <b>15</b> )	-	
Wood	Artocarpanone ( <b>5</b> )	Cytotoxicity, B16 melanoma cells, IC <sub>50</sub> = 122.2 µM	Arung <i>et al.</i> , 2010
	Morin ( <b>10</b> )	Cytotoxicity, B16 melanoma cells, IC <sub>50</sub> = 170.0 µM	
	Albanin A ( <b>12</b> )	Cytotoxicity, B16 melanoma cells, IC <sub>50</sub> = 84.7 µM	
	Artocarpin ( <b>16</b> )	Cytotoxicity, B16 melanoma cells, IC <sub>50</sub> = 2.0 µM	
	Cudraflavone C ( <b>17</b> )	Cytotoxicity, B16 melanoma cells, IC <sub>50</sub> = 9.2 µM	
	6-Prenylapigenin ( <b>18</b> )	Cytotoxicity, B16 melanoma cells, IC <sub>50</sub> = 32.5 µM	
	Kuwanon C ( <b>19</b> )	Cytotoxicity, B16 melanoma cells, IC <sub>50</sub> = 14.2 µM	
	Norartocarpin ( <b>20</b> )	Cytotoxicity, B16 melanoma cells, IC <sub>50</sub> = 7.8 µM	

**Table 1.1** (Continued)

Part of Plant	Compounds	Biological activity	References
Wood	Cudraflavone B ( <b>21</b> )	Cytotoxicity, B16 melanoma cells, IC <sub>50</sub> = 12.5 µM	Arung <i>et al.</i> , 2010
	Brosimone I ( <b>22</b> )	Cytotoxicity, B16 melanoma cells, IC <sub>50</sub> = 10.7 µM	
	2',4'-Dihydroxyflavone ( <b>23</b> )	Cytotoxicity, B16 melanoma cells, IC <sub>50</sub> = 114.7 µM	
	3-Prenyl luteolin ( <b>24</b> )	- Tyrosinase inhibition, IC <sub>50</sub> = 76.3 µM - Cytotoxicity, B16 melanoma cells, IC <sub>50</sub> = 56.7 µM	Arung <i>et al.</i> , 2010
	Artocarmin A ( <b>11</b> )	Tyrosinase inhibition, IC <sub>50</sub> = 18.7 ± 0.1 µM	
	Albanin A ( <b>12</b> )	Tyrosinase inhibition, IC <sub>50</sub> = 1.01 ± 0.05 µM	Nguyen <i>et al.</i> , 2012
	Cudraflavone C ( <b>17</b> )	Tyrosinase inhibition, IC <sub>50</sub> = 21.4 ± 0.2 µM	
	Norartocarpin ( <b>20</b> )	Tyrosinase inhibition, IC <sub>50</sub> = 17.3 ± 0.1 µM	
	Artocarmin B ( <b>25</b> )	Tyrosinase inhibition, IC <sub>50</sub> = 8.4 ± 0.1 µM	
	Artocarmin C ( <b>26</b> )	Tyrosinase inhibition, IC <sub>50</sub> = 40.0 ± 0.4 µM	
	Artocarmin D ( <b>27</b> )	Tyrosinase inhibition, IC <sub>50</sub> = 47.3 ± 0.4 µM	

**Table 1.1** (Continued)

Part of Plant	Compounds	Biological activity	References
Wood	Artocarmitin A ( <b>28</b> )	-	Nguyen <i>et al.</i> , 2012
	Artocarmitin B ( <b>29</b> )	Tyrosinase inhibition, $IC_{50} = 66.2 \pm 0.6 \mu M$	
	Artocarmitin C ( <b>30</b> )	Tyrosinase inhibition, $IC_{50} = 20.6 \pm 0.2 \mu M$	
	3'-[ $\gamma$ -Hydroxymethyl-(Z)- $\gamma$ -methylallyl]-4,2',4'-trihydroxychalcone ( <b>31</b> )	-	
	Gemichalcone B ( <b>32</b> )	Tyrosinase inhibition, $IC_{50} = 55.3 \pm 0.5 \mu M$	
	Gemichalcone A ( <b>33</b> )	Tyrosinase inhibition, $IC_{50} = 73.6 \pm 0.7 \mu M$	
	Isogemichalcone B ( <b>34</b> )	Tyrosinase inhibition, $IC_{50} = 82.2 \pm 0.8 \mu M$	
	Morachalcone A ( <b>35</b> )	Tyrosinase inhibition, $IC_{50} = 0.013 \pm 0.002 \mu M$	
	<i>p</i> -Hydroxybenzoic acid ( <b>36</b> )	Tyrosinase inhibition, $IC_{50} = 9.3 \pm 0.1 \mu M$	
	$\beta$ -Resorcylic acid ( <b>37</b> )	-	
	Vanillic acid ( <b>38</b> )	-	
	Goldfussinol ( <b>39</b> )	-	
	<i>p</i> -Coumaric acid ( <b>40</b> )	Tyrosinase inhibition, $IC_{50} = 2.3 \pm 0.1 \mu M$	
	2,3-Dihydro-5,7-dihydroxy-2-(2-hydroxy-4-methoxyphenyl)-4 <i>H</i> -1-benzopyran-4-one ( <b>4</b> )	-	Zheng <i>et al.</i> , 2014
	Artocarpanone ( <b>5</b> )	-	



**Table 1.1** (Continued)

Part of Plant	Compounds	Biological activity	References
Wood	Morin ( <b>10</b> )	-	Zheng <i>et al.</i> , 2014
	Artocarmin A ( <b>11</b> )	-	
	Albanin A ( <b>12</b> )	-	
	Steppogenin ( <b>14</b> )	-	
	Artocarpin ( <b>16</b> )	Cytotoxicity (IC <sub>50</sub> , µM) MCF-7: 11.3 ± 0.51 SMMC-7721: 15.85 ± 0.79 NCI-H460: 11.01 ± 0.81	
	Cudraflavone C ( <b>17</b> )	Cytotoxicity (IC <sub>50</sub> , µM) MCF-7: 10.81 ± 0.67 SMMC-7721: 12.06 ± 0.75 NCI-H460: 5.19 ± 0.14	
	Brosimone I ( <b>22</b> )	-	
	Gemichalcone A ( <b>33</b> )	-	
	Artoheterophyllin E ( <b>41</b> )	-	
	Artoheterophyllin F ( <b>42</b> )	-	
	Artoheterophyllin G ( <b>43</b> )	-	
	Artoheterophyllin H ( <b>44</b> )	-	

**Table 1.1** (Continued)

Part of Plant	Compounds	Biological activity	References
Wood	Artoheterophyllin I ( <b>45</b> )	Cytotoxicity (IC <sub>50</sub> , $\mu$ M) MCF-7: $26.14 \pm 0.95$ SMMC-7721: $25.28 \pm 1.21$ NCI-H460: $15.82 \pm 0.61$	Zheng <i>et al.</i> , 2014
	Artoheterophyllin J ( <b>46</b> )	-	
	2-Geranyl-2',3,4',5-tetrahydroxy- <i>cis</i> -stilbene ( <b>47</b> )	Cytotoxicity, NCI-H460, IC <sub>50</sub> = $16.66 \pm 0.87 \mu$ M	
	5-Methoxymoricin M ( <b>48</b> )	-	
	6-[(1 <i>S</i> ,2 <i>S</i> )-1,2-Dihydroxy-3-methylbutyl]-2-(2,4-dihydroxyphenyl)-5-hydroxy-7-methoxy-3-(3-methyl-2-buten-1-yl)-4 <i>H</i> -1-benzopyran-4-one ( <b>49</b> )	-	
	Cycloartocarpin ( <b>50</b> )	Cytotoxicity (IC <sub>50</sub> , $\mu$ M) MCF-7: $20.68 \pm 1.01$ SMMC-7721: $23.70 \pm 0.86$ NCI-H460: $20.72 \pm 0.63$	
	Cycloartocarpesin ( <b>51</b> )	-	
	Artocarpesin ( <b>52</b> )	-	
	Norartocarpetin ( <b>53</b> )	-	
	Isoartocarpesin ( <b>54</b> )	-	

**Table 1.1** (Continued)

Part of Plant	Compounds	Biological activity	References
Wood	Cyanomaclurin ( <b>55</b> )	-	Zheng <i>et al.</i> , 2014
	Apigenin ( <b>56</b> )	-	
	Artocarpetin ( <b>57</b> )	-	
	Artocarpfuranol ( <b>58</b> )	-	
	Moracin M ( <b>59</b> )	-	
	Artocarbene ( <b>60</b> )	-	
	Hypargyflavone A ( <b>61</b> )	-	
	2,4-Dihydroxybenzoic acid methyl ester ( <b>62</b> )	-	
	2,4-Dihydroxybenzaldehyde ( <b>63</b> )	-	Nguyen <i>et al.</i> , 2016
	Artocarpanone ( <b>5</b> )	Tyrosinase inhibition, IC <sub>50</sub> = 2.0 ± 0.1 µM	
	Steppogenin ( <b>14</b> )	Tyrosinase inhibition, IC <sub>50</sub> = 7.5 ± 0.5 µM	
	Norartocarpetin ( <b>53</b> )	-	
	Artocaepin E ( <b>64</b> )	Tyrosinase inhibition, IC <sub>50</sub> = 6.7 ± 0.8 µM	
	Artocaepin F ( <b>65</b> )	-	
	Liquiritigenin ( <b>66</b> )	Tyrosinase inhibition, IC <sub>50</sub> = 22.0 ± 2.5 µM	
	Dihydromorin ( <b>67</b> )	-	

**Table 1.1** (Continued)

Part of Plant	Compounds	Biological activity	References
Heartwood	Artocarpanone ( <b>5</b> )	Antibacterial (MIC, $\mu$ M) <i>Streptococcus mutans</i> : 25.8 <i>Streptococcus pyogenes</i> : 25.8 <i>Bacillus subtilis</i> : 25.8 <i>Staphylococcus aureus</i> : 413.5 <i>Staphylococcus epidermidis</i> : 413.5 <i>Staphylococcus epidermidis</i> : 413.5 <i>Escherichia coli</i> : 12.9	Septama <i>et al.</i> , 2015
	Artocarpin ( <b>16</b> )	Antibacterial (MIC, $\mu$ M) <i>Streptococcus mutans</i> : 4.4 <i>Streptococcus pyogenes</i> : 4.4 <i>Bacillus subtilis</i> : 17.8 <i>Staphylococcus aureus</i> : 8.9 <i>Staphylococcus epidermidis</i> : 4.4 <i>Pseudomonas aeruginosa</i> : 286.4 <i>Escherichia coli</i> : 71.6	

**Table 1.1** (Continued)

Part of Plant	Compounds	Biological activity	References
Heartwood	Cycloartocarpin ( <b>50</b> )	Antibacterial (MIC, $\mu\text{M}$ ) <i>Streptococcus mutans</i> : 35.9 <i>Streptococcus pyogenes</i> : 71.8 <i>Bacillus subtilis</i> : 35.9 <i>Staphylococcus aureus</i> : 71.8 <i>Staphylococcus epidermidis</i> : 35.9 <i>Escherichia coli</i> : 143.6	Septama <i>et al.</i> , 2015
	Cyanomaclurin ( <b>55</b> )	Antibacterial (MIC, $\mu\text{M}$ ) <i>Streptococcus mutans</i> : 6.8 <i>Streptococcus pyogenes</i> : 54.4 <i>Bacillus subtilis</i> : 217.6 <i>Staphylococcus aureus</i> : 217.6 <i>Staphylococcus epidermidis</i> : 54.4 <i>Escherichia coli</i> : 27.2	
	Artocarpin ( <b>16</b> )	Tyrosinase inhibition, $\text{IC}_{50} = 0.90 \pm 1.63 \mu\text{M}$	
	Cudraflavone B ( <b>21</b> )	Tyrosinase inhibition, $\text{IC}_{50} = 1.03 \pm 0.65 \mu\text{M}$	

**Table 1.1** (Continued)

Part of Plant	Compounds	Biological activity	References
Heartwood	Brosimone I ( <b>22</b> )	Tyrosinase inhibition, IC <sub>50</sub> = 1.78 ± 0.94 µM	Hanh <i>et al.</i> , 2015
	Morachalcone A ( <b>35</b> )	Tyrosinase inhibition, IC <sub>50</sub> = 0.18 ± 0.1 µM	
Twigs	Artocarpin ( <b>16</b> )	Cytotoxicity (IC <sub>50</sub> , µM) PC-3: 7.9 ± 0.6 NCI-H460: 8.3 ± 0.4	Di <i>et al.</i> , 2013
	Cudraflavone C ( <b>17</b> )	Cytotoxicity (IC <sub>50</sub> , µM) PC-3: 16.0 ± 0.1 NCI-H460: 19.8 ± 1.9	
	Norartocarpin ( <b>20</b> )	Cytotoxicity (IC <sub>50</sub> , µM) PC-3: 22.3 ± 0.9 NCI-H460: 20.7 ± 0.7	
	Artocarmitin A ( <b>28</b> )	Cytotoxicity (IC <sub>50</sub> , µM) PC-3: 41.6 ± 0.5 NCI-H460: 37.5 ± 4.4	
	Artocarmitin B ( <b>29</b> )	Cytotoxicity (IC <sub>50</sub> , µM) PC-3: 11.2 ± 0.7 NCI-H460: 16.2 ± 0.5	
	3'-[γ-Hydroxymethyl-(Z)-γ-methylallyl]-4,2',4'-trihydroxychalcone ( <b>31</b> )	Cytotoxicity (IC <sub>50</sub> , µM) PC-3: 26.2 ± 2.8 NCI-H460: 22.9 ± 1.0	

**Table 1.1** (Continued)

Part of Plant	Compounds	Biological activity	References
Twigs	Gemichalcone B ( <b>32</b> )	Cytotoxicity (IC <sub>50</sub> , $\mu$ M) PC-3: $9.8 \pm 0.2$ NCI-H460: $13.1 \pm 1.6$	Di <i>et al.</i> , 2013
	Gemichalcone A ( <b>33</b> )	Cytotoxicity (IC <sub>50</sub> , $\mu$ M) PC-3: $8.2 \pm 0.3$ NCI-H460: $9.5 \pm 0.4$	
	Isogemichalcone B ( <b>34</b> )	Cytotoxicity (IC <sub>50</sub> , $\mu$ M) PC-3: $14.9 \pm 0.5$ NCI-H460: $17.6 \pm 1.1$	
	Morachalcone A ( <b>35</b> )	Cytotoxicity (IC <sub>50</sub> , $\mu$ M) PC-3: $15.6 \pm 0.0$ NCI-H460: $16.1 \pm 1.6$	
	Norartocarpetin ( <b>53</b> )	Cytotoxicity (IC <sub>50</sub> , $\mu$ M) PC-3: $47.7 \pm 0.1$ NCI-H460: $18.6 \pm 3.0$	
	Artocarpusin C ( <b>68</b> )	Cytotoxicity, NCI-H460, IC <sub>50</sub> = $65.9 \pm 7.1 \mu$ M	
	Artocarstilene A ( <b>69</b> )	-	
	2,4,2',4'-Tetrahydroxy-3-(3-methyl-2-butenyl)-chalcone ( <b>70</b> )	Cytotoxicity (IC <sub>50</sub> , $\mu$ M) PC-3: $22.2 \pm 0.5$ NCI-H460: $29.9 \pm 0.5$	

**Table 1.1** (Continued)

Part of Plant	Compounds	Biological activity	References
Twigs	6-(3-Methylbut-2-enyl)-apigenin ( <b>71</b> )	Cytotoxicity (IC <sub>50</sub> , μM) PC-3: 43.8 ± 1.9 NCI-H460: 40.6 ± 1.7	Di <i>et al.</i> , 2013
	Arthocarpesin ( <b>72</b> )	Cytotoxicity (IC <sub>50</sub> , μM) PC-3: 16.3 ± 0.1 NCI-H460: 11.6 ± 0.3	
	5,7,4'-Trihydroxyflavone ( <b>73</b> )	Cytotoxicity (IC <sub>50</sub> , μM) PC-3: 75.4 ± 1.5 NCI-H460: 59.0 ± 1.1	
Leaves	Albanin A ( <b>12</b> )	-	Wang <i>et al.</i> , 2017
	Euchrenone a7 ( <b>13</b> )	Cytotoxicity (IC <sub>50</sub> , μM) PC-3: 17.0 ± 2.1 NCI-H460: 47.4 ± 2.5 A549: 35.2 ± 2.1	
	Norartocarpanone ( <b>15</b> )	-	
	Artocarpin ( <b>16</b> )	Cytotoxicity (IC <sub>50</sub> , μM) PC-3: 5.1 ± 0.3 NCI-H460: 10.2 ± 1.3 A549: 8.1 ± 0.7	
	Cudraflavone C ( <b>17</b> )	Cytotoxicity (IC <sub>50</sub> , μM) PC-3: 21.3 ± 1.1 NCI-H460: 15.4 ± 0.9 A549: 11.3 ± 1.6	



**Table 1.1** (Continued)

Part of Plant	Compounds	Biological activity	References
Leaves	Cudraflavone B ( <b>21</b> )	-	Wang <i>et al.</i> , 2017
	Brosimone I ( <b>22</b> )	-	
	Artocarmitin B ( <b>29</b> )	Cytotoxicity (IC <sub>50</sub> , μM) PC-3: 9.7 ± 0.6 NCI-H460: 11.3 ± 1.1 A549: 7.3 ± 1.0	
	Moracin M ( <b>59</b> )	-	
	Artocarbene ( <b>60</b> )	-	
	Artocarstilbene B ( <b>74</b> )	-	
	( <i>E</i> )-3,5-Dihydroxy-4-(3-methylbut-1-enyl)benzaldehyde ( <b>75</b> )	-	
	Moracin C ( <b>76</b> )	-	
	Albafuran B ( <b>77</b> )	Cytotoxicity (IC <sub>50</sub> , μM) PC-3: 43.4 ± 1.7 NCI-H460: 41.6 ± 2.3 A549: 46.5 ± 2.7	
	Artoindonesianin B-1 ( <b>78</b> )	Cytotoxicity (IC <sub>50</sub> , μM) PC-3: 13.9 ± 0.9 NCI-H460: 18.1 ± 1.9 A549: 16.2 ± 1.4	
	Demethylmoracin I ( <b>79</b> )	-	

**Table 1.1** (Continued)

Part of Plant	Compounds	Biological activity	References
Leaves	Moracin D ( <b>80</b> )	Cytotoxicity (IC <sub>50</sub> , $\mu$ M) PC-3: $14.4 \pm 2.4$ NCI-H460: $30.8 \pm 2.1$ A549: $23.7 \pm 1.9$	Wang <i>et al.</i> , 2017
	2,6,2',6'-Tetramethoxy-4,4'-bis(2,3-epoxy-1-hydroxy-propyl)biphenyl ( <b>81</b> )	-	
	Griffithine A ( <b>82</b> )	-	
	5 $\alpha$ ,6 $\alpha$ -Epoxy-24(R)-methylcholesta-7,22-dien-3 $\beta$ -ol ( <b>83</b> )	-	
Fruits	Artocarpesin ( <b>52</b> )	Antimicrobial (MIC, mg/mL) Methicillin-susceptible <i>Staphylococcus aureus</i> : 0.008 Methicillin-resistant <i>Staphylococcus aureus</i> : 0.016	Manuel <i>et al.</i> , 2012

ลิขสิทธิ์มหาวิทยาลัยเชียงใหม่  
Copyright© by Chiang Mai University  
All rights reserved

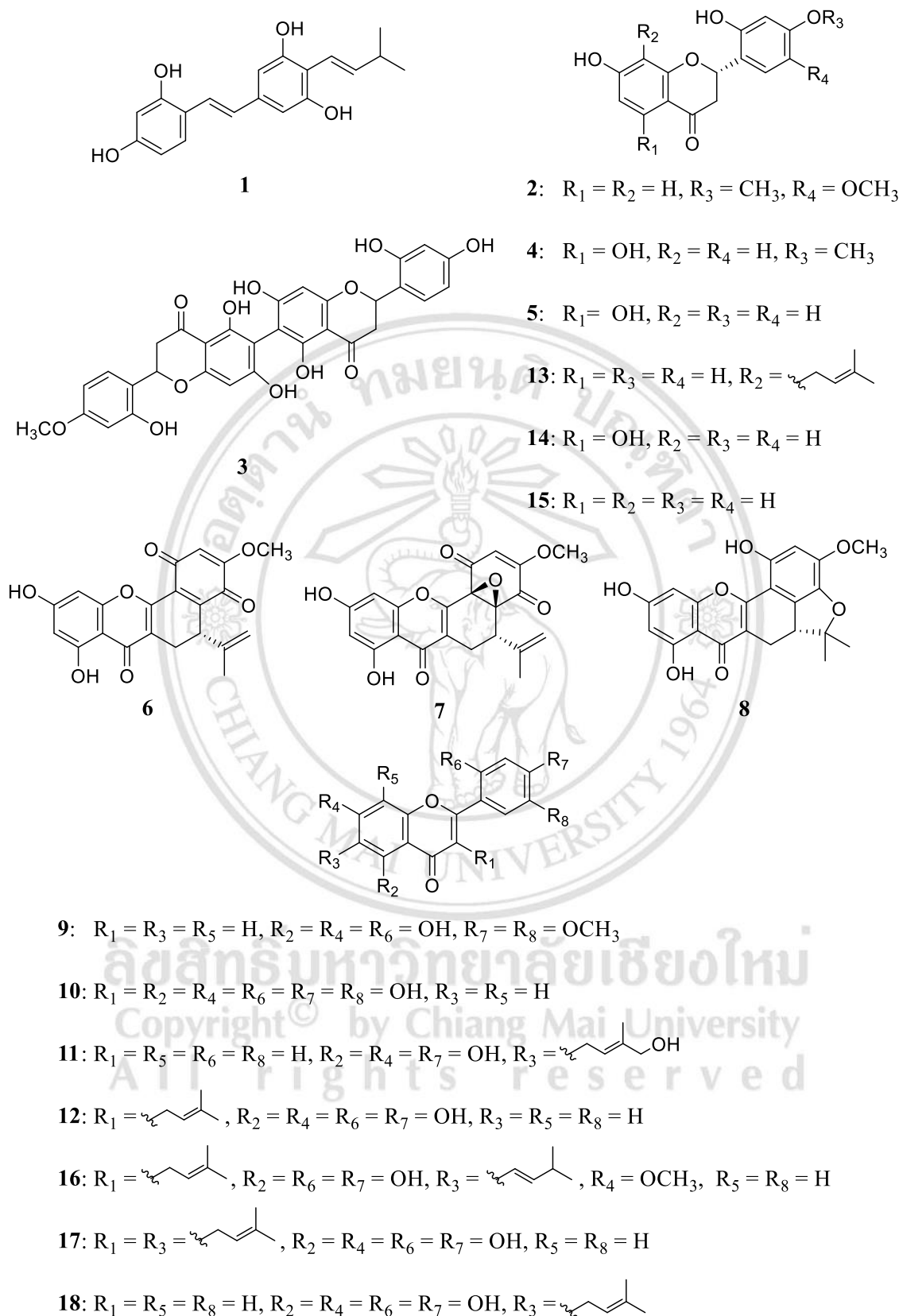
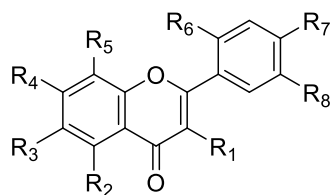


**Figure 1.2** The structures of isolated compounds from *A. heterophyllus*



19: R<sub>1</sub> = R<sub>5</sub> = , R<sub>2</sub> = R<sub>4</sub> = R<sub>6</sub> = R<sub>7</sub> = OH, R<sub>3</sub> = R<sub>8</sub> = H

20: R<sub>1</sub> = , R<sub>2</sub> = R<sub>4</sub> = R<sub>6</sub> = R<sub>7</sub> = OH, R<sub>3</sub> = , R<sub>5</sub> = R<sub>8</sub> = H

23: R<sub>1</sub> = R<sub>2</sub> = R<sub>3</sub> = R<sub>4</sub> = R<sub>5</sub> = R<sub>8</sub> = H, R<sub>6</sub> = R<sub>7</sub> = OH

24: R<sub>1</sub> = , R<sub>2</sub> = R<sub>4</sub> = R<sub>7</sub> = R<sub>8</sub> = OH, R<sub>3</sub> = R<sub>5</sub> = R<sub>6</sub> = H

27: R<sub>1</sub> = R<sub>5</sub> = R<sub>8</sub> = H, R<sub>2</sub> = R<sub>4</sub> = R<sub>6</sub> = R<sub>7</sub> = OH, R<sub>3</sub> =

43: R<sub>1</sub> = , R<sub>2</sub> = R<sub>4</sub> = R<sub>6</sub> = R<sub>7</sub> = OH, R<sub>3</sub> = R<sub>5</sub> = R<sub>8</sub> = H,

44: R<sub>1</sub> = , R<sub>2</sub> = R<sub>4</sub> = OCH<sub>3</sub>, R<sub>3</sub> = , R<sub>5</sub> = R<sub>6</sub> = R<sub>8</sub> = H, R<sub>7</sub> = OH

45: R<sub>1</sub> = , R<sub>2</sub> = R<sub>6</sub> = R<sub>7</sub> = OH, R<sub>3</sub> = , R<sub>4</sub> = OCH<sub>3</sub>, R<sub>5</sub> = R<sub>8</sub> = H

49: R<sub>1</sub> = , R<sub>2</sub> = R<sub>6</sub> = R<sub>7</sub> = OH, R<sub>3</sub> = , R<sub>4</sub> = OCH<sub>3</sub>, R<sub>5</sub> = R<sub>8</sub> = H

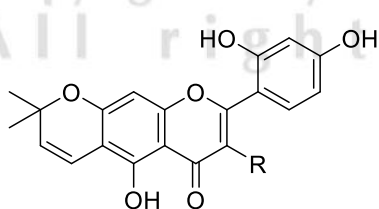
52: R<sub>1</sub> = R<sub>5</sub> = R<sub>8</sub> = H, R<sub>2</sub> = R<sub>4</sub> = R<sub>6</sub> = R<sub>7</sub> = OH, R<sub>3</sub> =

53: R<sub>1</sub> = R<sub>3</sub> = R<sub>5</sub> = R<sub>8</sub> = H, R<sub>2</sub> = R<sub>4</sub> = R<sub>6</sub> = R<sub>7</sub> = OH

54: R<sub>1</sub> = R<sub>5</sub> = R<sub>8</sub> = H, R<sub>2</sub> = R<sub>4</sub> = R<sub>6</sub> = R<sub>7</sub> = OH, R<sub>3</sub> =

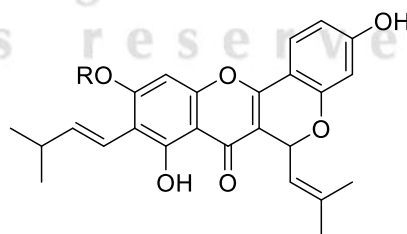
56: R<sub>1</sub> = R<sub>3</sub> = R<sub>5</sub> = R<sub>6</sub> = R<sub>8</sub> = H, R<sub>2</sub> = R<sub>4</sub> = R<sub>7</sub> = OH

57: R<sub>1</sub> = R<sub>3</sub> = R<sub>5</sub> = R<sub>8</sub> = H, R<sub>2</sub> = R<sub>6</sub> = R<sub>7</sub> = OH, R<sub>4</sub> = OCH<sub>3</sub>



21: R =

51: R = H



22: R = H

50: R = CH<sub>3</sub>

Figure 1.2 (continued)

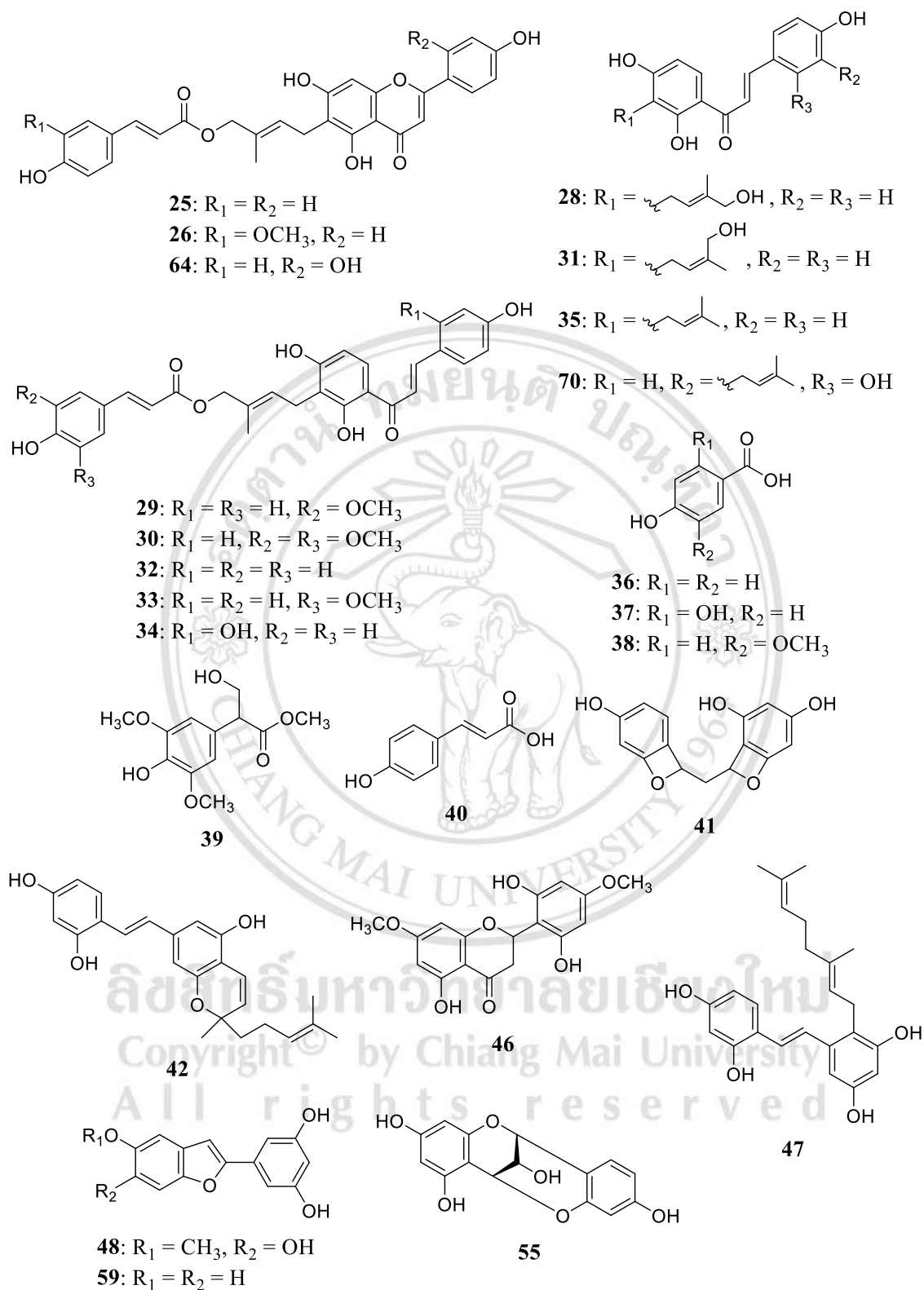


**Figure 1.2 (continued)**

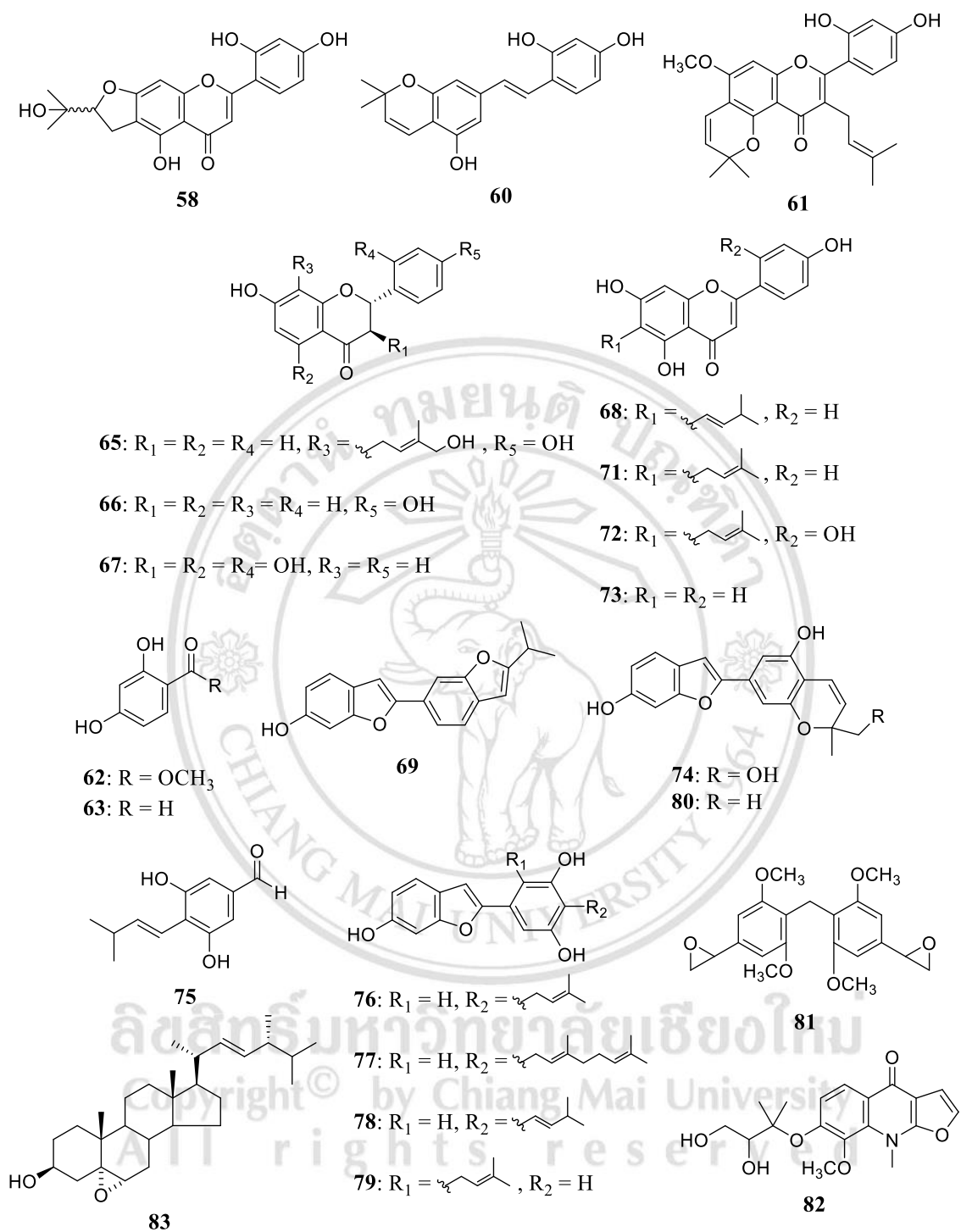


**Figure 1.2 (continued)**

### 1.3 *Artocarpus lakoocha*

*Artocarpus lakoocha* or monkey jack is belonged to the family Moraceae. Thai common name is Ma-Haad, Haad and Ka-Noon-Pah. It is distributed in Asia such as Thailand, Myanmar, Vietnam and Indonesia (Palanuvej *et al.*, 2007). It is around 15 meters in height. The leaves are green oblong around 10-25 centimeters. It has orange yellow male and green female flowers in the same tree. The young fruit is rounded green and ripen fruit is yellow and 250-300 grams weight. The seed has sticky latex (Bishnoi *et al.*, 2017). The parts of monkey jack tree are shown in **Figure 1.3**. The pulps of fruit can eat as fruit, pickle and curry. The durable heartwood and wood are used for furniture, house and construction especially railroad. Moreover, it can be used as folk traditional medicine. The heartwood is used for whitening lotion, (Hossain *et al.*, 2016) and are boiled and this water or Puak-Haad is used as an anthelmintic drug or removing tapeworm in the body (Puntumchai *et al.*, 2004). The many parts of monkey jack tree can be used to treat for malaria fever, diarrhea and inflammation (Namdaung *et al.*, 2018).

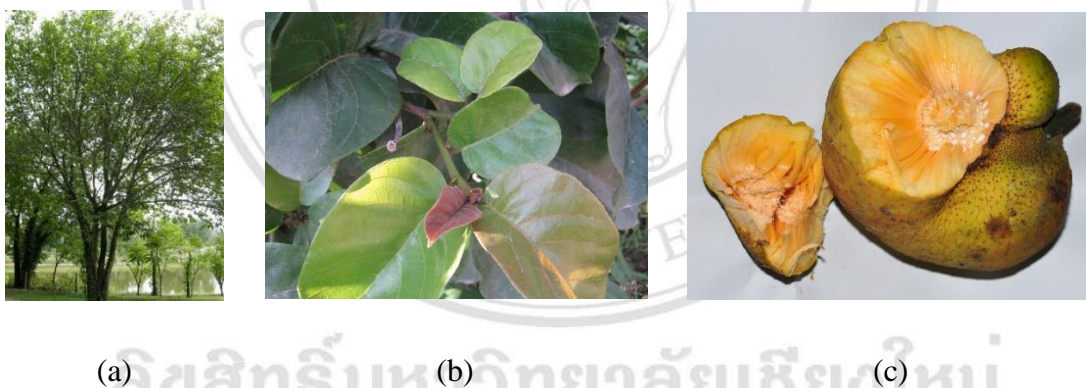


**Figure 1.3** The parts of *A. lakoocha* (a) tree, (b) young growth and (c) fruit  
(Artocarpus lacucha, 2019, <http://tropical.theferns.info/viewtropical.php?id=Artocarpus+lacucha> accessed on 15 February, 2019)

There are many publications to study the chemical constituents from the many parts of *A. lakoocha*. On the Scifinder Scholar Database, the isolated compounds on November 2010 - October 2017 are summarized in the **Table 1.2**. The structures are shown in **Figure 1.4**.

**Table 1.2** Isolated compounds with biological activities from *A. lakoocha*

Part of Plant	Compounds	Biological activity	References
Root barks	Cudraflavone C ( <b>17</b> )	Antiviral (IC <sub>50</sub> , $\mu$ M) HSV-1: $237 \pm 5.6$ HSV-2: $237 \pm 7.5$	Sritularak <i>et al.</i> , 2013
	5,7,2',4'-tetrahydroxy-6-geranyl-3-prenyl-flavone ( <b>84</b> )	Antiviral (IC <sub>50</sub> , $\mu$ M) HSV-1: $25.5 \pm 4.2$ HSV-2: $25.5 \pm 5.7$	
	(+)-afzelechin-3-O- $\alpha$ -L-rhamnose ( <b>85</b> )	-	
	(+)-catechin ( <b>86</b> )	-	Namdaung <i>et al.</i> , 2018
	Albafuran B ( <b>77</b> )	-	
	(+)-catechin ( <b>86</b> )	-	
	Lakoochin A ( <b>87</b> )	- Acetylcholinesterase inhibition, IC <sub>50</sub> = $27.42 \pm 0.42 \mu$ M - Butyrylcholinesterase inhibition, IC <sub>50</sub> = $13.88 \pm 0.03 \mu$ M	
	Lakoochin B ( <b>88</b> )	- Acetylcholinesterase inhibition, IC <sub>50</sub> = $1.08 \pm 0.01 \mu$ M - Butyrylcholinesterase inhibition, IC <sub>50</sub> = $0.10 \pm 0.0001 \mu$ M	



**Table 1.2** (Continued)

Part of Plant	Compounds	Biological activity	References
Root barks	Lakoochin C ( <b>89</b> )	- Acetylcholinesterase inhibition, IC <sub>50</sub> = 61.86 ± 0.19 μM - Butyrylcholinesterase inhibition, IC <sub>50</sub> = 47.21 ± 0.007 μM	Namdaung <i>et al.</i> , 2018
	Lakoochin D ( <b>90</b> )	-	
	Artolakoochol ( <b>91</b> )	- Acetylcholinesterase inhibition, IC <sub>50</sub> = 0.87 ± 0.23 μM - Butyrylcholinesterase inhibition, IC <sub>50</sub> = 14.93 ± 0.0001 μM	
	4-hydroxy artolakoochol ( <b>92</b> )	- Acetylcholinesterase inhibition, IC <sub>50</sub> = 1.10 ± 0.005 μM - Butyrylcholinesterase inhibition, IC <sub>50</sub> = 8.86 ± 0.04 μM	
	Cycloartolakoochol ( <b>93</b> )	Butyrylcholinesterase inhibition, IC <sub>50</sub> = 1.56 ± 0.001 μM	
	Oxyresveratrol ( <b>94</b> )	Butyrylcholinesterase inhibition, IC <sub>50</sub> = 2.95 ± 0.01 μM	

**Table 1.2** (Continued)

Part of Plant	Compounds	Biological activity	References
Heartwood	Oxyresveratrol ( <b>94</b> )	- Antiglycation, IC <sub>50</sub> = 2.0 µg/mL - DPPH· radical scavenging, IC <sub>50</sub> = 0.1 mg/mL - TBARS radical scavenging, IC <sub>50</sub> = 0.43 mg/mL	Povichit <i>et al.</i> , 2010
Seeds	Albanin A ( <b>12</b> )	-	Maneechai <i>et al.</i> , 2012
	Cudraflavone C ( <b>17</b> )	-	
	Norartocarpin ( <b>20</b> )	-	
	Cudraflavone B ( <b>21</b> )	-	
	Isoartocarpesin ( <b>54</b> )	-	
	(+)-catechin ( <b>86</b> )	-	
	2'-O-methylalbanin A ( <b>95</b> )	-	
	Cycloisoartocarpesin ( <b>96</b> )	-	
	Artolacuchin ( <b>97</b> )	- DPPH· radical scavenging, IC <sub>50</sub> = 37.5 µM - Tyrosinase inhibition, IC <sub>50</sub> = 12.8 µM	
	Isochlorophorin ( <b>98</b> )	- DPPH· radical scavenging, IC <sub>50</sub> = 34.3 µM - Tyrosinase inhibition, IC <sub>50</sub> = 66.0 µM	

**Table 1.2** (Continued)

Part of Plant	Compounds	Biological activity	References
Seeds	Chlorophorin ( <b>99</b> )	- DPPH <sup>•</sup> radical scavenging, IC <sub>50</sub> = 38.6 μM - Tyrosinase inhibition, IC <sub>50</sub> = 7.9 μM	Maneechai <i>et al.</i> , 2012
	Artotonkin ( <b>100</b> )	- DPPH <sup>•</sup> radical scavenging, IC <sub>50</sub> = 12.5 μM - Tyrosinase inhibition, IC <sub>50</sub> = 46.2 μM	
	Aesculin ( <b>101</b> )	-	

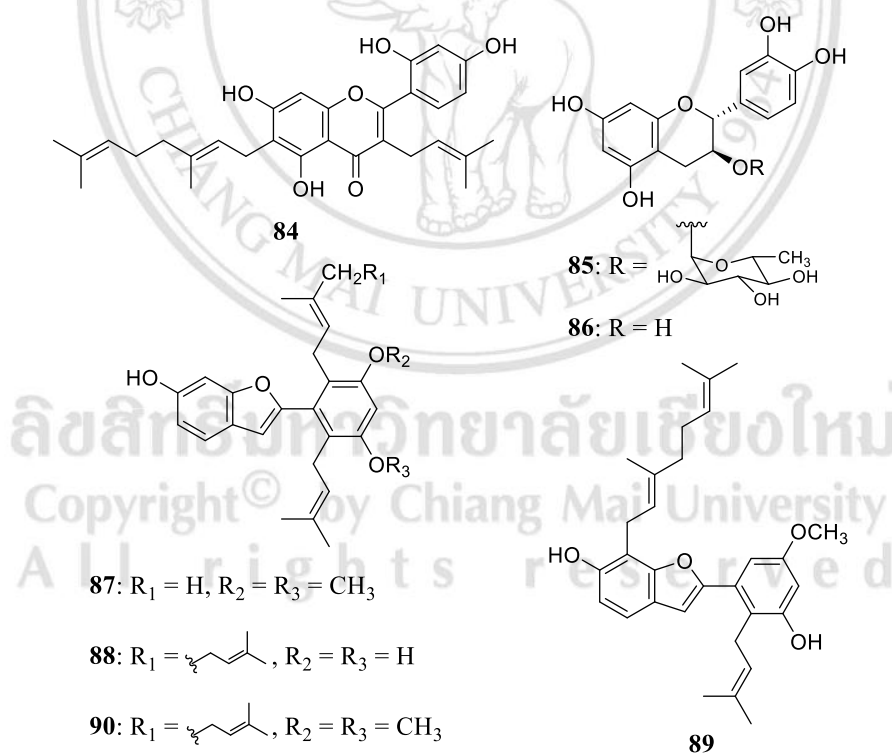


**Figure 1.4** The structures of isolated compounds from *A. lakoocha*

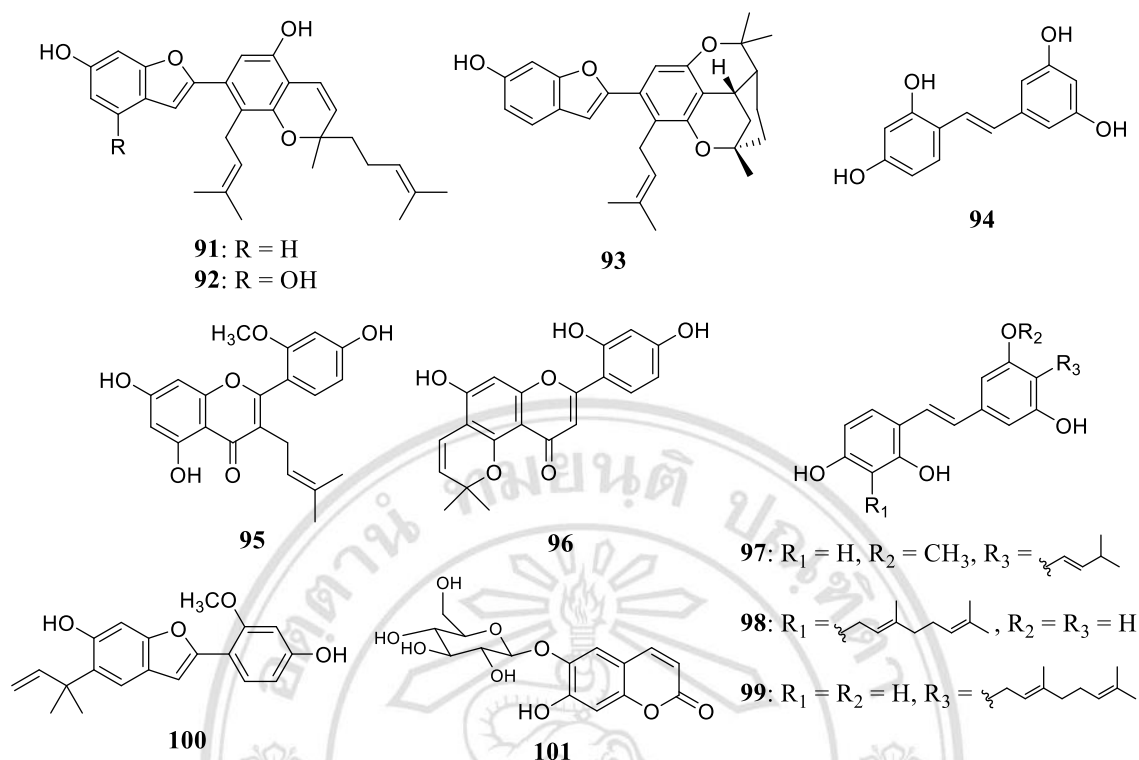


**Figure 1.4** (continued)

According to the **Table 1.1** and **1.2**, there are a few reports on the phytochemical investigation and biologically active compounds of the twigs of *A. heterophyllus* and no report about the biological activity of the twigs and barks of *A. lakoocha*. In addition, the extracts of the twigs of these plants exhibited antibacterial, antimalarial and cytotoxic activities as shown in **Table 1.3**. Interestingly, the extracts of *A. heterophyllus* and *A. lakoocha* were selectivity active against KB and MCF-7 cell lines, respectively. Consequently, the chemical constituents from the twigs of these plants are of interest. The investigation may lead to the finding of the new natural products with potential activities.

**Table 1.3** Biological activities of the extracts from the twigs of *A. heterophyllus* and *A. lakoocha*

Sample	Antibacterial (MIC, µg/mL)		Antimalarial (IC <sub>50</sub> , µg/mL)	Cytotoxicity (IC <sub>50</sub> , µg/mL)			
	SA	MRSA	<i>M. tuberculosis</i>	KB	MCF-7	NCI-H187	Vero
AHT	64	128	21.3	8.0	/	19.2	48.6
ALT	64	128	11.9	/	20.0	1.9	29.5
Doxorubicin <sup>a</sup>	-	-	-	0.9	13.2	0.2	-
Ellipticine <sup>a</sup>	-	-	-	2.2	-	-	1.6
Mefloquine <sup>b</sup>	-	-	0.0034	-	-	-	-
Vancomycin <sup>c</sup>	1	1	-	-	-	-	-

AHT = the methanolic extract from the twigs of *A. heterophyllus*,

ALT = the acetone extract from the twigs of *A. lakoocha*,

SA = *Staphylococcus aureus*, MRSA = Methicillin-resistant *S. aureus*,

KB = Oral human carcinoma cells, MCF-7 = Human breast cancer cells,

NCI-H187 = Small lung cancer cells, Vero = African green monkey kidney fibroblast,

/ = inactive, - = no test performed, <sup>a</sup> = standard compounds for cytotoxic assays,

<sup>b</sup> = standard antimalarial drug, <sup>c</sup> = standard compound for antibacterial assay

## 1.4 Objectives

1.4.1 To isolate and elucidate the structures of chemical constituents from the twigs of *A. heterophyllus* and the twigs and barks of *A. lakoocha*

1.4.2 To evaluate biological activities of some isolated compounds including cytotoxic activities against KB (human oral cancer cells), NCI-H187 (human small lung cancer cells), MCF-7 (human breast cancer cells), A2780 (human ovarian cancer cells) and Vero cell lines (African green monkey kidney fibroblasts), antibacterial activities against *Staphylococcus aureus* ATCC25923 and methicillin-resistant *Staphylococcus aureus* SK1, antifungal activities against *Cryptococcus neoformans* ATCC90113,

antimalarial activity against *Plasmodium falciparum* K1 and acetylcholinesterase inhibitory activity.



ลิขสิทธิ์มหาวิทยาลัยเชียงใหม่  
Copyright© by Chiang Mai University  
All rights reserved

## CHAPTER 2

### Experimental

#### 2.1 Chemicals and general experimental procedures

Thermo Scientific (evolution 201) and Shimadzu UV-Vis spectrometers were obtained ultraviolet spectra (UV), as well as Perkin Elmer and MIDAC M-series FT-IR spectrometers measured infrared spectra (IR).  $^1\text{H}$  and  $^{13}\text{C}$ -NMR spectra were recorded by 400 MHz Bruker FTNMR Ultra Shield and 500 MHz JEOL Eclipse 500 spectrometer with the internal standard, tetramethylsilane (TMS). MicroTOF, Bruker Daltonics and Agilent 622-LC-TOF-MS mass spectrometers recorded mass spectra (MS). Optical rotations were measured on AUTOPOL I and JASCO P-2000 polarimeters. Thin-layer chromatography (TLC) and precoated thin-layer chromatography (PLC) were performed on silica gel 60 F<sub>254</sub> (Merck), diol and reversed phase thin-layer chromatography. Column chromatography (CC) was performed on silica gel (Salicycle) type 100 (70-230 mesh ASTM) and type 60 (5-40 mesh ASTM for Quick column chromatography; QCC) or on Sephadex LH-20 or on diol (230-400 mesh ASTM) on reversed phase silica gel C18. Preparative HPLC was performed using Shimadzu LC-10AT pumps coupled with a semipreparative Varian Dynamax C18 column (5  $\mu\text{m}$ , 250 x 10 mm), a Shimadzu SPD M10A diode array detector and a SCL-10A system controller. Solvents for extraction and isolation were distilled prior to use.

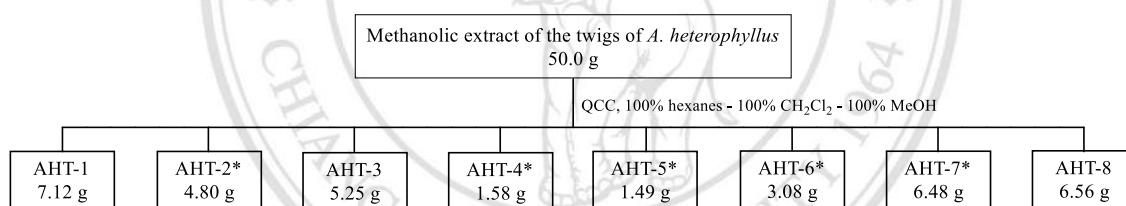
## 2.2 Twigs of *Artocarpus heterophyllus*

### 2.2.1 Plant materials and extraction

The twigs of *A. heterophyllus* were collected from Mae Rim District, Chiang Mai province, Thailand in February 2015. A voucher specimen No. QBG67505 deposited at the herbarium collection of the Queen Sirikit Botanic Garden, Mae Rim, Chiang Mai, Thailand. The air-dried twigs (4.0 kg) were extracted with 10 L of methanol for 7 days, and evaporated under reduced pressure to give a methanolic extract as a dark brown gum (50.0 g)

### 2.2.2 Purification of methanolic extract of the twigs of *A. heterophyllus*

The methanolic extract of the twigs of *A. heterophyllus* was subjected to QCC over silica gel with a gradient of 100% hexanes to 100% dichloromethane to 100% methanol to give eight fractions (AHT-1-AHT-8) as shown in **Figure 2.1**.



\*Fractions will be isolated.

**Figure 2.1** The isolation of the methanolic extract of the twigs of *A. heterophyllus*.

Fraction AHT-2 (brown gum, 4.80 g) was isolated using CC over silica gel eluting with 15% ethyl acetate in light petroleum ether to give three subfractions (AHT-21-AHT-23). Subfraction AHT-22 (brown gum, 182.9 mg) was further separated by silica gel CC using 20% ethyl acetate in light petroleum ether as a mobile phase to provide three subfractions (AHT-22A-AHT-22C). Compound **A24** (brown gum, 2.2 mg) was obtained from the second subfraction after purification by silica gel CC using 15% ethyl acetate in light petroleum ether, and followed by CC over Sephadex LH-20 with 100% methanol. Subfraction AHT-22C contained compound **A22** (brown gum, 17.9 mg). The isolation is shown in **Figure 2.2**.



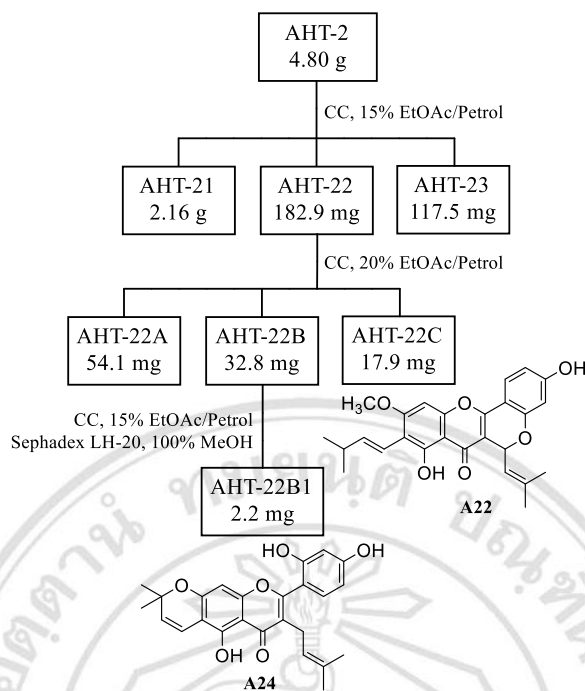


**Figure 2.2** The isolation of fraction AHT-2.

Fraction AHT-4 (brown gum, 1.58 g) was subjected to CC over silica gel using a gradient of 100% dichloromethane to 100% methanol to give five subfractions (AHT-41-AHT-45). Subfraction AHT-42 (brown gum, 701.9 mg) was separated by CC over Sephadex LH-20 eluting with 100% methanol to give four subfractions (AHT-42A-AHT-42D). Subfraction AHT-42B (brown gum, 190.5 mg) was further purified by silica gel CC with 30% ethyl acetate in light petroleum ether to afford compounds **A14** (brown gum, 1.6 mg) and **A25** (brown gum, 4.9 mg). Subfraction AHT-42C (brown gum, 43.3 mg) was separated by CC over silica gel eluting with a gradient of 100% dichloromethane to 100% methanol to provide three subfractions (AHT-42C1-AHT-42C3). Compounds **A1** (pale yellow gum, 3.0 mg) and **A21** (yellow gum, 7.7 mg) were isolated from the second subfraction after the purification with silica gel CC using 30% ethyl acetate in light petroleum ether as a mobile phase. Subfraction AHT-42D (brown gum, 35.6 mg) was further purified using the same procedure as subfraction AHT-42C to provide compounds **A2** (pale yellow gum, 7.6 mg) and **A16** (pale yellow gum, 1.3 mg). The isolation is shown in **Figure 2.3**.

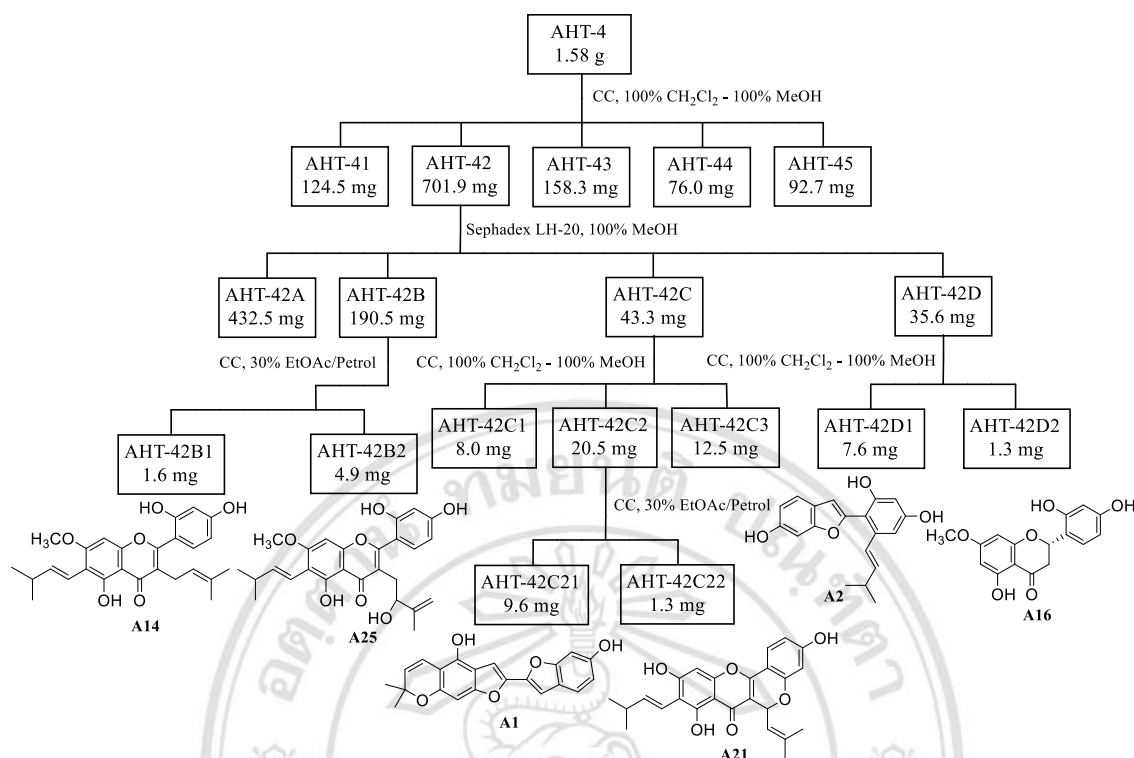


**Figure 2.3** The isolation of fraction AHT-4.

Fraction AHT-5 (brown gum, 1.49 g) was fractionated by CC over silica gel using a gradient of 100% dichloromethane to 100% methanol to give five subfractions (AHT-51-AHT-55). Subfraction AHT-52 (brown gum, 490.0 mg) was purified using same procedure as subfraction AHT-42 to give four subfractions (AHT-52A-AHT-52D). Compound **A18** (pale yellow gum, 4.2 mg) was obtained from the second subfraction. Subfraction AHT-53 (brown gum, 511.0 mg) was subjected to FCC using silica gel using 20% ethyl acetate in hexanes to give three subfractions (AHT-53A-AHT-53C). Compound **A6** (brown gum, 7.5 mg) was obtained from the third subfraction (brown gum, 16.8 mg) after purification on reverse phase silica gel CC using 75% methanol in water as a mobile phase. The isolation is shown in **Figure 2.4**.

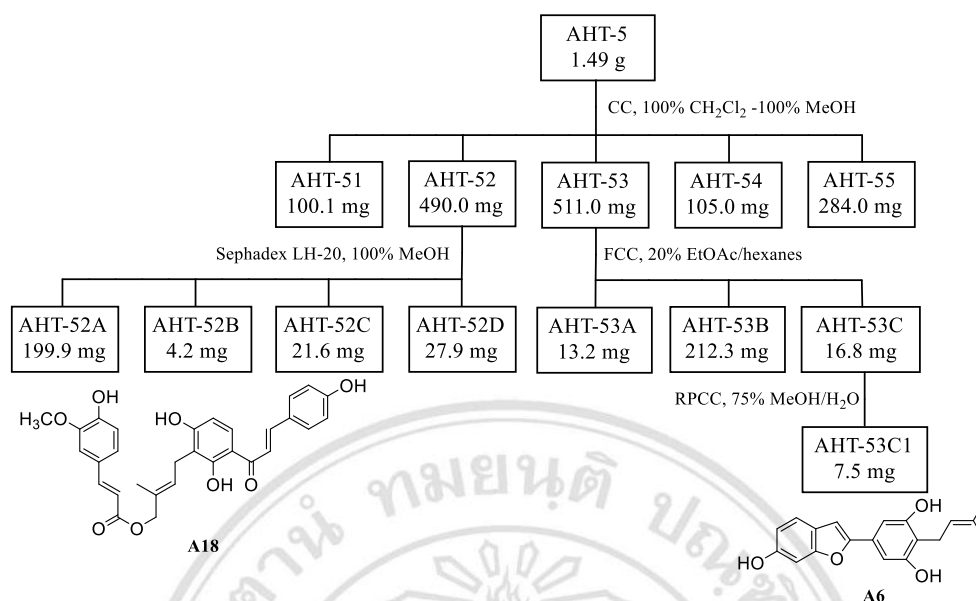


**Figure 2.4** The isolation of fraction AHT-5.

The separation of fraction AHT-6 (brown gum, 3.08 g) by QCC using a gradient of 100% hexanes to 100% dichloromethane to 100% methanol gave six subfractions (AHT-61-AHT-66). Separation of subfraction AHT-62 (brown gum, 536.9 mg) with Sephadex LH-20 CC using 100% methanol gave four subfractions (AHT-62A-AHT-62D). Compound **A23** (brown gum, 1.3 mg) was purified from the second subfraction (brown gum, 162.5 mg) with CC over silica gel using 30% ethyl acetate in hexanes as an eluent. The third subfraction (brown gum, 92.8 mg) was purified by silica gel CC with 40% ethyl acetate in hexanes followed by Sephadex LH-20 CC with 50% methanol in dichloromethane to furnish compound **A10** (pale yellow gum, 7.0 mg). Subfraction AHT-64 (brown gum, 354.1 mg) was subjected to CC over silica gel using a gradient of 100% dichloromethane to 100% methanol to afford three subfractions (AHT-64A-AHT-64C). Compound **A19** (pale yellow gum, 3.6 mg) was obtained from the second subfraction after purification by CC over silica gel with 40% ethyl acetate in hexanes. Separation of subfraction AHT-65 (brown gum, 382.0 mg) with Sephadex LH-20 CC using 100% methanol as a mobile phase gave five subfractions (AHT-65A-AHT-65E). Subfraction AHT-65B (brown gum, 162.1 mg) was further purified with silica gel CC using a gradient of 100% hexanes to 100% ethyl acetate to furnish compound **A9** (pale yellow gum, 3.9 mg). Compounds **A5** (brown gum, 3.7 mg) and **A20** (brown gum, 2.3 mg) were obtained from the subfraction AHT-65D (brown gum, 44.8 mg) after

purification using CC over silica gel with 50% ethyl acetate in hexanes. Purification of subfraction AHT-65E (brown gum, 17.6 mg) with silica gel CC using 5% methanol in dichloromethane as a mobile phase afforded compound **A17** (brown gum, 7.1 mg). The isolation is shown in **Figure 2.5** and **Figure 2.6**.

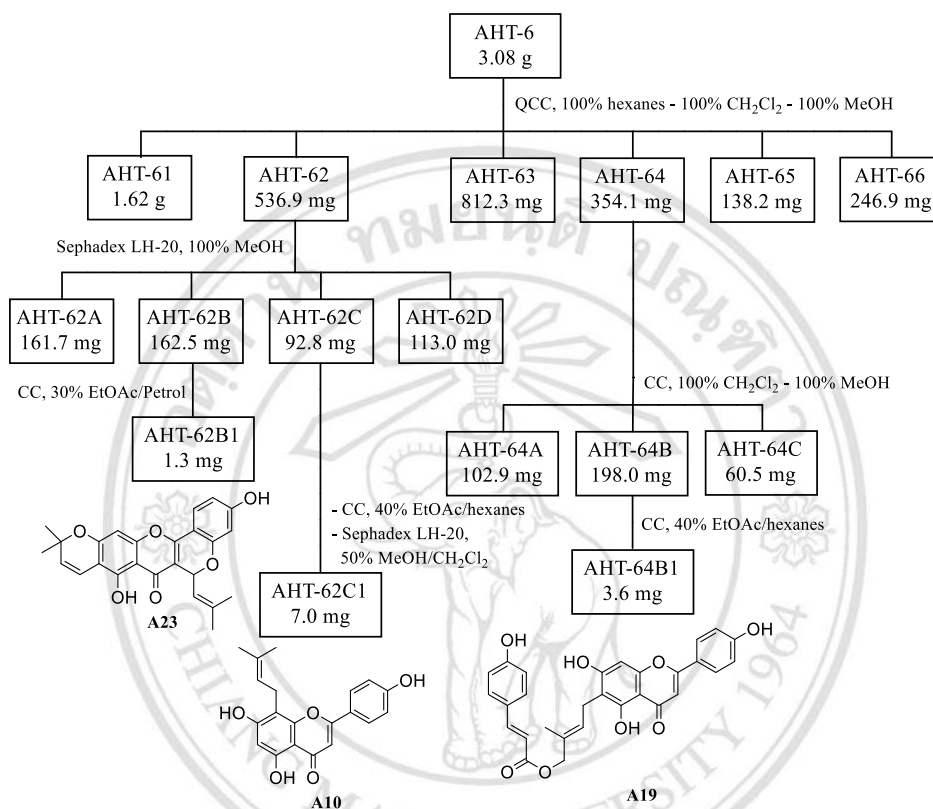


**Figure 2.5** The isolation of fraction AHT-6.

ลิขสิทธิ์มหาวิทยาลัยเชียงใหม่  
Copyright© by Chiang Mai University  
All rights reserved

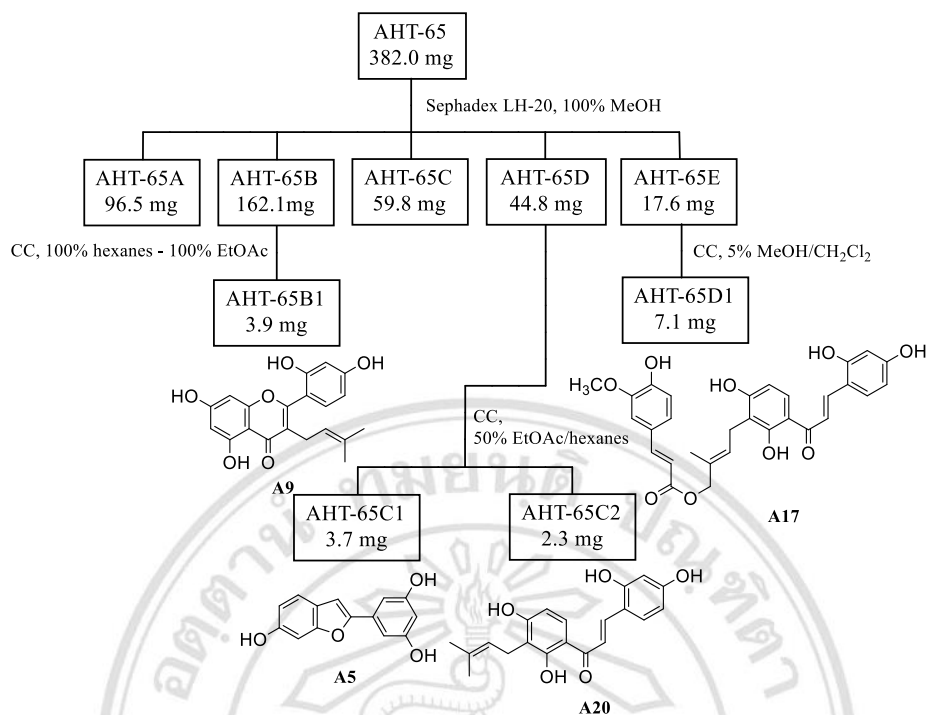


**Figure 2.6** The isolation of subfraction AHT-65.

Fraction AHT-7 (brown gum, 6.48 g) was fractionated with the same procedure as fraction AHT-6 to furnish five subfractions (AHT-71-AHT-75). The second subfraction (brown gum, 1.06 g) was separated by CC over silica gel using a gradient of 100% dichloromethane to 100% ethyl acetate to afford five subfractions (AHT-72A-AHT-72E). Purification of subfraction AHT-72B (brown gum, 116.2 mg) by CC over silica gel with 40% ethyl acetate in hexanes followed by reverse phase silica gel CC with 70% acetone in water gave compounds **A7** (brown gum, 3.3 mg), **A12** (brown gum, 2.2 mg) and **A13** (brown gum, 1.0 mg). Subfraction AHT-72C (brown gum, 238.3 mg) was further purified with silica gel CC using 20% ethyl acetate in light petroleum ether to afford compound **A11** (brown gum, 5.8 mg). Subfraction AHT-72D (brown gum, 224.0 mg) was subjected to CC silica gel using a gradient of 100% dichloromethane to 100% methanol to give four subfractions (AHT-72D1-AHT-72D4). Compound **A3** (pale yellow gum, 1.9 mg) was contained in the second subfraction. The third subfraction (brown gum, 34.5 mg) was further purified by reverse phase silica gel CC with 60% acetone in water to yield compound **A15** (brown gum, 5.7 mg). Separation of subfraction AHT-73 (brown gum, 1.01 g) by CC over silica gel with a gradient of 100% dichloromethane to 100% methanol furnished four subfractions (AHT-73A-AHT-73D). Subfraction AHT-73B

(brown gum, 82.3 mg) was purified with reverse phase silica gel using 50% acetone in water to give compounds **A4** (yellow gum, 2.2 mg) and **A8** (pale yellow gum, 1.0 mg). The isolation is shown in **Figure 2.7** and **Figure 2.8**.

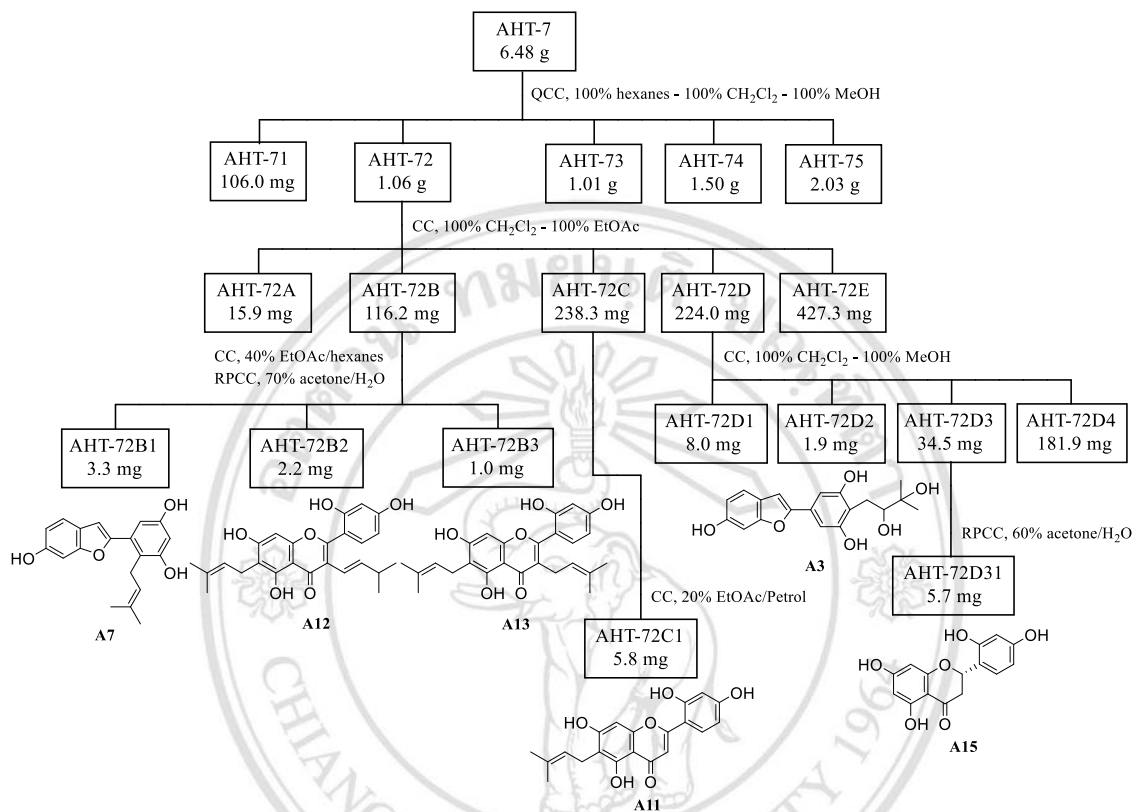


**Figure 2.7** The isolation of fraction AHT-7.

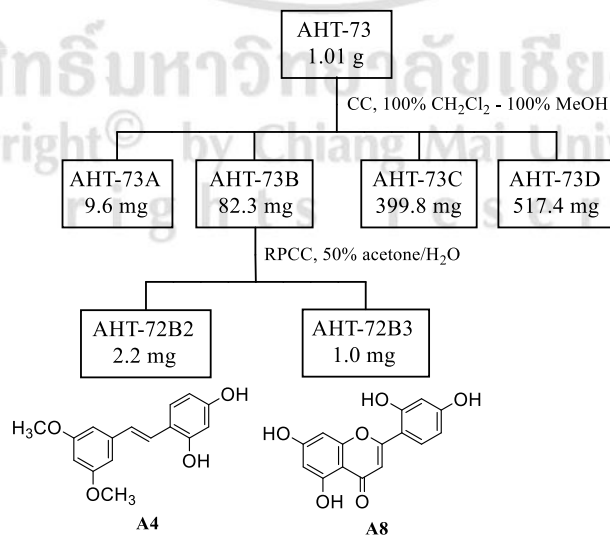


**Figure 2.8** The isolation of subfraction AHT-73.

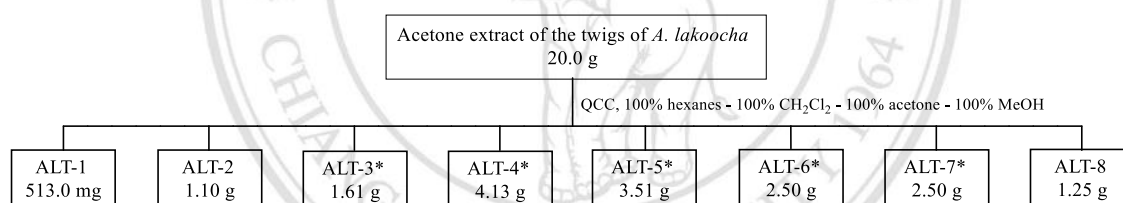
## 2.3 Twigs of *Artocarpus lakoocha*

### 2.3.1 Plant materials and extraction

The twigs of *A. lakoocha* were collected from Mae Rim district, Chiang Mai province, Thailand in January, 2016. A voucher specimen No.QBG91824 deposited at the herbarium collection of the Queen Sirikit Botanic Garden, Mae Rim, Chiang Mai, Thailand. The air-dried twigs (2.0 kg) were extracted with 10 L of acetone for 7 days two times. The extract was filtered and the acetone was then removed by under reduced pressure to give acetone extract as a dark brown gum 20.0 g.

### 2.3.2 Purification of acetone extract of the twigs of *A. lakoocha*

The extract was fractionated by QCC over silica gel with a gradient of 100% hexanes to 100% dichloromethane to 100% acetone to 100% methanol to give eight fractions (ALT1-ALT8) as shown in **Figure 2.9**.



\* Fractions will be isolated.

**Figure 2.9** The isolation of the acetone extract of the twigs of *A. lakoocha*.

Fraction ALT-3 (dark green gum, 1.61 g) was subjected to CC over silica gel eluting by the gradient of 100% hexanes to 100% dichloromethane to 100% methanol to give six subfractions (ALT-31-ALT-36). Subfraction ALT-33 (yellow green gum, 252.3 mg) was isolated by CC over silica gel eluting by 5% acetone in dichloromethane to give five subfractions (ALT-33A-ALT-33E). The second subfraction contained compound **A22** (yellow green gum, 3.5 mg). The fourth subfraction (yellow green gum, 21.3 mg) was further purified by CC over Sephadex LH-20 using 100% methanol as a mobile phase to give compound **A21** (yellow green gum, 2.3 mg). Subfraction ALT-35 (yellow green gum, 79.3 mg) was separated by the same procedure as subfraction ALT-33D to give compound **A18** (yellow green gum, 2.3 mg). The isolation is shown in **Figure 2.10**.

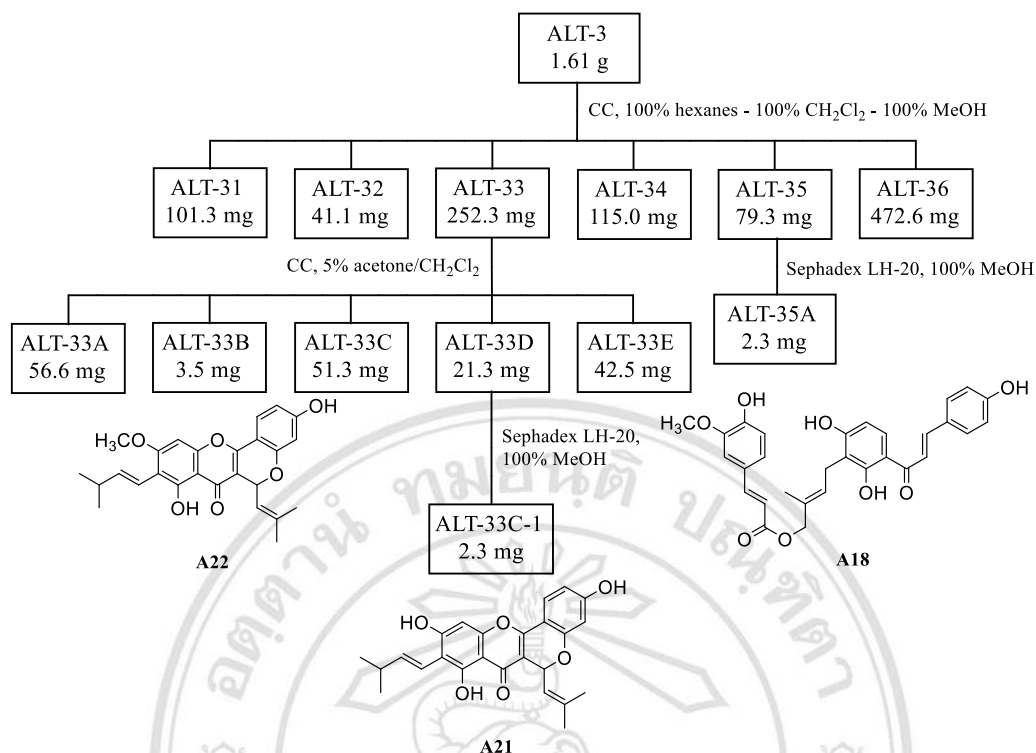


**Figure 2.10** The isolation of fraction ALT-3.

Fraction ALT-4 (brown gum, 4.13 g) was fractionated by CC over Sephadex LH-20 using 100% methanol as a mobile phase to give five subfractions (ALT-41-ALT-45). Subfraction ALT-42 (green gum, 413.5 mg) was isolated by CC over silica gel eluting by the gradient of 100% dichloromethane to 100% methanol to provide three subfractions (ALT-42A-ALT-42C). The second subfraction (green gum, 32.5 mg) was separated by the same procedure as subfraction ALT-42 to provide compounds **A2** (brown gum, 1.3 mg) and **A6** (brown gum, 2.1 mg). Subfraction ALT-44 (dark green gum, 556.7 mg) was isolated by CC over Sephadex LH-20 using 100% methanol as a mobile phase to give five subfractions (ALT-44A-ALT-44E). Compound **A32** (brown gum, 4.2 mg) was isolated from the second subfraction (dark green gum, 51.3 mg) after the purification with silica gel CC using 5% methanol in dichloromethane as a mobile phase. Subfraction ALT-44D (green gum, 41.5 mg) was further purified by CC over silica gel using a gradient of 100% dichloromethane to 100% methanol as a mobile phase followed by Sephadex LH-20 with 100% methanol to give compound **A31** (yellow gum, 2.1 mg) The isolation is shown in **Figure 2.11**.



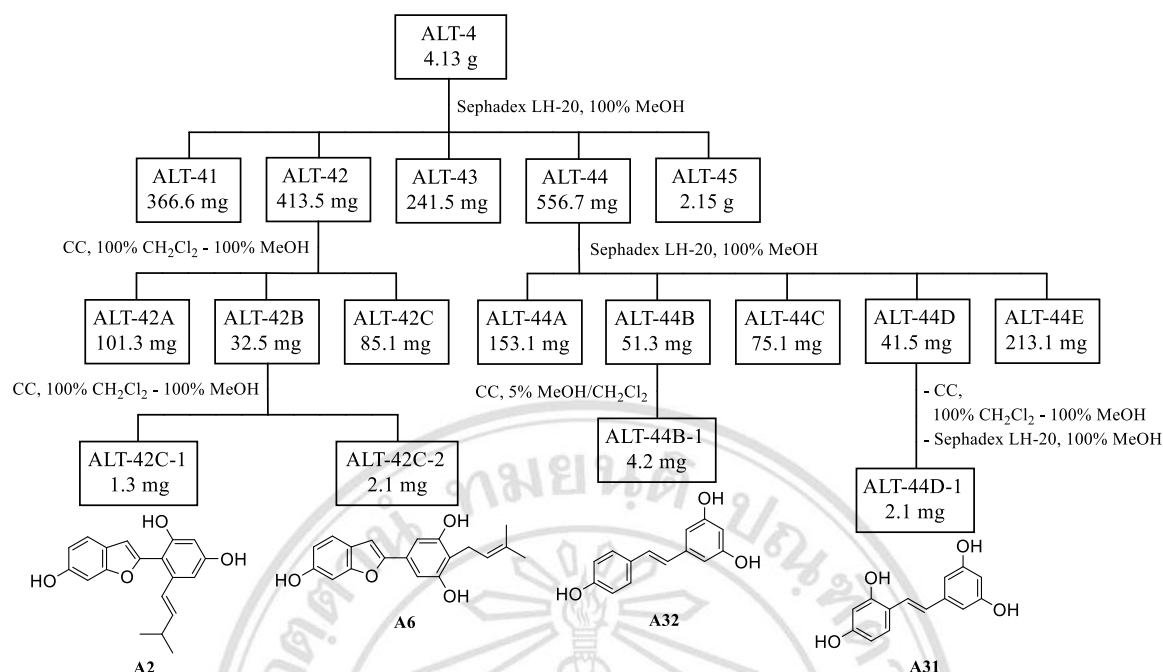


**Figure 2.11** The isolation of fraction ALT-4.

Fraction ALT-5 (brown gum, 3.51 g) was fractionated using QCC over silica gel eluting with a gradient from 100% dichloromethane to 100% methanol to give six subfractions (ALT-51-ALT-56). Subfraction ALT-52 (dark green gum, 356.2 mg) was isolated by CC over Sephadex LH-20 eluting by 100% methanol to provide three subfractions (ALT-52A-ALT-52C). Subfraction ALT-52B (green gum 63.1 mg) was further purified by CC over Sephadex LH-20 using 50% methanol in dichloromethane as a mobile phase to give three subfractions (ALT-52B-1-ALT-52B-3). Separation of subfraction ALT-52B-2 (yellow green gum, 19.3 mg) by CC silica gel with 2% methanol in dichloromethane gave compound **A28** (brown gum, 2.3 mg). Subfraction ALT-54 (dark green gum, 165.2 mg) was isolated by the same procedure as subfraction ALT-52B-1 to give three subfractions (ALT-54A-ALT-54C). Purification of subfraction ALT-54B (green gum, 35.2 mg) by CC over Sephadex LH-20 using 100% methanol as a mobile phase and silica gel CC with 10% acetone in dichloromethane gave compound **A26** (brown gum, 1.9 mg). Purification of subfraction ALT-54C (green gum, 25.6 mg) by CC silica gel with 15% acetone in dichloromethane furnished compound **A4** (brown gum, 1.5 mg). Subfraction ALT-55 (dark green gum, 65.3 mg) was purified by CC over Sephadex LH-20 with 50% methanol in dichloromethane followed by RPCC using 50% methanol

in water as a mobile phase to give compound **A5** (brown gum, 4.0 mg) The isolation is shown in **Figure 2.12**.

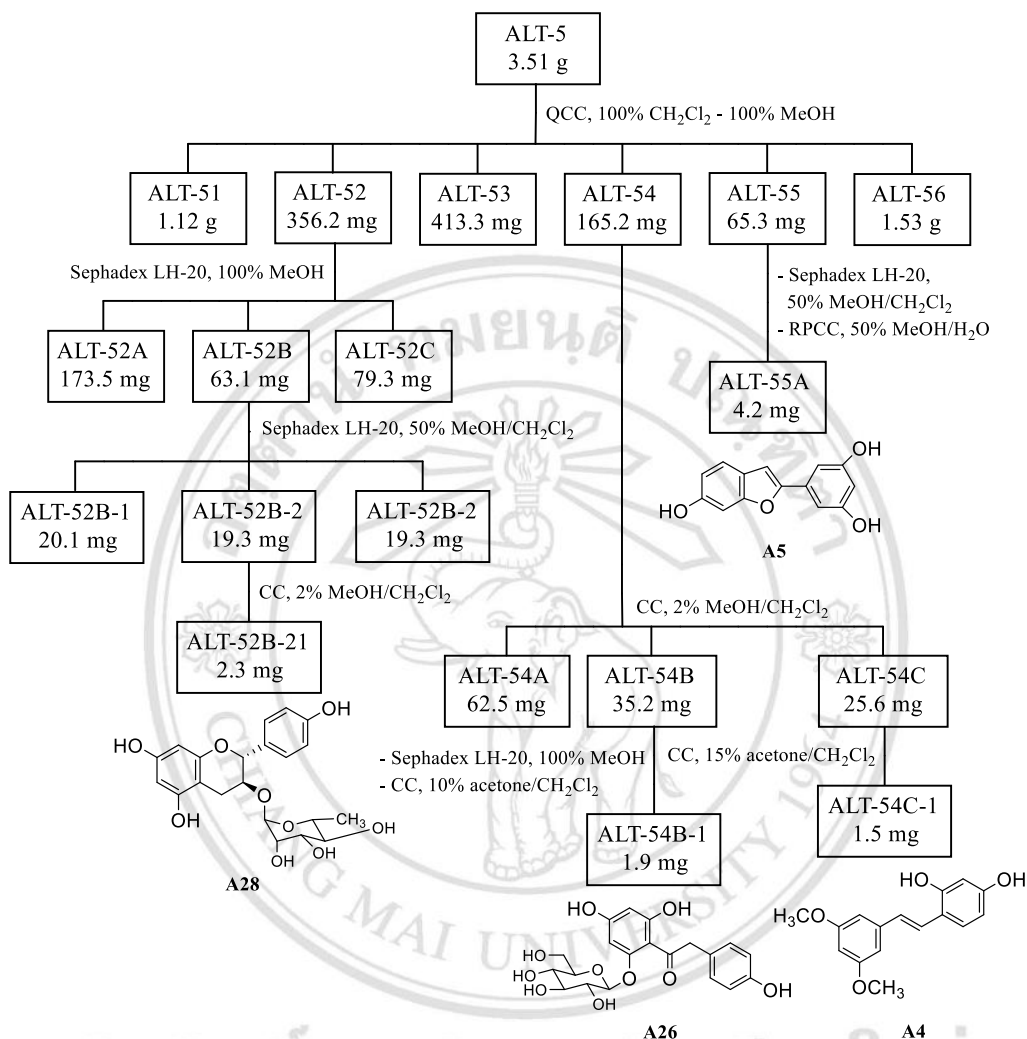


**Figure 2.12** The isolation of fraction ALT-5.

Fraction ALT-6 (dark green gum, 2.50 g) was fractionated by CC over Sephadex LH-20 with 100% methanol to give six subfractions (ALT-61-ALT-66). Subfraction ALT-62 (dark green gum, 120.0 mg) was purified by CC over silica gel using the gradient of 100% dichloromethane to 100% methanol to give four subfractions (ALT-62A-ALT-62D). Purification of subfraction ALT-62B (green gum, 51.3 mg) by Sephadex LH-20 CC using 100% methanol as a mobile phase and CC over silica gel with 2% methanol in dichloromethane gave compound **A30** (brown gum, 3.2 mg). Subfraction ALT-62C (green gum 31.2 mg) was further purified by CC over silica gel using 5%

methanol in dichloromethane as a mobile phase to provide compound **A29** (brown gum, 1.0 mg). Subfraction ALT-64 (dark green gum, 150.0 mg) was isolated by CC over Sephadex LH-20 with 100% methanol to provide three subfractions (ALT-64A-ALT-64C). The second subfraction (green gum, 51.3 mg) was purified by CC over Sephadex LH-20 using 50% methanol in dichloromethane as a mobile phase followed by RPCC with 40% methanol in water to provide compound **A7** (brown gum, 3.2 mg). Subfraction ALT-65 (dark green gum, 210.0 mg) was isolated by CC over silica gel eluting by the gradient of 100% dichloromethane to 100% ethyl acetate to give four subfractions (ALT-65A-ALT-65D). Subfraction ALT-65B (green gum 56.5 mg) was separated by the same as the procedure of subfraction ALT-65 to give three subfractions (ALT-65B1-ALT-65B3). The second (yellow gum, 15.3 mg) and third (yellow gum, 20.3 mg) subfractions were purified by CC over Sephadex LH-20 with 100% methanol to provide compounds **A9** (brown gum, 1.6 mg) and **A11** (brown gum 2.0 mg), respectively. Compound **A12** (brown gum 2.8 mg) was contained in the first subfraction after the purification of subfraction ALT-64D (green gum, 65.3 mg) by RPCC using 50% methanol in water. The isolation is shown in **Figure 2.13** and **Figure 2.14**.

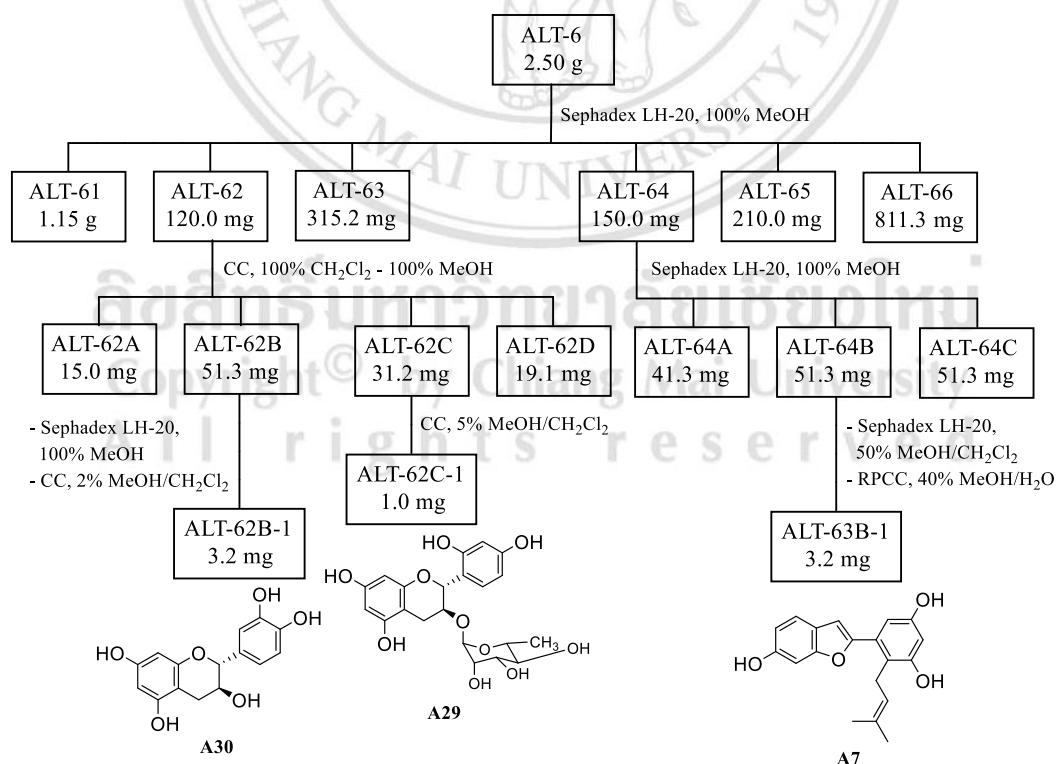


**Figure 2.13** The isolation of fraction ALT-6.

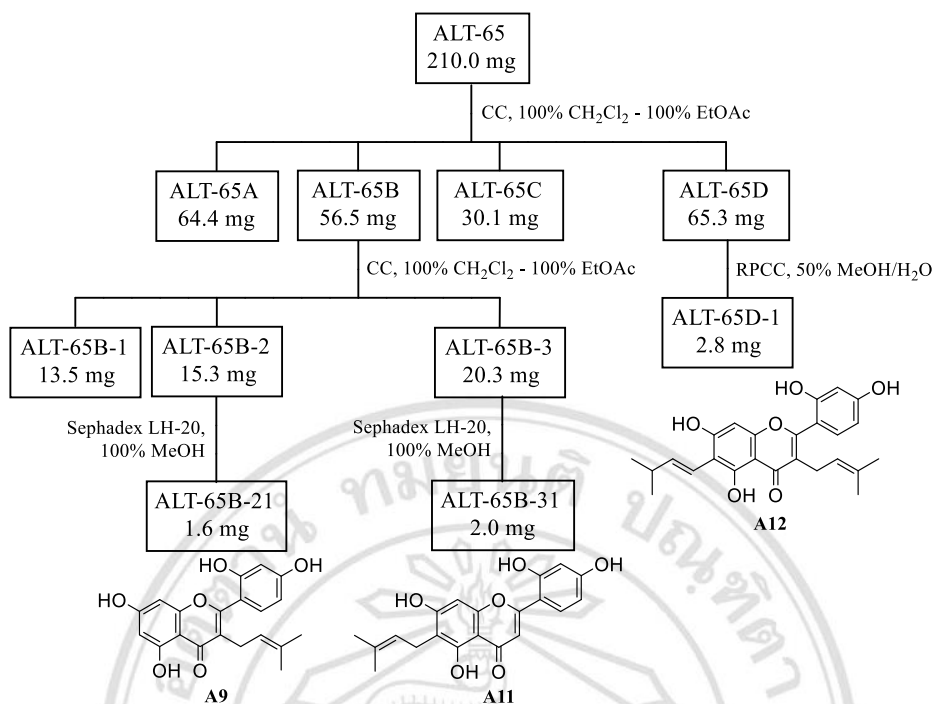


**Figure 2.14** The isolation of subfraction ALT-65.

Fraction ALT-7 (dark green gum, 2.50 g) was separated by CC over Sephadex LH-20 using 100% methanol as a mobile phase to give five subfractions (ALT-71-ALT-75). Subfraction ALT-72 (green gum, 230.2 mg) was further purified by silica gel CC with the gradient of 100% dichloromethane to 100% methanol to give three subfractions (ALT-72A-ALT-72C). Purification of the second subfraction (green gum, 43.1 mg) by CC over Sephadex LH-20 with 100% methanol gave compound **A27** (brown gum, 2.3 mg). Subfraction ALT-74 (green gum, 148.3 mg) was separated by CC over Sephadex LH-20 using 50% methanol in dichloromethane as a mobile phase to provide three subfractions (ALT-74A-ALT-74C). The purification of subfraction ALT-74B by silica gel CC with the gradient of 100% dichloromethane to 100% methanol and CC over Sephadex LH-20 with 100% methanol furnished compound **A16** (brown gum, 1.7 mg). The isolation was shown in **Figure 2.15**.

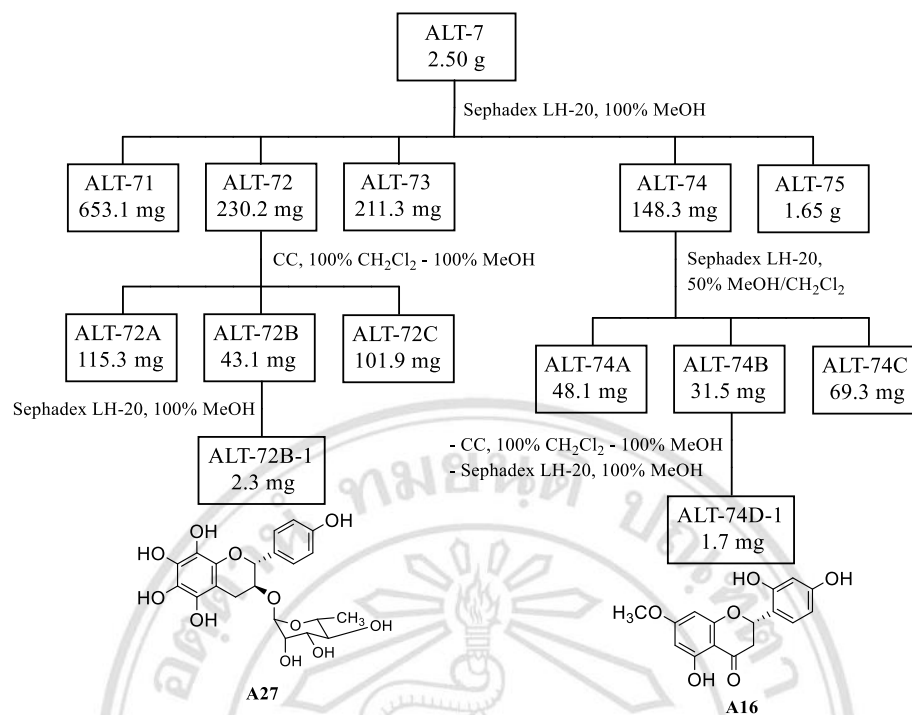


**Figure 2.15** The isolation of fraction ALT-7.

### 2.3.3 Acid hydrolysis of compound A26

A sample of compound **A26** (1.0 mg) in 2.0 N HCl (1.0 mL) in ethanol (5.0 mL) was heated at reflux for 2 h. After cooling, the reaction mixture was neutralized with 5% NaOH. The mixture was extracted with ethyl acetate (2 x 5.0 mL). The aqueous layer was concentrated under reduced pressure to yield D-glucose (0.5 mg), +43.6 (*c* 0.5, H<sub>2</sub>O) [D-glucose;  $[\alpha]^{25}_{\text{D}}$  +41.6 (*c* 0.50, H<sub>2</sub>O) (Yang *et al.*, 2001)]. The sugar was identified by TLC using CHCl<sub>3</sub>:AcOH:H<sub>2</sub>O (3:0.5:0.5) as a mobile phase by comparison with the authentic standard.

## 2.4 Barks of *Artocarpus lakoocha*

### 2.4.1 Plant materials and extraction

The barks of *A. lakoocha* were collected from Mae Rim district, Chiang Mai province, Thailand in January, 2016. A voucher specimen No. QBG91824 deposited at the herbarium collection of the Queen Sirikit Botanic Garden, Mae Rim, Chiang Mai, Thailand. The air-dried barks (4.0 kg) were extracted with 10 L of acetone for 7 days. The extract was filtered and acetone was then removed by under reduced pressure to give acetone extract as a dark brown (40.0 g). A portion extract (10.24 g) was dissolved by 300 mL 90% methanol in water and subjected to liquid-liquid partition using hexanes. The hexanes were removed by reduced pressure to give hexanes fraction as a brown gum (276.6 mg). Then, the aqueous solution was added 150 mL water, extracted by dichloromethane and removed the solution by rotary evaporator to afford a dark brown gum (232.8 mg) of dichloromethane and aqueous soluble fraction (9.56 g). The extraction is shown in **Figure 2.16**.

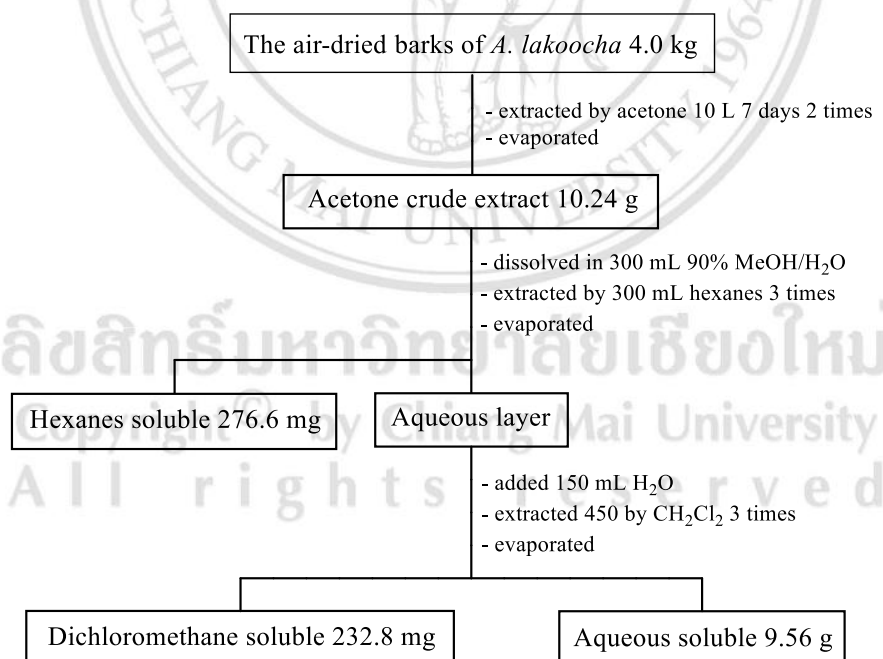
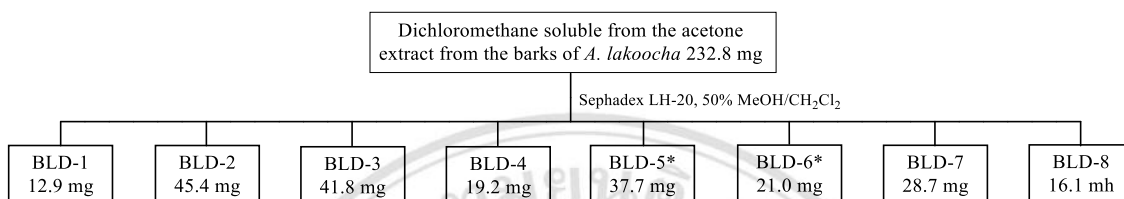


**Figure 2.16** The extraction of the barks of *A. lakoocha*.

#### 2.4.2 Purification of acetone extract from the barks of *A. lakoocha*

Chromatography of the dichloromethane fraction (brown gum, 232.8 mg) on Sephadex LH-20 using 50% methanol in dichloromethane as a mobile phase gave eight fractions (BLD-1-BLD-8) as shown in **Figure 2.17**.



\*Fractions will be isolated.

**Figure 2.17** The isolation of the dichloromethane fraction of the barks of *A. lakoocha*.

Fraction BLD-5 (brown gum, 37.7 mg) was separated by solid phase extraction with Hypersep C18 eluting with 50% and 80% methanol in water and 100% methanol to give three subfractions (BLD-51-BLD-53). High-performance liquid chromatography (HPLC) separation of subfraction BLD-51 (brown gum, 29.7 mg) on a C18 column with a solvent gradient from 50% to 99% methanol in water for 30 min and 99% methanol in water for 10 min gave compounds **A35** (brown gum, 0.9 mg,  $t_R = 15.50$  min) and **A34** (brown gum, 0.5 mg,  $t_R = 29.50$  min). Separation of subfraction BLD-52 (brown gum, 5.4 mg) by HPLC on a C18 column with the solvent gradient from 80% to 99% methanol in water for 30 min gave compound **A33** (brown gum, 0.5 mg,  $t_R = 23.50$  min). The isolation is shown in **Figure 2.18**.

Copyright© by Chiang Mai University  
All rights reserved

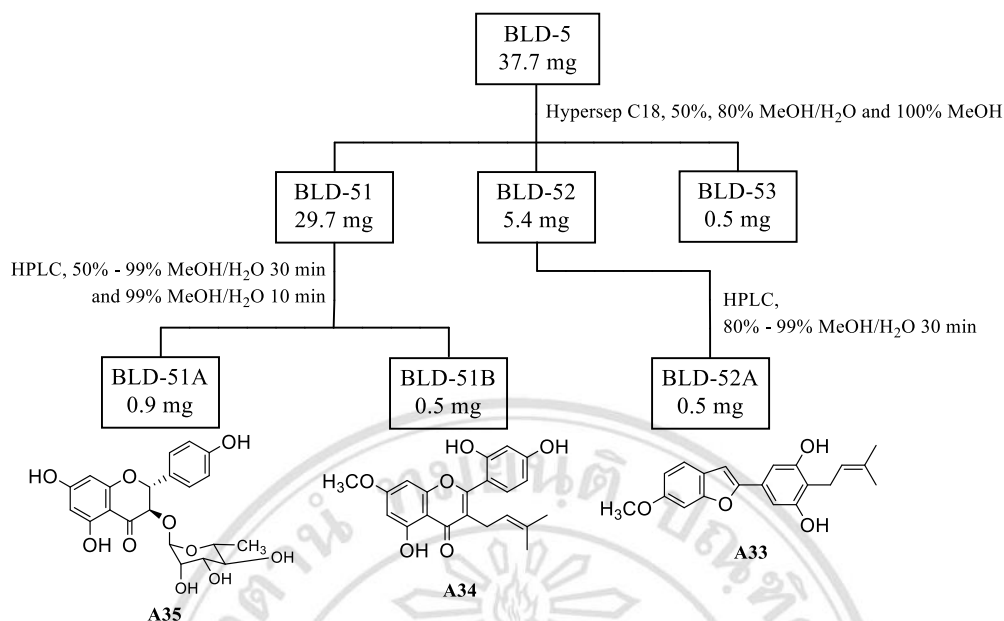


**Figure 2.18** The isolation of fraction BLD-5.

Fraction BLD-6 (brown gum, 21.0 mg) was separated by the same procedure as fraction BLD-5 to furnish three subfractions (BLD-61-BLD-63) and purification the first subfraction (brown gum, 16.9 mg) by HPLC on a C18 column with the solvent gradient from 50% methanol in water for 10 min and 50% to 99% methanol in water for 20 min gave compound **A36** (brown gum, 0.5 mg,  $t_R = 20.00$  min). Separation of subfraction BLD-62 (brown gum, 3.2 mg) by HPLC by the same procedure as subfraction BLD-52 to furnish compound **A6** (brown gum, 2.0 mg,  $t_R = 18.00$  min). The isolation is shown in **Figure 2.19**.



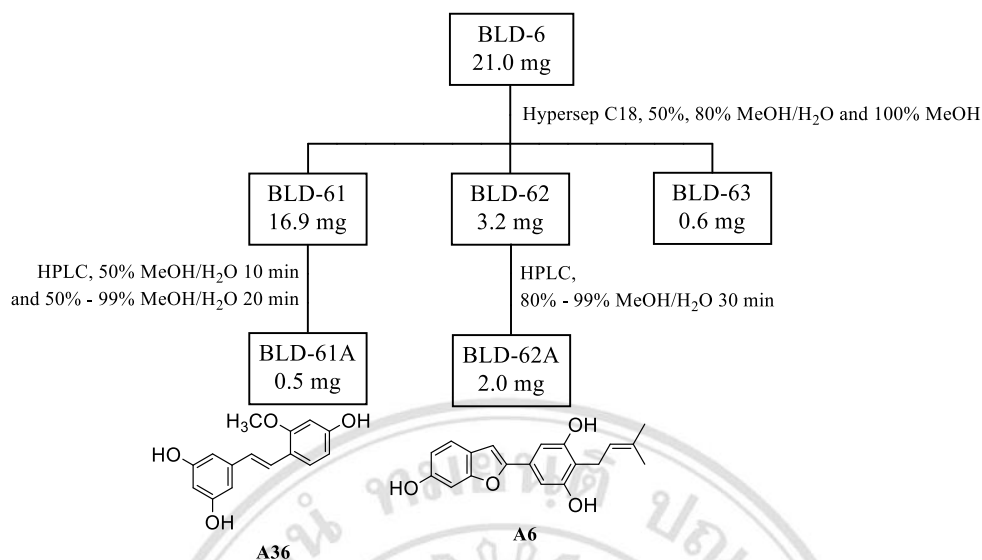
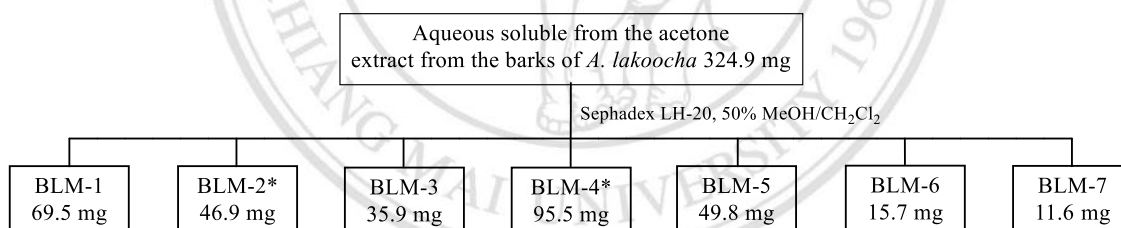


**Figure 2.19** The isolation of fraction BLD-6.

The portion aqueous fraction (brown gum, 324.9 mg) was fractionated by CC over Sephadex LH-20 using 50% methanol in dichloromethane as a mobile phase to give seven subfractions (BLM-1-BLM-7) as shown in **Figure 2.20**.



\*Fractions will be isolated.

**Figure 2.20** The isolation of the aqueous fraction of the barks of *A. lakoocha*.

Fraction BLM-2 (brown gum, 46.9 mg) was isolated by reverse phase column chromatography eluting by 30% methanol in water to 100% methanol to provide three subfractions (BLM-21-BLM-23). Subfraction BLM-22 (brown gum, 8.4 mg) was purified by diol silica gel column using the gradient of 100% dichloromethane to 100% methanol as a mobile phase to provide compound **A28** (brown gum, 1.4 mg). The isolation is shown in **Figure 2.21**.

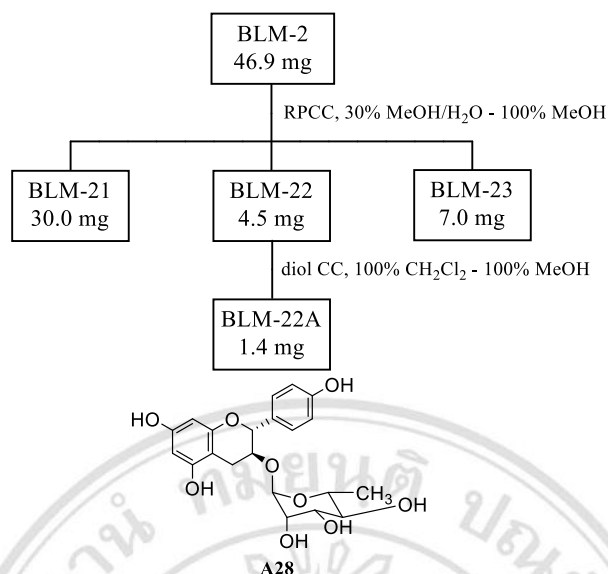


**Figure 2.21** The isolation of fraction BLM-2.

Fraction BLM-4 (brown gum, 95.5 mg) was subjected to CC using diol silica gel using the gradient of 100% dichloromethane to 100% methanol as a mobile phase to give two subfractions (BLM-41-BLM-42). Compound A30 (brown gum, 1.6 mg) was obtained from the second subfraction after purification the subfraction BLM-41 (brown gum, 15.4 mg) on Sephadex LH-20 using 100% methanol. The isolation is shown in **Figure 2.22**.

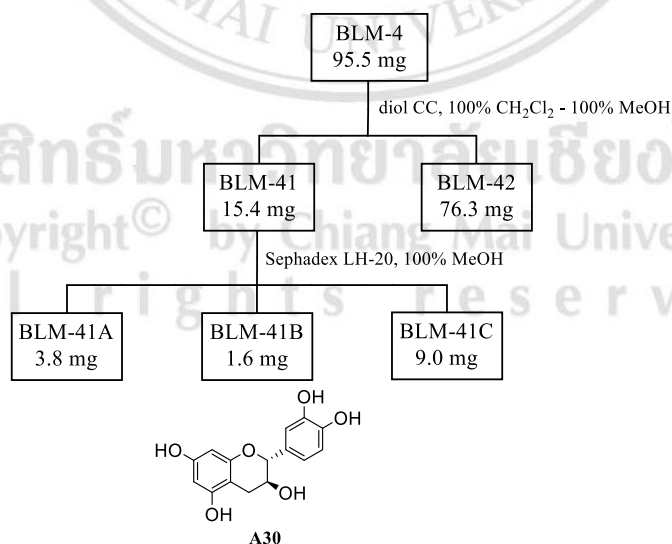


**Figure 2.22** The isolation of fraction BLM-4.

Compound **A1** (heterophyllene A): pale yellow gum; UV (MeOH)  $\lambda_{\max}$  nm (log  $\epsilon$ ): 224 (3.67), 245 (3.21), 275 (2.56), 310 (2.01); IR (neat)  $\nu_{\max}$   $\text{cm}^{-1}$ : 3420, 1645;  $^1\text{H}$ -NMR data (400 MHz,  $\text{CDCl}_3$ )  $\delta_{\text{H}}$ : 7.38 (1H, d,  $J = 8.4$  Hz), 6.97 (1H, s), 6.87 (1H, s), 6.85 (1H, s), 6.81 (1H, d,  $J = 2.0$  Hz), 6.76 (1H, dd,  $J = 8.4, 2.0$  Hz), 6.64 (1H, d,  $J = 10.0$  Hz), 5.64 (1H, d,  $J = 10.0$  Hz), 1.40 (6H, s);  $^{13}\text{C}$ -NMR data (100 MHz,  $\text{CDCl}_3$ )  $\delta_{\text{C}}$ : 155.6, 154.7, 154.1, 154.0, 153.6, 151.5, 129.6, 122.8, 121.2, 116.2, 113.8, 112.1, 105.6, 103.9, 101.6, 101.2, 98.2, 76.3, 27.8.

Compound **A2** (heterophyllene B): pale yellow gum; UV (MeOH)  $\lambda_{\max}$  nm (log  $\epsilon$ ): 226 (2.47), 248 (2.21), 265 (2.01); IR (neat)  $\nu_{\max}$   $\text{cm}^{-1}$ : 3400, 1667;  $^1\text{H}$ -NMR data (400 MHz, acetone- $d_6$ )  $\delta_{\text{H}}$ : 7.39 (1H, d,  $J = 8.4$  Hz), 6.96 (1H, d,  $J = 2.0$  Hz), 6.95 (1H, s), 6.93 (1H, d,  $J = 2.0$  Hz), 6.90 (1H, d,  $J = 2.0$  Hz), 6.81 (1H, dd,  $J = 8.4, 2.1$  Hz), 6.72 (1H, d,  $J = 16.4$  Hz), 6.71 (1H, dd,  $J = 16.4, 6.4$  Hz), 2.44 (1H, m), 1.09 (6H, d,  $J = 6.4$  Hz);  $^{13}\text{C}$ -NMR data (100 MHz, acetone- $d_6$ )  $\delta_{\text{C}}$ : 157.4, 156.8, 155.4, 142.1, 130.0, 122.7, 122.0, 119.1, 113.3, 104.1, 102.1, 98.5, 34.0, 23.3.

Compound **A3** (heterophyllene C): pale yellow gum;  $[\alpha]_{\text{D}}^{25} +48.2$  (c 0.53,  $\text{CHCl}_3$ ); UV (MeOH)  $\lambda_{\max}$  nm (log  $\epsilon$ ): 232 (2.41), 252 (2.31), 271 (2.01), 313 (1.89); IR (neat)  $\nu_{\max}$   $\text{cm}^{-1}$ : 3410, 1677;  $^1\text{H}$ -NMR data (400 MHz, acetone- $d_6$ )  $\delta_{\text{H}}$ : 7.39 (1H, d,  $J = 8.4$  Hz), 6.98 (1H, s), 6.97 (1H, d,  $J = 2.1$  Hz), 6.91 (2H, s), 6.80 (1H, dd,  $J = 8.4, 2.1$  Hz), 3.63 (1H, dd,  $J = 9.6, 2.0$  Hz), 3.24 (1H, dd,  $J = 14.0, 2.0$  Hz), 2.57 (1H, dd,  $J = 14.0, 9.6$  Hz), 1.26 (3H, s), 1.25 (3H, s);  $^{13}\text{C}$ -NMR data (100 MHz, acetone- $d_6$ )  $\delta_{\text{C}}$ : 157.2, 155.9, 155.3, 130.1, 121.9, 120.0, 113.1, 104.6, 101.7, 98.4, 81.2, 72.6, 26.8, 26.0, 25.0.

Compound **A4** (heterophyllene D): yellow gum; UV (MeOH)  $\lambda_{\max}$  nm (log  $\epsilon$ ): 228 (3.24), 300 (2.76), 334 (2.21); IR (neat)  $\nu_{\max}$   $\text{cm}^{-1}$ : 3389, 1640;  $^1\text{H}$ -NMR data (400 MHz, acetone- $d_6$ )  $\delta_{\text{H}}$ : 7.43 (1H, d,  $J = 8.8$  Hz), 7.42 (1H, d,  $J = 17.2$  Hz), 7.01 (1H, d,  $J = 17.2$  Hz), 6.69 (2H, d,  $J = 2.4$  Hz), 6.45 (1H, d,  $J = 2.4$  Hz), 6.40 (1H, dd,  $J = 8.8, 2.4$  Hz), 6.35 (1H, d,  $J = 2.4$  Hz), 3.80 (6H, s);  $^{13}\text{C}$ -NMR data (100 MHz, acetone- $d_6$ )  $\delta_{\text{C}}$ : 162.1, 159.4, 157.0, 141.7, 128.6, 126.3, 125.1, 117.1, 108.4, 104.8, 103.5, 117.1, 99.8, 55.6.

Compound **A5** (moracin M): brown gum; UV (MeOH)  $\lambda_{\max}$  nm (log  $\epsilon$ ): 214 (4.12), 316 (3.97); IR (neat)  $\nu_{\max}$   $\text{cm}^{-1}$ : 3427, 2916, 1629;  $^1\text{H-NMR}$  data (400 MHz, acetone- $d_6$ )  $\delta_{\text{H}}$ : 7.41 (1H, d,  $J = 8.4$  Hz), 7.04 (1H, d,  $J = 2.0$  Hz), 6.98 (1H, s), 6.85 (2H, d,  $J = 2.4$  Hz), 6.81 (1H, dd,  $J = 8.4, 2.0$  Hz), 6.36 (1H, t,  $J = 2.4$  Hz).

Compound **A6** (moracin C): brown gum; UV (MeOH)  $\lambda_{\max}$  nm (log  $\epsilon$ ): 214 (4.42), 319 (4.38); IR (neat)  $\nu_{\max}$   $\text{cm}^{-1}$ : 3329, 2912, 1622;  $^1\text{H-NMR}$  data (400 MHz, acetone- $d_6$ )  $\delta_{\text{H}}$ : 7.33 (1H, d,  $J = 8.4$  Hz), 6.88 (1H, d,  $J = 2.0$  Hz), 6.83 (1H, brs), 6.77 (2H, brs), 6.72 (1H, dd,  $J = 8.4, 2.0$  Hz), 5.26 (1H, t,  $J = 7.2$  Hz), 3.32 (2H, d,  $J = 7.2$  Hz), 1.78 (3H, s), 1.67 (3H, s).

Compound **A7** (demethylmoracin D): brown gum; UV (MeOH)  $\lambda_{\max}$  nm (log  $\epsilon$ ): 212 (4.13), 310 (3.56); IR (neat)  $\nu_{\max}$   $\text{cm}^{-1}$ : 3388, 2918, 1614;  $^1\text{H-NMR}$  data (400 MHz, acetone- $d_6$ )  $\delta_{\text{H}}$ : 7.42 (1H, d,  $J = 8.4$  Hz), 6.98 (1H, d,  $J = 2.4$  Hz), 6.81 (1H, dd,  $J = 8.4, 2.4$  Hz), 6.79 (1H, s), 6.74 (1H, d,  $J = 2.4$  Hz), 6.50 (1H, d,  $J = 2.4$  Hz), 5.18 (1H, t,  $J = 5.6$  Hz), 3.50 (2H, d,  $J = 5.6$  Hz), 1.67 (3H, s), 1.64 (3H, s).

Compound **A8** (norartocarpetin): pale yellow gum; UV (MeOH)  $\lambda_{\max}$  nm (log  $\epsilon$ ): 214 (4.25), 259 (3.91), 285 (3.85), 350 (3.99); IR (neat)  $\nu_{\max}$   $\text{cm}^{-1}$ : 3141, 2918, 1606;  $^1\text{H-NMR}$  data (400 MHz, acetone- $d_6$ )  $\delta_{\text{H}}$ : 13.14 (1H, s), 7.83 (1H, d,  $J = 8.8$  Hz), 7.07 (1H, s), 6.62 (1H, d,  $J = 2.4$  Hz), 6.56 (1H, dd,  $J = 8.8, 2.4$  Hz), 6.50 (1H, d,  $J = 1.8$  Hz), 6.23 (1H, d,  $J = 1.8$  Hz).

Compound **A9** (albanin A): pale yellow gum; UV (MeOH)  $\lambda_{\max}$  nm (log  $\epsilon$ ): 214 (3.95), 264 (3.59), 281 (3.55); IR (neat)  $\nu_{\max}$   $\text{cm}^{-1}$ : 3321, 2914, 1635, 1014;  $^1\text{H-NMR}$  data (400 MHz, acetone- $d_6$ )  $\delta_{\text{H}}$ : 13.16 (1H, s), 7.19 (1H, d,  $J = 8.4$  Hz), 6.56 (1H, d,  $J = 2.4$  Hz), 6.51 (1H, dd,  $J = 8.4, 2.4$  Hz), 6.32 (1H, d,  $J = 2.2$  Hz), 6.24 (1H, d,  $J = 2.2$  Hz), 5.11 (1H, t,  $J = 7.0$  Hz), 3.10 (2H, d,  $J = 7.0$  Hz), 1.56 (3H, s), 1.42 (3H, s).

Compound **A10** (licoflavone C): pale yellow gum; UV (MeOH)  $\lambda_{\max}$  nm (log  $\epsilon$ ): 214 (3.89), 276 (3.55), 332 (3.57); IR (neat)  $\nu_{\max}$   $\text{cm}^{-1}$ : 3365, 2918, 1602, 1454;  $^1\text{H-NMR}$  data (400 MHz, acetone- $d_6$ )  $\delta_{\text{H}}$ : 13.40 (1H, s), 7.94 (2H, d,  $J = 9.0$  Hz), 7.04 (2H, d,  $J = 9.0$  Hz), 6.65 (1H, s), 6.63 (1H, s), 5.29 (1H, t,  $J = 7.0$  Hz), 3.37 (2H, d,  $J = 7.0$  Hz), 1.79 (3H, s), 1.66 (3H, s).

Compound **A11** (artocarpesin): brown gum; UV (MeOH)  $\lambda_{\max}$  nm (log  $\epsilon$ ): 212 (4.33), 271 (3.79), 331 (3.84); IR (neat)  $\nu_{\max}$   $\text{cm}^{-1}$ : 3332, 2904, 1608, 1577;  $^1\text{H}$ -NMR data (400 MHz,  $\text{DMSO-}d_6$ )  $\delta_{\text{H}}$ : 13.30 (1H, s), 7.73 (1H, d,  $J = 8.8$  Hz), 6.98 (1H, s), 6.48 (2H, s), 6.43 (1H, d,  $J = 8.8$  Hz), 5.18 (1H, t,  $J = 6.4$  Hz), 3.21 (2H, d,  $J = 6.4$  Hz), 1.72 (3H, s), 1.62 (3H, s);  $^{13}\text{C}$ -NMR data (100 MHz,  $\text{DMSO-}d_6$ )  $\delta_{\text{C}}$ : 181.9, 161.8, 161.7, 161.5, 158.8, 158.3, 155.1, 130.5, 129.7, 122.3, 110.6, 108.7, 108.0, 106.7, 103.3, 93.0, 25.5, 21.0, 17.7.

Compound **A12** (norartocarpin): brown gum; UV (MeOH)  $\lambda_{\max}$  nm (log  $\epsilon$ ): 211 (4.30), 270 (4.25), 319 (3.94); IR (neat)  $\nu_{\max}$   $\text{cm}^{-1}$ : 3340, 2912, 1614, 1562;  $^1\text{H}$ -NMR data (400 MHz,  $\text{acetone-}d_6$ )  $\delta_{\text{H}}$ : 14.11 (1H, s), 7.23 (1H, d,  $J = 8.4$  Hz), 6.80 (1H, dd,  $J = 16.0$ , 6.8 Hz), 6.67 (1H, d,  $J = 16.0$  Hz), 6.60 (1H, d,  $J = 2.4$  Hz), 6.55 (1H, dd,  $J = 8.4$ , 2.4 Hz), 6.44 (1H, s), 5.16 (1H, t,  $J = 7.0$  Hz), 3.15 (2H, d,  $J = 7.0$  Hz), 2.48 (1H, m), 1.60 (3H, s), 1.46 (3H, s), 1.13 (6H, d,  $J = 6.8$  Hz).

Compound **A13** (cudraflavone C): brown gum; UV (MeOH)  $\lambda_{\max}$  nm (log  $\epsilon$ ): 212 (4.32), 258 (3.96), 312 (3.69); IR (neat)  $\nu_{\max}$   $\text{cm}^{-1}$ : 3313, 2914, 1612, 1566;  $^1\text{H}$ -NMR data (400 MHz,  $\text{acetone-}d_6$ )  $\delta_{\text{H}}$ : 13.44 (1H, s), 7.17 (1H, d,  $J = 8.4$  Hz), 6.56 (1H, d,  $J = 2.0$  Hz), 6.50 (1H, dd,  $J = 8.4$ , 2.0 Hz), 6.39 (1H, s), 5.27 (1H, t,  $J = 7.0$  Hz), 5.12 (1H, t,  $J = 6.8$  Hz), 3.35 (2H, d,  $J = 7.0$  Hz), 3.10 (2H, d,  $J = 6.8$  Hz), 1.77 (3H, s), 1.64 (3H, s), 1.56 (3H, s), 1.42 (3H, s).

Compound **A14** (artocarpin): brown gum; UV (MeOH)  $\lambda_{\max}$  nm (log  $\epsilon$ ): 200 (4.33), 267 (4.07), 330 (3.80); IR (neat)  $\nu_{\max}$   $\text{cm}^{-1}$ : 3369, 2951, 1631, 1614;  $^1\text{H}$ -NMR data (400 MHz,  $\text{CDCl}_3$ )  $\delta_{\text{H}}$ : 13.49 (1H, s), 7.13 (1H, d,  $J = 8.0$  Hz), 6.63 (1H, dd,  $J = 18.0$ , 6.8 Hz), 6.51 (1H, d,  $J = 18.0$  Hz), 6.51 (1H, d,  $J = 2.0$  Hz), 6.50 (1H, dd,  $J = 8.0$ , 2.0 Hz), 6.32 (1H, s), 5.10 (1H, t,  $J = 6.0$  Hz), 3.83 (3H, s), 3.10 (2H, d,  $J = 6.0$  Hz), 2.43 (1H, m), 1.57 (3H, s), 1.39 (3H, s), 1.07 (6H, d,  $J = 6.8$  Hz);  $^{13}\text{C}$ -NMR data (100 MHz,  $\text{CDCl}_3$ )  $\delta_{\text{C}}$ : 182.4, 162.9, 160.6, 159.5, 158.1, 156.2, 155.2, 142.6, 132.9, 131.5, 121.3, 120.9, 115.5, 112.2, 109.7, 108.2, 104.9, 103.8, 89.7, 55.9, 33.0, 25.6, 24.3, 22.5, 17.5.

Compound **A15** (steppogenin): brown gum;  $[\alpha]^{25}_D$  -21.6 (*c* 0.13, MeOH); UV (MeOH)  $\lambda_{\max}$  nm (log  $\epsilon$ ): 211 (4.22), 288 (3.98); IR (neat)  $\nu_{\max}$   $\text{cm}^{-1}$ : 3325, 2912, 1622, 1519;  $^1\text{H}$ -NMR data (400 MHz, acetone- $d_6$ )  $\delta_{\text{H}}$ : 12.22 (1H, s), 7.22 (1H, d,  $J$  = 8.4 Hz), 6.48 (1H, d,  $J$  = 2.0 Hz), 6.43 (1H, dd,  $J$  = 8.4, 2.0 Hz), 5.97 (1H, d,  $J$  = 1.6 Hz), 5.95 (1H, d,  $J$  = 1.6 Hz), 5.71 (1H, dd,  $J$  = 12.8, 2.8 Hz), 3.18 (1H, dd,  $J$  = 17.2, 12.8 Hz), 2.71 (1H, dd,  $J$  = 17.2, 2.8 Hz).

Compound **A16** (artocarpanone): pale yellow gum;  $[\alpha]^{25}_D$  -5.4 (*c* 0.19, acetone); UV (MeOH)  $\lambda_{\max}$  nm (log  $\epsilon$ ): 211 (4.36), 286 (4.10); IR (neat)  $\nu_{\max}$   $\text{cm}^{-1}$ : 3305, 2916, 1631, 1452;  $^1\text{H}$ -NMR data (400 MHz, acetone- $d_6$ )  $\delta_{\text{H}}$ : 12.17 (1H, s), 7.31 (1H, d,  $J$  = 8.4 Hz), 6.47 (1H, d,  $J$  = 2.4 Hz), 6.43 (1H, dd,  $J$  = 8.4, 2.4 Hz), 6.05 (1H, d,  $J$  = 2.0 Hz), 6.02 (1H, d,  $J$  = 2.0 Hz), 5.72 (1H, dd,  $J$  = 13.2, 2.8 Hz), 3.84 (3H, s), 3.20 (1H, dd,  $J$  = 17.2, 13.2 Hz), 2.73 (1H, dd,  $J$  = 17.2, 2.8 Hz).

Compound **A17** (isogemichalcone C): brown gum; UV (MeOH)  $\lambda_{\max}$  nm (log  $\epsilon$ ): 215 (4.02), 322 (3.80), 385 (3.65); IR (neat)  $\nu_{\max}$   $\text{cm}^{-1}$ : 3329, 2916, 1679, 1597;  $^1\text{H}$ -NMR data (400 MHz, acetone- $d_6$ )  $\delta_{\text{H}}$ : 14.23 (1H, s), 8.23 (1H, d,  $J$  = 15.6 Hz), 7.92 (1H, d,  $J$  = 9.0 Hz), 7.80 (1H, d,  $J$  = 15.6 Hz), 7.69 (1H, d,  $J$  = 8.8 Hz), 7.62 (1H, d,  $J$  = 16.0 Hz), 7.36 (1H, d,  $J$  = 2.0 Hz), 7.16 (1H, dd,  $J$  = 8.0, 2.0 Hz), 6.87 (1H, d,  $J$  = 8.8 Hz), 6.87 (1H, d,  $J$  = 8.0 Hz), 6.52 (1H, d,  $J$  = 9.0 Hz), 6.46 (1H, s), 6.44 (1H, d,  $J$  = 16.0 Hz), 5.58 (1H, t,  $J$  = 7.6 Hz), 3.91 (3H, s), 3.51 (2H, d,  $J$  = 7.6 Hz), 4.96 (2H, s), 1.75 (3H, s).

Compound **A18** (artocarmitin B): pale yellow gum; UV (MeOH)  $\lambda_{\max}$  nm (log  $\epsilon$ ): 210 (4.67), 335 (4.54), 362 (4.50); IR (neat)  $\nu_{\max}$   $\text{cm}^{-1}$ : 3361, 2914, 1597, 1510;  $^1\text{H}$ -NMR data (400 MHz, acetone- $d_6$ )  $\delta_{\text{H}}$ : 14.08 (1H, s), 8.01 (1H, d,  $J$  = 8.8 Hz), 7.84 (1H, d,  $J$  = 15.0 Hz), 7.80 (1H, d,  $J$  = 15.0 Hz), 7.73 (2H, d,  $J$  = 8.4 Hz), 7.62 (1H, d,  $J$  = 15.6 Hz), 7.37 (1H, d,  $J$  = 1.6 Hz), 7.16 (1H, dd,  $J$  = 8.0, 1.6 Hz), 6.93 (2H, d,  $J$  = 8.4 Hz), 6.87 (1H, d,  $J$  = 8.0 Hz), 6.56 (1H, d,  $J$  = 8.8 Hz), 6.44 (1H, d,  $J$  = 15.6 Hz), 5.58 (1H, t,  $J$  = 7.5 Hz), 4.95 (1H, s), 3.92 (3H, s), 3.50 (2H, d,  $J$  = 7.5 Hz), 1.75 (3H, s).

Compound **A19** (artocarmin B): pale yellow gum; UV (MeOH)  $\lambda_{\max}$  nm (log  $\epsilon$ ): 213 (4.53), 272 (4.07), 316 (4.12); IR (neat)  $\nu_{\max}$   $\text{cm}^{-1}$ : 3425, 2916, 1620, 1082;  $^1\text{H}$ -NMR data (400 MHz, acetone- $d_6$ )  $\delta_{\text{H}}$ : 13.35 (1H, s), 7.92 (2H, d,  $J$  = 8.8 Hz), 7.59 (1H, d,  $J$  = 16.0 Hz), 7.54 (2H, d,  $J$  = 8.4 Hz), 7.01 (2H, d,  $J$  = 8.8 Hz), 6.87 (2H, d,  $J$  = 8.4 Hz),

6.63 (2H, s), 6.35 (1H, d,  $J = 16.0$  Hz), 5.67 (1H, t,  $J = 7.2$  Hz), 4.54 (2H, s), 3.44 (2H, d,  $J = 7.2$  Hz), 1.81 (3H, s);  $^{13}\text{C}$ -NMR data (100 MHz, acetone- $d_6$ )  $\delta_{\text{C}}$ : 182.4, 166.3, 164.0, 161.2, 160.9, 159.8, 159.0, 155.3, 145.4, 131.0, 129.2, 128.4, 127.4, 126.0, 122.0, 116.8, 116.6, 115.7, 110.0, 104.2, 103.4, 94.0, 70.2, 21.8, 14.2.

Compound **A20** (morachalcone A): brown gum; UV (MeOH)  $\lambda_{\text{max}}$  nm (log  $\epsilon$ ): 212 (4.50), 306 (3.91), 382 (4.06); IR (neat)  $\nu_{\text{max}}$   $\text{cm}^{-1}$ : 3400, 2916, 1604, 1458;  $^1\text{H}$ -NMR data (400 MHz, acetone- $d_6$ )  $\delta_{\text{H}}$ : 14.19 (1H, s), 8.21 (1H, d,  $J = 15.4$  Hz), 7.88 (1H, d,  $J = 9.0$  Hz), 7.80 (1H, d,  $J = 15.4$  Hz), 7.66 (1H, d,  $J = 8.6$  Hz), 6.55 (1H, d,  $J = 2.0$  Hz), 6.52 (1H, d,  $J = 9.0$  Hz), 6.43 (1H, dd,  $J = 8.6, 2.0$  Hz), 5.26 (1H, t,  $J = 7.2$  Hz), 3.35 (2H, d,  $J = 7.2$  Hz), 1.74 (3H, s), 1.64 (3H, s).

Compound **A21** (brosimone D): yellow gum;  $[\alpha]_{\text{D}}^{25} +144.9$  ( $c$  0.15, MeOH); UV (MeOH)  $\lambda_{\text{max}}$  nm (log  $\epsilon$ ): 214 (4.37), 266 (4.11), 368 (4.11); IR (neat)  $\nu_{\text{max}}$   $\text{cm}^{-1}$ : 3269, 2918, 1614, 1560, 1454;  $^1\text{H}$ -NMR data (400 MHz,  $\text{CDCl}_3$ )  $\delta_{\text{H}}$ : 13.27 (1H, s), 7.64 (1H, d,  $J = 8.4$  Hz), 6.56 (1H, brd,  $J = 8.4$  Hz), 6.49 (1H, s), 6.40 (1H, d,  $J = 17.0$  Hz), 6.38 (1H, brs), 6.24 (1H, d,  $J = 9.6$  Hz), 6.21 (1H, dd,  $J = 17.0, 7.0$  Hz), 5.42 (1H, d,  $J = 9.6$  Hz), 2.20 (1H, m), 1.95 (3H, s), 1.68 (3H, s), 1.14 (6H, d,  $J = 6.4$  Hz);  $^{13}\text{C}$ -NMR data (100 MHz,  $\text{CDCl}_3$ )  $\delta_{\text{C}}$ : 178.6, 161.1, 159.3, 158.1, 155.5, 155.4, 155.2, 143.7, 139.5, 125.5, 121.0, 119.6, 109.7, 109.6, 108.8, 105.2, 104.5, 93.8, 69.7, 32.4, 25.8, 22.4, 18.6.

Compound **A22** (cycloartocarpin): brown gum;  $[\alpha]_{\text{D}}^{25} +125.0$  ( $c$  0.32, MeOH); UV (MeOH)  $\lambda_{\text{max}}$  nm (log  $\epsilon$ ): 212 (4.36), 269 (3.98), 369 (3.98); IR (neat)  $\nu_{\text{max}}$   $\text{cm}^{-1}$ : 3377, 2918, 1697, 1610, 1548, 1442;  $^1\text{H}$ -NMR data (400 MHz,  $\text{CDCl}_3$ )  $\delta_{\text{H}}$ : 13.42 (1H, s), 7.64 (1H, d,  $J = 8.4$  Hz), 6.70 (1H, dd,  $J = 16.2, 7.0$  Hz), 6.57 (1H, d,  $J = 16.2$  Hz), 6.53 (1H, dd,  $J = 8.4, 2.4$  Hz), 6.42 (1H, d,  $J = 2.4$  Hz), 6.37 (1H, s), 6.26 (1H, d,  $J = 9.2$  Hz), 5.42 (1H, d,  $J = 9.2$  Hz), 3.93 (3H, s), 2.47 (1H, m), 1.95 (3H, s), 1.68 (3H, s), 1.11 (6H, d,  $J = 6.4$  Hz).

Compound **A23** (cudraflavone A): brown gum;  $[\alpha]_{\text{D}}^{25} +172.8$  ( $c$  0.11, MeOH); UV (MeOH)  $\lambda_{\text{max}}$  nm (log  $\epsilon$ ): 213 (4.57), 293 (4.36), 368 (4.27); IR (neat)  $\nu_{\text{max}}$   $\text{cm}^{-1}$ : 3350, 2916, 1618, 1558, 1456;  $^1\text{H}$ -NMR data (400 MHz,  $\text{CDCl}_3$ )  $\delta_{\text{H}}$ : 13.03 (1H, s), 7.65 (1H, d,  $J = 8.4$  Hz), 6.71 (1H, d,  $J = 8.4$  Hz), 6.70 (1H, d,  $J = 10.0$  Hz), 6.41 (1H, brs), 6.37

(1H, s), 6.25 (1H, d,  $J = 9.9$  Hz), 5.60 (1H, d,  $J = 9.9$  Hz), 5.42 (1H, d,  $J = 10.0$  Hz), 1.97 (3H, s), 1.70 (3H, s), 1.46 (6H, s).

Compound **A24** (cudraflavone B): brown gum; UV (MeOH)  $\lambda_{\max}$  nm (log  $\epsilon$ ): 212 (4.68), 280 (4.49), 336 (4.15); IR (neat)  $\nu_{\max}$   $\text{cm}^{-1}$ : 3400, 2916, 1610, 1456;  $^1\text{H}$ -NMR data (400 MHz, acetone- $d_6$ )  $\delta_{\text{H}}$ : 13.57 (1H, s), 7.20 (1H, d,  $J = 8.4$  Hz), 6.67 (1H, d,  $J = 10.0$  Hz), 6.56 (1H, d,  $J = 2.4$  Hz), 6.51 (1H, dd,  $J = 8.4, 2.4$  Hz), 6.27 (1H, s), 5.74 (1H, d,  $J = 10.0$  Hz), 5.11 (1H, t,  $J = 7.0$  Hz), 3.11 (2H, d,  $J = 7.0$  Hz), 1.57 (3H, s), 1.45 (6H, s), 1.42 (3H, s).

Compound **A25** (artogomezianone): pale yellow gum;  $[\alpha]_{\text{D}}^{25} +6.3$  ( $c$  0.16, MeOH); UV (MeOH)  $\lambda_{\max}$  nm (log  $\epsilon$ ): 210 (4.45), 275 (4.36), 318 (4.02); IR (neat)  $\nu_{\max}$   $\text{cm}^{-1}$ : 3282, 2929, 1633, 1610, 1448;  $^1\text{H}$ -NMR data (400 MHz, acetone- $d_6$ )  $\delta_{\text{H}}$ : 13.82 (1H, s), 7.31 (1H, d,  $J = 8.0$  Hz), 6.72 (1H, dd,  $J = 16.0, 7.2$  Hz), 6.66 (1H, s), 6.54 (1H, dd,  $J = 16.0, 2.4$  Hz), 6.53 (1H, dd,  $J = 8.0, 2.4$  Hz), 6.52 (1H, d,  $J = 2.4$  Hz), 4.81 (1H, s), 4.67 (1H, s), 4.38 (1H, m), 3.96 (3H, s), 2.78 (1H, dd,  $J = 13.8, 5.0$  Hz), 2.58 (1H, dd,  $J = 13.8, 8.4$  Hz), 2.43 (1H, m), 1.57 (3H, s), 1.08 (6H, d,  $J = 8.6$  Hz);  $^{13}\text{C}$ -NMR data (100 MHz, acetone- $d_6$ )  $\delta_{\text{C}}$ : 183.0, 163.1, 162.5, 160.7, 158.9, 156.6, 156.1, 147.9, 141.5, 131.9, 119.0, 116.1, 112.1, 109.6, 109.1, 107.4, 104.6, 103.3, 89.7, 73.1, 55.8, 33.1, 32.1, 22.2, 16.8.

Compound **A26** (lakoochanoside A): pale yellow gum;  $[\alpha]_{\text{D}}^{25} +35.6$  ( $c$  0.10, MeOH); UV (MeOH)  $\lambda_{\max}$  nm (log  $\epsilon$ ): 217 (4.49), 280 (3.72); IR (neat)  $\nu_{\max}$   $\text{cm}^{-1}$ : 3300, 2947, 1693, 1450;  $^1\text{H}$ -NMR data (400 MHz, MeOD- $d_4$ )  $\delta_{\text{H}}$ : 7.08 (2H, d,  $J = 8.6$  Hz), 6.70 (2H, d,  $J = 8.6$  Hz), 6.14 (1H, d,  $J = 2.0$  Hz), 5.93 (1H, d,  $J = 2.0$  Hz), 5.06 (1H, d,  $J = 7.2$  Hz), 3.92 (1H, dd,  $J = 12.0, 2.0$  Hz), 3.74 (1H, dd,  $J = 12.0, 5.2$  Hz), 3.47 (1H, dd,  $J = 8.4, 7.2$  Hz), 3.45 (1H, t,  $J = 8.4$  Hz), 3.44 (1H, m), 3.42 (1H, dd,  $J = 9.2, 8.4$  Hz), 2.88 (2H, brd,  $J = 1.2$  Hz);  $^{13}\text{C}$ -NMR data (100 MHz, MeOD- $d_4$ )  $\delta_{\text{C}}$ : 206.1, 168.9, 162.4, 156.4, 134.0, 130.4, 116.1, 106.0, 102.0, 97.9, 96.4, 78.5, 78.4, 74.8, 71.1, 62.4, 31.0.

Compound **A27** (lakoochanoside B): pale yellow gum;  $[\alpha]_{\text{D}}^{25} -78.1$  ( $c$  0.32, MeOH); UV (MeOH)  $\lambda_{\max}$  nm (log  $\epsilon$ ): 215 (4.51), 277 (3.58); IR (neat)  $\nu_{\max}$   $\text{cm}^{-1}$ : 3346, 1606, 1439;  $^1\text{H}$ -NMR data (400 MHz, MeOD- $d_4$ )  $\delta_{\text{H}}$ : 7.18 (2H, d,  $J = 8.8$  Hz), 6.76 (2H, d,  $J = 8.8$  Hz), 4.62 (1H, d,  $J = 8.0$  Hz), 4.22 (1H, d,  $J = 1.6$  Hz), 3.90 (1H, ddd,  $J = 8.8,$



8.0, 5.8 Hz), 3.66 (1H, dq,  $J = 9.6, 6.4$  Hz), 3.55 (1H, dd,  $J = 9.6, 3.2$  Hz), 3.44 (1H, dd,  $J = 3.2, 1.6$  Hz), 3.27 (1H, t,  $J = 9.6$  Hz), 2.87 (1H, dd,  $J = 16.0, 5.8$  Hz), 2.61 (1H, dd,  $J = 16.0, 8.8$  Hz), 1.22 (1H, d,  $J = 6.4$  Hz);  $^{13}\text{C}$ -NMR data (100 MHz, MeOD- $d_4$ )  $\delta_{\text{C}}$ : 158.3, 157.7, 157.4, 156.7, 131.1, 129.3, 116.0, 102.1, 100.7, 81.0, 76.1, 73.9, 72.2, 71.9, 70.2, 28.1, 17.9.

Compound **A28** ((+)-afzelechin-3- $O$ - $\alpha$ -L-rhamnopyranoside): brown gum;  $[\alpha]^{25}_{\text{D}} -32.2$  ( $c$  0.28, MeOH); UV (MeOH)  $\lambda_{\text{max}}$  nm ( $\log \epsilon$ ): 213 (4.42), 275 (3.56); IR (neat)  $\nu_{\text{max}}$   $\text{cm}^{-1}$ : 3383, 1602;  $^1\text{H}$ -NMR data (400 MHz, MeOD- $d_4$ )  $\delta_{\text{H}}$ : 7.23 (2H, d,  $J = 8.4$  Hz), 6.80 (2H, d,  $J = 8.4$  Hz), 5.96 (1H, d,  $J = 2.2$  Hz), 5.87 (1H, d,  $J = 2.2$  Hz), 4.67 (1H, d,  $J = 8.0$  Hz), 4.27 (1H, d,  $J = 2.0$  Hz), 3.94 (1H, ddd,  $J = 8.8, 8.0, 5.6$  Hz), 3.70 (1H, dd,  $J = 9.6, 6.4$  Hz), 3.58 (1H, dd,  $J = 9.6, 3.2$  Hz), 3.48 (1H, dd,  $J = 3.2, 1.6$  Hz), 3.31 (1H, t,  $J = 9.5$  Hz), 2.91 (1H, dd,  $J = 16.0, 5.6$  Hz), 2.66 (1H, dd,  $J = 16.0, 8.8$  Hz), 1.26 (1H, d,  $J = 6.4$  Hz);  $^{13}\text{C}$ -NMR data (100 MHz, MeOD- $d_4$ )  $\delta_{\text{C}}$ : 158.4, 157.9, 157.5, 156.8, 131.2, 129.4, 116.1, 102.2, 100.7, 96.5, 95.5, 81.1, 76.2, 73.9, 72.2, 71.9, 70.3, 28.1, 17.9.

Compound **A29** ((+)-catechin-3- $O$ - $\alpha$ -L-rhamnopyranoside): brown gum;  $[\alpha]^{25}_{\text{D}} -43.8$  ( $c$  0.48, MeOH); UV (MeOH)  $\lambda_{\text{max}}$  nm ( $\log \epsilon$ ): 213 (4.49), 280 (3.72); IR (neat)  $\nu_{\text{max}}$   $\text{cm}^{-1}$ : 3340, 1606;  $^1\text{H}$ -NMR data (400 MHz, MeOD- $d_4$ )  $\delta_{\text{H}}$ : 6.84 (1H, d,  $J = 2.0$  Hz), 6.77 (1H, d,  $J = 8.4$  Hz), 6.72 (1H, dd,  $J = 8.4, 2.0$  Hz), 5.94 (1H, d,  $J = 2.2$  Hz), 5.86 (1H, d,  $J = 2.2$  Hz), 4.62 (1H, d,  $J = 7.6$  Hz), 4.30 (1H, d,  $J = 1.6$  Hz), 3.93 (1H, ddd,  $J = 8.4, 7.6, 5.6$  Hz), 3.68 (1H, dd,  $J = 9.4, 6.2$  Hz), 3.58 (1H, dd,  $J = 9.4, 3.4$  Hz), 3.52 (1H, dd,  $J = 3.4, 1.6$  Hz), 3.31 (1H, m), 2.87 (1H, dd,  $J = 16.0, 5.6$  Hz), 2.64 (1H, dd,  $J = 16.0, 8.4$  Hz), 1.25 (1H, d,  $J = 6.0$  Hz);  $^{13}\text{C}$ -NMR data (100 MHz, MeOD- $d_4$ )  $\delta_{\text{C}}$ : 158.0, 157.6, 156.9, 146.4, 146.3, 132.0, 119.8, 116.1, 115.1, 102.1, 100.7, 96.4, 95.5, 81.1, 76.0, 74.0, 72.3, 72.0, 70.3, 28.1, 17.9.

Compound **A30** ((+)-catechin): brown gum;  $[\alpha]^{25}_{\text{D}} -4.0$  ( $c$  0.25, MeOH); UV (MeOH)  $\lambda_{\text{max}}$  nm ( $\log \epsilon$ ): 214 (4.44), 281 (3.76); IR (neat)  $\nu_{\text{max}}$   $\text{cm}^{-1}$ : 3163, 1604;  $^1\text{H}$ -NMR data (400 MHz, acetone- $d_6$ )  $\delta_{\text{H}}$ : 8.24 (1H, s), 8.06 (1H, s), 7.97 (1H, s), 7.91 (1H, s), 6.89 (1H, d,  $J = 1.2$  Hz), 6.79 (1H, d,  $J = 8.0$  Hz), 6.75 (1H, dd,  $J = 8.0, 1.2$  Hz), 6.02 (1H, d,  $J = 2.0$  Hz), 5.87 (1H, d,  $J = 2.0$  Hz), 4.55 (1H, d,  $J = 7.6$  Hz), 3.99 (1H, m), 2.91 (1H, dd,  $J = 16.0, 5.4$  Hz), 2.52 (1H, dd,  $J = 16.0, 8.4$  Hz);  $^{13}\text{C}$ -NMR data (100 MHz,

acetone- $d_6$ )  $\delta_C$ : 156.9, 157.8, 157.2, 145.8, 145.7, 132.2, 120.1, 115.8, 115.3, 100.7, 96.2, 95.5, 82.7, 68.4, 28.8.

Compound **A31** (oxyresveratrol): brown gum; UV (MeOH)  $\lambda_{\max}$  nm (log  $\epsilon$ ): 214 (4.30), 304 (4.10) 281 (3.68); IR (neat)  $\nu_{\max}$   $\text{cm}^{-1}$ : 3280, 1591;  $^1\text{H}$ -NMR data (400 MHz, acetone- $d_6$ )  $\delta_H$ : 7.40 (1H, d,  $J$  = 8.4 Hz), 7.33 (1H, d,  $J$  = 16.4 Hz), 6.89 (1H, d,  $J$  = 16.4 Hz), 6.52 (2H, d,  $J$  = 2.4 Hz), 6.44 (1H, d,  $J$  = 2.4 Hz), 6.38 (1H, dd,  $J$  = 8.4, 2.4 Hz), 6.24 (1H, t,  $J$  = 2.4 Hz).

Compound **A32** (resveratrol): brown gum; UV (MeOH)  $\lambda_{\max}$  nm (log  $\epsilon$ ): 211 (4.28), 304 (4.10) 385 (4.16); IR (neat)  $\nu_{\max}$   $\text{cm}^{-1}$ : 3377, 1593;  $^1\text{H}$ -NMR data (400 MHz, acetone- $d_6$ )  $\delta_H$ : 7.41 (2H, d,  $J$  = 8.6 Hz), 7.01 (1H, d,  $J$  = 16.0 Hz), 6.88 (1H, d,  $J$  = 16.0 Hz), 6.84 (2H, d,  $J$  = 8.6 Hz), 6.53 (2H, d,  $J$  = 2.0 Hz), 6.27 (1H, t,  $J$  = 2.0 Hz).

Compound **A33** (sanggenofuran B): brown gum; UV (MeOH)  $\lambda_{\max}$  nm (log  $\epsilon$ ): 218 (4.59), 332 (4.49); IR (neat)  $\nu_{\max}$   $\text{cm}^{-1}$ : 3395, 2925, 1609;  $^1\text{H}$ -NMR data (500 MHz, acetone- $d_6$ )  $\delta_H$ : 7.45 (1H, d,  $J$  = 8.5 Hz), 7.10 (1H, d,  $J$  = 2.0 Hz), 6.94 (1H, s), 6.93 (2H, s), 6.86 (1H, dd,  $J$  = 8.5, 2.0 Hz), 5.34 (1H, t,  $J$  = 7.0 Hz), 3.86 (3H, s), 3.40 (2H, d,  $J$  = 7.0 Hz), 1.80 (3H, s), 1.62 (3H, s).

Compound **A34** (integrin): brown gum; UV (MeOH)  $\lambda_{\max}$  nm (log  $\epsilon$ ): 203 (4.16), 261 (3.71), 317 (3.60); IR (neat)  $\nu_{\max}$   $\text{cm}^{-1}$ : 3308, 2931, 1652, 1423;  $^1\text{H}$ -NMR data (500 MHz, acetone- $d_6$ )  $\delta_H$ : 13.12 (1H, s), 7.22 (1H, d,  $J$  = 8.5 Hz), 6.64 (1H, d,  $J$  = 2.0 Hz), 6.58 (1H, dd,  $J$  = 8.5, 2.0 Hz), 6.28 (1H, d,  $J$  = 2.0 Hz), 6.22 (1H, d,  $J$  = 2.0 Hz), 5.07 (1H, t,  $J$  = 6.5 Hz), 3.79 (3H, s), 3.00 (2H, d,  $J$  = 6.5 Hz), 1.57 (3H, s), 1.39 (3H, s).

Compound **A35** (engeletin): brown gum;  $[\alpha]_D^{20}$  -2.3 ( $c$  0.04, MeOH); UV (MeOH)  $\lambda_{\max}$  nm (log  $\epsilon$ ): 227 (4.12), 293 (3.83); IR (neat)  $\nu_{\max}$   $\text{cm}^{-1}$ : 3399, 2915, 1600, 1450;  $^1\text{H}$ -NMR data (500 MHz, acetone- $d_6$ )  $\delta_H$ : 12.02 (1H, s), 7.42 (2H, d,  $J$  = 8.5 Hz), 6.90 (2H, d,  $J$  = 8.5 Hz), 5.91 (1H, d,  $J$  = 2.0 Hz), 5.89 (1H, d,  $J$  = 2.0 Hz), 5.18 (1H, d,  $J$  = 11.0 Hz), 4.65 (1H, d,  $J$  = 11.0 Hz), 4.26 (1H, dd,  $J$  = 9.3, 3.2 Hz), 4.04 (1H, brs) 3.65 (1H, dd,  $J$  = 9.3, 3.2 Hz), 3.54 (1H, m), 3.31 (1H, t,  $J$  = 9.5 Hz), 1.14 (3H, d,  $J$  = 6.5 Hz).

Compound **A36** (*trans*-2-methoxy-4,3',5'-trihydroxystilbene): brown gum; UV (MeOH)  $\lambda_{\text{max}}$  nm (log  $\epsilon$ ): 213 (4.05), 281 (3.55), 331 (3.37); IR (neat)  $\nu_{\text{max}}$   $\text{cm}^{-1}$ : 3406, 1600;  $^1\text{H}$ -NMR data (500 MHz, acetone- $d_6$ )  $\delta_{\text{H}}$ : 7.46 (1H, d,  $J = 8.5$  Hz), 7.30 (1H, d,  $J = 16.5$  Hz), 6.88 (1H, d,  $J = 16.5$  Hz), 6.52 (2H, d,  $J = 2.0$  Hz), 6.50 (1H, d,  $J = 2.0$  Hz), 6.46 (1H, dd,  $J = 8.5, 2.0$  Hz), 6.25 (1H, t,  $J = 2.0$  Hz), 3.84 (3H, s).



ลิขสิทธิ์มหาวิทยาลัยเชียงใหม่  
Copyright© by Chiang Mai University  
All rights reserved

## CHAPTER 3

### Results and discussion

#### 3.1 Isolated compounds of the twigs of *Artocarpus heterophyllus*

The methanolic extract of twigs of *A. heterophyllus* was isolated to give four new compounds (**A1-A4**), together with twenty-one known compounds (**A5-A25**). The structures were identified by spectroscopic data.

##### 3.1.1 Compound A1

Compound **A1** was obtained as a pale yellow gum with the molecular formula  $C_{21}H_{16}O_5$  by HRESI-TOFMS ( $m/z$  349.1076  $[M+H]^+$ ). The UV spectrum showed maximum absorption bands at  $\lambda_{max}$  224, 245, 275 and 310 nm, suggesting the presence of a benzofuran chromophore (Trisuwan *et al.*, 2011), while the IR spectrum showed absorption bands for hydroxy ( $3420\text{ cm}^{-1}$ ) and double bond ( $1645\text{ cm}^{-1}$ ) functional groups. The  $^1\text{H}$ -NMR spectrum (**Table 3.1**) (**Figure 5**) showed signals of the three aromatic protons of a 1,2,4-trisubstituted benzene ring [ $\delta$  7.38 (d,  $J = 8.4\text{ Hz}$ , 1H), 6.81 (d,  $J = 2.0\text{ Hz}$ , 1H) and 6.76 (dd,  $J = 8.4, 2.0\text{ Hz}$ , 1H)], three singlet aromatic protons ( $\delta$  6.97, 6.87 and 6.85, each s, 1H), and a dimethylchromene ring [ $\delta$  6.64 and 5.64 (each d,  $J = 10.0\text{ Hz}$ , 1H) and 1.40 (s, 6H)]. Compound **A1** displayed carbon resonances for twenty-one carbons from the  $^{13}\text{C}$ -NMR and DEPT135 spectra (**Table 3.1**) (**Figure 6**), including eleven quaternary carbons ( $\delta$  155.6, 154.7, 154.1, 154.0, 153.6 (2C), 151.5, 122.8, 113.8, 101.2 and 76.3), eight methines ( $\delta$  129.6, 121.2, 116.2, 112.1, 105.6, 103.9, 101.6 and 98.2), and two methyls ( $\delta$  27.8 (2C)). Three aromatic protons resonating at  $\delta$  7.38, 6.81 and 6.76 were assigned as H-4', H-7' and H-5', respectively, on the basis of their multiplicities and coupling constants. The aromatic proton H-4' showed HMBC correlations with C-3' ( $\delta$  98.2), C-3'a ( $\delta$  122.8), C-6' ( $\delta$  155.6) and C-7'a ( $\delta$  153.6), H-7' was correlated with C-3'a, C-5', C-6' and C-7'a, and H-5' showed HMBC correlations with

C-3'a, C-6' and C-7'a. These data together with the chemical shifts of C-3'a, C-6' and C-7'a helped construct 2-substituted benzofuran moiety with the hydroxy group at C-6', supporting the benzofuran chromophore observed in the UV spectrum. The aromatic proton resonating at  $\delta$  6.87 was assigned at H-3 and showed HMBC cross peaks with C-2 ( $\delta$  154.1), C-3a ( $\delta$  113.8), C-4 ( $\delta$  151.5) and C-9a ( $\delta$  154.7). The remaining singlet aromatic proton at  $\delta$  6.85 was then assigned as H-9 on the basis of HMBC correlations with C-3a, C-4a ( $\delta$  101.2) and C-9a. The lower field olefinic proton of the dimethylchromene ring, H-5 ( $\delta$  6.64), displayed HMBC correlations with C-4, C-4a and C-8a ( $\delta$  154.0). These data established the 2-substituted benzofuran subunit with a hydroxy group at C-4 and a dimethylchromene ring which was fused to C-4a and C-8a with an ether linkage at C-8a. The HMBC correlation between H-3 of this benzofuran subunit and C-2' of the other benzofuran moiety indicated that the two benzofuran subunits were linked between C-2 and C-2'. Therefore, compound **A1** was identified as a new benzofuran derivative named heterophyllene A.

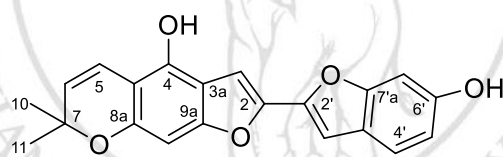


**Figure 3.1** The structure of heterophyllene A (**A1**)

**Table 3.1** The NMR data (400 MHz,  $\text{CDCl}_3$ ) of heterophyllene A (**A1**)

position	$\delta_{\text{H}}$ , mult. ( $J$ in Hz)	$\delta_{\text{C}}$ (Type)	HMBC	COSY
2	-	154.1 (C)	-	-
3	6.87, s	105.6 (CH)	C-2, C-3a, C-4, C-9a, C-2'	-
3a	-	113.8 (C)	-	-
4	-	151.5 (C)	-	-
4a	-	101.2 (C)	-	-
5	6.64, d (10.0)	116.2 (CH)	C-4, C-4a, C-7, C-8a	H-6
6	5.64, d (10.0)	129.6 (CH)	C-7, C-10	H-5
7	-	76.3 (C)	-	-

**Table 3.1** (continued)

position	$\delta_{\text{H}}$ , mult. ( $J$ in Hz)	$\delta_{\text{C}}$ (Type)	HMBC	COSY
8a	-	154.0 (C)	-	-
9	6.85, s	101.6 (CH)	C-3a, C-4a, C-9a	-
9a	-	154.7 (C)	-	-
10	1.40, s	27.8 (CH <sub>3</sub> )	C-6, C-7, C-11	H-11
11	1.40, s	27.8 (CH <sub>3</sub> )	C-6, C-7, C-10	H-10
2'	-	153.6 (C)	-	-
3'	6.97, s	98.2 (CH)	C-2', C-3'a, C-7'a	-
3'a	-	122.8 (C)	-	-
4'	7.38, d (8.4)	121.2 (CH)	C-3', C-3'a, C-6', C-7'a	H-5'
5'	6.76, dd (8.4, 2.0)	112.1 (CH)	C-3'a, C-6', C-7'a	H-4', H-7'
6'	-	155.6 (C)	-	-
7'	6.81, d (2.0)	103.9 (CH)	C-3'a, C-5', C-6', C-7'a	H-5'
7'a	-	153.6 (C)	-	-

### 3.1.2 Compound A2

Compound **A2** was isolated as a pale yellow gum with the molecular formula C<sub>19</sub>H<sub>18</sub>O<sub>4</sub> from HRESI-TOFMS ( $m/z$  311.1287 [M+H]<sup>+</sup>). The UV spectrum displayed absorption bands at  $\lambda_{\text{max}}$  226, 248 and 265 nm, whereas the IR spectrum showed hydroxy (3400 cm<sup>-1</sup>) and double bond (1667 cm<sup>-1</sup>) functional groups. The <sup>1</sup>H and <sup>13</sup>C-NMR spectral data of compound **A2** (Table 3.2) (Figure 7 and Figure 8) consisted of signals for a 2-substituted-6-hydroxy benzofuran moiety [ $\delta$  7.39 (d,  $J$  = 8.4 Hz, 1H), 6.95 (s, 1H), 6.93 (d,  $J$  = 2.0 Hz, 1H), 6.81 (dd,  $J$  = 8.4, 2.0 Hz, 1H),  $\delta$  157.4, 156.8, 155.4, 122.7, 122.0, 113.3, 104.1 and 102.1]. Additionally, the <sup>1</sup>H-NMR spectrum showed signals for a *trans*-3-methyl-1-butenyl subunit [ $\delta$  6.72 (d,  $J$  = 16.4 Hz, 1H), 6.71 (dd,  $J$  = 16.4, 6.4 Hz, 1H), 2.44 (m, 1H) and 1.09 (d,  $J$  = 6.4 Hz, 6H)], and two *meta*-coupled aromatic protons ( $\delta$  6.96 and 6.90, each d,  $J$  = 2.0 Hz, 1H). The presence of the *trans*-3-methyl-1-butenyl subunit was confirmed by <sup>1</sup>H-<sup>1</sup>H COSY correlations between the methine proton

H-16 ( $\delta$  2.44) with the methyl groups, H<sub>3</sub>-17 and H<sub>3</sub>-18 ( $\delta$  1.09), and one of the *trans*-coupled olefinic protons H-15 ( $\delta$  6.71). The *trans*-3-methyl-1-butenyl subunit was attached at C-9 ( $\delta$  130.0) position of the benzene ring according to HMBC correlations of the *trans*-olefinic proton H-14 ( $\delta$  6.72) with C-8 ( $\delta$  122.7), C-9, and C-10 ( $\delta$  98.5). The *meta*-coupled aromatic proton resonating at  $\delta$  6.96 was assigned as H-10 due to its HMQC correlations with C-10. Thus, the remaining *meta*-coupled aromatic proton at  $\delta$  6.90 was attributed to H-12 which displayed HMBC correlations with C-11 ( $\delta$  156.8) and C-13 ( $\delta$  157.4). The hydroxy groups were identified as substituents at C-11 and C-13 according to their chemical shifts. The HMBC correlation between H-3 ( $\delta$  6.95) of the benzofuran subunit and C-8 of the tetrasubstituted benzene ring was used to construct the 2-arylbenzofuran. Consequently, compound **A2** was identified as a new arylbenzofuran derivative named heterophyllene B.

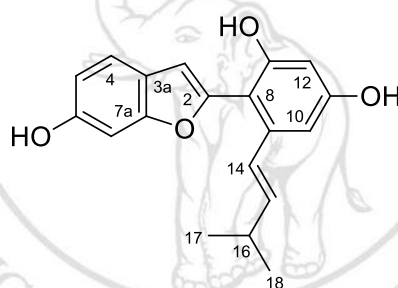


**Figure 3.2** The structure of heterophyllene B (**A2**)

**Table 3.2** The NMR data (400 MHz, acetone-*d*<sub>6</sub>) of heterophyllene B (**A2**)

position	$\delta_{\text{H}}$ , mult. ( <i>J</i> in Hz)	$\delta_{\text{C}}$ (Type)	HMBC	COSY
2	-	155.4 (C)	-	-
3	6.95, s	102.1 (CH)	C-4, C-5, C-8	-
3a	-	122.7 (C)	-	-
4	7.39, d (8.4)	122.0 (CH)	C-3, C-5, C-6	H-5
5	6.81, dd (8.4, 2.0)	113.3 (CH)	C-3a, C-4, C-6, C-7	H-4, H-7
6	-	157.4 (C)	-	-
7	6.93, d (2.0)	104.1 (CH)	C-5, C-6, C-7a	H-5
7a	-	156.8 (C)	-	-

**Table 3.2** (continued)

position	$\delta_{\text{H}}$ , mult. ( $J$ in Hz)	$\delta_{\text{C}}$ (Type)	HMBC	COSY
8	-	122.7 (C)	-	-
9	-	130.0 (C)	-	-
10	6.96, d (2.0)	98.5 (CH)	C-8, C-9, C-11	H-12
11	-	156.8 (C)	-	-
12	6.90, d (2.0)	104.1 (CH)	C-11, C-13	H-10
13	-	157.4 (C)	-	-
14	6.72, d (16.4)	119.1 (CH)	C-8, C-9, C-10, C-15	H-15
15	6.71, dd (16.4, 6.4)	142.1 (CH)	C-14, C-16, C-17, C-18	H-14, H-16
16	2.44, m	34.0 (CH)	C-14, C-15, C-17, C-18	H-15, H-17, H-18
17	1.09, d (6.4)	23.3 (CH <sub>3</sub> )	C-15, C-16	H-16
18	1.09, d (6.4)	23.3 (CH <sub>3</sub> )	C-15, C-16	H-16

### 3.1.3 Compound A3

Compound **A3** was isolated as a pale yellow gum with the molecular formula  $\text{C}_{19}\text{H}_{20}\text{O}_6$  from HRESI-TOFMS ( $m/z$  367.1156  $[\text{M}+\text{Na}]^+$ ). The UV and IR spectra of compound **A3** were similar to those of compound **A2**. The  $^1\text{H}$  and  $^{13}\text{C}$ -NMR data of compound **A3** (Table 3.3) (Figure 9 and Figure 10) consisted of the signals of 2-substituted-6-hydroxy benzofuran moiety [ $\delta$  7.39 (d,  $J = 8.4$  Hz, 1H), 6.98 (s, 1H), 6.97 (d,  $J = 2.1$  Hz, 1H), 6.80 (dd,  $J = 8.4, 2.1$  Hz, 1H),  $\delta$  155.9 (2C), 155.3, 121.9, 120.0, 113.1, 101.7 and 98.4] Additionally, the  $^1\text{H}$ -NMR spectrum showed signals for two singlet aromatic protons ( $\delta$  6.91, s, 2H), and a 2,3-dihydroxy-3-methylbutyl subunit [ $\delta$  3.63 (dd,  $J = 9.6, 2.0$  Hz, 1H), 3.24 (dd,  $J = 14.0, 2.0$  Hz, 1H), 2.57 (dd,  $J = 14.0, 9.6$  Hz, 1H), 1.26 and 1.25, each s, 3H]. The 2,3-dihydroxy-3-methylbutyl fragment was confirmed by the  $^1\text{H}$ - $^1\text{H}$  COSY correlations between the nonequivalent methylene protons, H<sub>2</sub>-14 ( $\delta$  3.24 and 2.57), and the oxymethine proton H-15 ( $\delta$  3.63) as well as the HMBC correlations of the methyl groups H<sub>3</sub>-17 ( $\delta$  1.26) and H<sub>3</sub>-18 ( $\delta$  1.25) with C-15



( $\delta$  81.2), and C-16 ( $\delta$  72.6). The two equivalent aromatic protons resonating as  $\delta$  6.91 were assigned as H-9 and H-13 according to HMQC correlations with C-9 ( $\delta$  104.6) and C-13 ( $\delta$  104.6), respectively, as well as the HMBC correlations; H-9/C-8 ( $\delta$  130.1), C-10 ( $\delta$  157.2), and C-11 ( $\delta$  113.1) and H-13/C-8, C-11, and C-12 ( $\delta$  157.2). The chemical shifts of C-10 and C-12 showed the hydroxy substituents at C-10 and C-12. The attachment of the 2,3-dihydroxy-3-methylbutyl subunit at C-11 of the benzene ring was supported by HMBC cross peaks of H<sub>2</sub>-14 with C-10, C-11 and C-12. The HMBC cross peak between H-3 ( $\delta$ <sub>H</sub> 6.98) of the benzofuran moiety with C-8 of the tetrasubstituted benzene ring was constructed the 2-arylbenzofuran. The absolute configuration at C-15 of compound **A3** was determined by the comparison of the specific rotation of (2*R*)-1,2-dihydroxy-1,1-dimethyl-3-phenylpropane (Hanessian *et al.*, 1998). The specific rotation of compound **A3**,  $[\alpha]^{25}_{\text{D}} +48.2$  ( $c = 0.53$ , CHCl<sub>3</sub>), was similar to (2*R*)-1,2-dihydroxy-1,1-dimethyl-3-phenylpropane,  $[\alpha]^{25}_{\text{D}} +52.0$  ( $c = 0.7$ , CHCl<sub>3</sub>), thus the absolute configuration at C-15 was assigned as *R*-configuration. Therefore, compound **A3** was identified as a new benzofuran derivative named heterophyllene C.

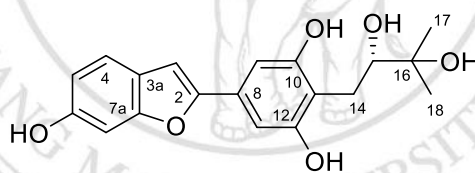


**Figure 3.3** The structure of heterophyllene C (**A3**)

**Table 3.3** The NMR data (400 MHz, acetone-*d*<sub>6</sub>) of heterophyllene C (**A3**)

position	$\delta_{\text{H}}$ , mult. ( <i>J</i> in Hz)	$\delta_{\text{C}}$ (Type)	HMBC	COSY
2	-	155.9 (C)	-	-
3	6.98, s	98.4 (CH)	C-4, C-8	-
3a	-	120.0 (C)	-	-
4	7.39, d (8.4)	121.9 (CH)	C-3, C-5, C-6	H-5
5	6.80, dd (8.4, 2.1)	113.1 (CH)	C-4, C-6, C-7	H-4, H-6
6	-	155.9 (C)	-	-
7	6.97, d (2.1)	101.7 (CH)	C-5, C-6, C-7a	H-5
7a	-	155.3 (C)	-	-

**Table 3.3** (continued)

position	$\delta_{\text{H}}$ , mult. ( $J$ in Hz)	$\delta_{\text{C}}$ (Type)	HMBC	COSY
8	-	130.1 (C)	-	-
9	6.91, s	104.6 (CH)	C-8, C-10, C-11	-
10	-	157.2 (C)	-	-
11	-	113.1 (C)	-	-
12	-	157.2 (C)	-	-
13	6.91, s	104.6 (CH)	C-8, C-11, C-12	-
14	a: 3.24, dd (14.0, 2.0) b: 2.57, dd (14.0, 9.6)	26.8 (CH <sub>2</sub> )	C-11, C-15, C-16	H <sub>b</sub> -14, H-15 H <sub>a</sub> -14, H-15
15	3.63, dd (9.6, 2.0)	81.2 (CH)	C-11, C-14, C-16	H <sub>2</sub> -14
16	-	72.6 (C)	-	-
17	1.26, s	26.0 (CH <sub>3</sub> )	C-15, C-16	-
18	1.25, s	25.0 (CH <sub>3</sub> )	C-15, C-16	-

### 3.1.4 Compound A4

Compound **A4** was obtained as a yellow gum with the molecular formula C<sub>16</sub>H<sub>16</sub>O<sub>4</sub> from HRESI-TOFMS ( $m/z$  295.0965 [M+Na]<sup>+</sup>). The UV spectrum displayed absorption bands at  $\lambda_{\text{max}}$  228, 300 and 334 nm, while the IR spectrum showed hydroxy (3389 cm<sup>-1</sup>) and double bond (1640 cm<sup>-1</sup>) functional groups. The <sup>1</sup>H-NMR spectrum (**Table 3.4**) (**Figure 11**) displayed characteristic signals for the three aromatic protons of a 1,2,4-trisubstituted benzene ring [ $\delta$  7.43 (d,  $J$  = 8.8 Hz, 1H), 6.45 (d,  $J$  = 2.4 Hz, 1H) and 6.40 (dd,  $J$  = 8.8, 2.4 Hz, 1H)], three aromatic protons of a 1,3,5-trisubstituted benzene ring [ $\delta$  6.69 (d,  $J$  = 2.4 Hz, 2H) and 6.35 (d,  $J$  = 2.4 Hz, 1H)], *trans*-coupled olefinic protons ( $\delta$  7.42 and 7.01, each d,  $J$  = 17.2 Hz, 1H), and two methoxyl groups ( $\delta$  3.80, s, 6H). The <sup>13</sup>C-NMR and DEPT135 spectra (**Figure 12**) showed thirteen carbon signal resonances for sixteen carbons; six quaternary carbons ( $\delta$  162.1 (2C), 159.2, 157.0, 141.7 and 117.1), eight methines ( $\delta$  128.6, 126.3, 125.1, 108.4, 104.8 (2C), 103.5 and 99.8), and two methoxyls ( $\delta$  55.6 (2C)). Three aromatic protons, which appeared at

$\delta$  7.43, 6.45 and 6.40, were assigned as H-6, H-3 and H-5, respectively, according to their multiplicities, coupling constants and HMBC correlations; H-3/C-1 ( $\delta$  117.1), C-2 ( $\delta$  157.0), C-4 ( $\delta$  159.2), and C-5 ( $\delta$  108.4); H-5/C-1, C-3 and C-4; H-6/C-1, and C-4. The substituents at C-2 and C-4 were identified as two hydroxy groups on the basis of their chemical shifts. One of the *trans*-olefinic proton H-7 ( $\delta$  7.42) showed HMBC cross peaks with C-1, C-2, and C-6 ( $\delta$  125.1) of the 1,2,4-trisubstituted benzene ring while the other one H-8 ( $\delta$  7.01) was correlated with C-1' ( $\delta$  141.7), C-2' ( $\delta$  104.8), and C-6' ( $\delta$  104.8) of the 1,3,5-trisubstituted benzene ring. Two equivalent aromatic protons ( $\delta$  6.69) were attributed to H-2' and H-6' according to their HMQC correlations with C-2' and C-6'. Accordingly, the remaining aromatic proton ( $\delta$  6.35) was assigned at H-4' on the basis of the coupling constants. Thus, the equivalent methoxyl groups H<sub>3</sub>-7' and H<sub>3</sub>-8' ( $\delta$  3.80) were located at C-3' ( $\delta$  162.1), and C-5' ( $\delta$  162.1), respectively. Consequently, compound **A4** was identified as 3',5'-dimethoxy-2,4-dihydroxystilbene named heterophyllene D.

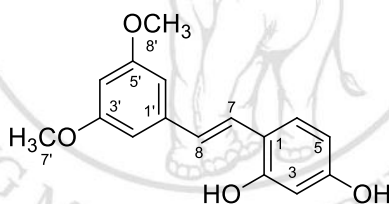


**Figure 3.4** The structure of heterophyllene D (**A4**)

**Table 3.4** The NMR data (400 MHz, acetone-*d*<sub>6</sub>) of heterophyllene D (**A4**)

position	$\delta_{\text{H}}$ , mult. ( <i>J</i> in Hz)	$\delta_{\text{C}}$ (Type)	HMBC	COSY
1	-	117.1 (C)	-	-
2	-	157.0 (C)	-	-
3	6.45, d (2.4)	103.5 (CH)	C-1, C-2, C-4, C-5	H-5
4	-	159.4 (C)	-	-
5	6.40, dd (8.8, 2.4)	108.4 (CH)	C-1, C-3, C-4	H-3, H-6
6	7.43, d (8.8)	125.1 (CH)	C-1, C-4	H-5
7	7.42, d (17.2)	128.6 (CH)	C-1, C-2, C-6	H-8

**Table 3.4** (continued)

position	$\delta_{\text{H}}$ , mult. ( $J$ in Hz)	$\delta_{\text{C}}$ (Type)	HMBC	COSY
8	7.01, d (17.2)	126.3 (CH)	C-1', C-2', C-6'	H-7
1'	-	141.7 (C)	-	-
2'	6.69, d (2.4)	104.8 (CH)	C-7, C-1', C-3', C-4'	H-4'
3'	-	162.1 (C)	-	-
4'	6.35, d (2.4)	99.8 (CH)	C-2', C-3', C-5', C-6'	H-2', H-6'
5'	-	162.1 (C)	-	-
6'	6.69, d (2.4)	104.8 (CH)	C-8, C-1', C-4', C-5'	H-4'
7'	3.80, s	55.6 (CH <sub>3</sub> )	C-3'	-
8'	3.80, s	55.6 (CH <sub>3</sub> )	C-5'	-

### 3.1.5 Compounds A5-A7

Compound **A5**, a brown gum, was a 2-arylbenzofuran derivative. The <sup>1</sup>H-NMR spectrum (Table 3.5) (Figure 13) of compound **A5** were similar to that of compound **A3** (Table 3.3) (Figure 3.3) except for the disappearance of 2,3-dihydroxy-3-methylbutyl subunit in compound **A3**, and the additional signal of triplet aromatic proton ( $\delta$  6.36, t,  $J$  = 2.4 Hz, 1H) in compound **A5**. Compound **A5** was identified as moracin M (Basnet *et al.*, 1993). Compound **A6**, a brown gum, had a same characteristic pattern of the <sup>1</sup>H-NMR data to compound **A5** (Table 3.5) (Figure 3.5). The main difference was found that the <sup>1</sup>H-NMR data (Table 3.5) (Figure 14) of compound **A6** displayed a prenyl unit [ $\delta$  5.26 (t,  $J$  = 7.2 Hz, 1H), 3.32 (d,  $J$  = 7.2 Hz, 2H), 1.78 and 1.67, each s, 3H] instead of the triplet aromatic proton in compound **A5**. Thus, the prenyl unit was located at C-11. Compound **A6** was assigned as moracin C (Kim *et al.*, 2012). Compound **A7**, a brown gum, showed 2-substituted-6-hydroxy benzofuran moiety [ $\delta$  7.42 (d,  $J$  = 8.4 Hz, 1H), 6.98 (d,  $J$  = 2.4 Hz), 6.81 (dd,  $J$  = 8.4, 2.4 Hz, 1H) and 6.79 (s, 1H)], two *meta*-coupled aromatic protons ( $\delta$  6.74 and 6.50, each d,  $J$  = 2.4 Hz, 1H) and a prenyl subunit [ $\delta$  5.18 (t,  $J$  = 5.6 Hz, 1H), 3.50 (d,  $J$  = 5.6 Hz, 2H), 1.67 and 1.64, each s, 3H] in the <sup>1</sup>H-NMR spectrum (Table 3.5) (Figure 15). The <sup>1</sup>H-NMR spectrum of compound **A7** was similar

to that of compound **A6** (Table 3.5) (Figure 3.5) except for the splitting pattern of the aromatic protons H-11 ( $\delta_H$  6.50) and H-13 ( $\delta_H$  6.74) as doublet. Thus, the prenyl unit was attached at C-9. Comparison the  $^1H$ -NMR data of compound **A7** with demethylmoracin I was similar. Consequently, compound **A7** was identified as demethylmoracin I (Lee *et al.*, 2001).

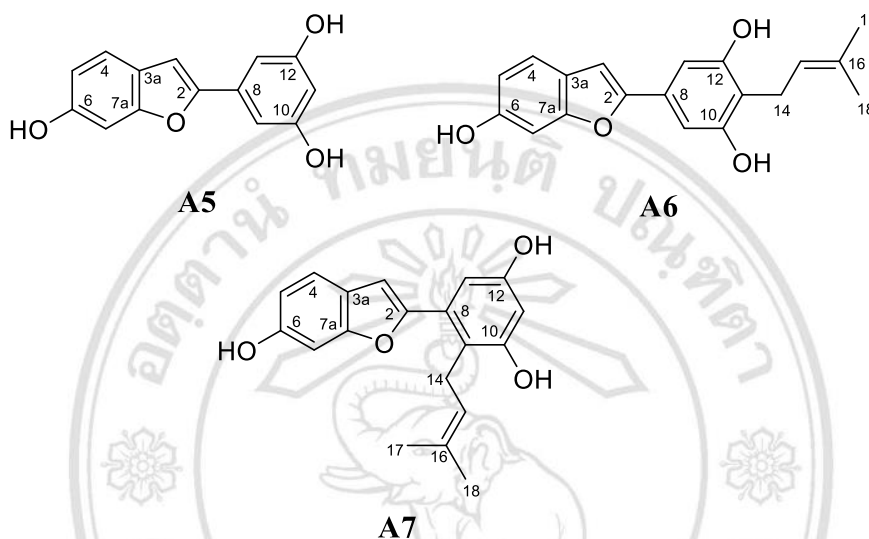


**Figure 3.5** The structures of compounds **A5-A7**

**Table 3.5** The <sup>1</sup>H-NMR data of compounds **A5-A7** (400 MHz, acetone-*d*<sub>6</sub>), moracin M (400 MHz, acetone-*d*<sub>6</sub>), moracin C (300 MHz, acetone-*d*<sub>6</sub>) and demethylmoracin I (500 MHz, acetone-*d*<sub>6</sub>)

position	$\delta_H$ , mult. ( <i>J</i> in Hz)				
	compound <b>A5</b>	moracin M	compound <b>A6</b>	moracin C	compound <b>A7</b> demethylmoracin I
3	6.98, s	6.88, s	6.83, brs	6.82, d (0.9)	6.79, s 6.66, s
4	7.41, d, (8.4)	7.33, d (8.5)	7.33, d (8.4)	7.32, d (8.4)	7.42, d (8.4) 7.33, d (8.4)
5	6.81, dd (8.4, 2.0)	6.73, dd (8.5, 2.5)	6.72, dd (8.4, 2.0)	6.72, dd (8.4, 2.1)	6.81, dd (8.4, 2.4) 6.72, dd (8.4, 2.2)
7	7.04, d (2.0)	6.91, d (2.5)	6.87, d (2.0)	6.88, d (2.1)	6.98, d (2.4) 6.87, d (2.1)
9	6.85, d (2.4)	6.77, d (2.5)	6.77, brs	6.78, s	6.74, d, (2.4) 6.61, d (2.5)
11	6.36, t, (2.4)	6.26, t (2.5)	-	-	6.50, d (2.4) 6.33, d (2.5)
13	6.85, d, (2.4)	6.77, d (2.5)	6.77, brs	6.78, s	-
14	-	-	3.32, d, (7.2)	3.32, d (6.9)	3.50, d (5.6) 3.42, d (6.3)
15	-	-	5.26, t (7.2)	5.26, t (6.9)	5.18, t (5.6) 5.13, m
16	-	-	-	-	-
17	-	-	1.78, s	1.78, s	1.67, s 1.64, s
18	-	-	1.67, s	1.66, s	1.64, s

### 3.1.6 Compounds A8-A14

Compounds **A8-A14** were obtained as a pale yellow gum. The UV spectrum showed maximum absorption bands in the range of  $\lambda_{\max}$  211-350 nm, indicating the flavone skeleton (Ryu *et al.*, 2008), while the IR spectrum displayed hydroxy (3365-3141  $\text{cm}^{-1}$ ) and conjugated ketone carbonyl (1635-1602  $\text{cm}^{-1}$ ) functional groups. The  $^1\text{H-NMR}$  spectrum of compound **A8** (Table 3.6) (Figure 16) showed signals for one chelated hydroxy proton ( $\delta$  13.14, s, 1H), three aromatic protons of a 1,2,4-trisubstituted benzene ring [ $\delta$  7.83 (d,  $J$  = 8.8 Hz, 1H), 6.62 (d,  $J$  = 2.4 Hz, 1H) and 6.56 (dd,  $J$  = 8.8, 2.4 Hz, 1H)], one olefinic proton ( $\delta$  7.07, s, 1H), and *meta*-coupled aromatic protons ( $\delta$  6.50 and 6.23, each d,  $J$  = 1.8 Hz, 1H). These  $^1\text{H-NMR}$  data was similar to that of norartocarpetin. Thus, compound **A8** was identified as norartocarpetin (Zheng *et al.*, 2008). The  $^1\text{H-NMR}$  spectrum of compound **A9** (Table 3.6) (Figure 17) was similar to that of compound **A8** except for the replacement of an olefinic proton in compound **A8** by a prenyl unit [ $\delta$  5.11 (t,  $J$  = 7.0 Hz, 1H), 3.10 (d,  $J$  = 7.0 Hz, 2H), 1.56 and 1.42, each s, 3H)]. Thus, the prenyl unit was located at C-3. Therefore, compound **A9** was identified as albanin A (Sun *et al.*, 2014). Compound **A10** displayed four aromatic protons of a *para*-disubstituted benzene ring ( $\delta$  7.94 and 7.04, each d,  $J$  = 9.0 Hz, 2H), one olefinic proton ( $\delta$  6.65, s, 1H), singlet aromatic proton ( $\delta$  6.63, s, 1H), and a prenyl unit [ $\delta$  5.29 (t,  $J$  = 7.0 Hz, 1H), 3.37 (d,  $J$  = 7.0 Hz, 2H), 1.79 and 1.66 each s, 3H)] in the  $^1\text{H-NMR}$  spectrum (Table 3.6) (Figure 18). The *para*-disubstituted aromatic protons and the prenyl unit in compound **A10** instead of the aromatic protons of the 1,2,4-trisubstituted benzene ring and one of the *meta*-coupled aromatic protons in compound **A8**. Comparison of the  $^1\text{H-NMR}$  data with licoflavone C found that compound **A10** was licoflavone C (Kajiyama *et al.*, 1992). The  $^1\text{H-NMR}$  spectrum of compound **A11** (Table 3.7) (Figure 19) was similar to that of compound **A8** except for the replacement of the one of *meta*-coupled aromatic protons of compound **A8** with a prenyl unit [ $\delta$  5.18 (t,  $J$  = 6.4 Hz, 1H), 3.21 (d,  $J$  = 6.4 Hz, 2H), 1.72 and 1.62, each s, 3H)] in  $^1\text{H-NMR}$  spectrum. These data was similar to that of artocarpesin. Thus, compound **A11** was assigned as artocarpesin (Zheng *et al.*, 2008). Comparison of the  $^1\text{H-NMR}$  spectrum (Table 3.7) (Figure 20) of compounds **A12** with compound **A9** found that compound **A12** displayed signals of a *trans*-3-methyl-1-butenyl unit [ $\delta$  6.80 (dd,  $J$  = 16.0, 6.8 Hz, 1H), 6.67 (d,  $J$  = 16.0 Hz, 1H), 2.48 (m, 1H) and 1.13 (d,  $J$  = 6.4

Hz, 6H)] instead of one of the *meta*-coupled aromatic proton of compound **A9**. The  $^1\text{H-NMR}$  data of compound **A12** was almost similar to that of norartocarpin. Therefore, compound **A12** was identified as norartocarpin (Zhang *et al.*, 2013). The  $^1\text{H-NMR}$  spectrum (Table 3.7) (Figure 21) of compound **A13** was similar to that of compound **A12**. The  $^1\text{H-NMR}$  spectrum of compound **A13** showed additional signals of a prenyl unit [ $\delta$ 5.12 (t,  $J = 6.8$  Hz, 1H), 3.10 (d,  $J = 6.8$  Hz, 1H), 1.77 and 1.56, each s, 3H] instead of the *trans*-3-methyl-1-butenyl unit in compound **A12**. Compound **A13** was cudraflavone C (Quang *et al.*, 2015). Furthermore, compound **A14** showed an additional signal for a methoxyl group ( $\delta$ 3.83) in the  $^1\text{H-NMR}$  spectrum (Table 3.8) (Figure 22) of **A14**, by comparison the  $^1\text{H-NMR}$  spectrum with compound **A12**. The  $^1\text{H-NMR}$  spectrum of compound **A14** was almost similar to that of artocarpin. Thus, compound **A14** was assigned as artocarpin (Septama *et al.*, 2015).

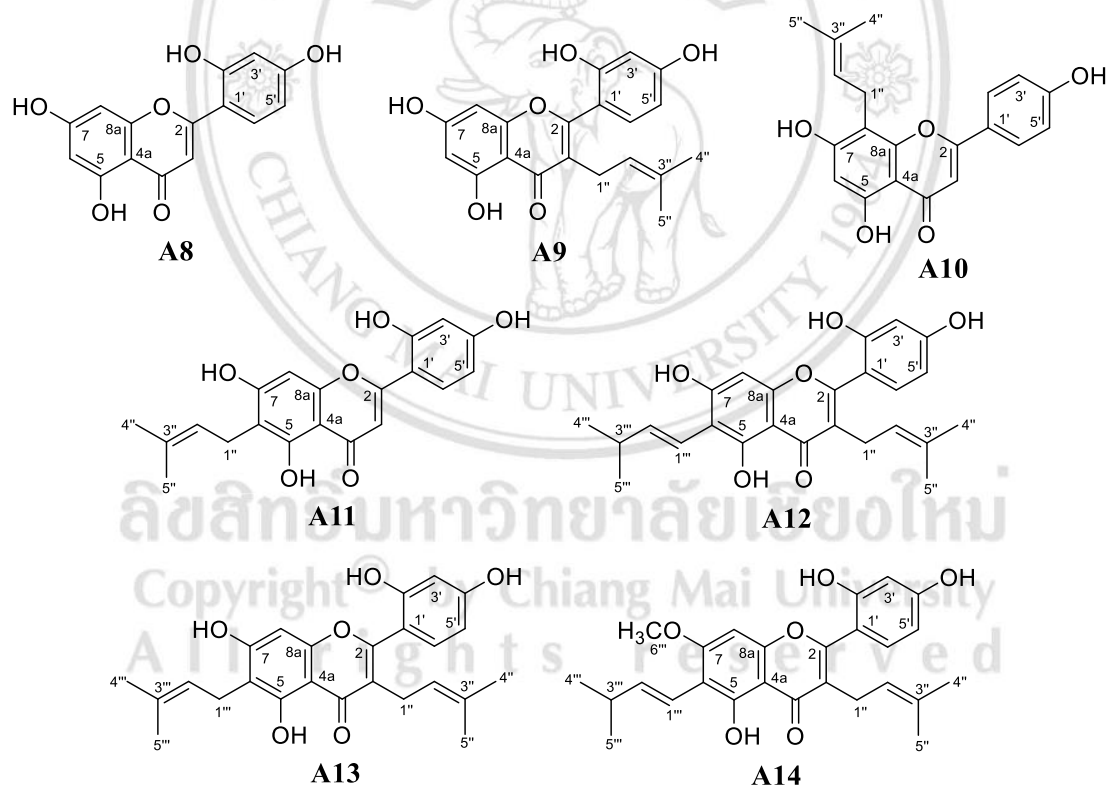


**Figure 3.6** The structures of compounds **A8-A14**



**Table 3.6** The <sup>1</sup>H-NMR data of compounds **A8-A10** (400 MHz, acetone-*d*<sub>6</sub>), norartocarpetin (300 MHz, DMSO-*d*<sub>6</sub>), albanin **A** (400 MHz, DMSO-*d*<sub>6</sub>) and licoflavone **C** (400 MHz, acetone-*d*<sub>6</sub>)

position	$\delta_{\text{H}}$ , mult. ( <i>J</i> in Hz)					
	compound <b>A8</b>	norartocarpetin	compound <b>A9</b>	albanin <b>A</b>	compound <b>A10</b>	licoflavone <b>C</b>
3	7.07, s	7.00, s	-	-	6.65, s	6.63, s
5-OH	13.14, s	-	13.16, s	13.13, brs	13.40, s	13.00, s
6	6.23, d (1.8)	6.15, d (1.8)	6.24, d (2.2)	6.23, d (3.2)	6.63, s	6.34, s
8	6.50, d (1.8)	6.48, d (1.8)	6.32, d (2.2)	6.31, d (3.2)	-	-
3'	6.62, d (2.4)	6.53, d (3.0)	6.56, d (2.4)	6.56, d (2.4)	7.04, d (9.0)	7.05, d (9.0)
5'	6.56, dd (8.8, 2.4)	6.42, dd (8.7, 3.0)	6.51, dd (8.4, 2.4)	6.51, dd (8.4, 2.4)	7.04, d (9.0)	7.05, d (9.0)
6'	7.83, d (8.8)	7.75, d (8.7)	7.19, d (8.4)	7.18, d (8.4)	7.94, d (9.0)	7.96, d (9.0)
1''	-	-	3.10, d (7.0)	3.10, d (6.8)	3.37, d (7.0)	3.57, brd (6.8)
2''	-	-	5.11, t (7.0)	5.11, t (6.8)	5.29, t (7.0)	5.30, brt (6.8)
3''	-	-	-	-	-	-
4''	-	-	1.56, s	1.56, s	1.79, s	1.82, s
5''	-	-	1.42, s	1.42, s	1.66, s	1.67, s

**Table 3.7** The <sup>1</sup>H-NMR data of compounds **A11** (400 MHz, DMSO-*d*<sub>6</sub>), **A12** (400 MHz, acetone-*d*<sub>6</sub>), **A13** (400 MHz, acetone-*d*<sub>6</sub>), artocarpesin (300 MHz, DMSO-*d*<sub>6</sub>), norartocarpin (400 MHz, acetone-*d*<sub>6</sub>) and cudraflavone C (400 MHz, acetone-*d*<sub>6</sub>)

position	$\delta_{\text{H}}$ , mult. ( <i>J</i> in Hz)				
	compound <b>A11</b>	artocarpesin	compound <b>A12</b>	norartocarpin	compound <b>A13</b>
3	6.98, s	6.98, s	-	-	-
5-OH	13.30, s	-	14.11, s	14.08, s	13.44, s
8	6.48, s	6.48, s	6.44, s	6.43, s	6.39, s
3'	6.48, s	6.48, d (1.8)	6.60, d (2.4)	6.57, d (2.0)	6.54, d (2.4)
5'	6.43, d (8.8)	6.43, dd (8.7, 2.1)	6.55, dd (8.4, 2.4)	6.52, dd (8.4, 2.0)	6.50, dd (8.4, 2.4)
6'	7.73, d (8.8)	7.73, d (8.7)	7.23, d (8.4)	7.20, d (8.4)	7.17, d (8.4)
1''	3.21, d (6.4)	3.18, brd (6.6)	3.15, d (7.0)	3.13, d (7.2)	3.35, d (7.2)
2''	5.18, t (6.4)	5.17, brt (6.6)	5.16, t (7.0)	5.13, t (7.2)	5.27, t (7.0)
4''	1.62, s	1.62, s	1.60, s	1.58, s	1.42, s
5''	1.72, s	1.73, s	1.46, s	1.44, s	1.64, s
					1.62, s

**Table 3.7** (continued)

position	$\delta_{\text{H}}$ , mult. ( $J$ in Hz)					
	compound <b>A11</b>	artocarpesin	compound <b>A12</b>	norartocarpin	compound <b>A13</b>	cudraflavone C
1"	-	-	6.67, d (16.0)	6.65, dd (16.4, 1.0)	3.10, d (6.8)	3.10, d (6.8)
2"	-	-	6.80, dd (16.0, 6.8)	6.78, dd (16.4, 7.2)	5.12, t (6.8)	5.11, d (6.8)
3"	-	-	2.48, m	2.42, m	-	-
4"	-	-	1.13, d (6.8)	1.11, d (6.8)	1.56, s	1.55, s
5"	-	-	1.13, d (6.8)	1.11, d (6.8)	1.77, s	1.76, s

**Table 3.8** The NMR data of compound **A14** (400 MHz, CDCl<sub>3</sub>), and artocarpin (500 MHz, CDCl<sub>3</sub>)

position	Compound <b>A14</b>		artocarpin	
	$\delta_{\text{H}}$ , mult. ( <i>J</i> in Hz)	$\delta_{\text{C}}$ (Type)	$\delta_{\text{H}}$ , mult. ( <i>J</i> in Hz)	$\delta_{\text{C}}$ (Type)
2	-	160.6 (C)	-	159.3 (C)
3	-	121.3 (C)	-	120.8 (C)
4	-	182.4 (C)	-	182.2 (C)
4a	-	103.8 (C)	-	104.9 (C)
5-OH	13.49, s	158.1 (C)	13.47, s	158.6 (C)
6	-	109.7 (C)	-	109.7 (C)
7	-	162.9 (C)	-	162.8 (C)
8	6.32, s	89.7 (CH)	6.38, s	89.4 (CH)
8a	-	156.2 (C)	-	155.0 (C)
1'	-	112.2 (C)	-	112.5 (C)
2'	-	155.2 (C)	-	155.1 (C)
3'	6.51, d (2.0)	104.9 (CH)	6.48, d (2.2)	103.8 (CH)
4'	-	159.5 (C)	-	158.9 (C)
5'	6.50, dd (8.0, 2.0)	108.2 (CH)	6.49, dd (9.0, 2.2)	108.6 (CH)
6'	7.13, d (8.0)	131.5 (CH)	7.18, d (8.8)	131.5 (CH)
1''	3.10, d (6.0)	24.3 (CH <sub>2</sub> )	3.09, d (7.0)	24.4 (CH <sub>2</sub> )
2''	5.10, t (6.0)	120.9 (CH)	5.12, t (6.7)	121.5 (CH)
3''	-	132.9 (C)	-	133.3 (C)
4''	1.57, s	17.5 (CH <sub>3</sub> )	1.60, s	17.7 (CH <sub>3</sub> )
5''	1.39, s	25.6 (CH <sub>3</sub> )	1.42, s	25.7 (CH <sub>3</sub> )
1'''	6.51, d (18.0)	115.5 (CH)	6.53, brd (16.4)	115.6 (CH)
2'''	6.63, dd (18.0, 6.8)	142.6 (CH)	6.68, dd (16.4, 7.1)	142.6 (CH)
3'''	2.43, m	33.0 (CH)	2.44, m	33.0 (CH)
4'''	1.07, d (6.8)	22.5 (CH <sub>3</sub> )	1.08, d (7.0)	22.3 (CH <sub>3</sub> )
5'''	1.07, d (6.8)	22.5 (CH <sub>3</sub> )	1.08, d (7.0)	22.7 (CH <sub>3</sub> )
6'''	3.83, s	55.9 (CH <sub>3</sub> )	3.84, s	55.9 (CH <sub>3</sub> )

### 3.1.7 Compounds A15 and A16

Compound **A15** was obtained as a brown gum. The UV spectrum displayed absorption bands at  $\lambda_{\max}$  211 and 288 nm, while the IR spectrum showed hydroxy ( $3325\text{ cm}^{-1}$ ) and carbonyl ( $1622\text{ cm}^{-1}$ ) functional groups. The  $^1\text{H-NMR}$  (**Table 3.9**) (**Figure 24**) spectrum of compound **A15** was similar to that of norartocarpetin (**A8**) except for the replacement of the olefinic proton in compound **A8** with the signals of oxymethine proton ( $\delta$  5.71, dd,  $J = 12.8, 2.8\text{ Hz}$ , 1H) and non-equivalent methylene protons [ $\delta$  3.18 (dd,  $J = 17.2, 12.8\text{ Hz}$ , 1H) and 2.71 (dd,  $J = 17.2, 2.8\text{ Hz}$ , 1H)]. The oxymethine and methylene protons were assigned as H-2 and H<sub>2</sub>-3, respectively, according to their chemical shifts. The absolute configuration at C-2 of compound **A15** was determined by the comparison of the specific rotation of steppogenin (Jeong *et al.*, 2009). The specific rotation of compound **A15**,  $[\alpha]^{25}_{\text{D}} -21.63$  ( $c = 0.125$ , MeOH), was similar to that of steppogenin,  $[\alpha]^{24}_{\text{D}} -3.5$  ( $c = 0.125$ , MeOH), thus the absolute configuration at C-2 was assigned as *S*-configuration. Thus, compound **A15** was identified as steppogenin (Zheng *et al.*, 2008). Compound **A16**, a pale yellow gum, had a same characteristic  $^1\text{H-NMR}$  pattern with compound **A15** and displayed the additional signal of a methoxyl group at  $\delta$  3.84 (s, 3H) in  $^1\text{H-NMR}$  spectrum (**Table 3.9**) (**Figure 25**) of compound **A16**. The specific rotation of compound **A16**,  $[\alpha]^{25}_{\text{D}} -5.4$  ( $c = 0.19$ , acetone), was similar to that of artocarpanone,  $[\alpha]^{24}_{\text{D}} -2.0$  ( $c = 0.2$ , acetone) (Wei *et al.*, 2005), thus the absolute configuration at C-2 was assigned as *S*-configuration. Consequently, compound **A16** was identified as artocarpanone (Wei *et al.*, 2005).

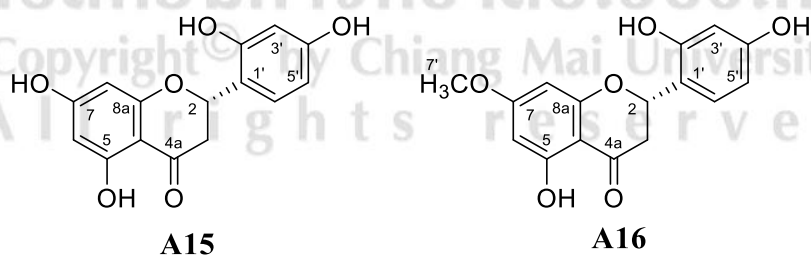


**Figure 3.7** The structures of compounds **A15** and **A16**

**Table 3.9** The  $^1\text{H}$ -NMR data of compounds **A15** and **A16** (400 MHz, acetone- $d_6$ ), steppogenin (500 MHz, acetone- $d_6$ ) and artocarpanone (400 MHz, acetone- $d_6$ )

position	$\delta_{\text{H}}$ , mult. ( $J$ in Hz)			
	compound <b>A15</b>	steppogenin	compound <b>A16</b>	artocarpanone
2	5.71, dd (12.8, 2.8)	5.59, dd (13.2, 2.9)	5.72, dd (13.2, 2.8)	5.73, dd (14.0, 3.0)
3	a: 3.18, dd (17.2, 12.8) b: 2.71, dd (17.2, 2.8)	a: 3.06, dd (17.2, 13.1) b: 2.69, dd (17.2, 2.9)	a: 3.20, dd (17.2, 13.2) b: 2.73, dd (17.2, 2.8)	a: 3.21, dd (17.0, 14.0) b: 2.74, dd (17.0, 3.0)
5-OH	12.22, s	-	12.17, s	12.17, s
6	5.95, d (1.6)	5.86, d (2.2)	6.02, d (2.0)	6.02, d (2.0)
8	5.97, d (1.6)	5.90, d (2.2)	6.05, d (2.0)	6.05, d (2.0)
3'	6.48, d (2.0)	6.31, d (2.1)	6.47, d (2.4)	6.47, d (2.0)
5'	6.43, dd (8.4, 2.0)	6.33, dd (8.2, 2.4)	6.43, dd (8.4, 2.4)	6.43, dd (8.0, 2.0)
6'	7.22, d (8.4)	7.22, d (8.2)	7.31, d (8.4)	7.32, d (8.0)
7'	-	-	3.84, s	3.85, s

### 3.1.8 Compounds **A17** and **A18**

Compound **A17** was isolated as a brown gum. The UV spectrum showed maximum absorption bands at  $\lambda_{\text{max}}$  215, 322 and 385 nm, while the IR spectrum displayed hydroxy ( $3329\text{ cm}^{-1}$ ) and conjugated ketone carbonyl ( $1679\text{ cm}^{-1}$ ) functional groups. The  $^1\text{H}$ -NMR spectrum (**Table 3.10**) (**Figure 26**) showed resonances for a chelated hydroxy proton ( $\delta$  14.23, s, 1H), two sets of *trans*-coupled olefinic protons ( $\delta$  8.23 and 7.80, each d,  $J = 15.6\text{ Hz}$ , 1H and 7.62 and 6.44, each d,  $J = 16.0\text{ Hz}$ , 1H), two *ortho*-coupled aromatic protons ( $\delta$  7.92 and 6.52, each d,  $J = 9.0\text{ Hz}$ , 1H), two sets of three aromatic protons of a 1,2,4-trisubstituted benzene ring [ $\delta$  7.69 (d,  $J = 8.8\text{ Hz}$ , 1H), 6.87 (d,  $J = 8.8$

Hz, 1H), 6.46 (s, 1H) and 7.36 (d,  $J = 2.0$  Hz, 1H), 7.16 (dd,  $J = 8.0, 2.0$  Hz, 1H) and 6.87 (d,  $J = 8.0$  Hz, 1H)], and olefinic proton ( $\delta$  5.58, t,  $J = 7.6$  Hz, 1H), one methoxy group ( $\delta$  3.91, s, 3H), two methylene protons [ $\delta$  4.96 (s, 2H) and 3.51 (d,  $J = 7.6$  Hz, 2H)], and a methyl group ( $\delta$  1.75, s, 3H). Comparison of the  $^1\text{H}$ -NMR data of compound **A17** with isogemichalcone C, they are the same compound. Thus, compound **A17** was isogemichalcone C (Lee *et al.*, 2001). Furthermore, comparison of the  $^1\text{H}$ -NMR spectrum of compound **A18**, a pale yellow gum, with compound **A17** was similar except for the replacement of three aromatic protons of 1,2,4-trisubstituted benzene ring of compound **A17** with four aromatic protons of *para*-disubstituted benzene ring ( $\delta$  7.73 and 6.93, each d,  $J = 8.4$  Hz, 2H) (Table 3.10) (Figure 27). Compound **A18** was artocarmitin B (Nguyen *et al.*, 2012).

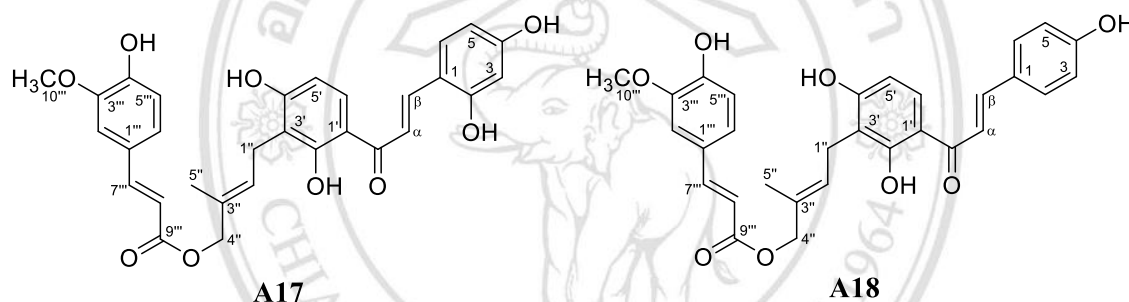


**Figure 3.8** The structures of compounds **A17** and **A18**

**Table 3.10** The  $^1\text{H}$ -NMR data of compounds **A17** and **A18** (400 MHz, acetone- $d_6$ ), isogemichalcone C and artocarmitin B (500 MHz, acetone- $d_6$ )

position	$\delta_{\text{H}}$ , mult. ( $J$ in Hz)			
	compound <b>A17</b>	isogemichalcone C	compound <b>A18</b>	artocarmitin B
2	-	-	7.73, d (8.4)	7.73, d (8.5)
3	6.46, s	6.51, brs	6.93, d (8.4)	6.93, d (8.5)
5	6.87, d (8.8)	6.93, d (8.5)	6.93, d (8.4)	6.93, d (8.5)
6	7.69, d (8.8)	7.68, d (8.5)	7.73, d (8.4)	7.73, d (8.5)
$\alpha$	7.80, d (15.6)	7.80, d (15.4)	7.80, d (15.0)	7.76, d (15.5)
$\beta$	8.23, d (15.6)	8.22, d (15.4)	7.84, d (15.0)	7.84, d (15.5)

**Table 3.10** (continued)

position	$\delta_{\text{H}}$ , mult. ( $J$ in Hz)			
	compound <b>A17</b>	isogemichalcone C	compound <b>A18</b>	artocarmitin B
2'-OH	14.23, s	-	14.08, s	14.06, s
5'	6.52, d (9.0)	6.51, d (8.9)	6.56, d (8.8)	6.56, d (9.0)
6'	7.92, d (9.0)	7.91, d (8.8)	8.01, d (8.8)	8.00, d (9.0)
1''	3.51, d (7.6)	3.46, d (7.4)	3.50, d (7.5)	3.47, d (7.5)
2''	5.58, t (7.6)	5.69, brt (8.0)	5.58, t (7.5)	5.68, t (7.5)
4''	4.96, s	4.54, s	4.95, s	4.55, s
5''	1.75, s	1.88, s	1.75, s	1.88, s
2'''	7.36, d (2.0)	7.36, d (2.0)	7.37, d (1.6)	7.34, d (1.5)
5'''	6.87, d (8.0)	6.87, d (8.0)	6.87, d (8.0)	6.86, d (8.5)
6'''	7.16, dd (8.0, 2.0)	7.16, dd (8.0, 2.0)	7.16, dd (8.0, 1.6)	7.34, dd (8.5, 1.5)
7'''	7.62, d (16.0)	7.62, d (16.0)	7.62, d (15.6)	7.58, d (16.0)
8'''	6.44, d (16.0)	6.44, d (16.0)	6.44, d (15.6)	6.40, d (16.0)
10'''	3.91, s	3.91, s	3.92, s	3.91, s

### 3.1.9 Compound A19

Compound **A19** was obtained as a pale yellow gum. The  $^1\text{H}$ -NMR spectrum (**Table 3.11**) (**Figure 28**) showed the signals of one chelated hydroxy proton ( $\delta$  13.35, s, 1H), two *trans*-coupled olefinic protons ( $\delta$  7.59 and 6.35, each d,  $J$  = 16.0 Hz, 1H), two sets of four aromatic protons of a *para*-disubstituted benzene ring [ $\delta$  7.92 and 7.01, each d,  $J$  = 8.8 Hz, 2H and 7.54 and 6.87, each d,  $J$  = 8.4 Hz, 2H], singlet aromatic proton ( $\delta$  6.63, s, 1H), two olefinic proton [ $\delta$  6.63 (s, 1H) and 5.67 (t,  $J$  = 7.2 Hz, 1H)], two methylene protons [ $\delta$  4.54 (s, 2H) and 3.44 (d,  $J$  = 7.2 Hz, 2H)] and one methyl group ( $\delta$  1.81, s, 3H). Compound **A19** displayed carbon resonances for twenty-nine carbons from the  $^{13}\text{C}$ -NMR spectrum (**Table 3.11**) (**Figure 29**) including thirteen quaternary carbons ( $\delta$  182.4, 166.3, 164.0, 161.2, 160.9, 159.8, 159.0, 155.3, 131.0, 126.0, 122.0,



110.0 and 104.2), thirteen methines ( $\delta$  145.4, 129.2 (2C), 128.4 (2C), 127.4, 116.8 (2C), 116.6 (2C), 115.7, 103.4 and 94.0), two methylenes ( $\delta$  70.2 and 21.8) and one methyl ( $\delta$  14.2). When the NMR data of compound **A19** were compared with artocarmin B, they displayed almost similar data. Thus, compound **A19** was assigned as artocarmin B (Nguyen *et al.*, 2012).

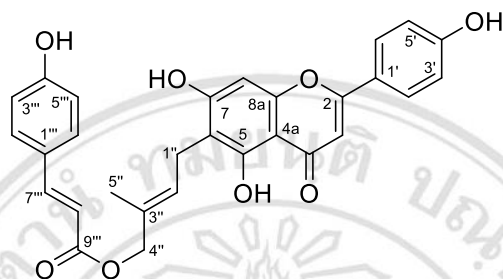


**Figure 3.9** The structure of artocarmin B (**A19**)

**Table 3.11** The NMR data of compound **A19** (400 MHz, acetone- $d_6$ ) and artocarmin B (500 MHz, DMSO- $d_6$ )

position	compound <b>A19</b>		artocarmin B	
	$\delta_H$ , mult. ( $J$ in Hz)	$\delta_C$ (Type)	$\delta_H$ , mult. ( $J$ in Hz)	$\delta_C$ (Type)
2	-	164.0 (C)	-	163.9 (C)
3	6.63, s	103.4 (CH)	6.76, s	103.0 (CH)
4	-	182.4 (C)	-	182.4 (C)
4a	-	104.2 (C)	-	103.8 (C)
5-OH	13.35, s	159.0 (C)	13.27, s	158.8 (C)
6	-	110.0 (C)	-	110.2 (C)
7	-	161.2 (C)	-	162.1 (C)
8	6.63, s	94.0 (CH)	6.55, s	93.4 (CH)
8a	-	155.3 (C)	-	155.5 (C)

**Table 3.11** (continued)

position	compound <b>A19</b>		artocarmin B	
	$\delta_{\text{H}}$ , mult. ( <i>J</i> in Hz)	$\delta_{\text{C}}$ (Type)	$\delta_{\text{H}}$ , mult. ( <i>J</i> in Hz)	$\delta_{\text{C}}$ (Type)
1'	-	122.0 (C)	-	121.6 (C)
2'	7.92, d (8.8)	128.4 (CH)	7.91, d (8.8)	128.5 (CH)
3'	7.01, d (8.8)	116.8 (CH)	6.92, d (8.8)	116.1 (CH)
4'	-	160.9 (C)	-	160.9 (C)
5'	7.01, d (8.8)	116.8 (CH)	6.92, d (8.8)	116.1 (CH)
6'	7.92, d (8.8)	128.4 (CH)	7.91, d (8.8)	128.5 (CH)
1''	3.44, d (7.2)	21.8 (CH <sub>2</sub> )	3.30, d (7.1)	20.9 (CH <sub>2</sub> )
2''	5.67, t (7.2)	127.4 (CH)	5.56, t (7.1)	127.4 (CH)
3''	-	131.0 (C)	-	131.0 (C)
4''	4.54, s	70.2 (CH <sub>2</sub> )	4.52, s	70.2 (CH <sub>2</sub> )
5''	1.81, s	14.2 (CH <sub>3</sub> )	1.80, s	13.9 (CH <sub>3</sub> )
1'''	-	126.0 (C)	-	125.4 (C)
2'''	7.54, d (8.4)	129.2 (CH)	7.54, d (8.6)	130.3 (CH)
3'''	6.87, d (8.4)	116.6 (CH)	6.78, d (8.6)	115.9 (CH)
4'''	-	159.8 (C)	-	160.0 (C)
5'''	6.87, d (8.4)	116.6 (CH)	6.78, d (8.6)	115.9 (CH)
6'''	7.54, d (8.4)	129.2 (CH)	7.54, d (8.6)	130.3 (CH)
7'''	7.59, d (16.0)	145.4 (CH)	7.54, d (16.0)	144.9 (CH)
8'''	6.35, d (16.0)	115.7 (CH)	6.39, d (16.0)	115.7 (CH)
9'''	-	166.3 (C)	-	166.6 (C)

### 3.1.10 Compound A20

Compound **A20** was isolated as a pale brown gum. The  $^1\text{H}$ -NMR spectrum (**Table 3.12**) (**Figure 30**) showed the resonances of a chelated hydroxy proton ( $\delta$  14.19, s, 1H), two *trans*-coupled olefinic protons ( $\delta$  8.21 and 7.80, each d,  $J = 15.4$  Hz, 1H), two *ortho*-coupled aromatic protons ( $\delta$  7.88 and 6.52, each d,  $J = 9.0$  Hz, 1H), three aromatic protons of a 1,2,4-trisubstituted benzene ring [ $\delta$  7.66 (d,  $J = 8.6$  Hz, 1H), 6.55 (d,  $J = 2.0$  Hz, 1H) and 6.43 (d,  $J = 8.6, 2.2$  Hz, 1H)], and a prenyl unit [ $\delta$  5.26 (t,  $J = 7.2$  Hz, 1H), 3.35 (d,  $J = 7.2$  Hz, 2H), 1.74 and 1.64, each s, 3H]. The  $^1\text{H}$ -NMR data was the same to those of morachalcone A. Thus, compound **A20** was morachalcone A (Zhang *et al.*, 2009).

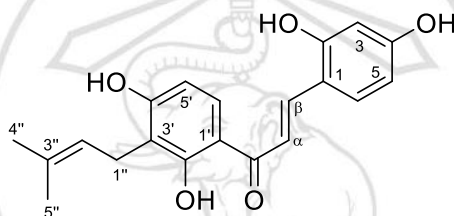


**Figure 3.10** The structure of morachalcone A (**A20**)

**Table 3.12** The  $^1\text{H}$ -NMR data of compound **A20** (400 MHz, acetone- $d_6$ ) and morachalcone A (500 MHz, acetone- $d_6$ )

position	$\delta_{\text{H}}$ , mult. ( $J$ in Hz)	
	compound <b>A20</b>	morachalcone A
3	6.55, d (2.0)	6.53, d (2.0)
5	6.43, dd (8.6, 2.0)	6.45, dd (8.5, 2.0)
6	7.66, d (8.6)	7.67, d (8.5)
$\alpha$	7.80, d (15.4)	7.79, d (15.4)
$\beta$	8.21, d (15.4)	8.21, d (15.4)
2'-OH	14.19, s	14.15, s
5'	6.52, d (9.0)	6.52, d (8.9)
6'	7.88, d (9.0)	7.88, d (8.9)

**Table 3.12** (continued)

position	$\delta_{\text{H}}$ , mult. ( $J$ in Hz)	
	compound <b>A20</b>	morachalcone A
1''	3.35, d (7.2)	3.37, d (7.2)
2''	5.26, t (7.2)	5.28, t (7.2)
4''	1.64, s	1.64, s
5''	1.74, s	1.78, s

### 3.1.11 Compounds A21-A24

Compound **A21** was obtained as a yellow gum. The  $^1\text{H}$ -NMR spectrum (**Table 3.13**) (**Figure 31**) showed resonances of a chelated hydroxy proton ( $\delta$  13.27, s, 1H), three aromatic protons of a 1,2,4-trisubstituted benzene ring [ $\delta$  7.64 (d,  $J$  = 8.4 Hz, 1H), 6.56 (brd,  $J$  = 8.4 Hz, 1H) and 6.38 (brs, 1H)], one singlet aromatic proton ( $\delta$  6.49, s, 1H), a *trans*-3-methyl-1-butenyl fragment [ $\delta$  6.40 (d,  $J$  = 17.0 Hz, 1H), 6.21 (dd,  $J$  = 17.0, 7.0 Hz, 1H), 2.20 (m, 1H) and 1.14 (d,  $J$  = 6.4 Hz, 6H)] and a 3-methyl-1-oxy-2-butenyl subunit [ $\delta$  6.24 (d,  $J$  = 9.6 Hz, 1H), 5.42 (d,  $J$  = 9.6 Hz, 1H), 1.95 and 1.68, each s, 3H]. To identify of compound **A21** was established by comparison of its  $^1\text{H}$ -NMR data to those of brosimone I (Zheng *et al.*, 2008). Thus, compound **A21** was brosimone I. Compound **A22** was isolated as a brown gum. The  $^1\text{H}$ -NMR spectrum (**Table 3.13**) (**Figure 32**) was similar to that of compound **A21** except for the additional resonance of a methoxyl group ( $\delta$  3.93, s, 3H) in compound **A22**. After comparison the  $^1\text{H}$ -NMR data of compound **A22** with that of cycloartocarpin, they are similar data. Therefore, compound **A22** was identified as cycloartocarpin (Septama *et al.*, 2015). Comparison of the  $^1\text{H}$ -NMR spectrum of compound **A23** (**Table 3.14**) (**Figure 33**), a brown gum, with those of compound **A21** showed similar data except for the replacement of the *trans*-3-methyl-1-butenyl unit in compound **A21** with a dimethylchromene ring [ $\delta$  6.70 (d,  $J$  = 10.0 Hz, 1H), 5.42 (d,  $J$  = 10.0 Hz, 1H) and 1.68 (s, 6H)] in compound **A23**, indicating that the dimethylchromene ring was fused at C-6 and C-7 with an ether linkage at C-7. Therefore, compound **A23** was cudraflavone A (Wei *et al.*, 2005). Compound **A24**,

brown gum, had the same characteristic  $^1\text{H-NMR}$  pattern (**Table 3.14**) (**Figure 34**) with compound **A23**. The main difference was found that the resonances of prenyl fragment [ $\delta$  5.11 (t,  $J = 7.0$  Hz, 1H), 3.11 (d,  $J = 7.0$  Hz, 2H), 1.57 and 1.42, each s, 3H] in compound **A24** replaced of the signals of 3-methyl-1-oxy-2-butenyl subunit in compound **A23**. Thus, compound **A24** was cudraflavone B (Zheng *et al.*, 2008).

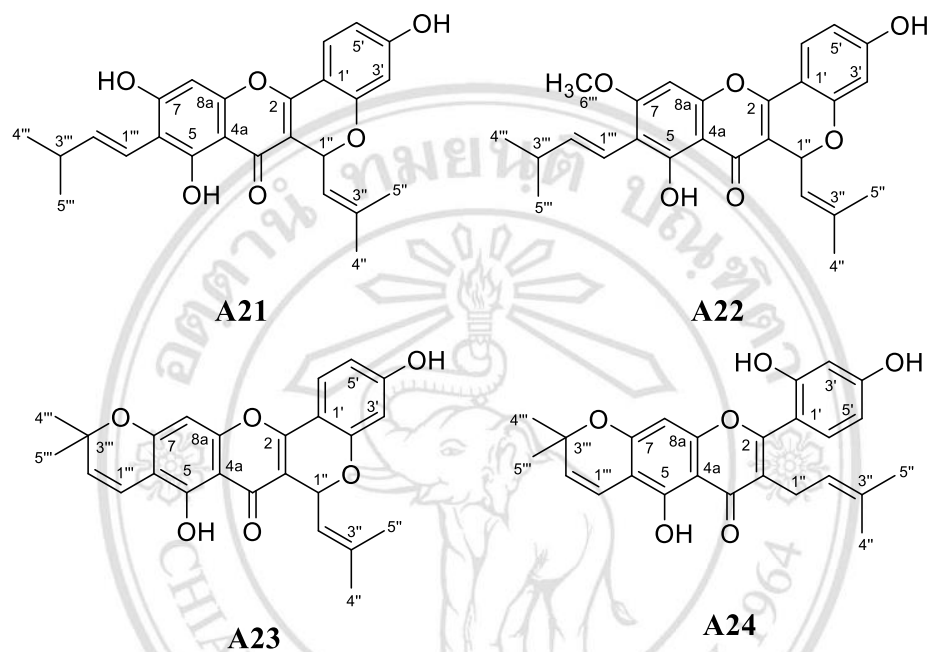


**Figure 3.11** The structures of compounds **A21-A24**

**Table 3.13** The  $^1\text{H-NMR}$  data of compounds **A21** and **A22** (400 MHz,  $\text{CDCl}_3$ ), brosimone I (300 MHz,  $\text{CDCl}_3$ ) and cycloartocarpin (500 MHz,  $\text{CDCl}_3$ )

position	$\delta_{\text{H}}$ , mult. ( $J$ in Hz)			
	compound <b>A21</b>	brosimone I	compound <b>A22</b>	cycloartocarpin
5-OH	13.27, s	-	13.42, s	13.41, s
8	6.49, s	6.26, s	6.37, s	6.44, s
3'	6.38, brs	6.16, d (1.8)	6.42, d (2.4)	6.40, d (2.5)
5'	6.56, brd (8.4)	6.25, dd (8.7, 1.8)	6.53, dd (8.4, 2.4)	6.52, dd (8.5, 2.5)
6'	7.64, d (8.4)	7.34, d (8.7)	7.64, d (8.4)	7.65, d (8.5)

**Table 3.13** (continued)

position	$\delta_{\text{H}}$ , mult. ( <i>J</i> in Hz)			
	compound <b>A21</b>	brosimone I	compound <b>A22</b>	cycloartocarpin
1''	6.24, d (9.6)	5.93, d (9.3)	6.26, d (9.2)	6.24, d (9.2)
2''	5.42, d (9.6)	5.18, d (9.3)	5.42, d (9.2)	5.41, d (9.2)
4''	1.68, s	1.44, s	1.68, s	1.67, s
5''	1.95, s	1.71, s	1.95, s	1.95, s
1'''	6.40, d (17.0)	6.31, d (16.5)	6.57, d (16.2)	6.56, d (16.2)
2'''	6.21, dd (17.0, 7.0)	6.48, dd (16.5, 6.9)	6.70, dd (16.2, 7.0)	6.69, dd (16.1, 7.5)
3'''	2.20, m	2.22, m	2.47, m	2.46, m
4'''	1.14, d (6.4)	0.87, d (6.9)	1.11, d (6.4)	1.08, d (6.5)
5'''	1.14, d (6.4)	0.84, d (6.9)	1.11, d (6.4)	1.08, d (6.5)
6'''	-	-	3.93, s	3.92, s

**Table 3.14** The  $^1\text{H}$ -NMR data of compounds **A23** (400 MHz,  $\text{CDCl}_3$ ), **A24** (400 MHz, acetone- $d_6$ ), cudraflavone A (400 MHz,  $\text{CDCl}_3$ ) and cudraflavone B (300 MHz,  $\text{DMSO}-d_6$ )

position	$\delta_{\text{H}}$ , mult. ( <i>J</i> in Hz)			
	compound <b>A23</b>	cudraflavone A	compound <b>A24</b>	cudraflavone B
5-OH	13.03, s	12.95, s	13.57, s	-
8	6.37, s	6.30, s	6.27, s	6.37, s
3'	6.41, brs	6.35, d (2.0)	6.56, d (2.4)	6.43, d (2.1)
5'	6.71, d (8.4)	6.48, dd (7.5, 2.0)	6.51, dd (8.4, 2.4)	6.34, dd (8.4, 2.1)
6'	7.65, d (8.4)	7.58, d (7.5)	7.20, d (8.4)	7.07, d (8.4)

**Table 3.14** (continued)

position	$\delta_{\text{H}}$ , mult. ( $J$ in Hz)			
	compound <b>A23</b>	cudraflavone A	compound <b>A24</b>	cudraflavone B
1''	6.25, d (9.9)	6.18, d (9.5)	3.11, d (7.0)	2.97, d (6.9)
2''	5.60, d (9.9)	5.54, d (9.5)	5.11, t (7.0)	5.01, t (6.9)
4''	1.70, s	1.63, s	1.42, s	1.36, s
5''	1.97, s	1.90, s	1.57, s	1.54, s
1'''	6.70, d (10.0)	6.63, d (9.9)	6.67, d (10.0)	6.61, d (9.9)
2'''	5.42, d (10.0)	5.35, d (9.9)	5.74, d (10.0)	5.77, d (9.9)
4'''	1.46, s	1.43, s	1.45, s	1.41, s
5'''	1.46, s	1.43, s	1.45, s	1.41, s

### 3.1.12 Compound A25

Compound **A25** was obtained as a pale yellow gum. The  $^1\text{H}$ -NMR spectrum (**Table 3.15**) (**Figure 35**) showed resonances for a chelated hydroxy proton ( $\delta$  13.28, s, 1H), three aromatic protons of a 1,2,4-trisubstituted benzene ring [ $\delta$  7.31 (d,  $J$  = 8.0 Hz, 1H), 6.53 (dd,  $J$  = 8.0, 2.4 Hz, 1H) and 6.52 (d,  $J$  = 2.4 Hz, 1H)], one olefinic proton ( $\delta$  6.66, s, 1H), a *trans*-3-methyl-1-butenyl fragment [ $\delta$  6.72 (dd,  $J$  = 16.0, 7.2 Hz, 1H), 6.54 (dd,  $J$  = 16.0, 7.2 Hz, 1H), 2.43 (m, 1H) and 1.08 (d,  $J$  = 6.4 Hz, 6H)], a 2-hydroxy-3-methyl-3-butenyl unit [ $\delta$  4.81 and 4.67, each s, 1H, 4.38 (m, 1H), 2.78 (dd,  $J$  = 13.8, 5.0 Hz, 1H), 2.58 (dd,  $J$  = 13.8, 8.4 Hz, 1H) and 1.57 (s, 3H)], and methoxyl group ( $\delta$  3.96, s, 3H). Compound **A25** displayed carbon resonances for twenty-six carbons from the  $^{13}\text{C}$ -NMR spectrum (**Table 3.14**) (**Figure 36**) including twelve quaternary carbons ( $\delta$  183.0, 163.1, 162.5, 160.7, 158.9, 156.6, 156.1, 147.9, 119.0, 112.1, 109.1 and 104.6), eight methines ( $\delta$  141.5, 131.9, 116.1, 107.4, 103.3, 89.7, 73.1 and 33.1), two methylenes ( $\delta$  109.6 and 32.1) and four methyls ( $\delta$  55.8, 22.2 (2C) and 16.8). The  $^1\text{H}$ -NMR spectrum of compound **A25** was similar to that of compound **A14** except for the replacement of a prenyl unit in compound **A14** with 2-hydroxy-3-methyl-3-butenyl unit in compound **A25**. The presence of 2-hydroxy-3-methyl-3-butenyl unit was confirmed by the HMBC cross

peaks (**Table 3.16**) of methyl proton H-5'' ( $\delta_{\text{H}}$  1.57) with C-2'' ( $\delta$  73.1), C-3'' ( $\delta$  147.9), and C-4'' ( $\delta$  109.6), as well as the non-equivalent methylene protons H<sub>2</sub>-4'' ( $\delta$  4.81 and 4.67), with C-2'', and C-5'' ( $\delta$  16.8). In addition, the <sup>1</sup>H-<sup>1</sup>H COSY correlations (**Table 3.16**) between the remaining non-equivalent methylene protons H<sub>2</sub>-1'' ( $\delta$  2.78 and 2.58) with methine proton H-2'' ( $\delta$  4.38). The chemical shift of C-2'' ( $\delta$  73.1) showed the hydroxy substituent on this carbon. The 2-hydroxy-3-methyl-3-butenyl unit was attached at C-3 based on the HMBC correlations between the methylene proton H<sub>2</sub>-1'' with C-3 ( $\delta$  119.0). The NMR data of compound **A25** is the same compound with these of artogomezianone. Therefore, compound **A25** was artogomezianone (Likhitwitayawuid *et al.*, 2006)

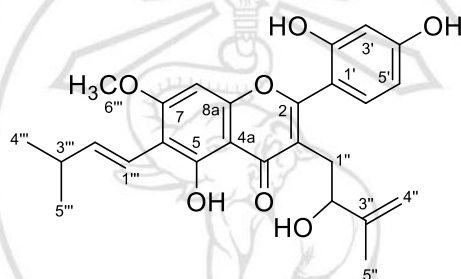


**Figure 3.12** The structure of artogomezianone (**A25**)

**Table 3.15** The NMR data of compound **A25** (400 MHz, acetone-*d*<sub>6</sub>) and artogomezianone (500 MHz, acetone-*d*<sub>6</sub>)

position	compound <b>A25</b>		artogomezianone	
	$\delta_{\text{H}}$ , mult. ( <i>J</i> in Hz)	$\delta_{\text{C}}$ (Type)	$\delta_{\text{H}}$ , mult. ( <i>J</i> in Hz)	$\delta_{\text{C}}$ (Type)
2	-	163.1 (C)	-	163.3 (C)
3	-	119.0 (C)	-	119.8 (C)
4	-	183.0 (C)	-	183.9 (C)
4a	-	104.6 (C)	-	105.4 (C)
5-OH	13.82, s	158.9 (C)	13.81, s	159.7 (C)
6	-	109.1 (C)	-	109.9 (C)
7	-	162.5 (C)	-	164.0 (C)
8	6.66, s	89.7 (CH)	6.57, s	90.6 (CH)



**Table 3.15** (continued)

position	compound <b>A25</b>		artogomezianone	
	$\delta_{\text{H}}$ , mult. ( <i>J</i> in Hz)	$\delta_{\text{C}}$ (Type)	$\delta_{\text{H}}$ , mult. ( <i>J</i> in Hz)	$\delta_{\text{C}}$ (Type)
8a	-	156.1 (C)	-	156.9 (C)
1'	-	112.1 (C)	-	112.9 (C)
2'	-	156.6 (C)	-	157.4 (C)
3'	6.52, d (2.4)	103.3 (CH)	6.54, d (2.5)	104.1 (CH)
4'	-	160.7 (C)	-	161.5 (C)
5'	6.53, dd (8.0, 2.4)	107.4 (CH)	6.53, dd (8.0, 2.5)	108.2 (CH)
6'	7.31, d (8.0)	131.9 (CH)	7.31, d (8.0)	132.8 (CH)
1''	a: 2.78, dd (13.8, 5.0) b: 2.58, dd (13.8, 8.4)	32.1 (CH <sub>2</sub> )	a: 2.78, dd (14.0, 5.0) b: 2.57, dd (14.0, 9.0)	33.0 (CH <sub>2</sub> )
2''	4.38, m	73.1 (CH)	4.39 - 4.42, m	74.0 (CH)
3''	-	147.9 (C)	-	148.7 (C)
4''	a: 4.81, s b: 4.67, s	109.6 (CH <sub>2</sub> )	a: 4.81, s b: 4.66, s	110.5 (CH <sub>2</sub> )
5''	1.57, s	16.8 (CH <sub>3</sub> )	1.57, s	17.6 (CH <sub>3</sub> )
1'''	6.54, dd (16.0, 2.4)	116.1 (CH)	6.59, dd (16.5, 1.0)	116.9 (CH)
2'''	6.72, dd (16.0, 7.2)	141.5 (CH)	6.72, dd (16.5, 7.5)	142.3 (CH)
3'''	2.43, m	33.1 (CH)	2.39 - 2.47, m	33.9 (CH)
4'''	1.08, d (6.8)	22.2 (CH <sub>3</sub> )	1.08, d (6.5)	23.0 (CH <sub>3</sub> )
5'''	1.08, d (6.8)	22.2 (CH <sub>3</sub> )	1.08, d (6.5)	23.0 (CH <sub>3</sub> )
6'''	3.96, s	55.8 (CH <sub>3</sub> )	3.97, s	56.6 (CH <sub>3</sub> )

**Table 3.16** The HMBC and COSY correlations of compound **A25**

position	HMBC	COSY
OH-5	C-4, C-4a, C-6	-
H-8	C-7, C-8a, C-6'''	-
H-3'	C-2', C-4'	-
H-5'	C-4', C-6'	H-6'
H-6'	C-1', C-5'	H-5'
H-1''	C-3, C-4, C-2''	H-2''
H-2''	C-1''	H-1''
H-4''	C-2'', C-5''	H-5''
H-5''	C-2'', C-3'', C-4''	H-2''
H-1'''	C-2''', C-3''', C-4'''	H-2'''
H-2'''	C-1''', C-3''', C-4''', C-5'''	H-1''', H-3'''
H-3'''	C-2''', C-4''', C-5'''	H-2''', H-4''', H-5'''
H-4'''	C-2''', C-3'''	H-3'''
H-5'''	C-2''', C-3'''	H-3'''
H-6'''	C-7	-

### 3.2 Isolated compounds of the twigs of *A. lakoocha*

Purification of acetone extract of the twigs of *A. lakoocha* led to the isolation of two new compounds (**A26-A27**) together with seventeen known compounds (**A2, A4-A7, A9, A11-A12, A16, A18, A21-A22, A28-A32**). The structures were identified by spectroscopic data.

#### 3.2.1 Compound **A26**

Compound **A26** was obtained as a pale yellow gum with a specific rotation of  $[\alpha]^{25}_D +35.6$  ( $c = 0.1$ , MeOH). The molecular formula  $C_{20}H_{22}O_{10}$  was assigned by HRESI-TOFMS ( $m/z$  445.1115  $[M+Na]^+$ ). The UV spectrum showed maximum absorption bands at  $\lambda_{max}$  217 and 280 nm. The IR spectrum displayed hydroxy (3300

$\text{cm}^{-1}$ ), conjugated carbonyl ( $1693\text{ cm}^{-1}$ ) and double bond ( $1450\text{ cm}^{-1}$ ) functional groups. The  $^1\text{H}$ -NMR spectrum (**Table 3.17**) (**Figure 37**) consisted of signals for four aromatic protons of a *para*-disubstituted benzene ring ( $\delta$  7.08 and 6.70, each d,  $J = 8.6\text{ Hz}$ , 2H), two *meta*-coupled aromatic protons ( $\delta$  6.14 and 5.93, each d,  $J = 2.0\text{ Hz}$ , 1H), signals of  $\beta$ -D-glucose moiety [ $\delta$  5.06 (d,  $J = 7.2\text{ Hz}$ , 1H), 3.92 (dd,  $J = 12.0, 2.0\text{ Hz}$ , 1H), 3.74 (dd,  $J = 12.0, 5.2\text{ Hz}$ , 1H), 3.47 (dd,  $J = 8.4, 7.2\text{ Hz}$ , 1H), 3.45 (t,  $J = 8.4\text{ Hz}$ , 1H), 3.44 (m, 1H) and 3.42 (dd,  $J = 9.2, 8.4\text{ Hz}$ , 1H)], and methylene protons ( $\delta$  2.88, brd,  $J = 1.2\text{ Hz}$ , 2H). Compound **A26** displayed twenty carbons from the  $^{13}\text{C}$ -NMR and DEPT135 spectra (**Table 3.17**) (**Figure 38**) including seven quaternary carbons ( $\delta$  206.1, 168.9, 162.4 (2C), 156.4, 134.0 and 106.0), eleven methines ( $\delta$  130.4 (2C), 116.1 (2C), 102.0, 97.9, 96.4, 78.5, 78.4, 74.8 and 71.1), and two methylenes ( $\delta$  62.4 and 31.0). The presence of D-glucose moiety unit was confirmed by the following  $^1\text{H}$ ,  $^{13}\text{C}$ -NMR spectra and  $^1\text{H}$ - $^1\text{H}$  COSY correlations (**Table 3.17**); H-1" ( $\delta$  5.06)/H-2" ( $\delta$  3.47) and H-3" ( $\delta$  3.45), H-4" ( $\delta$  3.42)/ H-3" and H-5" ( $\delta$  3.44), H-5"/H-4", H<sub>a</sub>-6" ( $\delta$  3.92) and H<sub>b</sub>-6" ( $\delta$  3.74) and from its isolation after acid hydrolysis of **A26** via TLC and specific rotation (Yang et al., 2011). The *meta*-coupled aromatic proton resonating at  $\delta$  6.14 was assigned H-3, according to HMBC correlations (**Table 3.17**) with C-1 ( $\delta$  97.9), C-2 ( $\delta$  162.4), and C-4 ( $\delta$  168.1). Thus, the remaining *meta*-coupled aromatic proton,  $\delta$  5.93 was located at H-5 based on HMBC correlations with C-1, C-4, and C-6 ( $\delta$  168.1). The chemical shifts of C-4 and C-6 established the hydroxy substituents at C-4 and C-6 while the chemical shift of C-2 showed the oxysubstituent at C-2. The methylene proton H-8 ( $\delta$  2.88) showed HMBC cross peaks with C-1' ( $\delta$  134.0), C-2' ( $\delta$  130.4), and C-6' ( $\delta$  130.4) of the *para*-disubstituted benzene ring and carbonyl carbon C-7 ( $\delta$  206.1). The chemical shift of C-4' ( $\delta$  162.4) of the *para*-disubstituted benzene ring indicated that the hydroxy group was the substituent at C-4'. These data constructed a 2-(4-hydroxyphenyl)acetyl fragment. This fragment was attached at C-1 of benzene ring on the basis of the chemical shift of C-1 and HMBC correlations between H-3 and H-5 of the benzene ring with the carbonyl group. Therefore, the glucose moiety was attached at C-2 of the benzene ring with an ether linkage confirming by the HMBC correlation between anomeric proton, H-1" ( $\delta$  5.06), with C-2 of benzene ring. Consequently, compound **A26** was identified as new compound named lakoochanoside A.

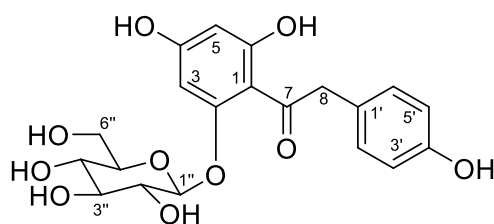


**Figure 3.13** The structure of lakoochanoside A (**A26**)

**Table 3.17** The NMR data (400 MHz, MeOD-*d*<sub>4</sub>) of lakoochanoside A (**A26**)

position	$\delta_H$ , mult. ( <i>J</i> in Hz)	$\delta_C$ (Type)	HMBC	COSY
1	-	106.0 (C)	-	-
2	-	162.4 (C)	-	-
3	6.14, d (2.0)	96.4 (CH)	C-1, C-2, C-4, C-7	H-5
4	-	168.9 (C)	-	-
5	5.93, d (2.0)	97.9 (CH)	C-1, C-4, C-6, C-7	H-3
6	-	162.4 (C)	-	-
7	-	206.1 (C)	-	-
8	2.88, brd (1.2)	31.0 (CH <sub>2</sub> )	C-7, C-1', C-2', C-6'	-
1'	-	134.0 (C)	-	-
2'	7.08, d (8.6)	130.4 (CH)	C-1', C-3', C-4'	H-3'
3'	6.70, d (8.6)	116.1 (CH)	C-1', C-2', C-4'	H-2'
4'	-	156.4 (C)	-	-
5'	6.70, d (8.6)	116.1 (CH)	C-1', C-4', C-6'	H-6'
6'	7.08, d (8.6)	130.4 (CH)	C-1', C-4', C-5'	H-5'
1''	5.06, d (7.2)	102.0 (CH)	C-2, C-3, C-2''	H-2''
2''	3.47, dd (8.4, 7.2)	74.8 (CH)	C-1'', C-3'', C-4''	H-1'', H-3''
3''	3.45, t (8.4)	78.5 (CH)	C-1'', C-2'', C-4''	H-2'', H-4''
4''	3.42, dd (9.2, 8.4)	71.1 (CH)	C-2'', C-3'', C-5''	H-3'', H-5''
5''	3.44, m	78.4 (CH)	C-1'', C-2'', C-3'', C-4'', C-6''	H-4'', H <sub>ab</sub> -6''
6''	a: 3.92, dd (12.0, 2.0) b: 3.74, dd (12.0, 5.2)	62.4 (CH <sub>2</sub> )	C-4'', C-5''	H-5'', H <sub>b</sub> -6'' H-5'', H <sub>a</sub> -6''

### 3.2.2 Compounds A27 and A28

Compound **A28** was obtained as a brown gum. The UV spectrum showed maximum absorption bands at  $\lambda_{\text{max}}$  213 and 275 nm. The IR spectrum displayed bands hydroxy ( $3383\text{ cm}^{-1}$ ) and double bond ( $1602\text{ cm}^{-1}$ ) functional groups. The  $^1\text{H}$ -NMR spectrum of **A28** (Table 3.19) (Figure 41) displayed the signals for four aromatic protons of a *para*-disubstituted benzene ring ( $\delta$  7.23 and 6.80, each d,  $J = 8.4\text{ Hz}$ , 2H), two *meta*-coupled aromatic protons [ $\delta$  5.96 and 5.87, each d,  $J = 2.2\text{ Hz}$ , 1H], signals of rhamnose moiety [ $\delta$  4.27 (d,  $J = 2.0\text{ Hz}$ , 1H), 3.70 (dd,  $J = 9.6, 6.4\text{ Hz}$ , 1H), 3.58 (dd,  $J = 9.6, 3.2\text{ Hz}$ , 1H), 3.48 (dd,  $J = 3.2, 1.6\text{ Hz}$ , 1H), 3.31 (t,  $J = 9.6\text{ Hz}$ , 1H) and 1.26 (d,  $J = 6.4\text{ Hz}$ , 3H)], two oxymethine proton [ $\delta$  4.67 (d,  $J = 8.0\text{ Hz}$ , 1H) and 3.94 (ddd,  $J = 8.8, 8.0, 5.6\text{ Hz}$ , 1H)], and two non-equivalent methylene protons [ $\delta$  2.91 (dd,  $J = 16.0, 5.6\text{ Hz}$ , 1H) and 2.66 (dd,  $J = 16.0, 8.8\text{ Hz}$ , 1H)]. Compound **A28** displayed twenty-one carbons from the  $^{13}\text{C}$ -NMR and DEPT135 spectra (Table 3.19) (Figure 42) including six quaternary carbons ( $\delta$  158.4, 157.9, 157.5, 156.8, 131.2 and 100.7) thirteen methines ( $\delta$  129.4 (2C), 116.1 (2C), 102.2, 96.5, 95.5, 81.1, 76.2, 73.9, 72.2, 71.9 and 70.3) one methylene ( $\delta$  28.1) and one methyl ( $\delta$  17.9). The presence of rhamnose moiety unit was confirmed by the following  $^1\text{H}$ - $^1\text{H}$  COSY correlations; H-1" ( $\delta$  4.27)/H-2" ( $\delta$  3.48), H-2"/H-1" and H-3" ( $\delta$  3.58), H-3"/H-2" and H-4" ( $\delta$  3.31), H-4"/H-3" and H-5" ( $\delta$  3.70), H-5"/H-4" and H-6" ( $\delta$  1.226) and H-6"/H-5". The *meta*-coupled aromatic protons of **A28** resonating at  $\delta$  5.96 was assigned as H-6 due to its HMQC correlation with C-6 ( $\delta$  96.5) and the HMBC correlations (Table 3.20) with C-4 ( $\delta$  28.1), C-5 ( $\delta$  156.8), and C-7 ( $\delta$  157.5). Thus, the remaining *meta*-coupled aromatic proton at  $\delta$  5.87 was located at C-8 ( $\delta$  95.5). One of oxymethine proton resonating of  $\delta$  4.67 was located as H-2 according to its  $^1\text{H}$ - $^1\text{H}$  COSY correlation with H-3 ( $\delta$  3.94) as well as the HMBC correlations of H-2 with C-3 ( $\delta$  76.2), C-4 ( $\delta$  28.1) and C-8a ( $\delta$  158.4), while the oxymethine proton H-3, displayed  $^1\text{H}$ - $^1\text{H}$  COSY cross peaks with the non-equivalent oxymethylene protons H<sub>2</sub>-4 ( $\delta$  2.91 and 2.66). In addition, the methylene protons, H<sub>ab</sub>-4, showed HMBC correlations with C-2 ( $\delta$  81.1), C-3, C-4a ( $\delta$  100.7), and C-8a. These data together with the chemical shifts of C-5 ( $\delta$  156.8) and C-7 ( $\delta$  157.5) established a chromane ring with the hydroxy substituents at C-5 and C-7. The *para*-disubstituted benzene ring was attached at C-2 of chromane ring

based on the HMBC correlations of H-2' and H-6' ( $\delta$  7.43) with C-2. The chemical shift of C-4' ( $\delta$  157.9) was identified the hydroxy substituent at C-4'. These data of **A28** constructed the flavan-3-ol moiety with the hydroxy substituents at C-5, C-7 and C-4'. The HMBC correlation between the anomeric proton (H-1'') and C-3 gave the glycoside linkage between C-3 of chroman moiety and C-1'' ( $\delta$  102.2) of rhamnose unit. As H-2 coupled with H-3 with a relatively large coupling constant of 8.0 Hz, both of them were located at pseudoaxial positions, indicating a *trans* relationship between these protons. The specific rotation of **A28**,  $[\alpha]^{25}_{\text{D}} -32.2$  ( $c = 0.28$ , MeOH), was similar to (+)-afzelechin-3-*O*- $\alpha$ -L-rhamnopyranoside,  $[\alpha]^{25}_{\text{D}} -83.4$  ( $c = 0.3$ , MeOH) (Choi *et al.*, 2015), thus the absolute configuration at C-2 and C-3 were assigned as 2*R*,3*S*-configurations. Therefore, compound **A28** was (+)-afzelechin-3-*O*- $\alpha$ -L-rhamnopyranoside (Choi *et al.*, 2015). Compound **A27** was obtained as a brown gum with molecular formula  $\text{C}_{21}\text{H}_{24}\text{O}_{11}$  from HRESI-TOFMS ( $m/z$  475.1206  $[\text{M}+\text{Na}]^+$ ). The  $^1\text{H}$ -NMR spectrum (Table 3.18) (Figure 39) of compound **A27** were similar to that of compound **A28**. The main difference between compound **A27** and compound **A28** was the disappearance of the *meta*-coupled aromatic protons in compound **A27** when comparison with the  $^1\text{H}$ -NMR spectrum of compound **A28**. The  $^{13}\text{C}$ -NMR spectrum of compound **A27** (Table 3.18) (Figure 40) showed the signals for two additional quaternary carbons ( $\delta$  157.7 and 157.4) instead of two methine carbons ( $\delta$  96.5 and 95.5) in compound **A28**, indicating that the *meta*-coupled aromatic protons in compound **A28** were substituted with hydroxy groups in compound **A27**. The above conclusion established a 3,5,6,7,8,4'-hexahydroxyflavan (Zeng *et al.*, 2011). In addition, absolute configuration at C-2 and C-3 of compound **A27** were determined by the comparison of the specific rotation of (+)-afzelechin-3-*O*- $\alpha$ -L-rhamnopyranoside (Choi *et al.*, 2015) and coupling constants of H-2 and H-3. The specific rotation of compound **A27**,  $[\alpha]^{25}_{\text{D}} -28.1$  ( $c = 0.32$ , MeOH), was similar to (+)-afzelechin-3-*O*- $\alpha$ -L-rhamnopyranoside,  $[\alpha]^{25}_{\text{D}} -83.4$  ( $c = 0.3$ , MeOH), thus the absolute configuration at C-2 and C-3 were assigned as 2*R*,3*S*-configuration. Consequently, compound **A27** was identified as new flavan-3-ol derivative named lakoochanoside B.

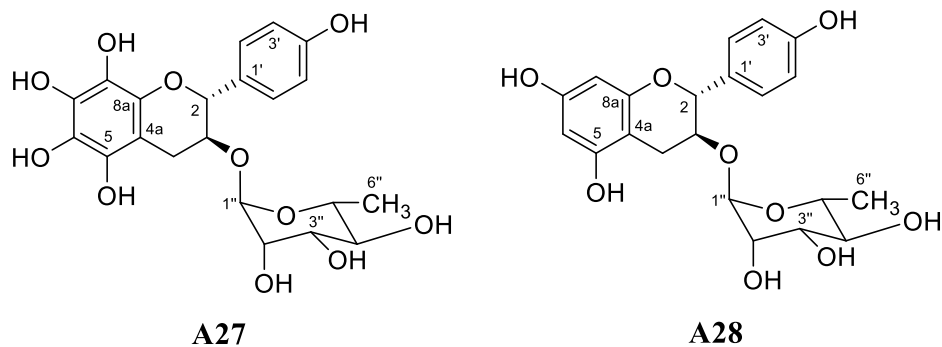


**Figure 3.14** The structures of compounds **A27** and **A28**

**Table 3.18** The NMR data (400 MHz, MeOD-*d*<sub>4</sub>) of lakoochanoside B (**A27**)

position	$\delta_{\text{H}}$ , mult. ( <i>J</i> in Hz)	$\delta_{\text{C}}$ (Type)	HMBC	COSY
2	4.62, d (8.0)	81.0 (CH)	C-4, C-8a, C-1', C-2, C-6'	H-3
3	3.90, ddd (8.8, 8.0, 5.8)	76.1 (CH)	C-2, C-4a	H-2, H <sub>ab</sub> -4
4	a: 2.87, dd (16.0, 5.8) b: 2.61, dd (16.0, 8.8)	28.1 (CH <sub>2</sub> )	C-2, C-4a, C-5, C-8a	H-2, H-3
4a	-	100.7 (C)	-	-
5	-	158.3 (C)	-	-
6	-	157.7 (C)	-	-
7	-	157.7 (C)	-	-
8	-	157.4 (C)	-	-
8a	-	156.7 (C)	-	-
1'	-	131.1 (C)	-	-
2'	7.18, d (8.8)	129.3 (CH)	C-2, C-4'	H-3'
3'	6.76, d (8.8)	116.0 (CH)	C-1', C-4'	H-2'
4'	-	158.3 (C)	-	-
5'	6.76, d (8.8)	116.0 (CH)	C-1', C-4'	H-6'
6'	7.18, d (8.8)	129.3 (CH)	C-2, C-4'	H-5'

**Table 3.18** (continued)

position	$\delta_{\text{H}}$ , mult. ( $J$ in Hz)	$\delta_{\text{C}}$ (Type)	HMBC	COSY
1"	4.22, d (1.6)	102.1 (CH)	C-3, C-2", C-3" C-5"	H-2"
2"	3.44, dd (3.2, 1.6)	71.9 (CH)	C-1", C-4"	H-1", H-3"
3"	3.55, dd (9.6, 3.2)	72.2 (CH)	C-1", C-5"	H-2", H-4"
4"	3.27, t (9.6)	73.9 (CH)	C-2", C-3", C-6"	H-3", H-5"
5"	3.66, dq (9.6, 6.4)	70.2 (CH)	C-1", C-3", C-6"	H-4", H-6"
6"	1.22, d (6.4)	17.9 (CH <sub>3</sub> )	C-4", C-5"	H-5"

ลิขสิทธิ์มหาวิทยาลัยเชียงใหม่  
 Copyright© by Chiang Mai University  
 All rights reserved



**Table 3.19** The NMR data (400 MHz, MeOD-*d*<sub>4</sub>) of compounds **A27** and **A28** and (+)-afzelechin-3-*O*- $\alpha$ -L-rhamnopyranoside (500 MHz, MeOD-*d*<sub>4</sub>)

position	compound <b>A27</b> (lakoochanoside B)		compound <b>A28</b>		(+) -afzelechin-3- <i>O</i> - $\alpha$ -L-rhamnopyranoside	
	$\delta_{\text{H}}$ , mult. ( <i>J</i> in Hz)	$\delta_{\text{C}}$ (Type)	$\delta_{\text{H}}$ , mult. ( <i>J</i> in Hz)	$\delta_{\text{C}}$ (Type)	$\delta_{\text{H}}$ , mult. ( <i>J</i> in Hz)	$\delta_{\text{C}}$ (Type)
2	4.62, d (8.0)	81.0 (CH)	4.67, d (8.0)	81.1 (CH)	4.66, d (7.9)	81.3 (CH)
3	3.90, ddd (8.8, 8.0, 5.8)	76.1 (CH)	3.94, ddd (8.8, 8.0, 5.6)	76.2 (CH)	3.94, m	76.4 (CH)
4	a: 2.87, dd (16.0, 5.8) b: 2.61, dd (16.0, 8.8)	28.1 (CH <sub>2</sub> )	a: 2.91, dd (16.0, 5.6) b: 2.66, dd (16.0, 8.8)	28.1 (CH <sub>2</sub> )	a: 2.91, dd (15.9, 5.7) b: 2.65, dd (16.3, 8.9)	28.4 (CH <sub>2</sub> )
4a	-	100.7 (C)	-	100.7 (C)	-	100.8 (C)
5	-	158.3 (C)	-	156.8 (C)	-	157.1 (C)
6	-	157.7 (C)	5.96, d (2.2)	96.5 (CH)	5.94, d (2.2)	95.6 (CH)
7	-	157.7 (C)	-	157.5 (C)	-	157.7 (C)
8	-	157.4 (C)	5.87, d (2.2)	95.5 (CH)	5.85, d (2.4)	96.6 (CH)
8a	-	156.7 (C)	-	158.4 (C)	-	158.1 (C)
1'	-	131.1 (C)	-	131.2 (C)	-	131.4 (C)
2'	7.18, d (8.8)	129.3 (CH)	7.23, d (8.4)	129.4 (CH)	7.23, d (8.5)	129.5 (CH)
3'	6.76, d (8.8)	116.0 (CH)	6.80, d (8.4)	116.1 (CH)	6.79, d (8.5)	116.2 (CH)

**Table 3.19** (continued)

position	compound <b>A27</b> (lakoochanoside B)		compound <b>A28</b>		(+) - afzelechin-3- <i>O</i> - $\alpha$ -L-rhamnopyranoside	
	$\delta_{\text{H}}$ , mult. ( <i>J</i> in Hz)	$\delta_{\text{C}}$ (Type)	$\delta_{\text{H}}$ , mult. ( <i>J</i> in Hz)	$\delta_{\text{C}}$ (Type)	$\delta_{\text{H}}$ , mult. ( <i>J</i> in Hz)	$\delta_{\text{C}}$ (Type)
4'	-	158.3 (C)	-	157.9 (C)	-	158.7 (C)
5'	6.76, d (8.8)	116.0 (CH)	6.80, d (8.4)	116.1 (CH)	6.79, d (8.5)	116.2 (CH)
6'	7.18, d (8.8)	129.3 (CH)	7.23, d (8.4)	129.4 (CH)	7.23, d (8.5)	129.5 (CH)
1"	4.22, d (1.6)	102.1 (CH)	4.27, d (2.0)	102.2 (CH)	4.25, brs	102.4 (CH)
2"	3.44, dd (3.2, 1.6)	71.9 (CH)	3.48, dd (3.2, 1.6)	71.9 (CH)	- *	72.1 (CH)
3"	3.55, dd (9.6, 3.2)	72.2 (CH)	3.58, dd (9.6, 3.2)	72.2 (CH)	- *	72.4 (CH)
4"	3.27, t (9.6)	73.9 (CH)	3.31, t (9.5)	73.9 (CH)	- *	74.1 (CH)
5"	3.66, dq (9.6, 6.4)	70.2 (CH)	3.70, dd (9.6, 6.4)	70.3 (CH)	- *	70.5 (CH)
6"	1.22, d (6.4)	17.9 (CH <sub>3</sub> )	1.26, d (6.4)	17.9 (CH <sub>3</sub> )	1.25, d (6.3)	18.1 (CH <sub>3</sub> )

\* not appear in reference

**Table 3.20** The HMBC and COSY correlations of compound **A28**

position	HMBC	COSY
H-2	C-3, C-4, C-8a, C-1'	H-3
H-3	C-2, C-4, C-4a, C-1', C-1''	H-2, H-4 <sub>a</sub> , H-4 <sub>b</sub>
H-4	C-2, C-3, C-4a, C-8a	H-2, H-3
H-6	C-4a, C-5, C-7	H-8
H-8	C-6, C-8, C-8a	H-6
H-2'	C-2, C-1', C-3', C-4'	H-3'
H-3'	C-1', C-2', C-4'	H-2'
H-5'	C-2, C-4', C-6'	H-6'
H-6'	C-2, C-1', C-4', C-5'	H-5'
H-1''	C-3, C-2'', C-5''	H-2''
H-2''	C-1'', C-3''	H-1'', H-3''
H-3''	C-2'', C-4''	H-2'', H-4''
H-4''	C-3'', C-5'', C-6''	H-3'', H-5''
H-5''	C-3, C-1'', C-4'', C-6''	H-4'', H-6''
H-6''	C-5''	H-5''

### 3.2.3 Compounds **A29** and **A30**

Compound **A29** was isolated as brown gum. Comparison of <sup>1</sup>H-NMR spectra of compound **A29** (Table 3.21) (Figure 43) with compound **A28** found that compound **A29** displayed the signals of three aromatic protons of a 1,2,4-trisubstituted benzene ring [ $\delta$  6.84 (d,  $J$  = 2.0 Hz, 1H), 6.77 (d,  $J$  = 8.4 Hz, 1H) and 6.72 (dd,  $J$  = 8.4 and 2.0 Hz, 1H)] instead of the *para*-disubstituted aromatic protons [ $\delta$  7.23 and 6.80, each d,  $J$  = 8.4 Hz, 2H] of compound **A28**. The hydroxy groups were located at C-3' ( $\delta$  146.4) and C-4' ( $\delta$  146.3) according to their chemical shifts. Therefore, compound **A29** was (+)-catechin-3-*O*- $\alpha$ -L-rhamnopyranoside (Kim *et al.*, 2012). Compound **A30** obtained as brown gum. The <sup>1</sup>H-NMR spectrum (Table 3.21) (Figure 45) of compound **A30** was similar to those of compound **A29** except for the disappearance of the signals of rhamnose moiety in

compound **A30**. The absolute configuration at C-2 and C-3 of compound **A30** were assigned to be 2*R*,3*S*-configuration due to comparison of the specific rotation,  $[\alpha]^{25}_D$  -13.6 ( $c = 0.22$ , MeOH) with those of (+)-catechin,  $[\alpha]^{25}_D$  -18.8 ( $c = 0.5$ , MeOH). Therefore, compound **A30** was (+)-catechin (Hye *et al.*, 2009).

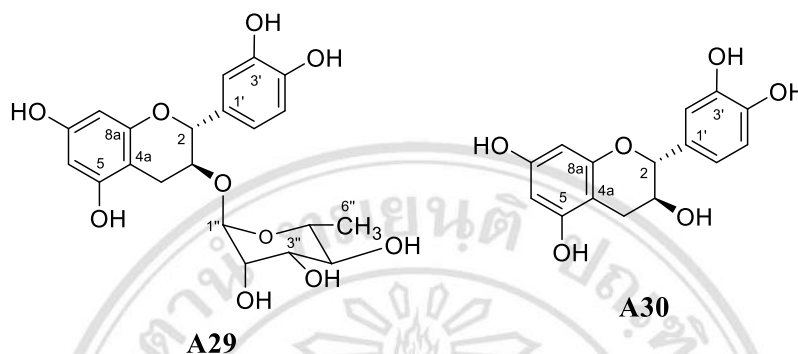


**Figure 3.15** The structures of compounds **A29** and **A30**

**Table 3.21** The  $^1\text{H}$ -NMR data of compounds **A29** (400 MHz, MeOD- $d_4$ ), **A30** (400 MHz, acetone- $d_6$ ), (+)-catechin-3-*O*- $\alpha$ -L-rhamnopyranoside (400 MHz, MeOD- $d_4$ ) and (+)-catechin (400 MHz, acetone- $d_6$ )

position	$\delta_H$ , mult. ( $J$ in Hz)			
	compound <b>A29</b>	(+)-catechin-3- <i>O</i> - $\alpha$ -L-rhamno pyranoside	compound <b>A30</b>	(+)-catechin
2	4.62, d (7.6)	4.62, d (7.6)	4.55, d (7.6)	4.56, d (7.8)
3	3.93, ddd (8.4, 7.6, 5.6)	3.93, m	3.99, m	4.00, ddd (8.5, 7.8, 5.6)
4	a: 2.87, dd (16.0, 5.6)	a: 2.88, dd (16.0, 5.5)	a: 2.91, dd (16.0, 5.4)	a: 2.90, dd (16.1, 5.5)
	b: 2.64, dd (16.0, 8.4)	b: 2.64, dd (16.0, 8.5)	b: 2.52, dd (16.0, 8.4)	b: 2.54, dd (16.0, 8.5)
5	-	-	8.24, s	-

**Table 3.21** (continued)

position	$\delta_{\text{H}}$ , mult. ( <i>J</i> in Hz)			
	compound <b>A29</b>	(+)-catechin-3- <i>O</i> - $\alpha$ -L-rhamno pyranoside	compound <b>A30</b>	(+)-catechin
6	5.94, d (2.2)	5.94, d (2.3)	5.87, d (2.0)	5.87, d (2.3)
7	-	-	8.06, s	-
8	5.86, d (2.2)	5.86, d (2.3)	6.02, d (2.0)	6.01, d (2.3)
2'	6.84, d (2.0)	6.84, d (1.8)	6.89, d (1.2)	6.89, d (1.9)
5'	6.77, d (8.4)	6.77, d (8.0)	6.79, d (8.0)	6.79, d (8.1)
6'	6.72, dd (8.4, 2.0)	6.72, dd (8.0, 1.8)	6.75, dd (8.0, 1.2)	6.73, dd (8.1, 1.9)
1"	4.30, d (1.6)	4.29, d (1.4)	-	-
2"	3.52, dd (3.4, 1.6)	3.51, dd (3.2, 1.8)	-	-
3"	3.58, dd (9.4, 3.4)	3.57, dd (3.2, 1.8)	-	-
4"	3.31, m	3.31, m	-	-
5"	3.68, dd (9.4, 6.2)	3.68, m	-	-
6"	1.25, d (6.0)	1.25, d (6.2)	-	-

ลิขสิทธิ์มหาวิทยาลัยเชียงใหม่  
Copyright© by Chiang Mai University  
All rights reserved

**Table 3.22** The  $^{13}\text{C}$ -NMR data of compounds **A29** (100 MHz,  $\text{MeOD-}d_4$ ), **A30** (100 MHz,  $\text{acetone-}d_6$ ), (+)-catechin-3-*O*- $\alpha$ -L-rhamnopyranoside (100 MHz,  $\text{MeOD-}d_4$ ) and (+)-catechin (100 MHz,  $\text{DMSO-}d_6$ )

position	$\delta_c$ (Type)			
	compound <b>A29</b>	(+)-catechin-3- <i>O</i> - $\alpha$ -L-rhamnopyranoside	compound <b>A30</b>	(+)-catechin
2	81.1 (CH)	81.3 (CH)	82.7 (CH)	80.9 (CH)
3	76.0 (CH)	76.1 (CH)	68.4 (CH)	66.3 (CH)
4	28.1 ( $\text{CH}_2$ )	28.1 ( $\text{CH}_2$ )	28.8 ( $\text{CH}_2$ )	27.7 ( $\text{CH}_2$ )
4a	102.1 (C)	100.8 (C)	100.7 (C)	99.1 (C)
5	157.6 (C)	157.5 (C)	156.9 (C)	155.3 (C)
6	95.5 (CH)	95.6 (CH)	95.5 (CH)	93.6 (CH)
7	156.9 (C)	157.0 (C)	157.2 (C)	156.1 (C)
8	96.4 (CH)	95.6 (CH)	96.2 (CH)	95.1 (CH)
8a	158.0 (C)	158.1 (C)	157.8 (C)	156.4 (C)
1'	132.0 (C)	132.1 (C)	132.2 (C)	139.6 (C)
2'	115.1 (CH)	115.2 (CH)	115.3 (CH)	114.5 (CH)
3'	146.4 (C)	146.4 (C)	145.8 (C)	144.6 (C)
4'	146.3 (C)	146.5 (C)	145.7 (C)	144.8 (C)
5'	116.1 (CH)	116.2 (CH)	115.8 (CH)	115.1 (CH)
6'	119.8 (CH)	120.0 (CH)	120.1 (CH)	118.4 (CH)
1''	100.7 (CH)	102.3 (CH)	-	-
2''	72.0 (CH)	72.1 (CH)	-	-
3''	72.3 (CH)	72.4 (CH)	-	-
4''	74.0 (CH)	74.1 (CH)	-	-
5''	70.3 (CH)	70.5 (CH)	-	-
6''	17.9 ( $\text{CH}_3$ )	18.1 ( $\text{CH}_3$ )	-	-

### 3.2.4 Compounds A31 and A32

Compound **A31** was isolated as a brown gum. The  $^1\text{H-NMR}$  spectrum (**Table 3.23**) (**Figure 47**) showed resonances of three aromatic protons of a 1,2,4-trisubstituted benzene ring [ $\delta$ 7.40 (d,  $J = 8.4$  Hz, 1H), 6.44 (d,  $J = 2.4$  Hz, 1H) and 6.38 (dd,  $J = 8.4$ , 2.4 Hz, 1H)], two *trans*-coupled olefinic protons ( $\delta$ 7.33 and 6.89, each d,  $J = 16.4$  Hz, 1H), and three aromatic protons of a 1,3,5-trisubstituted benzene ring [ $\delta$ 6.52 (d,  $J = 2.0$  Hz, 2H) and 6.24 (t,  $J = 2.0$  Hz, 1H)]. The  $^1\text{H-NMR}$  spectral data of compound **A31** was similar to those of heterophyllene D (**A4**) isolated from the twigs of *A. heterophyllus*. The main differences were the disappearance of two methoxyl groups in compound **A31** when comparison with compound **A4**. Thus, the hydroxy groups were assigned to C-3' and C-5'. Compound **A31** was identified as oxyresveratrol (Ban *et al.*, 2006). Compound **A32** was isolated as a brown gum. Comparison of its  $^1\text{H-NMR}$  data of compound **A32** (**Table 3.16**) (**Figure 48**) with compound **A31** found that compound **A32** displayed signals of four aromatic protons of a *para*-disubstituted benzene ring ( $\delta$  7.41 and 6.84, each d,  $J = 8.6$  Hz, 2H) instead of the three aromatic protons of a 1,2,4-trisubstituted benzene ring in compound **A31**. The hydroxy groups were assigned as the substituent at C-4 according to the chemical shifts of H-3 and H-5, respectively. Therefore, compound **A32** was resveratrol (Chi *et al.*, 2014).

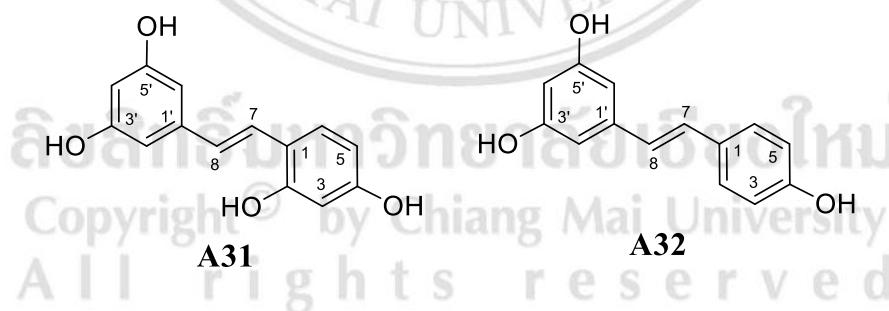


**Figure 3.16** The structures of compounds **A31** and **A32**

**Table 3.23** The  $^1\text{H}$ -NMR data (400 MHz, acetone- $d_6$ ) of compounds **A31** and **A32**, oxyresveratrol (400 MHz, MeOD- $d_4$ ) and resveratrol (400 MHz, MeOD- $d_4$ )

position	$\delta_{\text{H}}$ , mult. ( $J$ in Hz)			
	compound <b>A31</b>	oxyresveratrol	compound <b>A32</b>	resveratrol
2	-	-	6.84, d (8.6)	6.83, d (9.0)
3	6.44, d (2.4)	6.30, d (2.5)	7.41, d (8.6)	7.40, d (9.0)
5	6.38, dd (8.4, 2.4)	6.30, dd (8.7, 2.5)	6.84, d (8.6)	6.83, d (9.0)
6	7.40, d (8.4)	7.32, d (8.7)	7.41, d (8.6)	7.40, d (9.0)
7	7.33, d (16.4)	7.26, d (16.4)	7.01, d (16.0)	6.99, d (16.5)
8	6.89, d (16.4)	6.80, d (16.4)	6.88, d (16.0)	6.89, d (16.5)
2'	6.52, d (2.0)	6.43, d (2.1)	6.53, d (2.0)	6.54, d (1.8)
4'	6.24, t (2.0)	6.12, t (2.1)	6.27, t (2.0)	6.26, t (1.8)
6'	6.52, d (2.0)	6.43, t (2.1)	6.53, d (2.0)	6.54, d (1.8)

### 3.3 Isolated compounds from the barks of *A. lakoocha*

The separation of the acetone extract of the barks of *A. lakoocha* provided seven known compounds (**A6**, **A28**, **A30** and **A33-A36**). The structures were identified by spectroscopic data.

#### 3.3.1 Compound **A33**

Compound **A33** was isolated as a brown gum. The  $^1\text{H}$ -NMR spectrum (**Table 3.24**) (**Figure 49**) showed resonances for three aromatic protons of a 1,2,4-trisubstituted benzene ring [ $\delta$  7.45 (d,  $J$  = 8.5 Hz, 1H), 7.10 (d,  $J$  = 2.0 Hz, 1H) and 6.86 (dd,  $J$  = 8.5, 2.0 Hz, 1H)], three singlet aromatic protons [ $\delta$  6.94 (s, 1H) and 6.93 (s, 2H)], one methoxyl group ( $\delta$  3.86 (s, 6H)), and a prenyl unit [ $\delta$  5.34 (t,  $J$  = 7.0 Hz, 1H), 3.40 (d,  $J$  = 7.0 Hz, 2H), 1.80 and 1.62, each s, 3H]. The  $^1\text{H}$ -NMR data of compound **A33** was the same characteristic pattern of compound **A6**. In addition, compound **A33** showed the additional a methoxyl group at 3.86 in the  $^1\text{H}$ -NMR spectrum. Thus, compound **A33** was sanggenofuran B (Shi *et al.*, 2007).



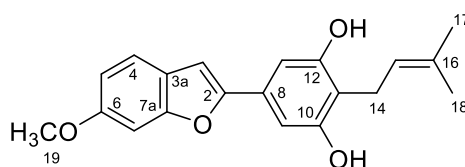


**Figure 3.17** The structure of sanggenofuran B (**A33**)

**Table 3.24** The  $^1\text{H}$ -NMR data of compound **A33** (500 MHz, acetone- $d_6$ ) and sanggenofuran B (500 MHz,  $\text{CDCl}_3$ )

position	$\delta_{\text{H}}$ , mult. ( $J$ in Hz)	
	compound <b>A33</b>	sanggenofuran B
3	6.94, s	6.84, s
4	7.45, d (8.5)	7.40, d (8.5)
5	6.86, dd (8.5, 2.0)	6.85, dd (8.5, 2.0)
7	7.10, d (2.0)	7.03, d (2.0)
9	6.93, s	6.87, s
13	6.93, s	6.87, s
14	3.40, d (7.0)	3.44, d (7.0)
15	5.34, t (7.0)	5.28, m
17	1.62, s	1.77, s
18	1.80, s	1.83, s
19	3.86, s	3.86, s

### 3.3.2 Compound **A34**

Compound **A34** was obtained as a brown gum. The  $^1\text{H}$ -NMR spectrum (**Table 3.25**) (**Figure 50**) showed resonances of a chelated hydroxy proton ( $\delta$  13.12, s, 1H), three aromatic protons of a 1,2,4-trisubstituted benzene ring [ $\delta$  7.22 (d,  $J$  = 8.5 Hz, 1H), 6.64 (d,  $J$  = 2.0 Hz, 1H) and 6.58 (dd,  $J$  = 8.5, 2.0 Hz, 1H)], two *meta*-coupled aromatic protons ( $\delta$  6.64 and 6.28, each d,  $J$  = 2.0 Hz, 1H), a prenyl unit [ $\delta$  5.07 (t,  $J$  = 6.5 Hz, 1H), 3.00 (d,  $J$  = 6.5 Hz, 2H), 1.57 and 1.39, each s, 3H], and a methoxyl proton ( $\delta$  3.79, s, 3H). The  $^1\text{H}$ -NMR spectrum of compound **A34** was similar to that of

compound **A9** except for the additional signal of methoxyl group of compound **A34**. Thus, compound **A34** was assigned as integrin (Smith *et al.*, 2019).

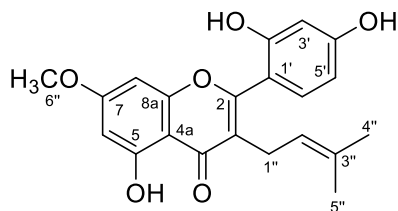


**Figure 3.18** The structure of integrin (**A34**)

**Table 3.25** The  $^1\text{H}$ -NMR data (500 MHz, acetone- $d_6$ ) of compound **A34** and integrin

position	$\delta_{\text{H}}$ , mult. ( $J$ in Hz)	
	compound <b>A34</b>	integrin
5	13.12, s	13.10, s
6	6.22, d (2.0)	6.30, d (2.3)
8	6.28, d (2.0)	6.45, d (2.3)
3'	6.64, d (2.0)	6.57, d (2.3)
5'	6.58, dd (8.5, 2.0)	6.52, dd (8.3, 2.3)
6'	7.22, d (8.5)	7.21, d (8.3)
1''	3.00, d (6.5)	3.11, d (7.1)
2''	5.07, t (6.5)	5.12, tq (7.1, 1.4)
4''	1.57, s	1.57, s
5''	1.39, s	1.43, s
6''	3.79, s	3.89, s

### 3.3.3 Compound A35

Compound **A35** was obtained as brown gum. The  $^1\text{H-NMR}$  spectrum (**Table 3.26**) (**Figure 51**) showed resonances of a chelated hydroxy proton ( $\delta$  12.02, s, 1H), four aromatic protons of a *para*-disubstituted benzene ring [ $\delta$  7.42 and 6.90, each d,  $J$  = 8.5 Hz, 2H], two *meta*-coupled aromatic protons [ $\delta$  5.91 and 5.89, each d,  $J$  = 2.0 Hz, 1H], two methine protons [ $\delta$  5.18 and 4.65, each d,  $J$  = 11.0 Hz, 1H], and signals of rhamnose moiety [ $\delta$  4.26 (m, 1H), 4.04 (brs, 1H), 3.65 (dd,  $J$  = 9.3, 3.2 Hz, 1H), 3.54 (m, 1H), 3.31 (t,  $J$  = 9.5 Hz, 1H), and 1.14 (d,  $J$  = 6.5 Hz, 3H)]. The  $^1\text{H-NMR}$  spectral data of compound **A35** showed characteristic signals similar to those of compound **A28**. The main differences were the disappearance of methylene protons in compound **A35** when comparison with compound **A28**. Thus, the carbonyl group was identified as substituents at C-4 on the basis of their chemical shifts, and the additional resonance of a chelated hydroxy proton ( $\delta$  12.02) at C-5. The specific rotation of compound **A35**,  $[\alpha]^{20}_{\text{D}} -2.3$  ( $c$  = 0.04, MeOH), was similar to those of engeletin,  $[\alpha]^{20}_{\text{D}} -14.2$  ( $c$  = 0.32, MeOH) (Su *et al.*, 2001). Thus, the absolute configuration at C-2 and C-3 was assigned as 2*S*,3*R*-configurations. Consequently, compound **A35** was engeletin (Huang *et al.*, 2011).

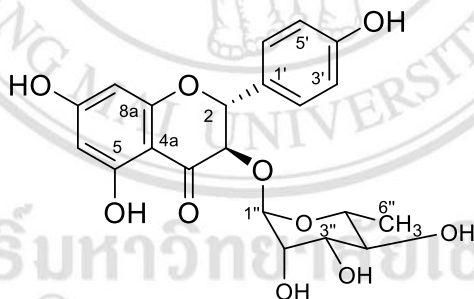


**Figure 3.19** The structure of engeletin (**A35**)

**Table 3.26** The  $^1\text{H}$ -NMR data of compounds **A35** (500 MHz, acetone- $d_6$ ) and engeletin (400 MHz, MeOD- $d_4$ )

position	$\delta_{\text{H}}$ , mult. ( $J$ in Hz)	
	compound <b>A35</b>	engeletin
2	5.18, d (11.0)	5.31, d (10.8)
3	4.65, d (11.0)	4.62, d (10.8)
5	12.02, s	-
6	5.91, d (2.0)	5.92, d (1.6)
8	5.89, d (2.0)	5.89, d (1.6)
2'	7.42, d (8.5)	7.36, d (8.4)
3'	6.90, d (8.5)	6.85, d (8.4)
5'	6.90, d (8.5)	6.85, d (8.4)
6'	7.42, d (8.5)	7.36, d (8.4)
1''	4.04, brs	3.99, s
2''	4.26, m	4.30, m
3''	3.65, dd (9.3, 3.2)	3.67, dd (9.2, 2.8)
4''	3.54, m	3.50, m
5''	3.31, t (9.5)	3.34, m
6''	1.14, d (6.5)	1.19, d (6.0)

### 3.3.4 Compound **A36**

Compound **A36** was isolated as a brown gum. The  $^1\text{H}$ -NMR spectrum (**Table 3.27**) (**Figure 52**) consisted of signals for three aromatic protons of a 1,2,4-trisubstituted benzene ring [ $\delta$  7.46 (d,  $J$  = 8.5 Hz, 1H), 6.50 (d,  $J$  = 2.0 Hz, 1H) and 6.46 (dd,  $J$  = 8.5, 2.5 Hz, 1H)], two *trans*-coupled olefinic protons ( $\delta$  7.30 and 6.88, each d,  $J$  = 16.5 Hz, 1H), three aromatic protons of a 1,3,5-trisubstituted benzene ring [ $\delta$  6.52 (d,  $J$  = 2.0 Hz, 2H) and 6.25 (t,  $J$  = 2.0 Hz, 1H)], and one methoxyl group ( $\delta$  3.84, s, 3H). The  $^1\text{H}$ -NMR data of compound **A36** was similar to those of compound **A31** except for the additional

signal of the methoxyl proton at  $\delta$  3.84 (s, 3H). Therefore, compound **A36** was *trans*-2-methoxy-4,3',5'-trihydroxystilbene (Likhitwitayawuid *et al.*, 2006).

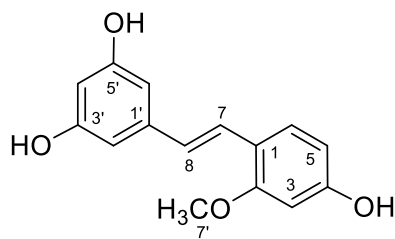


**Figure 3.20** The structure of *trans*-2-methoxy-4,3',5'-trihydroxystilbene (**A36**)

**Table 3.27** The  $^1\text{H}$ -NMR data of compound **A36** (500 MHz, acetone- $d_6$ ) and *trans*-2-methoxy-4,3',5'-trihydroxystilbene (300 MHz, acetone- $d_6$ )

position	$\delta_{\text{H}}$ , mult. ( <i>J</i> in Hz)	
	compound <b>A36</b>	<i>trans</i> -2-methoxy-4,3',5'-trihydroxystilbene
3	6.50, d (2.0)	6.45, brs
5	6.46, dd (8.5, 2.0)	6.42, brd (8.4)
6	7.46, d (8.5)	7.41, d (8.4)
7	7.30, d (16.5)	7.25, d (16.5)
8	6.88, d (16.5)	6.83, d (16.5)
2'	6.52, d (2.0)	6.45, brs
4'	6.25, t (2.0)	6.21, brs
6'	6.52, d (2.0)	6.45, brs
7'	3.84, s	3.80, s

### 3.4 Biological activities of some isolated compounds from *A. heterophyllus* and *A. lakoocha*

Some isolated compounds were evaluated for their cytotoxicities against oral human carcinoma (KB), human breast cancer (MCF-7), small lung cancer (NCI-H187), human ovarian cancer (A2780) and non-cancerous Vero cells (African green monkey kidney fibroblasts) (Table 3.28). Compounds **A1**, **A12**, **A17**, **A18**, **A21**, **A24**, and **A25** exhibited moderate to weak cytotoxicity against KB cell with the IC<sub>50</sub> values in the range of 16.7-33.6 µM, while compound **A14** with a IC<sub>50</sub> value of 13.6 µM displayed good activity compared with that of the standard drug, ellipticine, IC<sub>50</sub> 13.5 µM. Compounds **A3** and **A12** showed strong cytotoxicity against MCF-7 cell line with the IC<sub>50</sub> values of 12.6 and 10.0 µM, respectively, whereas the other compounds displayed weaker activity with the IC<sub>50</sub> values in the range of 17.6-37.9 µM. Compounds **A1**, **A10**, **A17-A19**, **A21**, **A24**, and **A25** showed weak activity against NCI-H187 cell line with IC<sub>50</sub> values in the range of 18.7-37.5 µM, while compounds **A12** and **A14** exhibited moderate activity with the IC<sub>50</sub> values of 14.8 and 14.2 µM, respectively. Moreover, compounds **A6** and **A22** had selectively moderate and weak cytotoxicity against NCI-H187 cells with the IC<sub>50</sub> values of 28.7 and 44.2 µM, respectively, and were not toxic against Vero cell lines. Furthermore, compound **A6** displayed cytotoxic activity against A2780 cell lines with an IC<sub>50</sub> value of 15 ± 1.6 µM, while compound **A33** showed weaker activity than compound **A6** with an IC<sub>50</sub> value of 57.1 ± 4.6 µM. Regarding cytotoxicity against the vero cell lines, compounds **A1** and **A12** exhibited moderate activity with the IC<sub>50</sub> values of 9.6 and 10.0 µM, respectively, while the other compounds were milder activity with the IC<sub>50</sub> values in the range of 11.3-49.7 µM.

In addition, some of isolated compounds were tested for antibacterial activity against *Staphylococcus aureus* and methicillin-resistant *Staphylococcus aureus*, antifungal activity against *Cryptococcus neoformans* (Table 3.29), antimalarial activity against *Plasmodium falciparum* K1 and acetylcholinesterase inhibitory activity (Table 3.30). Compounds **A7**, **A16**, **A26**, **A28-A30** and **A32** were inactive in all assays. Compounds **A4-A6**, **A9**, **A11**, **A21**, **A27** and **A31** were weak to inactive antibacterial activity against *S. aureus* with the MIC values in the range of 16-128 µg/mL. Compound

**A22** exhibited the strongest antibacterial activity against *S. aureus* with the MIC value of 2 µg/mL, whereas compounds **A12** and **A18** showed weaker activity with the MIC values of 4 and 8 µg/mL, respectively. For antibacterial activity against methicillin-resistant *S. aureus*, compound **A22** was two-fold more active than compound **A12** with a MIC value of 2 µg/mL, whereas the remaining compounds exhibited only moderate, weak or no activity. In addition, compound **A22** displayed strong antifungal activity against *C. neoformans* with a MIC value of 4 µg/mL, while compound **A18** showed mild activity with a MIC value of 8 µg/mL. The remaining compounds exhibited moderate activities or were inactive. Compound **A31** showed weak acetylcholinesterase inhibitory activity with % inhibition value of  $43.1 \pm 2.7$ , while compounds **A4**, **A6**, **A9**, **A11** and **A21**, exhibited weak activity with % inhibition values in the range of 12.1-31.1. Among the isolated compounds, compounds **A6**, **A21-A22** and **A27**, displayed moderately antimalarial activity against *P. falciparum* K1 with the IC<sub>50</sub> values in the range of 2.7-7.3 µM. The remaining compounds **A2**, **A11** and **A18** exhibited mild activity with the IC<sub>50</sub> values in the range of 10.2-26.7 µM.

The flavone-type compounds displayed cytotoxicities against the tested cell lines. Flavones with prenyl group, compounds **A9**, **A10**, **A11**, **A13** and **A34**, exhibited weak to inactive cytotoxicities whereas compounds **A12** and **A14** containing the prenyl group and *trans*-3-methyl-1-butenyl unit at C-6 demonstrated good activity to all tested cell lines. These results indicated that the *trans*-3-methyl-1-butenyl group might play an important responsibility for the cytotoxicities.

The study could be concluded that six new and thirty known compounds, isolated from the twigs of *A. heterophyllus* and the twigs and barks of *A. lakoocha* were flavonoids, arylbenzofurans, stilbenoids and deoxybenzoin. These compounds are common metabolites produced in *Artocarpus* trees (Jagtap *et al.*, 2010). The isolated compounds showed biological activities including cytotoxic, antimicrobial, antimalarial and acetylcholinesterase inhibitory activities.

**Table 3.28** Cytotoxic activities of some isolated compounds

Compound	Cytotoxicities (IC <sub>50</sub> , $\mu$ M)			
	KB	MCF-7	NCI-H187	Vero
<b>A1</b>	30.8 $\pm$ 0.3	/	18.7 $\pm$ 0.4	9.6 $\pm$ 1.7
<b>A3</b>	/	12.6 $\pm$ 1.5	/	38.5 $\pm$ 3.6
<b>A6</b>	/	/	28.7 $\pm$ 0.5	/
<b>A10</b>	/	/	31.7 $\pm$ 1.0	38.2 $\pm$ 0.3
<b>A12</b>	18.5 $\pm$ 3.8	10.0 $\pm$ 1.0	14.8 $\pm$ 3.2	10.0 $\pm$ 0.2
<b>A14</b>	13.6 $\pm$ 0.1	17.6 $\pm$ 0.03	14.2 $\pm$ 2.2	14.2 $\pm$ 2.4
<b>A16</b>	/	/	/	49.7 $\pm$ 2.3
<b>A17</b>	16.7 $\pm$ 0.2	28.5 $\pm$ 2.5	29.8 $\pm$ 2.0	15.2 $\pm$ 0.1
<b>A18</b>	33.6 $\pm$ 4.3	21.9 $\pm$ 2.3	31.3 $\pm$ 4.6	11.3 $\pm$ 0.2
<b>A19</b>	/	/	37.5 $\pm$ 2.1	32.5 $\pm$ 0.2
<b>A21</b>	22.3 $\pm$ 0.2	37.9 $\pm$ 0.3	23.4 $\pm$ 1.2	23.5 $\pm$ 1.1
<b>A22</b>	/	/	44.2 $\pm$ 2.2	/
<b>A24</b>	25.8 $\pm$ 0.02	34.7 $\pm$ 0.3	35.5 $\pm$ 1.2	29.3 $\pm$ 1.1
<b>A25</b>	19.4 $\pm$ 0.2	/	21.1 $\pm$ 0.3	37.0 $\pm$ 1.0
Ellipticine <sup>a</sup>	13.48	-	10.96	2.85
Doxorubicin <sup>a</sup>	1.95	15.44	0.15	-
Tamoxifen <sup>a</sup>	-	23.12	-	-

<sup>a</sup> reference compounds for cytotoxicity assays, / inactive, - no test performed, Paclitaxal was the standard compound for cytotoxicity against A2780 cell lines, IC<sub>50</sub> = 0.013  $\pm$  0.001  $\mu$ M



**Table 3.29** Antimicrobial activities of some isolated compounds

Compound	Antimicrobial activity (MIC, $\mu\text{g/mL}$ )		
	<i>S. aureus</i>	methilicin-resistant <i>S. aureus</i>	<i>C. neoformans</i>
<b>A4</b>	16	16	16
<b>A5</b>	32	64	32
<b>A6</b>	32	32	32
<b>A9</b>	128	/	/
<b>A11</b>	/	128	/
<b>A12</b>	4	4	16
<b>A18</b>	8	8	8
<b>A21</b>	128	128	/
<b>A22</b>	2	2	4
<b>A27</b>	64	/	/
<b>A32</b>	16	16	16
Vancomycin <sup>a</sup>	0.5	0.5	-
Amphotericin B <sup>a</sup>	-	-	0.25

<sup>a,b</sup> Standard drug for antimicrobial assays, / inactive, - no test performed

**Table 3.30** Acetylcholinesterase inhibitory and antimalarial activities of some isolated compounds

Compound	Acetylcholinesterase inhibition (% inhibition at 100 $\mu\text{M}$ )	Antimalarial activity, <i>P. falciparum</i> K1 (IC <sub>50</sub> , $\mu\text{M}$ )
<b>A2</b>	/	20.5
<b>A4</b>	31.1 $\pm$ 1.4	/
<b>A6</b>	23.5 $\pm$ 2.5	3.5
<b>A9</b>	18.3 $\pm$ 4.6	/
<b>A11</b>	12.6 $\pm$ 4.3	26.7

**Table 3.30** Acetylcholinesterase inhibitory and antimalarial activities of some isolated compounds

Compound	Acetylcholinesterase inhibition (% inhibition at 100 $\mu$ M)	Antimalarial activity, <i>P. falciparum</i> K1 (IC <sub>50</sub> , $\mu$ M)
<b>A18</b>	/	10.2
<b>A21</b>	12.1 $\pm$ 3.7	7.3
<b>A22</b>	/	2.7
<b>A27</b>	/	2.8
<b>A31</b>	43.1 $\pm$ 2.7	/
Galantamine <sup>a</sup>	98.4 $\pm$ 0.6	-
Dihydroartemisinin <sup>b</sup>	-	3.25 nM

<sup>a</sup> positive control for acetylcholinesterase inhibitory assay, <sup>b</sup> reference compound for antimalarial activity, / inactive, - no test performed

## CHAPTER 4

### Conclusions

The separation and structural elucidation of the extracts of the twigs of *Artocarpus heterophyllus* and the twigs and bark of *A. lakoocha* led to the isolation of 36 compounds. Three new 2-arylbenzofuran compounds, heterophyllenes A-C (**A1-A3**), and one new stilbenoid compound, heterophyllene D (**A4**), together with twenty-one known compounds, including moracin M (**A5**), moracin C (**A6**), demethylmoracin I (**A7**), norartocarpetin (**A8**), albanin A (**A9**), licoflavone C (**A10**), artocarpesin (**A11**), norartocarpin (**A12**), cudraflavone C (**A13**), artocarpin (**A14**), steppogenin (**A15**), artocarpanone (**A16**), isogemichalcone C (**A17**), artocarmitin B (**A18**), artocarmin B (**A19**), morachalcone A (**A20**), brosimone I (**A21**), cycloartocarpin (**A22**), cudraflavone A (**A23**), cudraflavone B (**A24**) and artogomezianone (**A25**) were isolated from the methanolic extract of the twigs of *A. heterophyllus*. One new deoxybenzoin derivative, lakoochanoside A (**A26**), one new flavan compound, lakoochanoside B (**A27**), along with seventeen known compounds including heterophyllene B (**A2**), heterophyllene D (**A4**), moracin M (**A5**), moracin C (**A6**), demethylmoracin I (**A7**), albanin A (**A9**), artocarpesin (**A11**), norartocarpin (**A12**), artocarpanone (**A16**), artocarmitin B (**A18**), brosimone I (**A21**), cycloartocarpin (**A22**), (+)-afzelechin-3-*O*- $\alpha$ -L-rhamnopyranoside (**A28**), (+)-catechin-3-*O*- $\alpha$ -L-rhamnopyranoside (**A29**), (+)-catechin (**A30**), oxyresveratrol (**A31**) and resveratrol (**A32**) were isolated from the acetone extract of the twigs of *A. lakoocha*. In addition, moracin C (**A6**), afzelechin-3-*O*- $\alpha$ -L-rhamnopyranoside (**A28**), (+)-catechin (**A30**), oxyresveratrol (**A31**), sanggenofuran B (**A33**), integrin (**A34**), engeletin (**A35**) and *trans*-2-methoxy-4,3',5'-trihydroxystilbene (**A36**) were isolated and identified from the acetone extract of the barks of *A. lakoocha*.

Heterophyllene C (**A3**) showed cytotoxicity against MCF-7 cell line. Prenylated flavonoids especially norartocarpin (**A12**) and artocarpin (**A14**) exhibited the good cytotoxic activities against KB, MCF-7 NCI-H187 and Vero cell lines and strong antimicrobial activities against *Staphylococcus aureus*, methicillin-resistant *Staphylococcus aureus*, and *Cryptococcus neoformans*, while cycloartocarpin (**A22**) displayed strong antimicrobial activities. New flavan lakoochanoside B (**A27**) showed moderate antibacterial and antimalarial activities. The stilbenoid oxyresveratrol (**A31**) showed weak acetylcholinesterase inhibitory activity. However, this is the first report on the separation and structural elucidation of deoxybenzoin obtained from the twigs of *A. lakoocha* which offers the potential clinical application of *A. lakoocha*.



ลิขสิทธิ์มหาวิทยาลัยเชียงใหม่  
Copyright© by Chiang Mai University  
All rights reserved

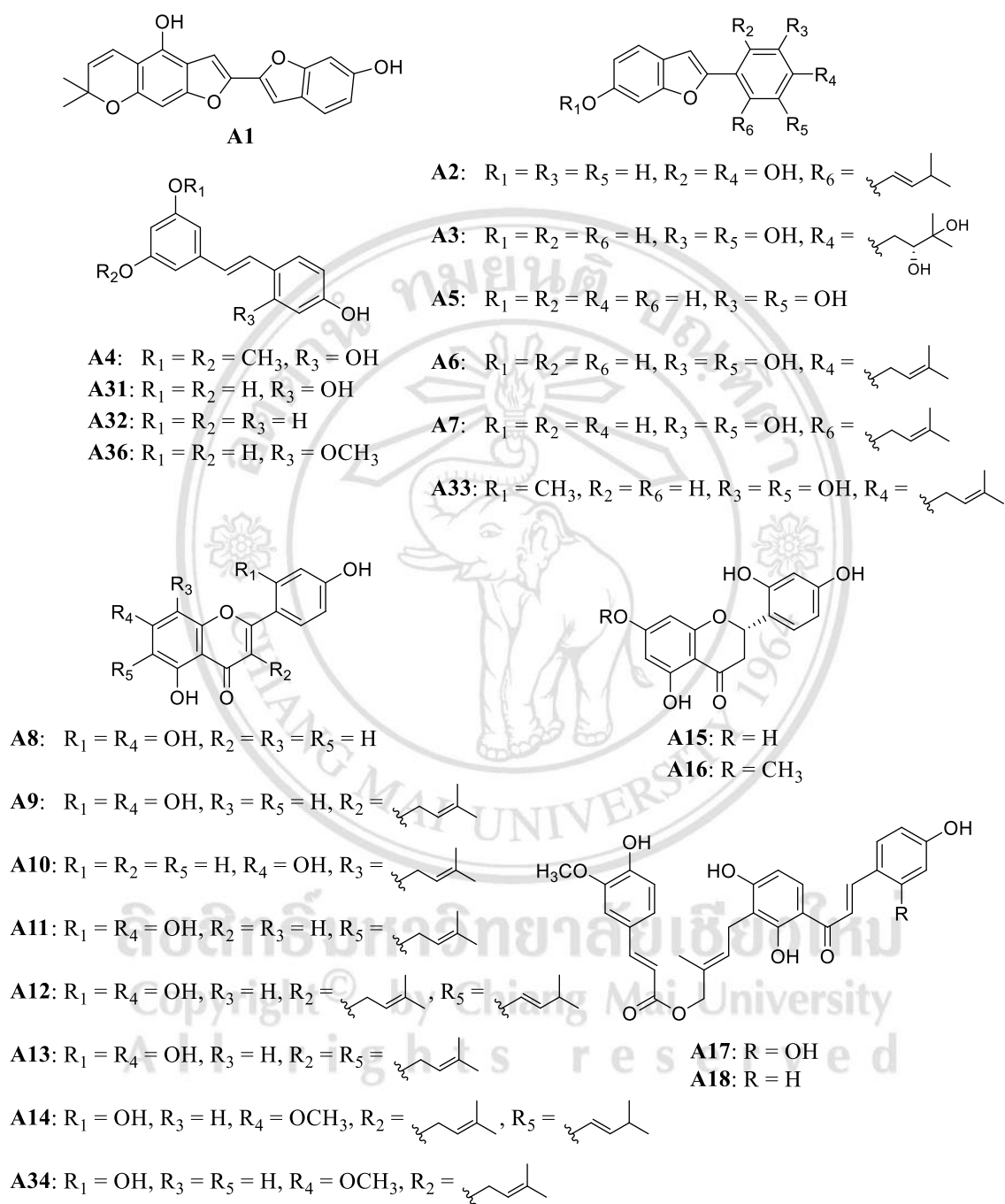


**Figure 4.1** The structures of isolated compounds from *A. heterophyllus* and *A. lakoocha* (A1-A36)

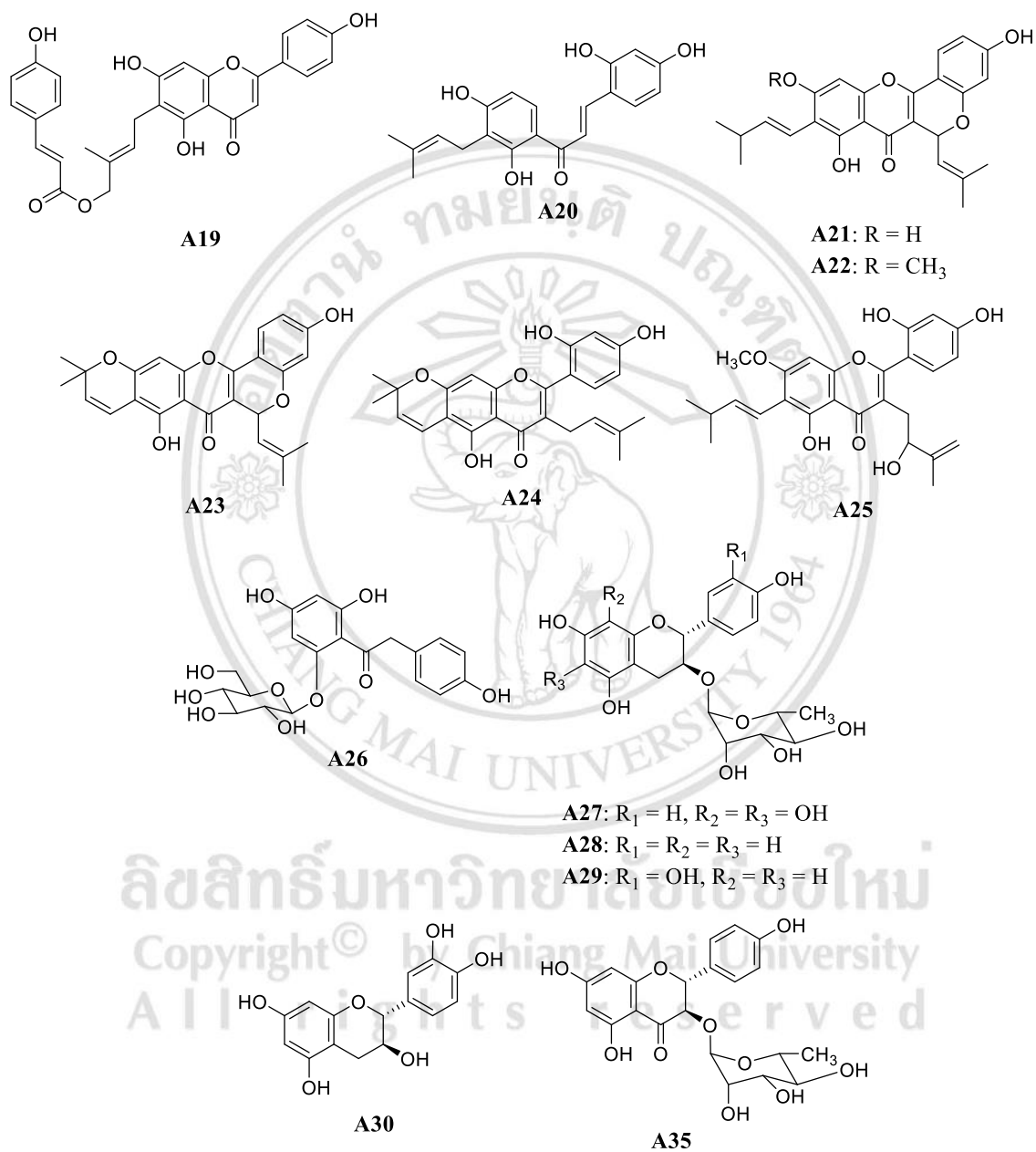


**Figure 4.1** (continued)

## REFERENCES

- Arung, E.T., Yoshikawa, K., Shimizu, K. and Kondo, R. 2010. Isoprenoid-substituted flavonoids from wood of *Artocarpus heterophyllus* on B16 melanoma cells: cytotoxicity and structural criteria. *Fitoterapia* 81, 120-123.
- Arung, E.T., Shimizu, K., Tanaka, H. and Kondo, R. 2010. 3-Prenyl luteolin, a new prenylated flavone with melanin biosynthesis inhibitory activity from wood of *Artocarpus heterophyllus*. *Fitoterapia* 81, 640-643.
- Baliga, M.S., Shivashankara, A.R., Haniadka, R., Dsouza, J. and Bhat, H.P. 2011. Phytochemistry, nutritional and pharmacological properties of *Artocarpus heterophyllus* Lam (jackfruit): a review. *Food Research International* 44, 1800-1811.
- Ban, J.Y., Jeon, S.-Y., Nguyen, T.T.H., Bae, K., Song, K.-S. and Seong, Y. H. 2006. Neuroprotective effect of oxyresveratrol from *Smilacis chinae* rhizome on amyloid  $\beta$  protein (25-35)-indeed neurotoxicity in cultured rat cortical neurons. *Biological and Pharmaceutical Bulletin* 29(12), 2419-2424.
- Basnet, P., Kadota, S., Terashima, S., Shimizu, M. and Namba, T. 1993. Two new 2-arylbenzofuran derivatives from hypoglycemic activity-bearing fractions of *Morus insignis*. *Chemical and Pharmaceutical Bulletin* 41(7), 1238-1243.
- Bishnoi, S.K., Shinde, R. and Sarkar, P.K. Monkey jack (*Artocarpus lakoocha* Roxb.): hope for sustaining livelihood in fruits for livelihood: production technology and management, Agrobios, Jodhpur, India. 199-213.
- Chi, X., Xing, Y., Xiao, Y., Dong, Q. and Hu, F. 2014. Separation and purification of three stilbenes from the radix of *polygonum cillinerve* (Nakai) ohwl by microporous resin column chromatography combined with high-speed counter-current chromatography. *Quimica Nova* 37(9), 1465-1468.

- Choi, J., Cho, J.Y., Kim, Y.-D., Htwe, K.M., Lee, W.-S., Lee, J.C., Kim, J. and Yoon, K.D. 2015. Phenolic compounds and triterpenes from the barks of *Diospyros burmanica*. *Natural Product Sciences* 21(2), 76-81.
- Di, X., Wang, S., Wang, B., Liu, Y., Yuan, H., Lou, H and Wang, X. 2013. New phenolic compounds from the twigs of *Artocarpus heterophyllus*. *Drug Discovery Therapeutics* 7(1), 24-28.
- Fang, S.-C., Hsu, C.-L., Yu, Y.-S. and Yen, G.-C. 2008. Cytotoxic effects of new geranyl chalcone derivatives isolated from the leaves of *Artocarpus communis* in SW 872 human liposarcoma cells. *Journal of Agricultural and Food Chemistry* 56, 8859-8868.
- Hanessian, S. and Xie, F. 1998. Exploring functional and molecular diversity with polymer-bound *p*-alkoxybenzyl ethers-scope and applications of preparatively useful organic reactions. *Tetrahedron Letters* 39, 737-740.
- Hanh, N.H. and Hoa, L.T.P. 2015. Tyrosinase inhibitors from the heartwood of Vietnamese *Artocarpus heterophyllus*. *Journal of Natural Products and Resources* 5(4), 1-4.
- Hossain, M.F., Islam, M.A., Akhtar, S. and Numan, S.M. 2016. Nutritional value and medicinal uses of monkey jack fruit (*Artocarpus lakoocha*). *International Research Journal of Biological Sciences* 5(1), 60-63.
- Huang, H., Cheng, Z., Shi, H., Xin, W., Wang, T.T.Y. and Yu, L. 2011. Isolation and characterization of two flavonoids, engeletin and astilbin, from the leaves of *Engelhardia roxburghiana* and their potential anti-inflammatory properties. *Journal of Agricultural and Food Chemistry* 59, 4562-4569.
- Hye, M.A., Taher, M.A., Ali, M.Y., Ali, M.U. and Zaman, S. 2009. Isolation of (+)-catechin from *Acacia Catechu* (Cutch Tree) by a convenient method. *Journal of Scientific Research* 2, 300-305.
- Jagtap, U.B. and Bapat, V.A. 2010. *Artocarpus*: a review of its traditional uses, phytochemistry and pharmacology. *Journal of Ethnopharmacology* 129, 142-166.



- Jeong, S.H., Ryu, Y.B., Curtis-Long, M.J., Ryu, H.W., Beak, Y.S., Kang, J.E., Lee, W.S. and Park, K.H. 2009. Tyrosinase inhibitory polyphenols from roots of *Morus lhou*. *Journal of Agricultural and Food Chemistry* 57, 1195-1203.
- Kajiyama, K., Demizu, S., Hiraga, Y., Kinoshita, K., Koyama, K., Takahashi, K., Tamura, Y., Okada, K. and Kinoshita, T. 1992. New prenylflavones and dibenzoylmethane from *Glycyrrhiza inflata*. *Journal of Natural Products* 55, 1197-1203.
- Kim, J.E., Kim, S.S., Hyun, C.-G. and Lee, N.H. 2012. Antioxidative chemical constituents from the stems of *Cleyera japonica* Thunberg. *International Journal of Pharmacology* 8(5), 410-415.
- Kim, Y.J., Sohn, M.-J. and Kim, W.-G. 2012. Chalcomoracin and moracin C, new inhibitors of *Staphylococcus aureus* enoyl-acyl carrier protein reductase from *Morus alba*. *Biological and Pharmaceutical Bulletin* 35(5), 791-795.
- Lee, D., Bhat, K.P.L., Fong, H.H.S., Farnsworth, N.R., Pezzuto, J.M. and Kinghorn, A.D. 2001. Aromatase inhibitors from *Broussonetia papyrifera*. *Journal of Natural Products* 64, 1286-1293.
- Likhitwitayawuid, K., Chaiwiriyi, S., Sritularak, B. and Lipipun, V. 2006. Antiherpetic flavones from the heartwood of *Artocarpus gomezianus*. *Chemistry & Biodiversity* 3, 1138-1143.
- Likhitwitayawuid, K., Sornsute, A., Sritularak, B. and Ploypradith, P. 2006. Chemical transformations of oxyresveratrol (*trans*-2,4,3',5'-tetrahydroxystilbene) into a potent tyrosinase inhibitor and a strong cytotoxic agent. *Bioorganic & Medicinal Chemistry Letters* 16, 5650-5653.
- Mai, N.T.T., Hai, N.X., Phu, D.H., Trong, P.N.H. and Nhan, N.T. 2012. Three new geranyl aurones from the leaves of *Artocarpus altilis*. *Phytochemistry Letters* 5, 647-650.

- Maneechai, S., De-Eknamkul, W., Umehara, K., Noguchi, H. and Likhitwitayawuid, K. 2012. Flavonoid and stilbenoid production in callus cultures of *Artocarpus lakoocha*. *Phytochemistry* 81, 42-49.
- Manuel, N.-G.V., Osvaldo, S.-S.D., Alejandra, R.-F.T., Rodolfo, A.-V. and Lucila A.-L. 2012. Antimicrobial activity of artocarpesin from *Artocarpus heterophyllus* Lam. against methicillin-resistant *Staphylococcus aureus* (MRSA). *Journal of Medicinal Plants Research* 6(34), 4879-4882.
- Namdaung, U., Athipornchai, A., Khammee, T., Kuno, M. and Suksamrarn, S. 2018. 2-Arylbenzofurans from *Artocarpus lakoocha* and methyl ether analogs with potent cholinesterase inhibitory activity. *European Journal of Medicinal Chemistry* 143, 1301-1311.
- Nguyen, N.T., Nguyen, M.H.K., Nguyen, H.X., Bui, N.K.N. and Nguyen, M.T.T. 2012. Tyrosinase inhibitors from the wood of *Artocarpus heterophyllus*. *Journal of Natural Products* 75, 1951-1955.
- Nguyen, H.X., Nguyen, N.T., Nguyen, M.H.K., Le, T.H., Do, T.N.V., Hung, T.M. and Nguyen, M.T.T. 2016. Tyrosinase inhibitory activity of flavonoids from *Artocarpus heterophyllus*. *Chemistry Central Journal* 10, 2-7.
- Palanuvej, C., Issaravanich, S., Tunsaringkarn, T., Rungsiyothin, A., Vipunngun, N., Ruangrunsi, N. and Likhitwitayawuid, K. 2007. Pharmacognostic study of *Artocarpus lakoocha* heartwood. *Journal of Health Research* 21(4), 257-262.
- Puntumchai, A., Kittakoo, P., Rajviroongit, S., Vimuttipong, S., Likhitwitayawuid, K. and Thebtaranonth, Y. 2004. Lakoochins A and B, new antimycobacterial stilbene derivatives from *Artocarpus lakoocha*. *Journal of Natural Products* 67, 485-486.
- Povichit, N., Phrutivorapongkul, A., Suttajit, M. and Leelapornpisid, P. 2010. Antiglycation and antioxidant activities of oxyresveratrol extracted from the heartwood of *Artocarpus lakoocha* Roxb. *Maejo International Journal of Science and Technology* 4(3), 454-461.

- Quang, T.H., Ngan, N.T.T., Yoon, C.-S., Cho, K.-H., Kang, D.G., Lee, H.S., Kim, Y.-C. and Oh, H. 2015. Protein tyrosine phosphatase 1B inhibitors from the roots of *Cudrania tricuspidata*. *Molecules* 20, 11173-11183.
- Rao, G.V. and Mukhopadhyay, T. 2010. Artoindonesianin F, a potent tyrosinase inhibitor from the roots of *Artocarpus heterophyllus* Lam. *Indian Journal of Chemistry* 49B, 1264-1266.
- Ren, G., Peng, J., Liu, A., Liang, J., Yuan, W., Wang, H. and He, J. 2015. Structure elucidation and NMR assignments of two new flavanones from the roots of *Artocarpus heterophyllus*. *Magnetic Resonance in Chemistry* 53, 872-874.
- Ryu, Y.B., Ha, T.J., Curtis-Long, M.J., Ryu, H.W., Gal, S.W. and Park, K.H. 2008. Inhibitory effects on mushroom tyrosinase by flavones from the stem barks of *Morus lhou* (S.) Koidz. *Journal of Enzyme Inhibition and Medicinal Chemistry* 23(6), 922-930.
- Septama, A.W. and Panichayupakaranant, P. 2015. Antibacterial assay-guided isolation of active compounds from *Artocarpus heterophyllus* heartwoods. *Pharmaceutical Biology* 53(11), 1608-1613.
- Shi, Y.-Q., Nomura, T. and Fukai, T. 2007. A new 2-arylbenzofuran from the root bark of Chinese *Morus cathayana*. *Fitoterapia* 78, 617-618.
- Smith, R.J., Bower, R.L., Ferguson, S.A., Rosengren, R.J., Cook, G.M. and Hawkins, B.C. 2019. The synthesis of ( $\pm$ )-oxyisocyclointegrin. *European Journal of Organic Chemistry*, 1571-1573.
- Sritularak, B., Tantrakarnsakul, K., Likhitwitayawuid, K. and Lipipun, V. 2010. New 2-arylbenzofurans from the root bark of *Artocarpus lakoocha*. *Molecules* 15, 6548-6558.
- Sritularak, B., Tantrakarnsakul, K., Lipipun, V. and Likhitwitayawuid, K. 2013. Flavonoids with anti-HSV activity from the root bark of *Artocarpus lakoocha*. *Natural Product Research* 8(8), 1079-1080.

- Su, B.-N., Cuendet, M., Hawthorne, M.E., Kardono, L.B.S., Riswan, S., Fong, H.H.S., Mehta, R.G., Pezzuto, J.M. and Kinghorn, A.D. 2002. Constituents of the bark and twigs of *Artocarpus dadah* with cyclooxygenase inhibitory activity. *Journal of Natural Products* 65, 163-169.
- Sun, J., He, X.-M., Zhao, M.-M., Li, L., Li, C.-B. and Dong, Y. 2014. Antioxidant and nitrite-scavenging capacities of phenolic compounds from sugarcane (*Saccharum officinarum* L.) Tops. *Molecules* 19, 13147-13160.
- Trisuwan, K., Rukachaisirikul, V., Kaewpet, M., Phongpaichit, S., Hutadilok-Towatana, N., Preedanon, S. and Sakayaroj, J. 2011. Sesquiterpene and xanthone derivatives from the sea fan-derived fungus *Aspergillus sydowii* PSU-F154. *Journal of Natural Products* 74, 1663-1667.
- Wang, X.-L., Di, X.-X., Shen, T., Wang, S.-Q. and Wang, X.-N. 2017. New phenolic compounds from the leaves of *Artocarpus heterophyllus*. *Chinese Chemical Letters* 28, 37-40.
- Wei, B.-L., Weng, J.-R., Chiu, P.-H., Hung, C.-F., Wang, J.-P. and Lin, C.-N. 2005. Antiinflammatory flavonoids from *Artocarpus heterophyllus* and *Artocarpus communis*. *Journal of Agricultural and Food Chemistry* 53, 3867-3871.
- Yang, J.-H., Kondratyuk, T.P., Jermihov, K.C., Marler, L.E., Qiu, X., Choi, Y., Cao, H., Yu, R., Sturdy, M., Huang, R., Liu, Y., Wang, L.-Q., Mesecar, A.D., Breemen, R.B., Pezzuto, J.M., Fong, H.H.S., Chen, Y.-G. and Zhang, H.-J. 2011. Bioactive compounds from the fern *Lepisorus contortus*, *Journal of Natural Products* 74, 129-136.
- Yuan, W.-J., Yuan, J.-B., Peng, J.-B., Ding, Y.-Q., Zhu, J.-X. and Ren, G. 2017. Flavonoids from the roots of *Artocarpus heterophyllus*. *Fitoterapia* 117, 133-137.
- Zeng, X., Qiu, Q., Jiang, C., Jing, Y., Qiu, G. and He, X. 2011. Antioxidant flavones from *Livistona chinensis*. *Fitoterapia* 82, 609-614.
- Zhang, W.-J., Wu, J.-F., Zhou, P.-F., Wang, Y. and Hou, A.-J. 2013. Total syntheses of norartocarpin and artocarpin. *Tetrahedron* 69, 5850-5858.

- Zhang, X., Hu, X., Hou, A. and Wang, H. 2009. Inhibitory effect of 2,4,2',4'-tetrahydroxy-3-(3-methyl-2-butenyl)-chalcone on tyrosinase activity and melatonin biosynthesis. *Biological and Pharmaceutical Bulletin* 32(1), 86-90.
- Zheng, Z.-P., Cheng, K.-W., To, J.T.-K., Li, H. and Wang, M. 2008. Isolation of tyrosinase inhibitors from *Artocarpus heterophyllus* and use of its extract as antibrowning agent. *Molecular Nutrition & Food Research* 52, 1530-1538.
- Zheng, Z.-P., Xu, Y., Qin, C., Zhang, S., Gu, X., Lin, Y., Xie, G., Wang, M. and Chen, J. 2014. Characterization of antiproliferative activity constituents from *Artocarpus heterophyllus*. *Journal of Agricultural and Food Chemistry* 62, 5519-5527.
- Medthai. 2017. ขนุน สรรพคุณและประโยชน์ของขนุน 32 ข้อ. Medthai.com. <http://medthai.com/ขนุน/>. (accessed 15 February, 2019).
- Useful tropical plants database. 2019. *Artocarpus lacucha*. Useful tropical plants database. <http://tropical.theferns.info/viewtropical.php?id=Artocarpus+lacucha> (accessed 15 February, 2019).



APPENDIX

ลิขสิทธิ์มหาวิทยาลัยเชียงใหม่

Copyright© by Chiang Mai University  
All rights reserved

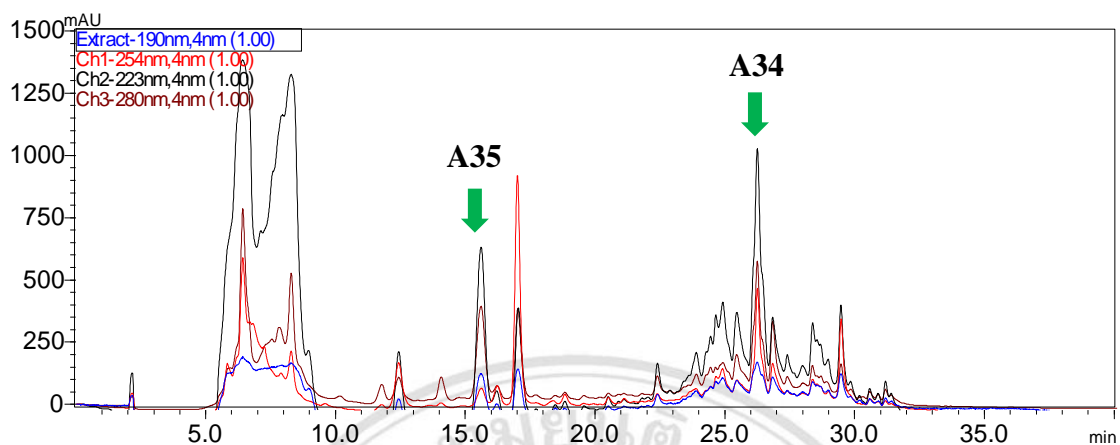


**Figure 1** HPLC chromatogram of subfraction BLD-51

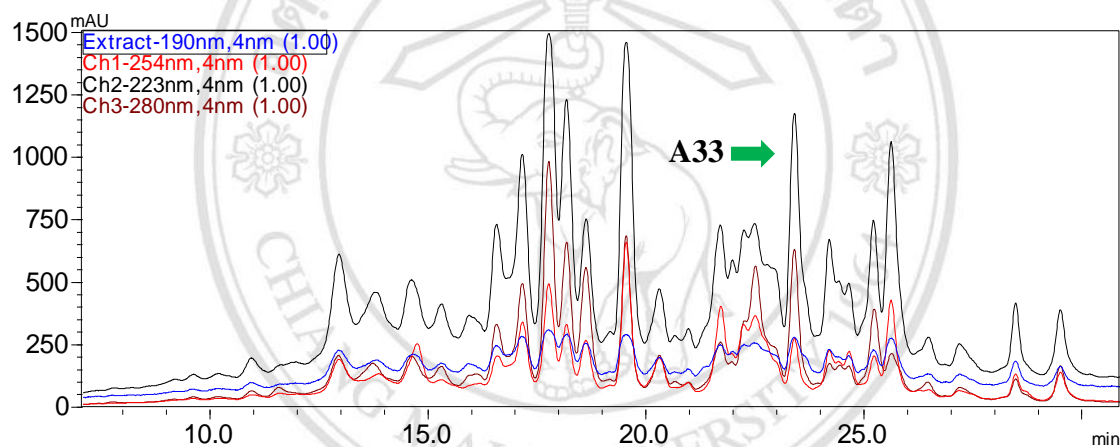


**Figure 2** HPLC chromatogram of subfraction BLD-52

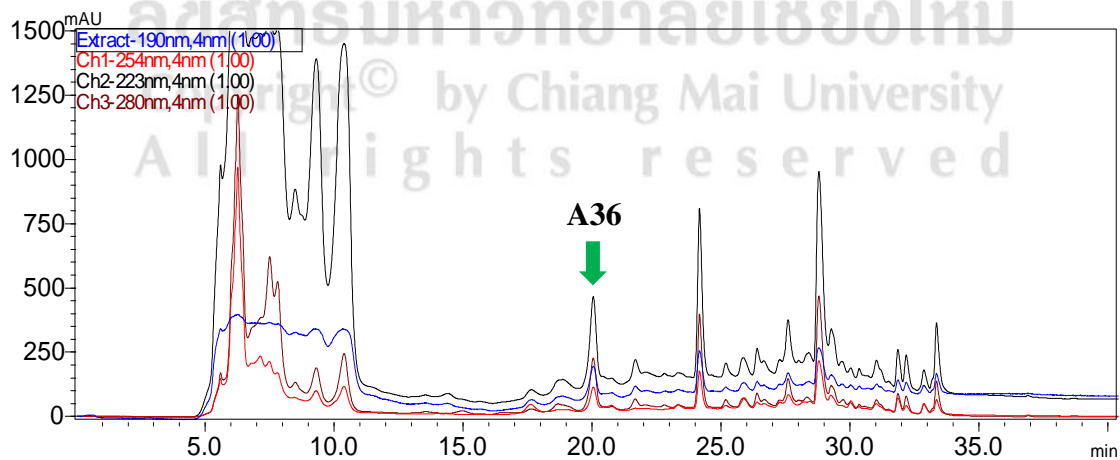


**Figure 3** HPLC chromatogram of subfraction BLD-61

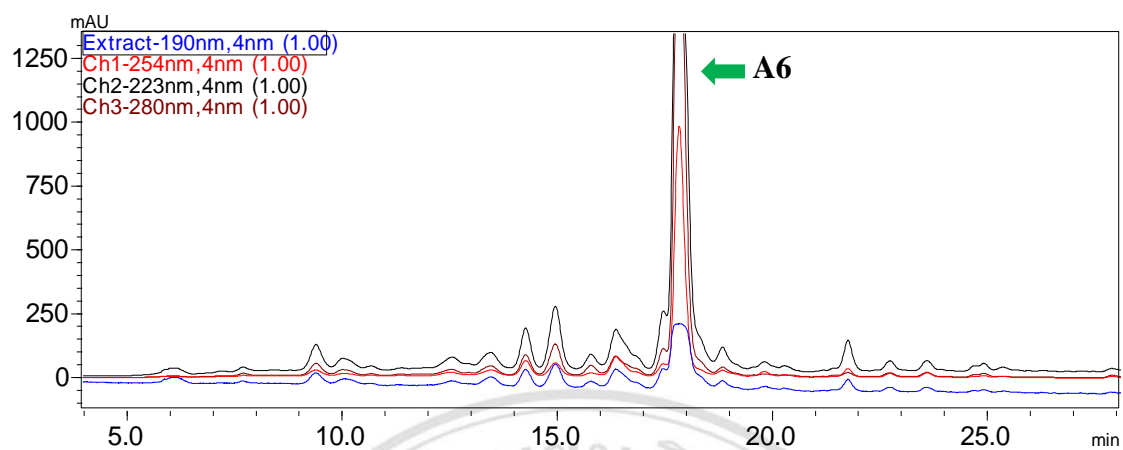


**Figure 4** HPLC chromatogram of subfraction BLD-62

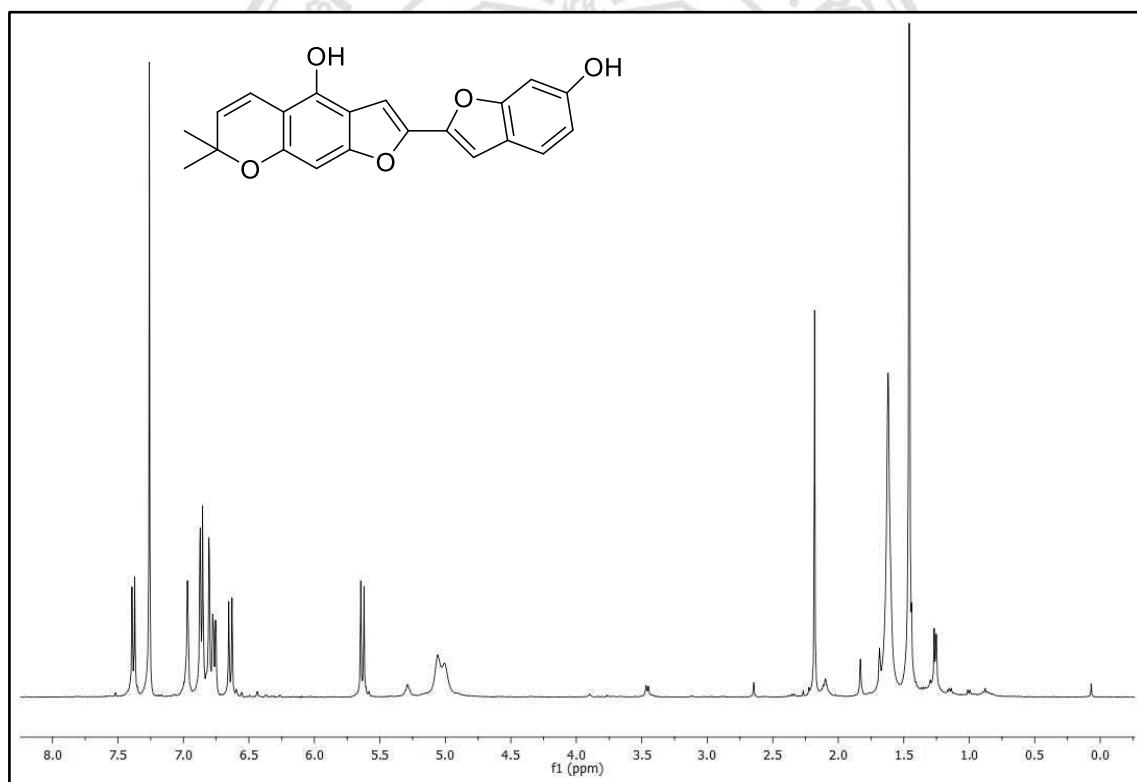


**Figure 5** The  $^1\text{H}$ -NMR (400 MHz,  $\text{CDCl}_3$ ) spectrum of compound A1



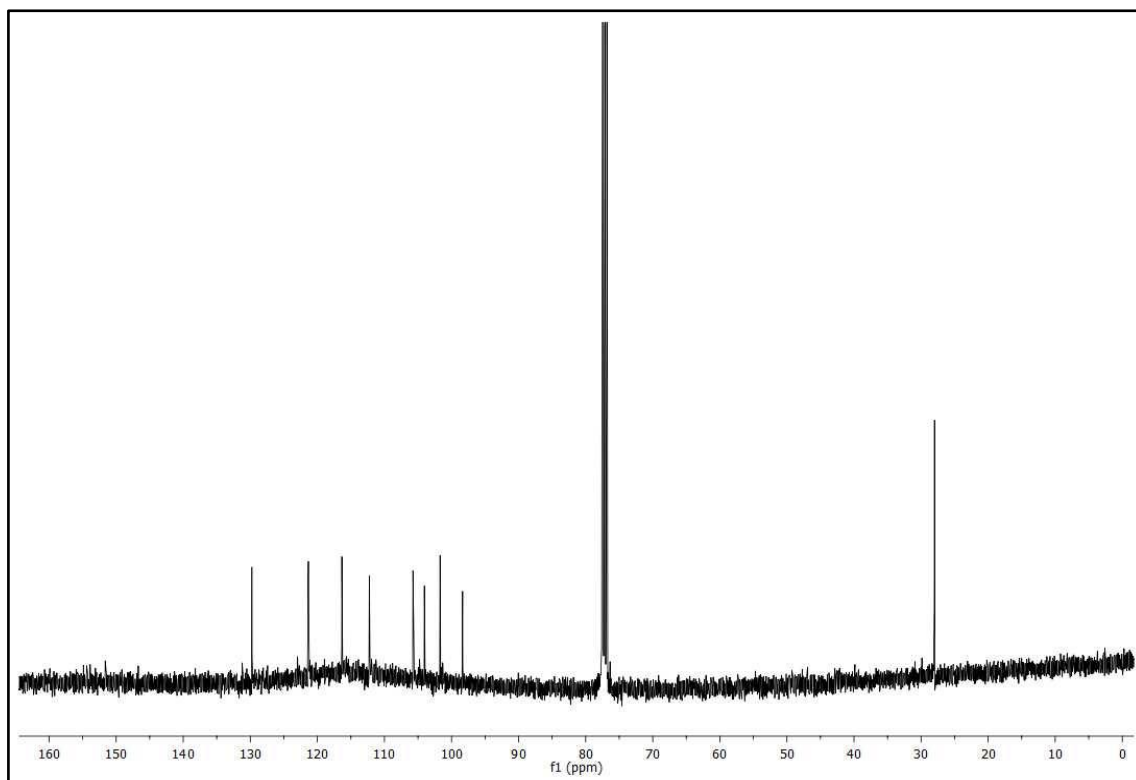


**Figure 6** The  $^{13}\text{C}$ -NMR (100 MHz,  $\text{CDCl}_3$ ) spectrum of compound **A1**

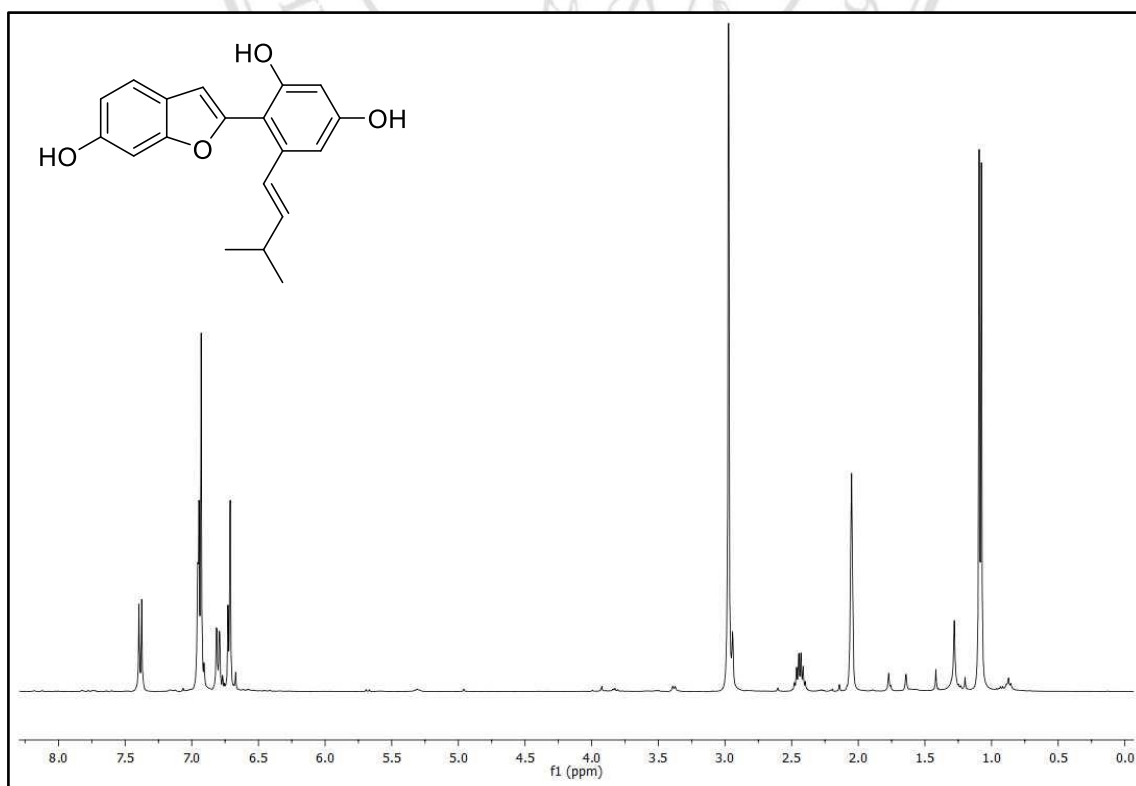


**Figure 7** The  $^1\text{H}$ -NMR (400 MHz,  $\text{acetone-}d_6$ ) spectrum of compound **A2**

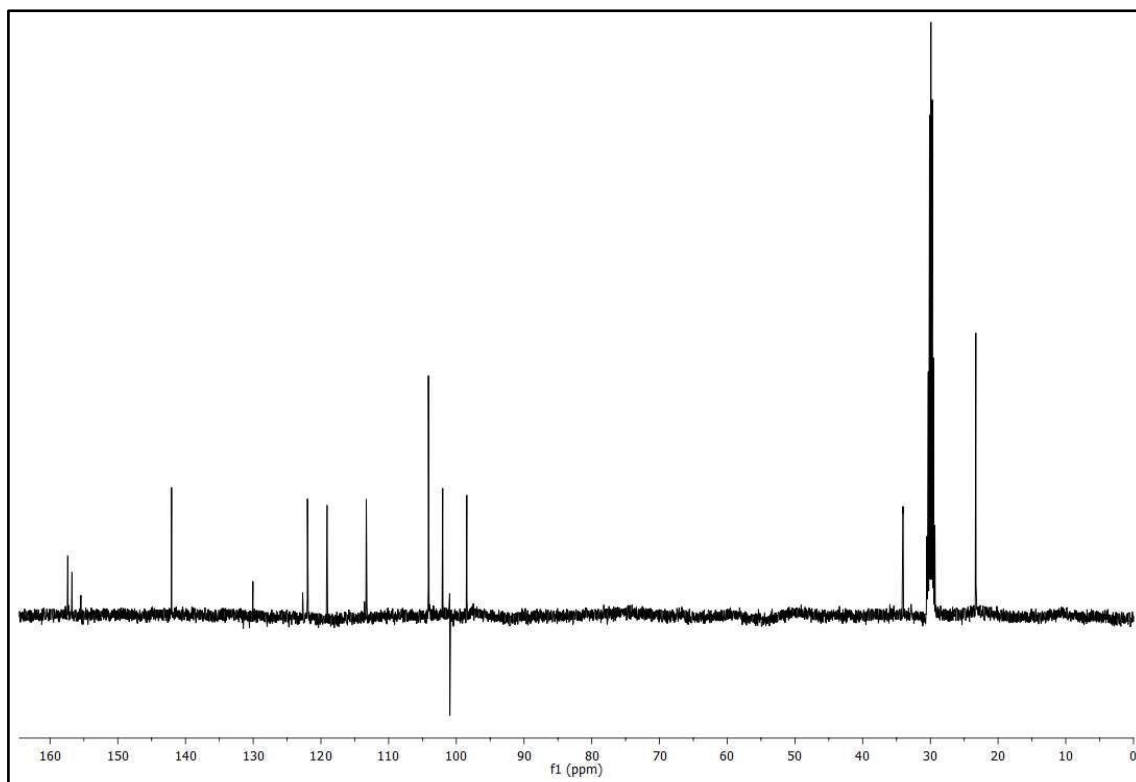


**Figure 8** The  $^{13}\text{C}$ -NMR (100 MHz, acetone- $d_6$ ) spectrum of compound **A2**

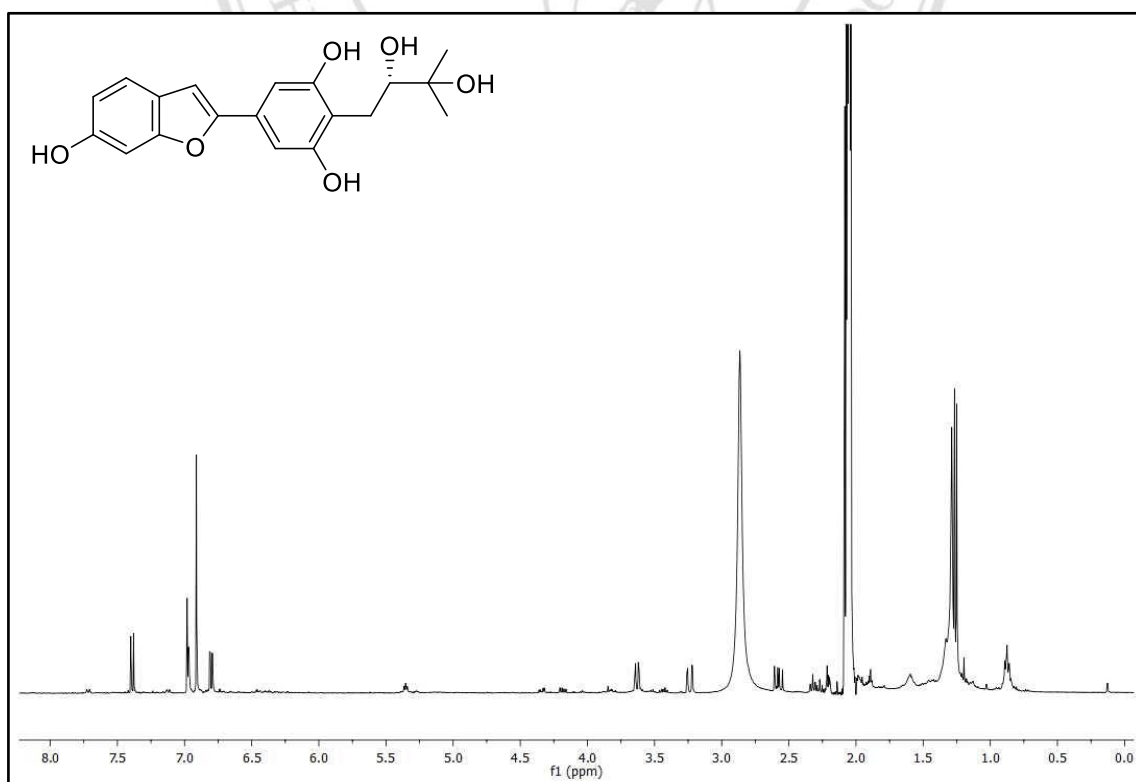


**Figure 9** The  $^1\text{H}$ -NMR (400 MHz, acetone- $d_6$ ) spectrum of compound **A3**

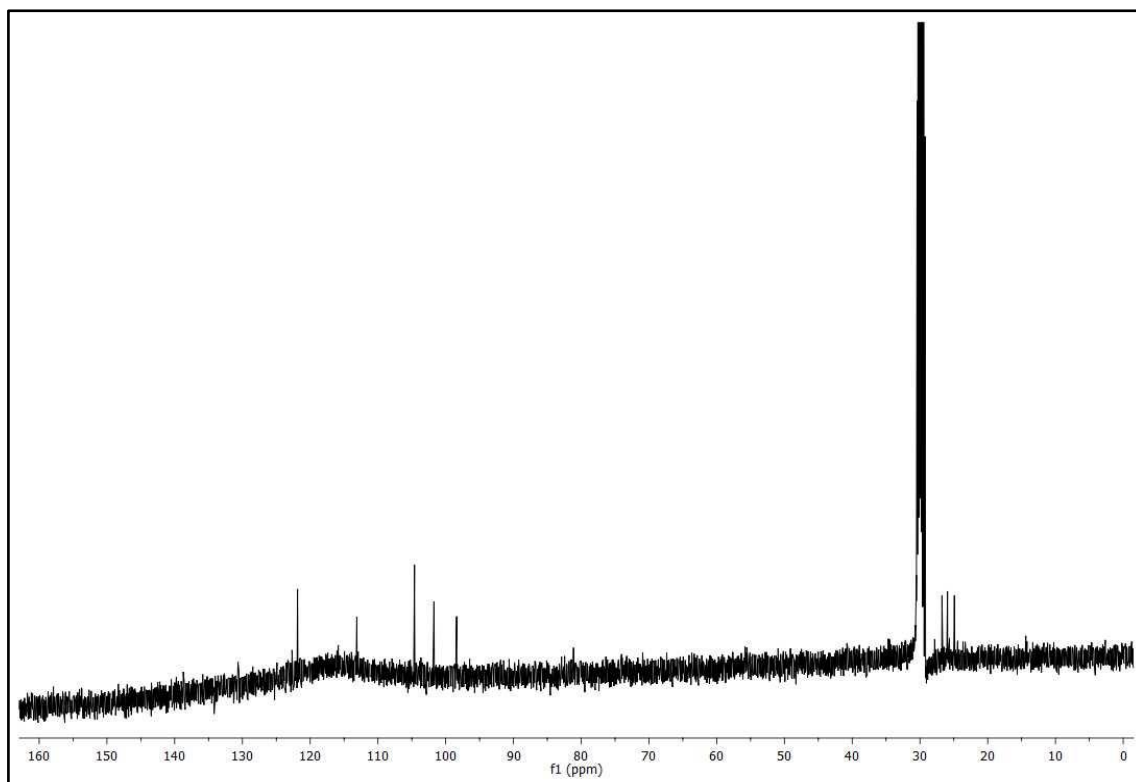


**Figure 10** The  $^{13}\text{C}$ -NMR (100 MHz, acetone- $d_6$ ) spectrum of compound A3

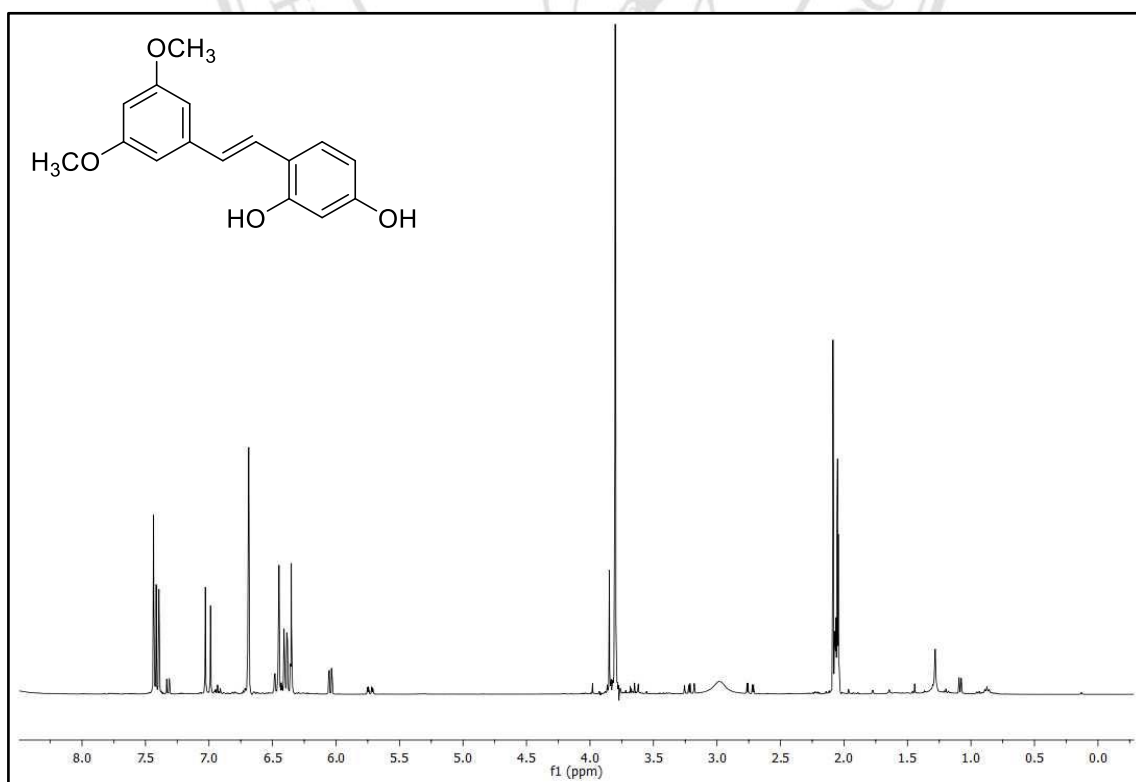


**Figure 11** The  $^1\text{H}$ -NMR (400 MHz, acetone- $d_6$ ) spectrum of compound A4

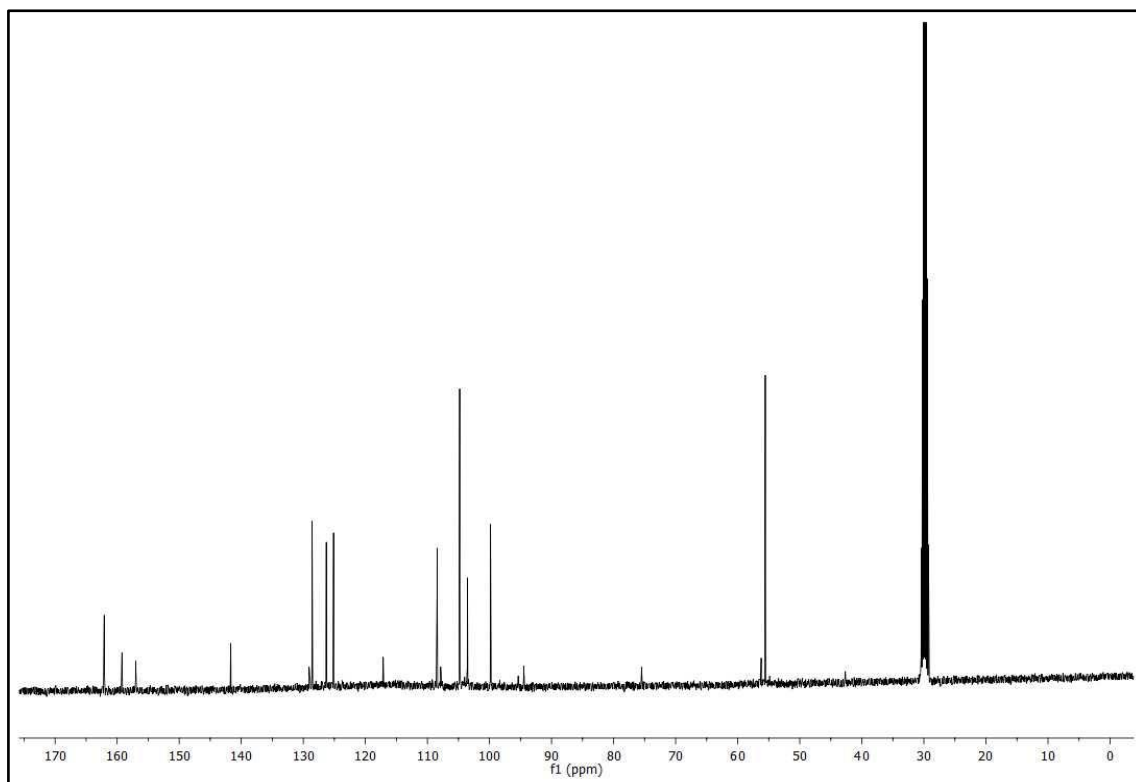


**Figure 12** The  $^{13}\text{C}$ -NMR (100 MHz, acetone- $d_6$ ) spectrum of compound **A4**

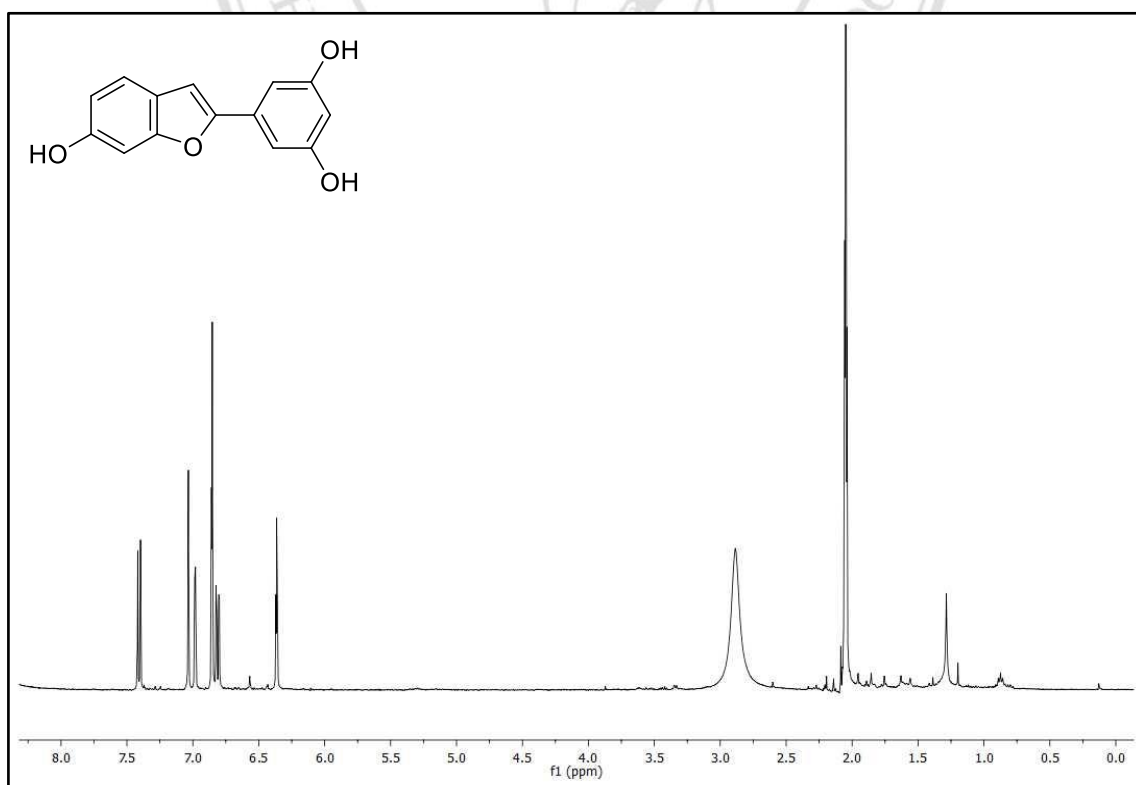


**Figure 13** The  $^1\text{H}$ -NMR (400 MHz, acetone- $d_6$ ) spectrum of compound **A5**

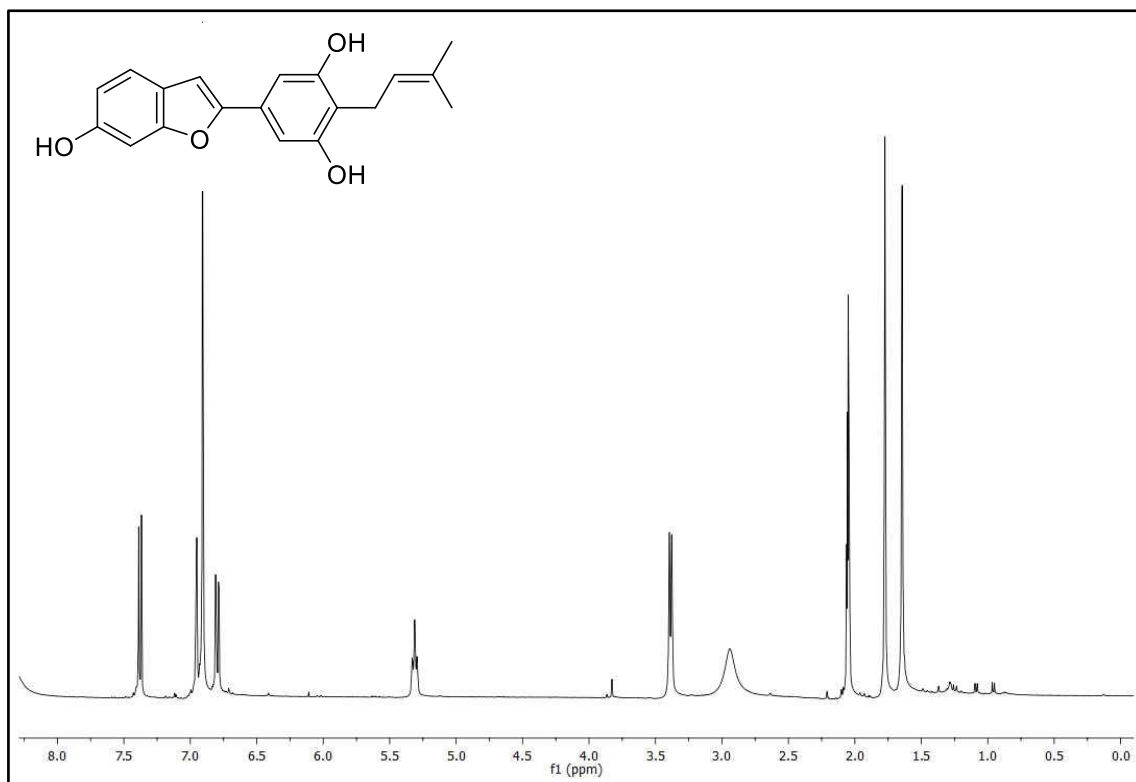


**Figure 14** The <sup>1</sup>H-NMR (400 MHz, acetone-*d*<sub>6</sub>) spectrum of compound A6

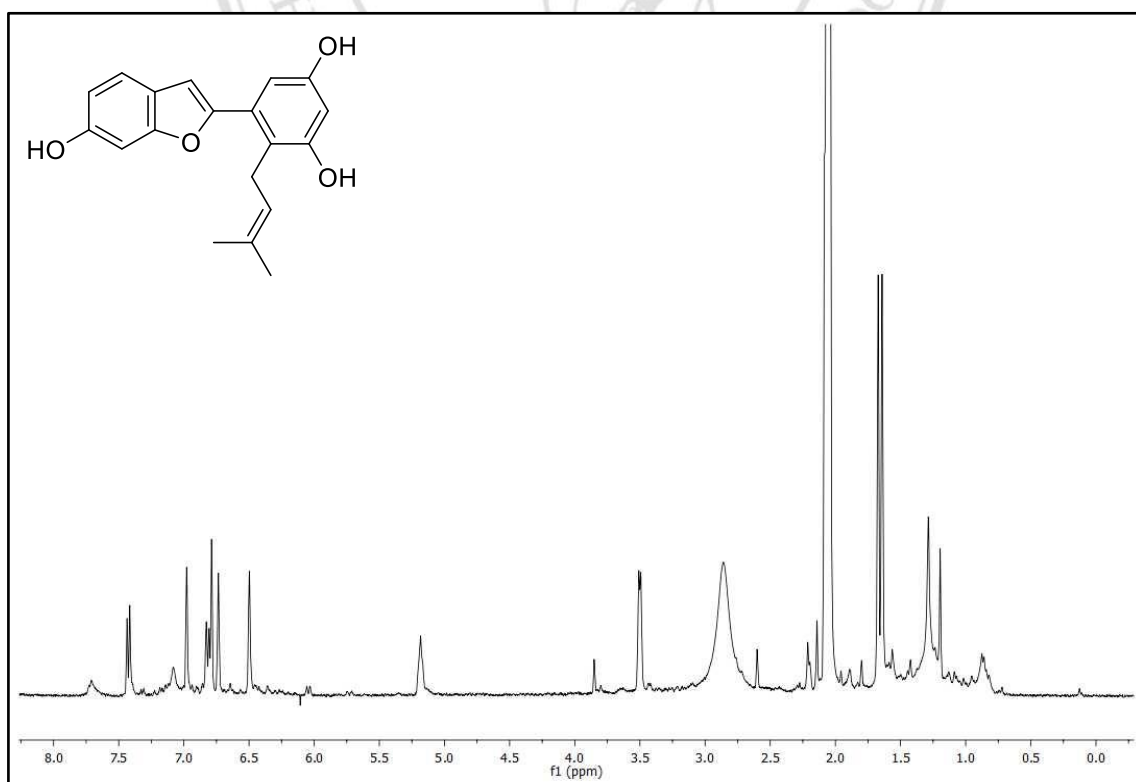


**Figure 15** The <sup>1</sup>H-NMR (400 MHz, acetone-*d*<sub>6</sub>) spectrum of compound A7

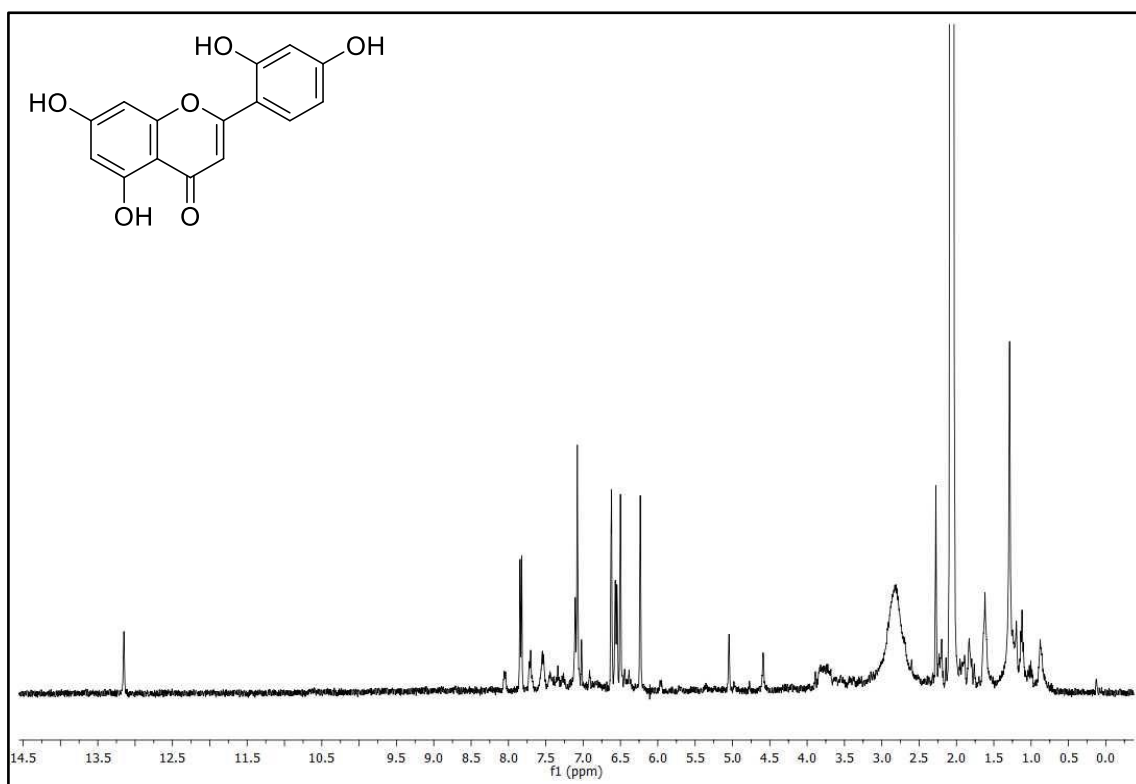


**Figure 16** The <sup>1</sup>H-NMR (400 MHz, acetone-*d*<sub>6</sub>) spectrum of compound **A8**

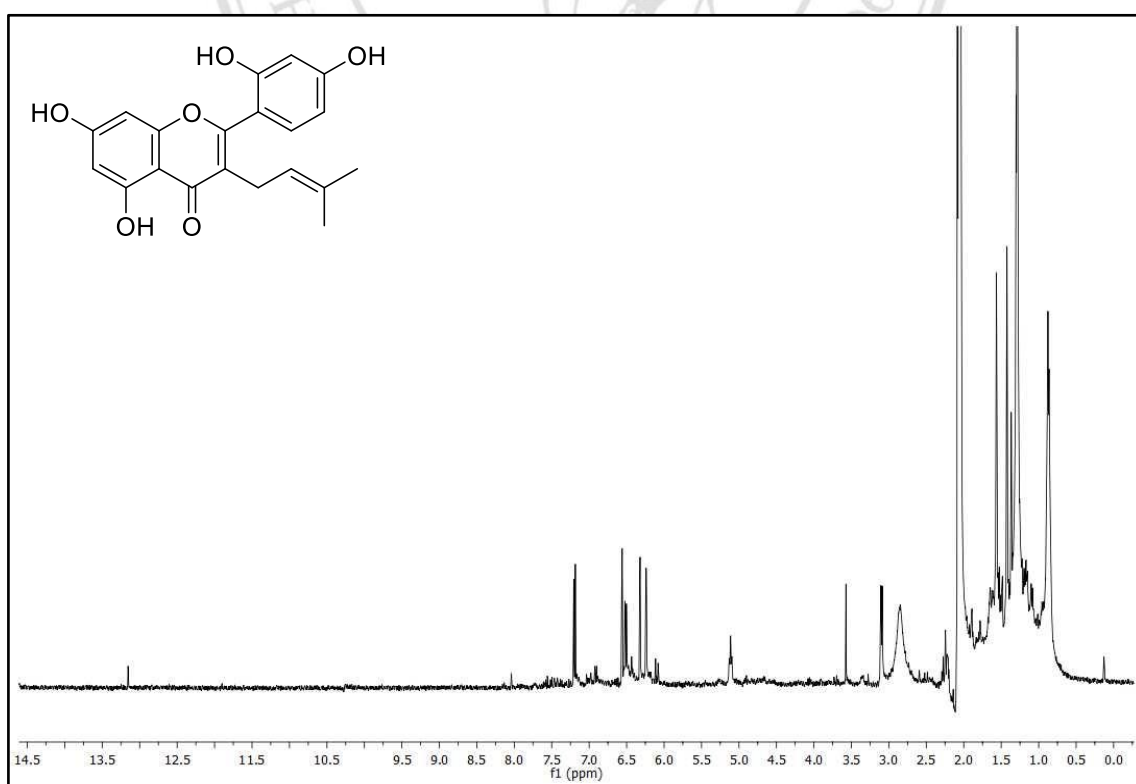


**Figure 17** The <sup>1</sup>H-NMR (400 MHz, acetone-*d*<sub>6</sub>) spectrum of compound **A9**

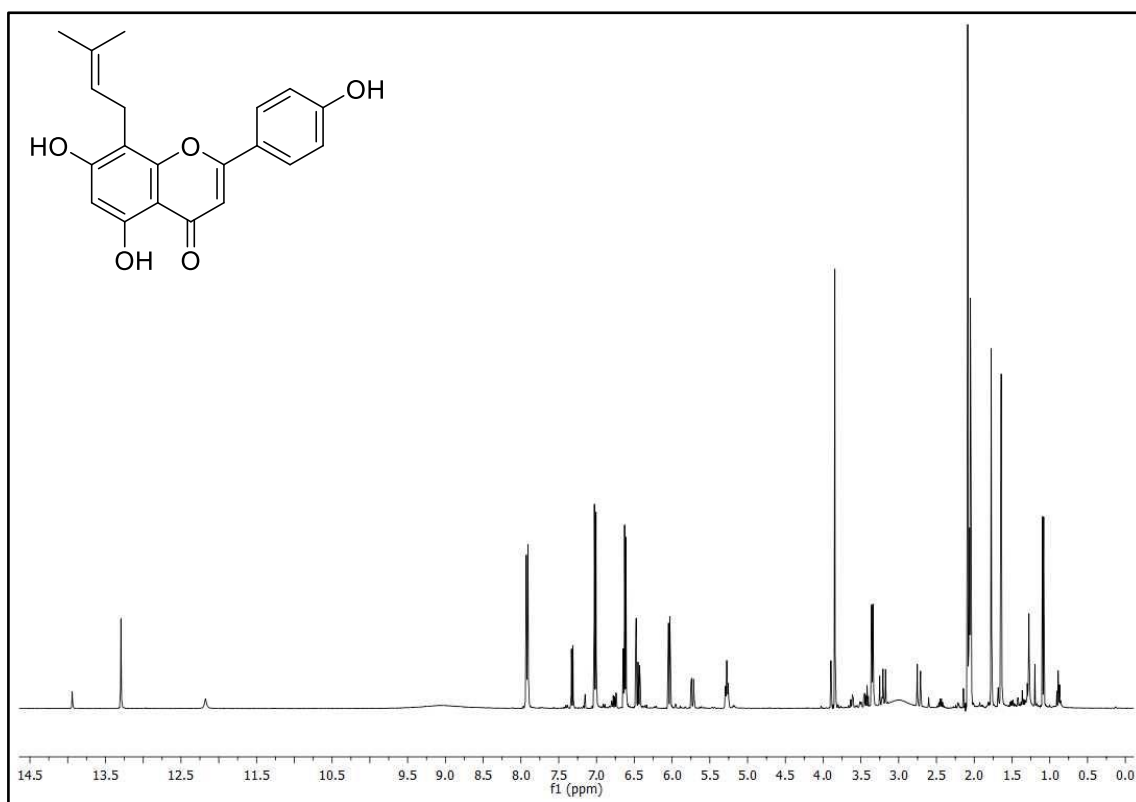


**Figure 18** The  $^1\text{H}$ -NMR (400 MHz, acetone- $d_6$ ) spectrum of compound **A10**

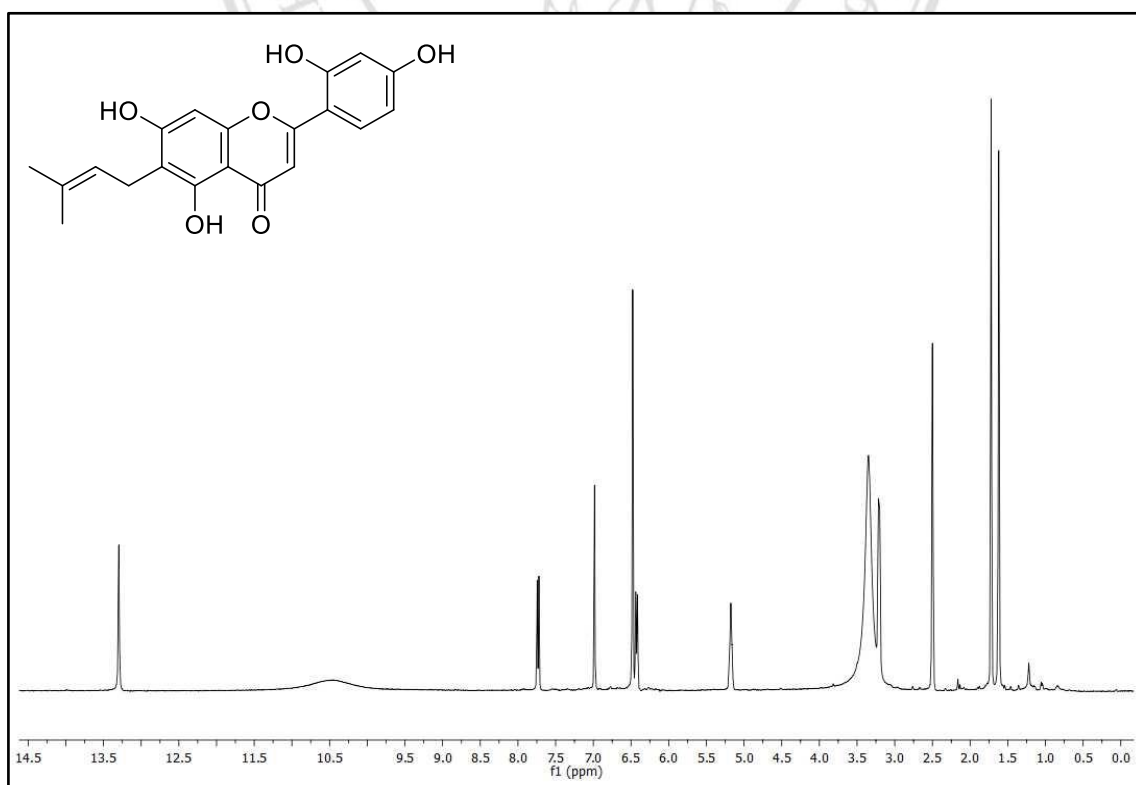


**Figure 19** The  $^1\text{H}$ -NMR (400 MHz, DMSO- $d_6$ ) spectrum of compound **A11**

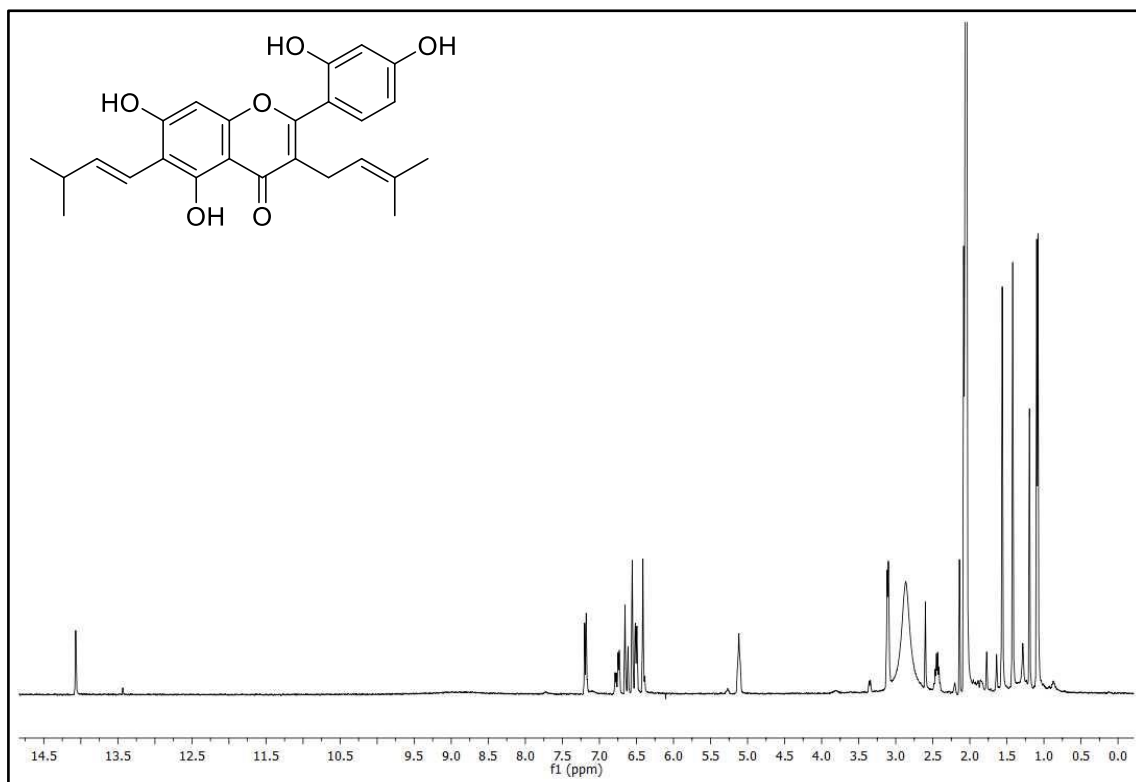


**Figure 20** The <sup>1</sup>H-NMR (400 MHz, acetone-*d*<sub>6</sub>) spectrum of compound A12

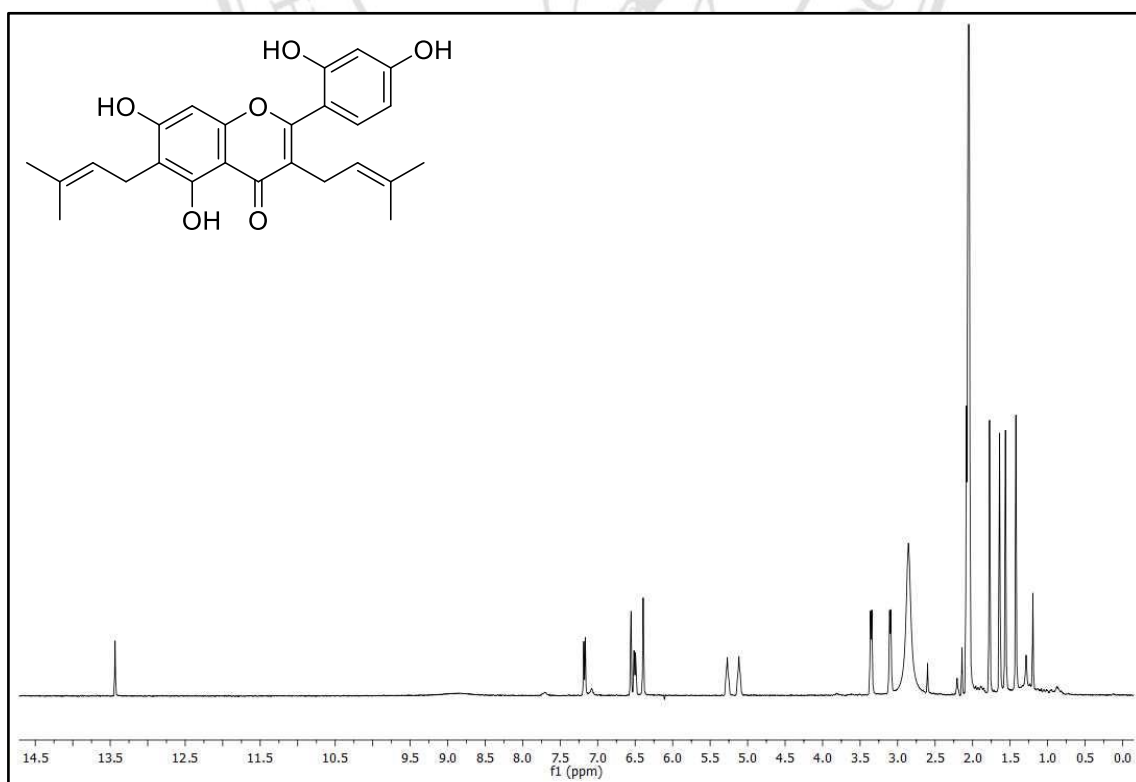


**Figure 21** The <sup>1</sup>H-NMR (400 MHz, acetone-*d*<sub>6</sub>) spectrum of compound A13



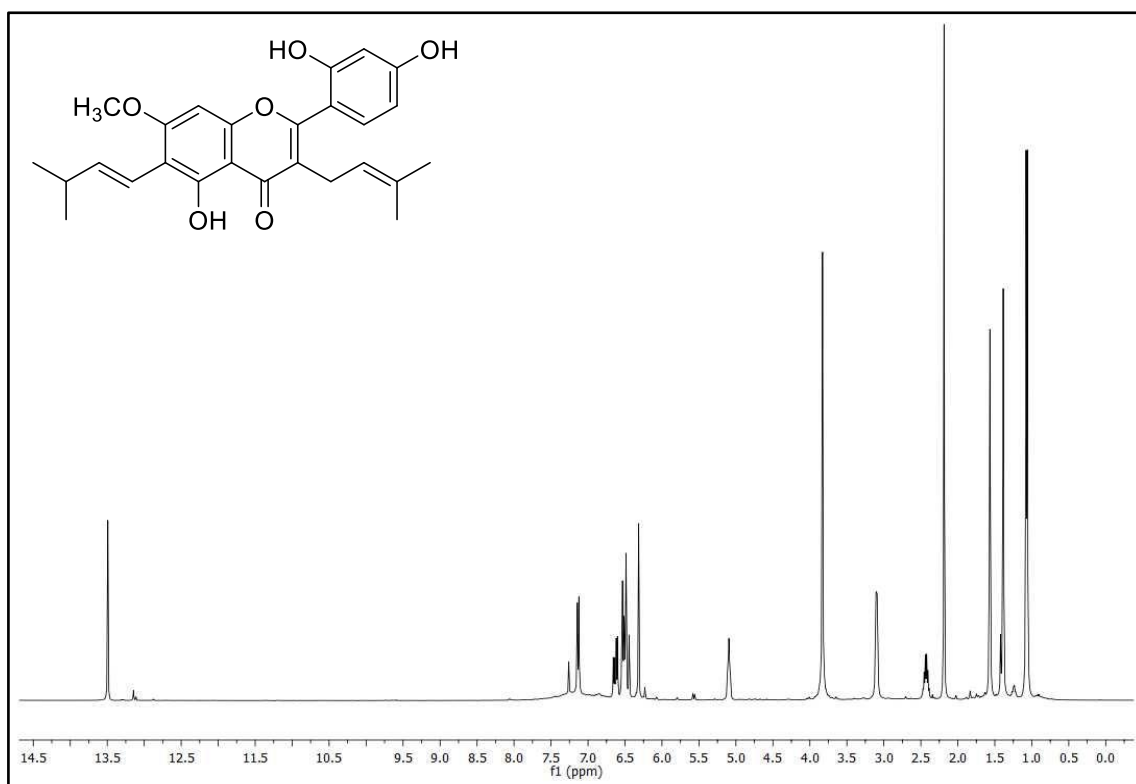


**Figure 22** The  $^1\text{H}$ -NMR (400 MHz,  $\text{CDCl}_3$ ) spectrum of compound **A14**

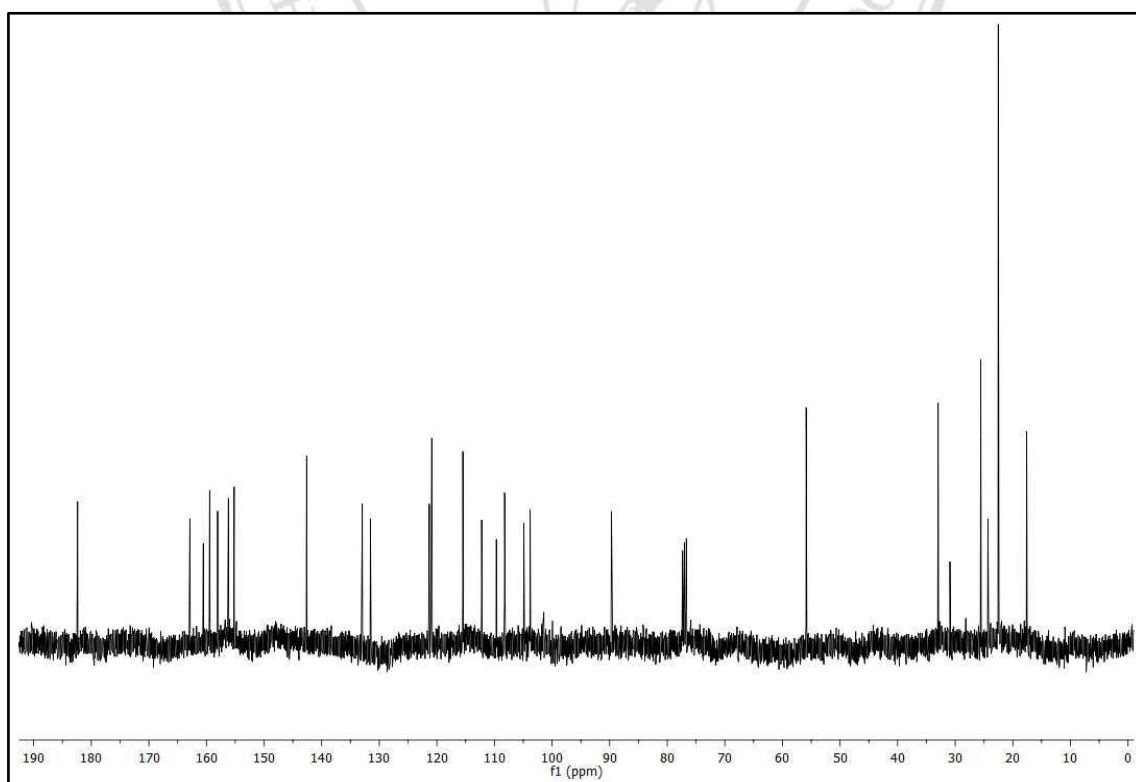


**Figure 23** The  $^{13}\text{C}$ -NMR (400 MHz,  $\text{CDCl}_3$ ) spectrum of compound **A14**

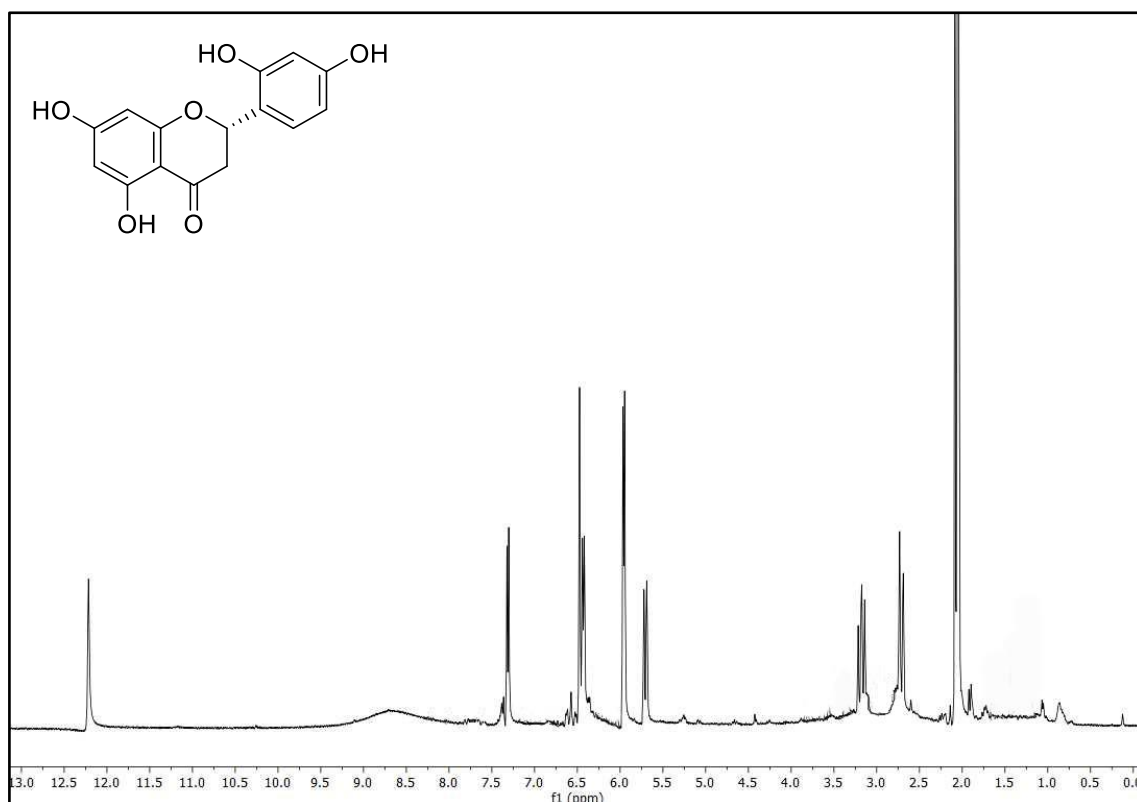


**Figure 24** The <sup>1</sup>H-NMR (400 MHz, acetone-*d*<sub>6</sub>) spectrum of compound A15

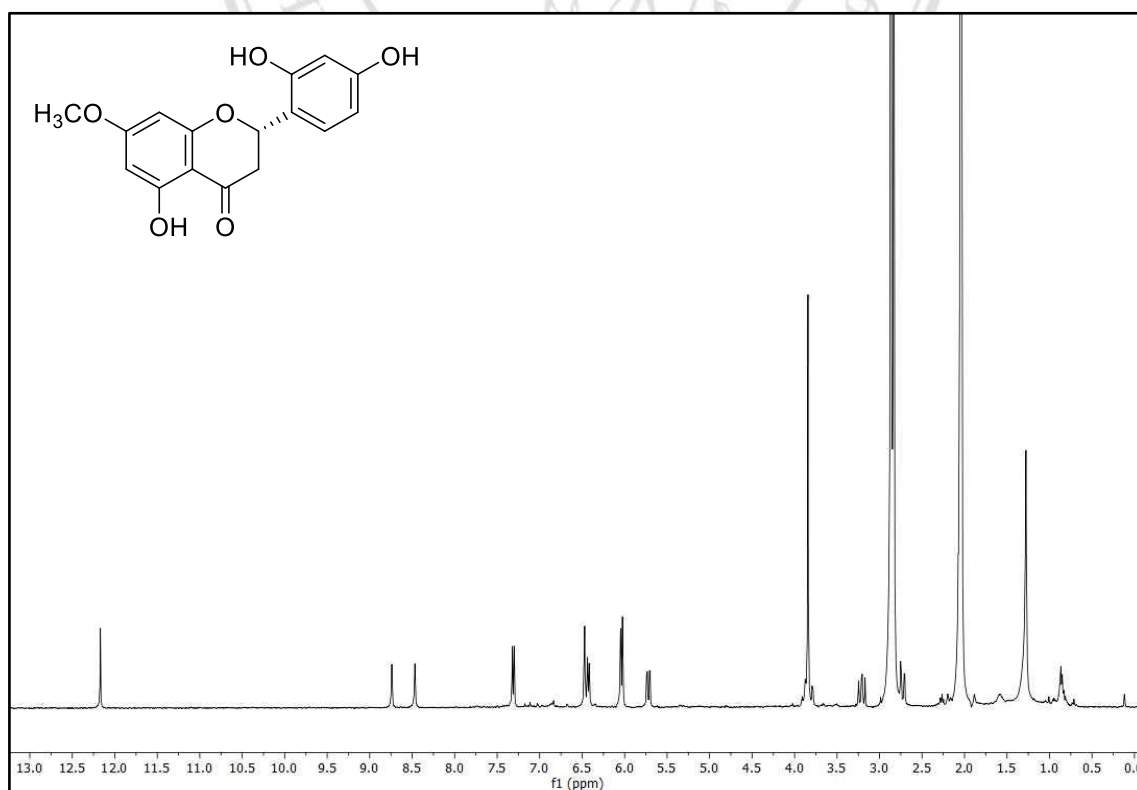


**Figure 25** The <sup>1</sup>H-NMR (400 MHz, acetone-*d*<sub>6</sub>) spectrum of compound A16

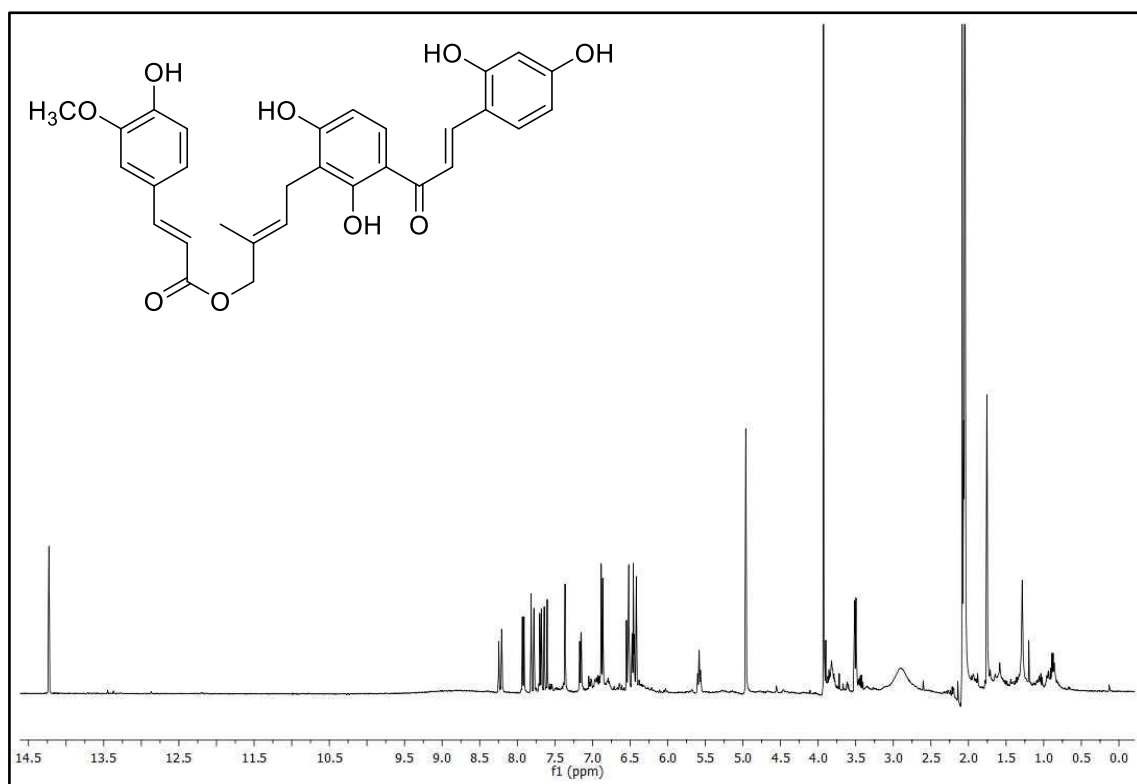


**Figure 26** The  $^1\text{H}$ -NMR (400 MHz, acetone- $d_6$ ) spectrum of compound **A17**

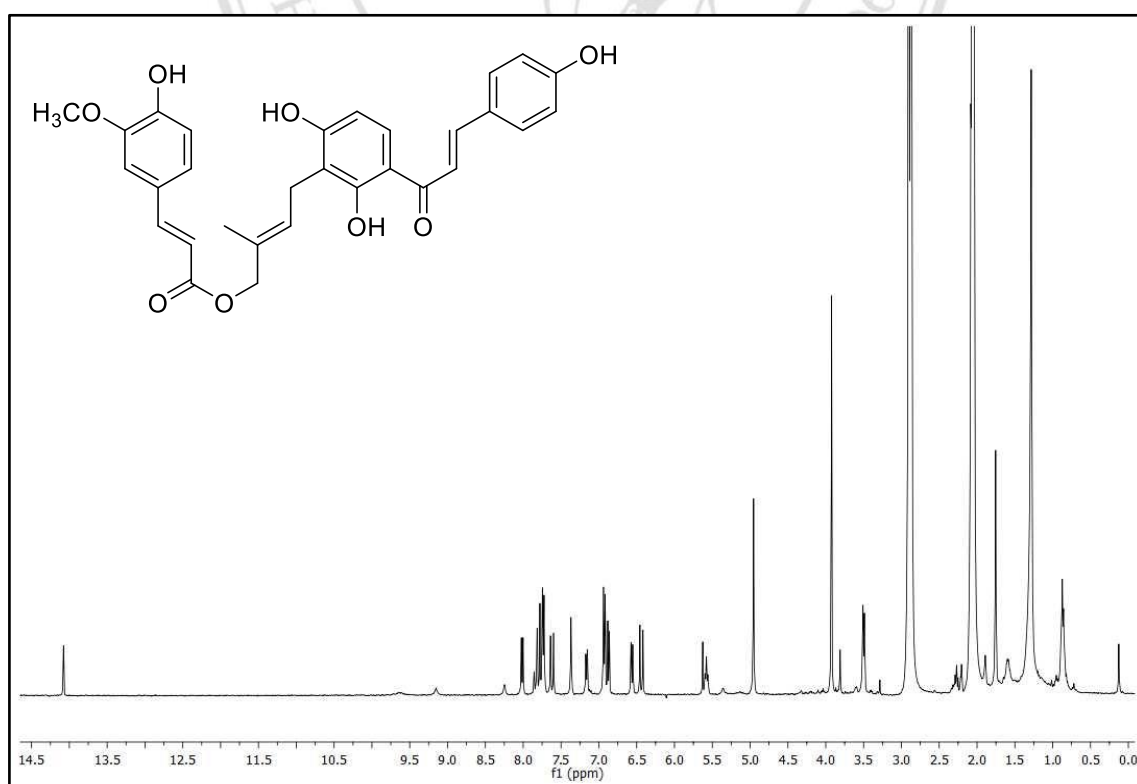


**Figure 27** The  $^1\text{H}$ -NMR (400 MHz, acetone- $d_6$ ) spectrum of compound **A18**

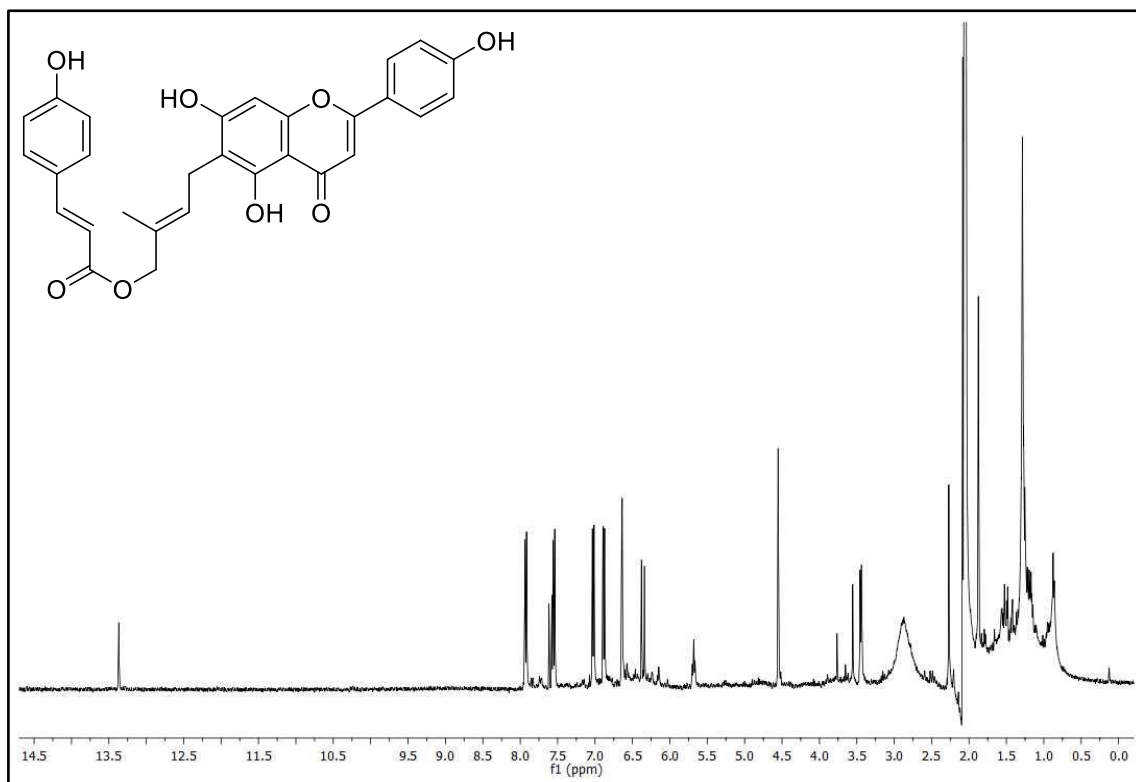


**Figure 28** The <sup>1</sup>H-NMR (400 MHz, acetone-*d*<sub>6</sub>) spectrum of compound A19

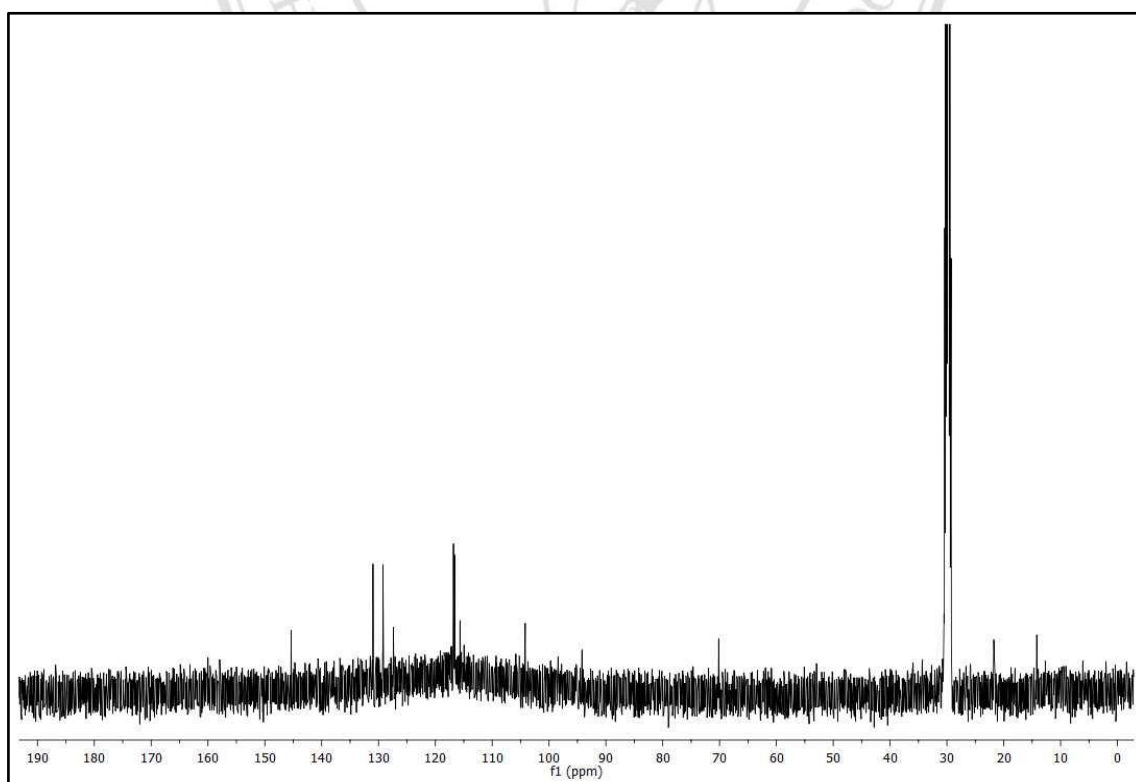


**Figure 29** The <sup>13</sup>C-NMR (100 MHz, acetone-*d*<sub>6</sub>) spectrum of compound A19

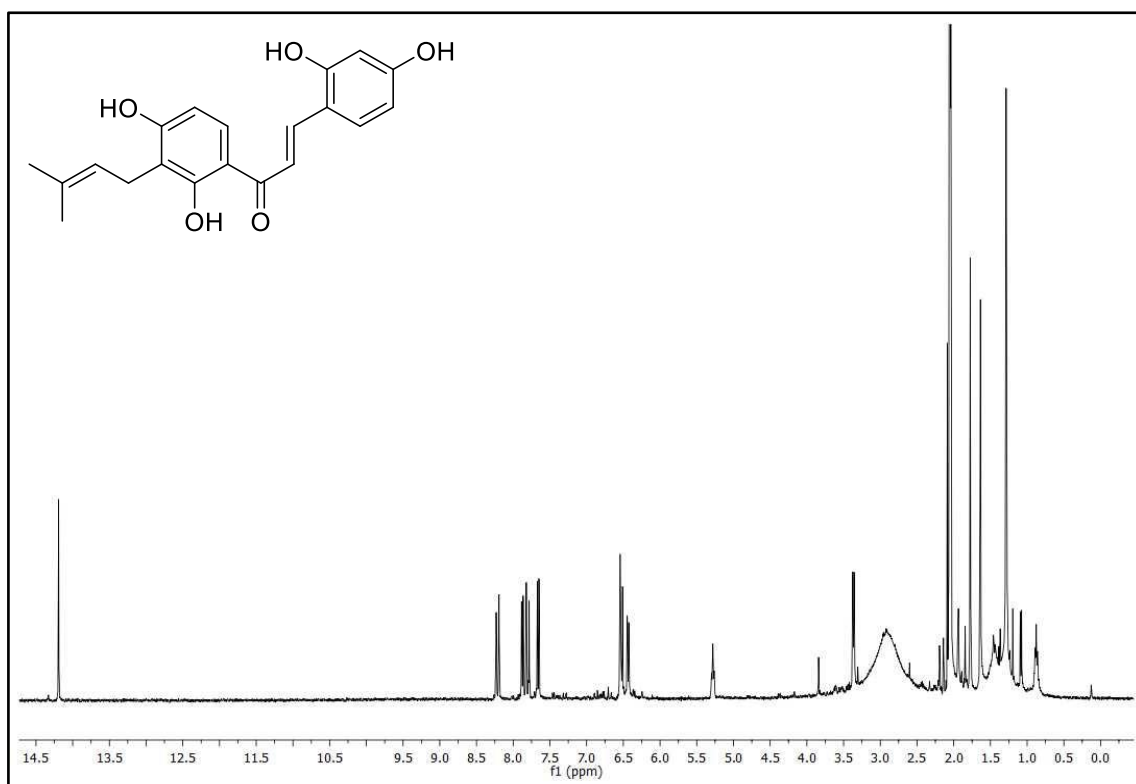


**Figure 30** The  $^1\text{H}$ -NMR (400 MHz, acetone- $d_6$ ) spectrum of compound **A20**

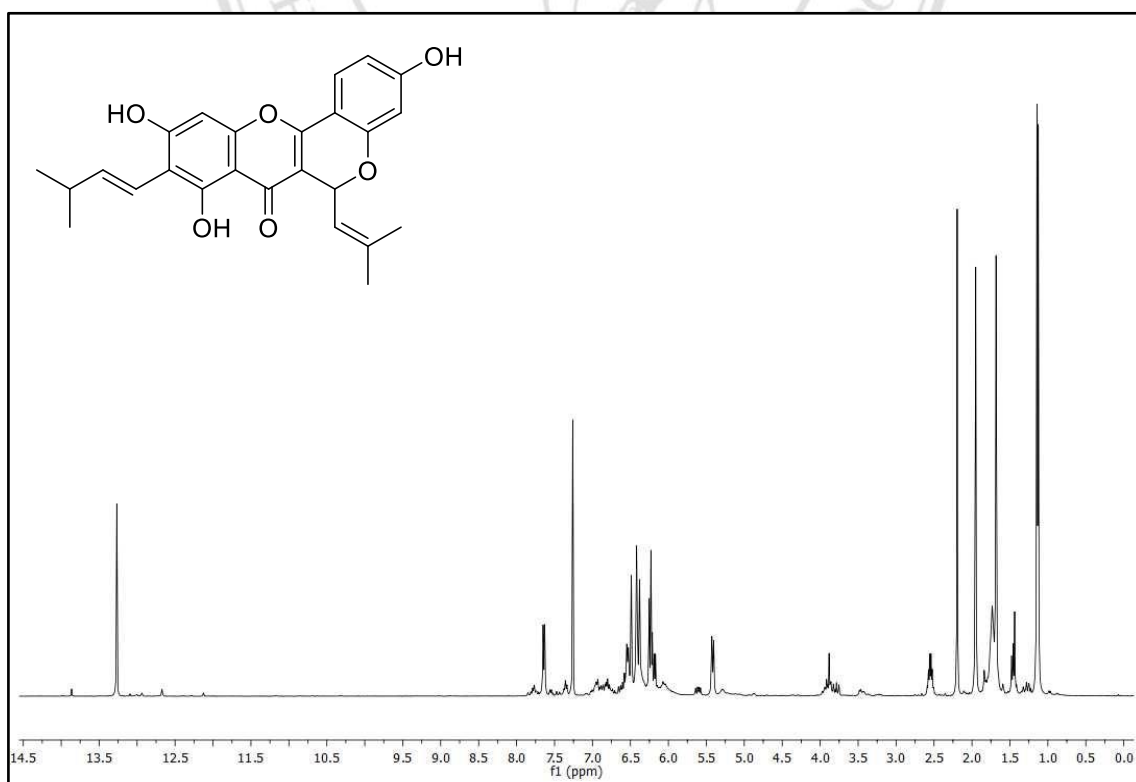


**Figure 31** The  $^1\text{H}$ -NMR (400 MHz,  $\text{CDCl}_3$ ) spectrum of compound **A21**

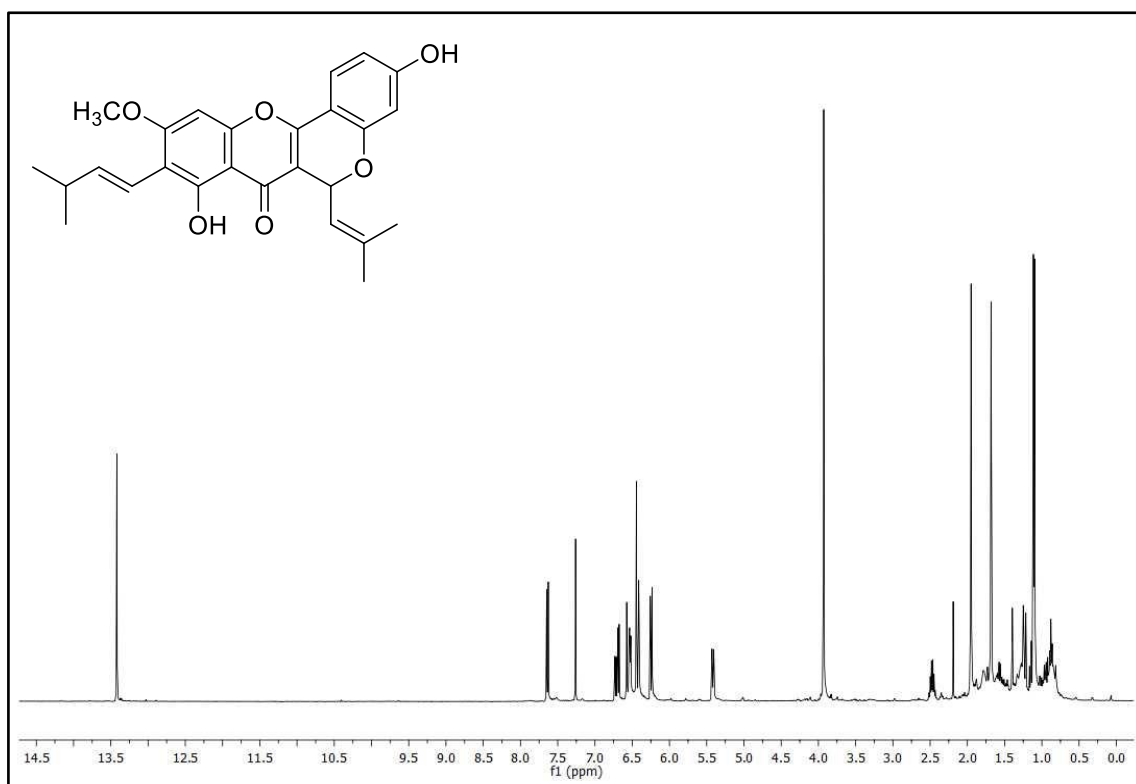


**Figure 32** The <sup>1</sup>H-NMR (400 MHz, CDCl<sub>3</sub>) spectrum of compound **A22**

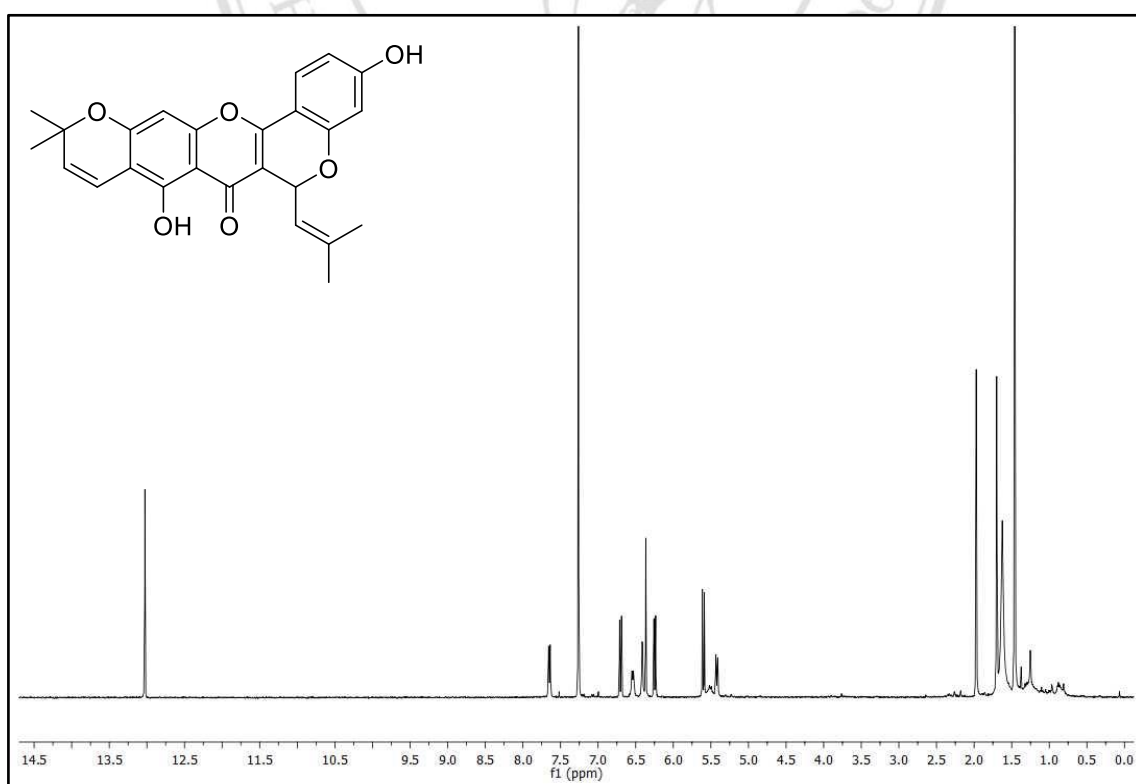


**Figure 33** The <sup>1</sup>H-NMR (400 MHz, CDCl<sub>3</sub>) spectrum of compound **A23**

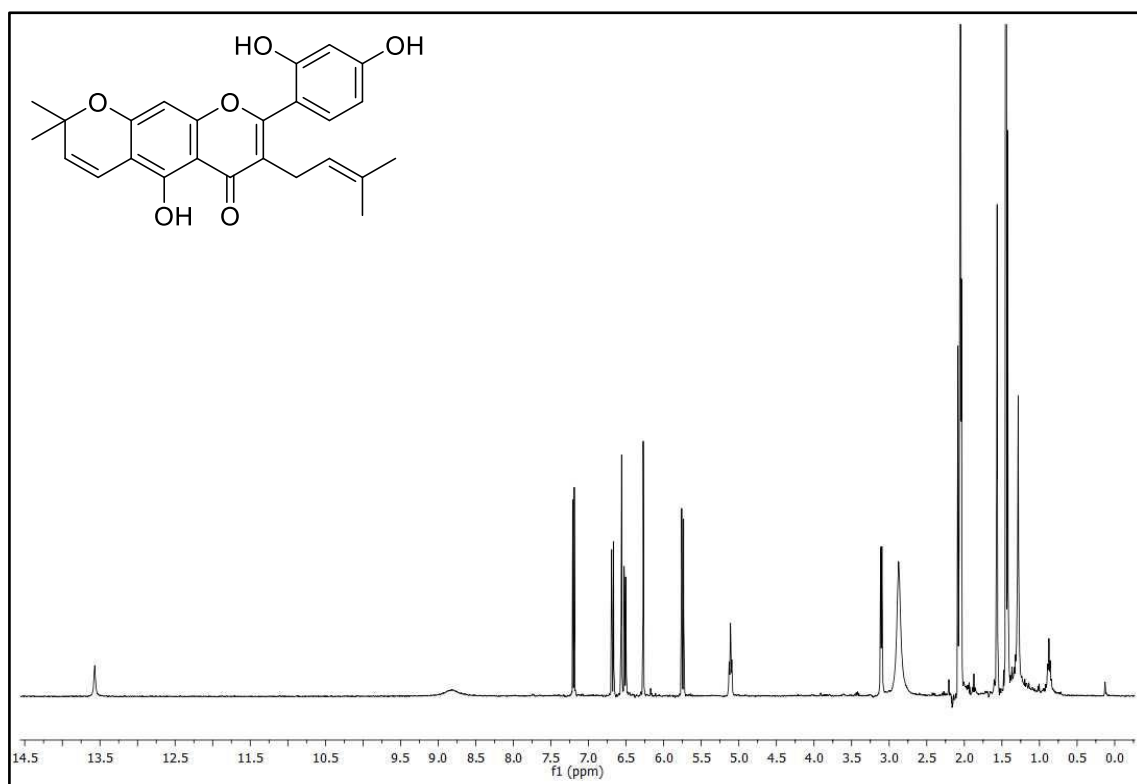


**Figure 34** The  $^1\text{H}$ -NMR (400 MHz, acetone- $d_6$ ) spectrum of compound **A24**

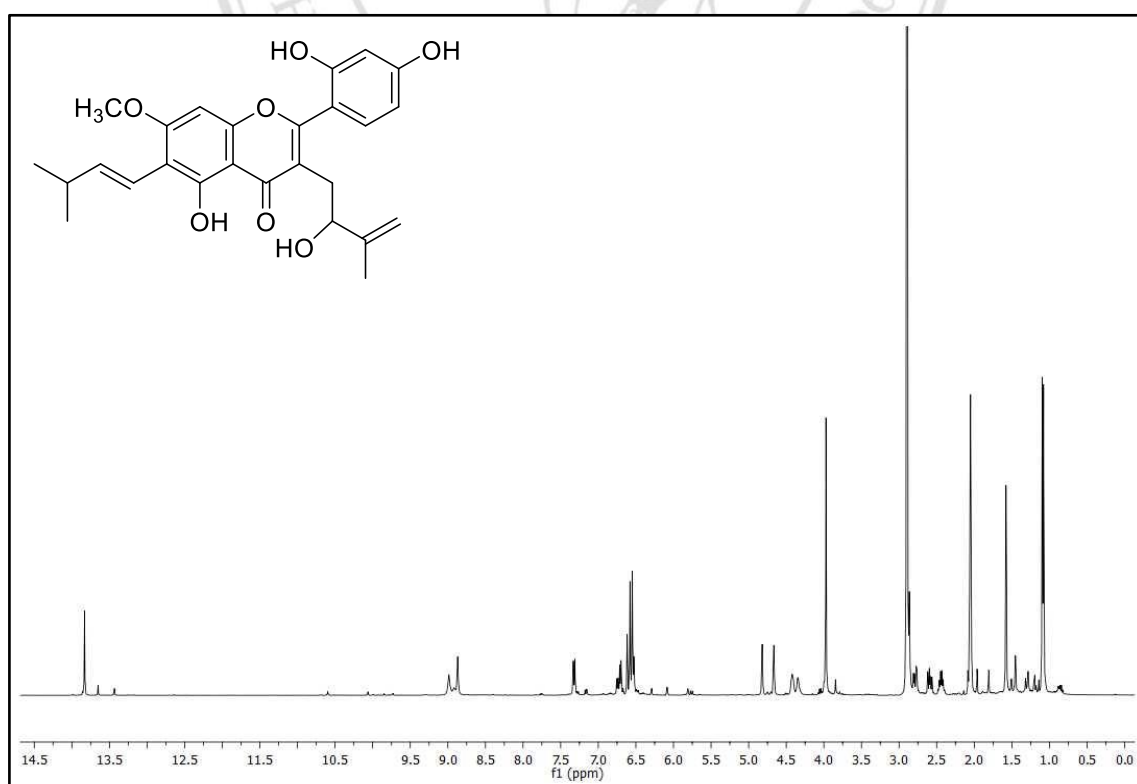


**Figure 35** The  $^1\text{H}$ -NMR (400 MHz, acetone- $d_6$ ) spectrum of compound **A25**

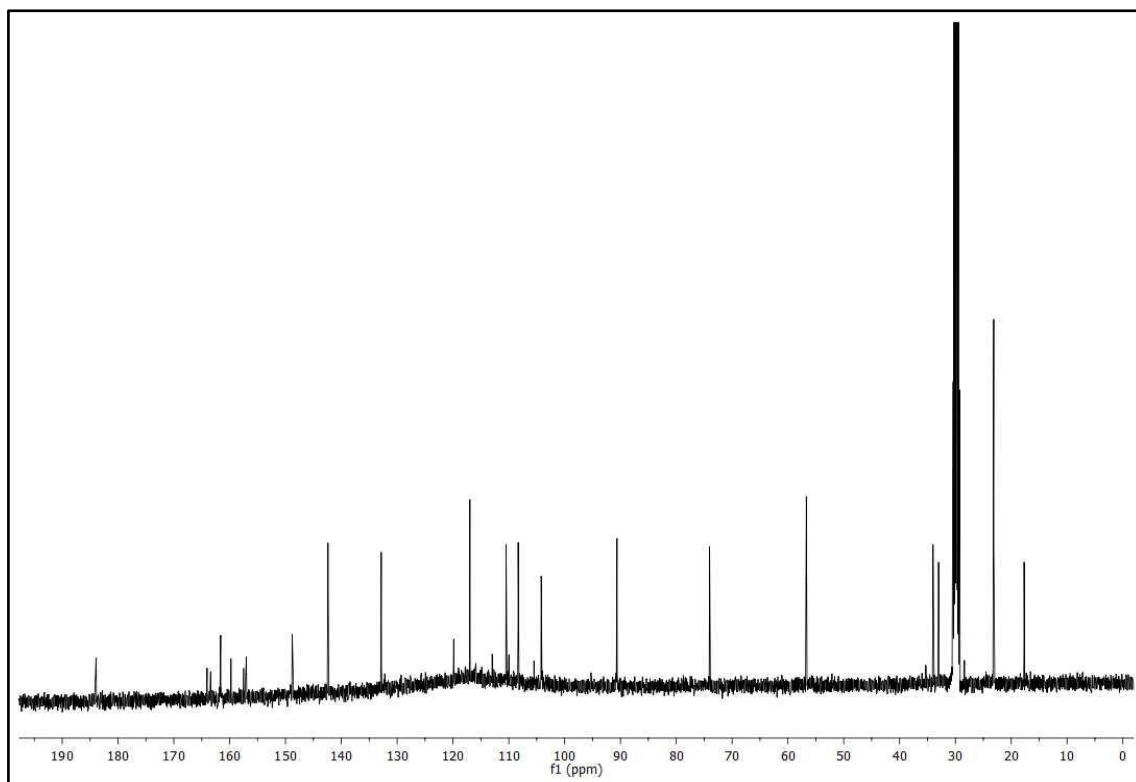


**Figure 36** The  $^{13}\text{C}$ -NMR (100 MHz, acetone- $d_6$ ) spectrum of compound **A25**

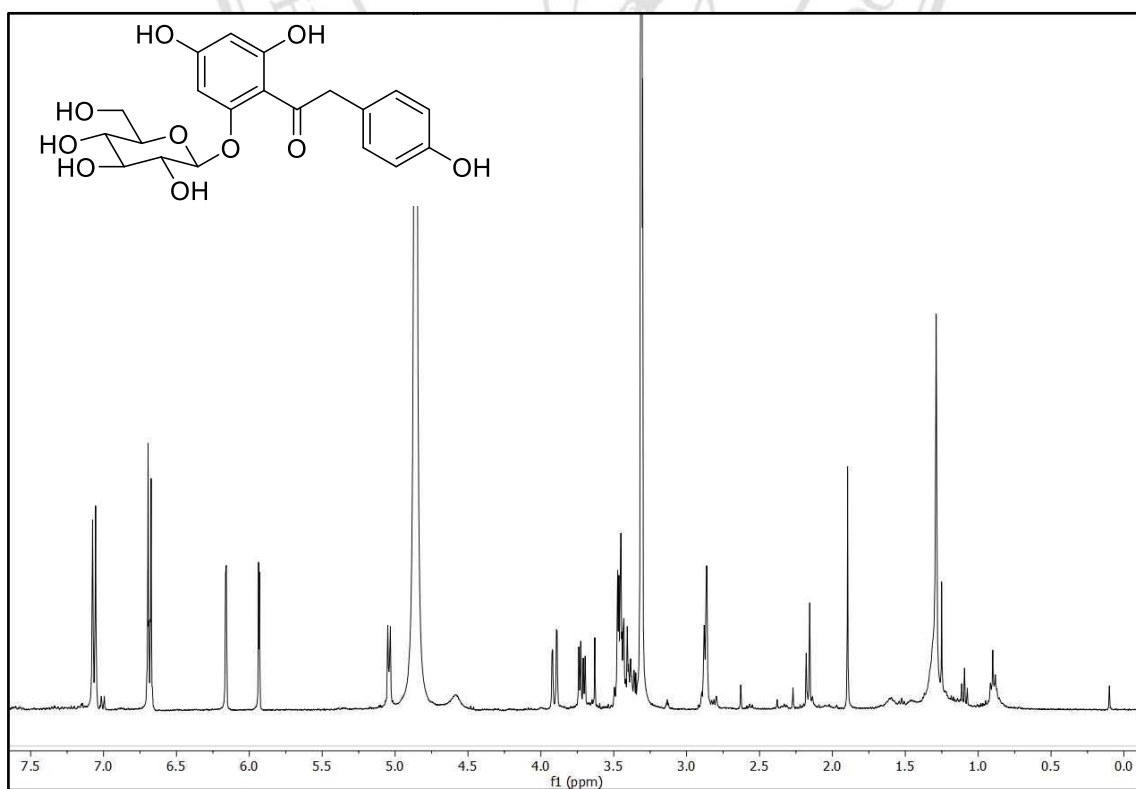


**Figure 37** The  $^1\text{H}$ -NMR (400 MHz, MeOD- $d_4$ ) spectrum of compound **A26**



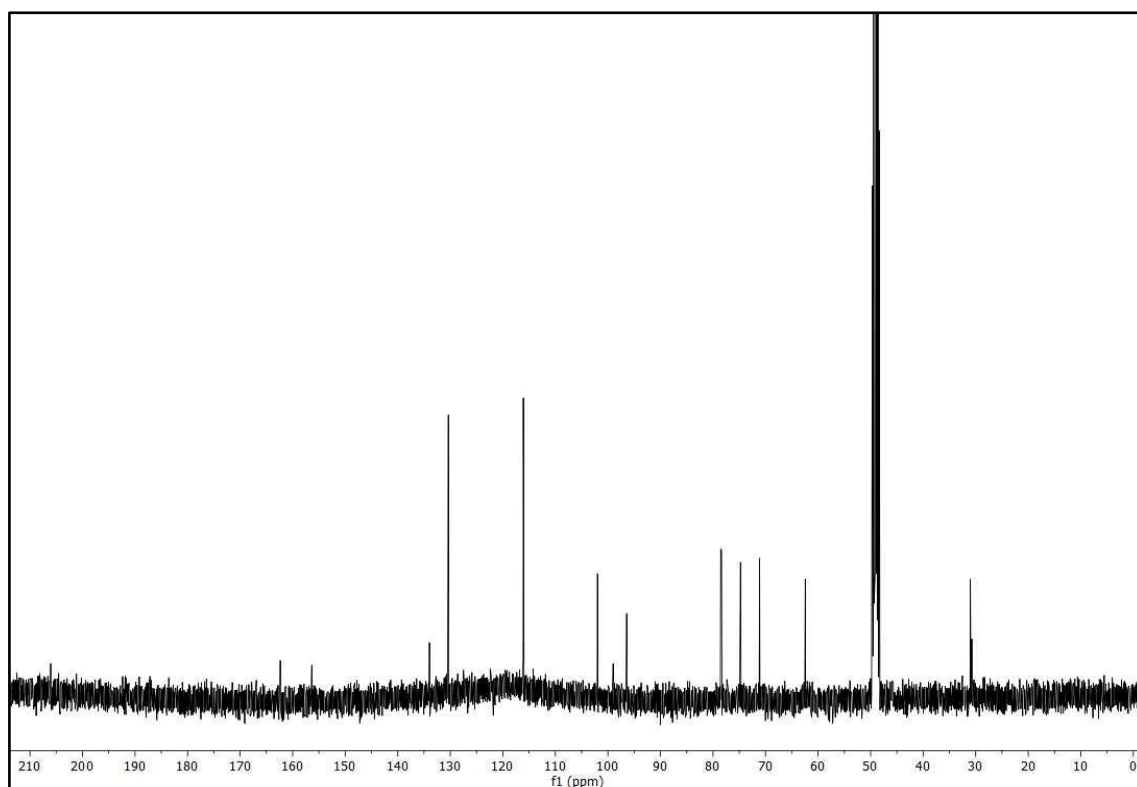


**Figure 38** The  $^{13}\text{C}$ -NMR (100 MHz,  $\text{MeOD-}d_4$ ) spectrum of compound **A26**

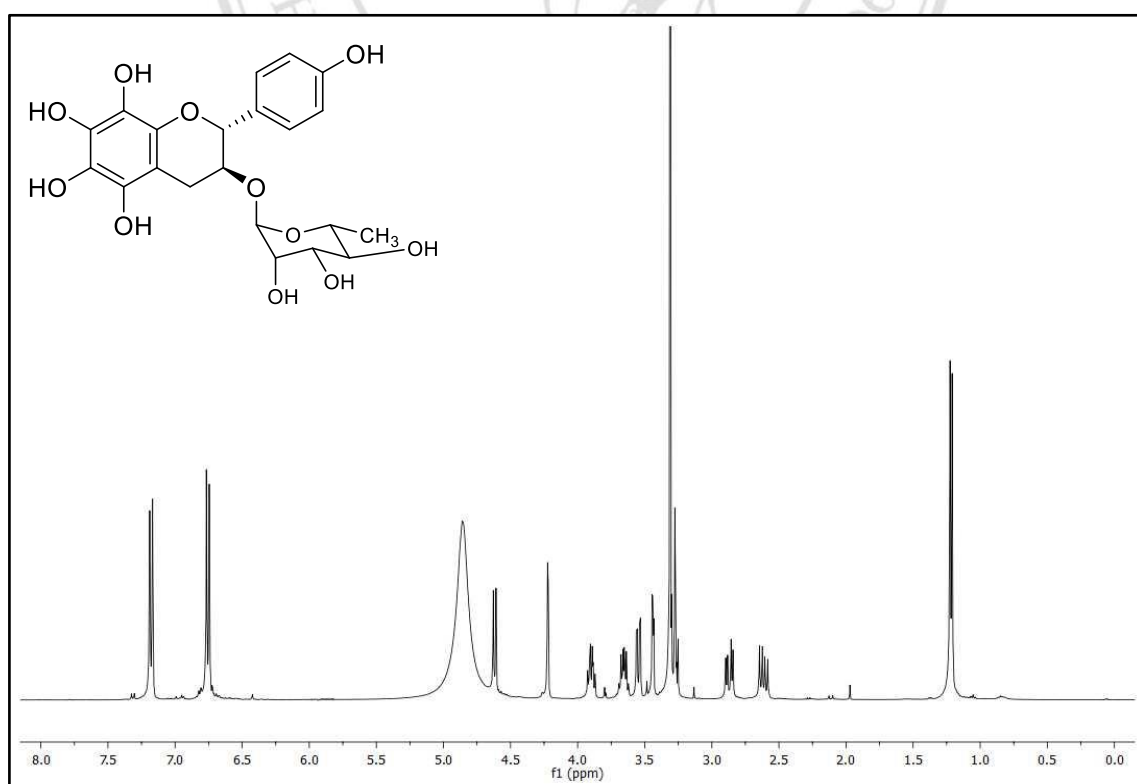


**Figure 39** The  $^1\text{H}$ -NMR (400 MHz,  $\text{MeOD-}d_4$ ) spectrum of compound **A27**

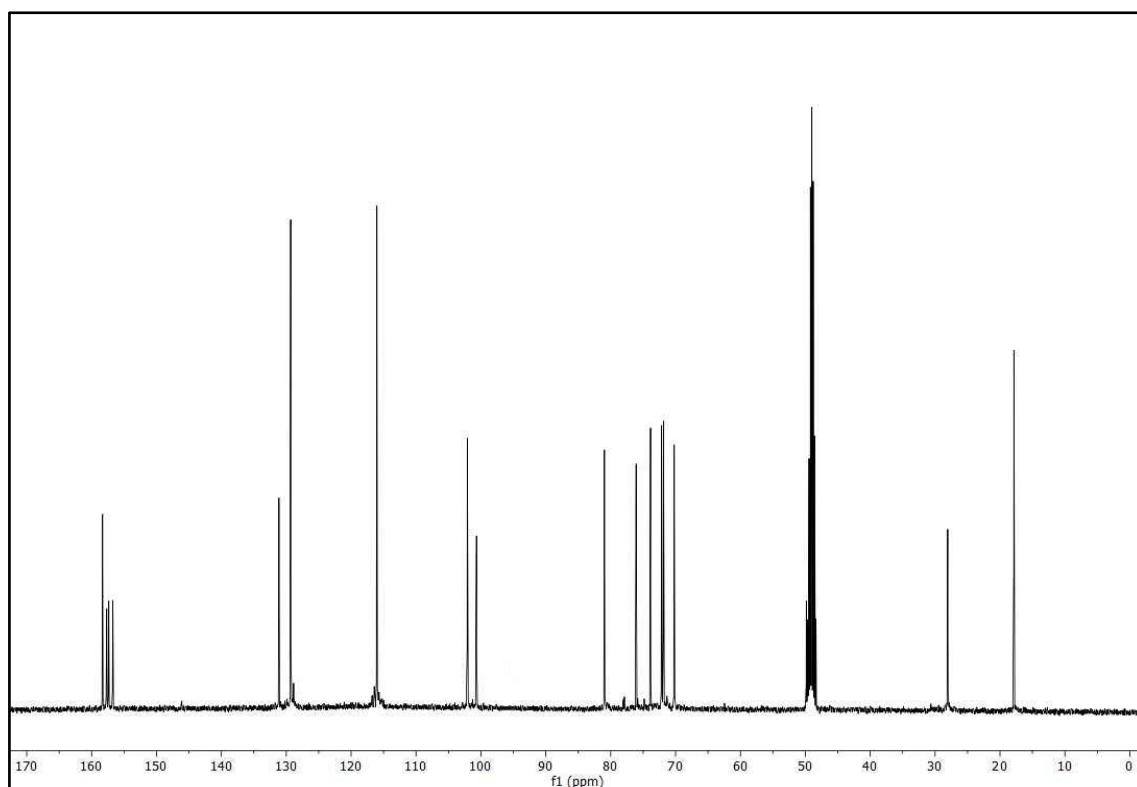


**Figure 40** The  $^{13}\text{C}$ -NMR (100 MHz,  $\text{MeOD-}d_4$ ) spectrum of compound **A27**

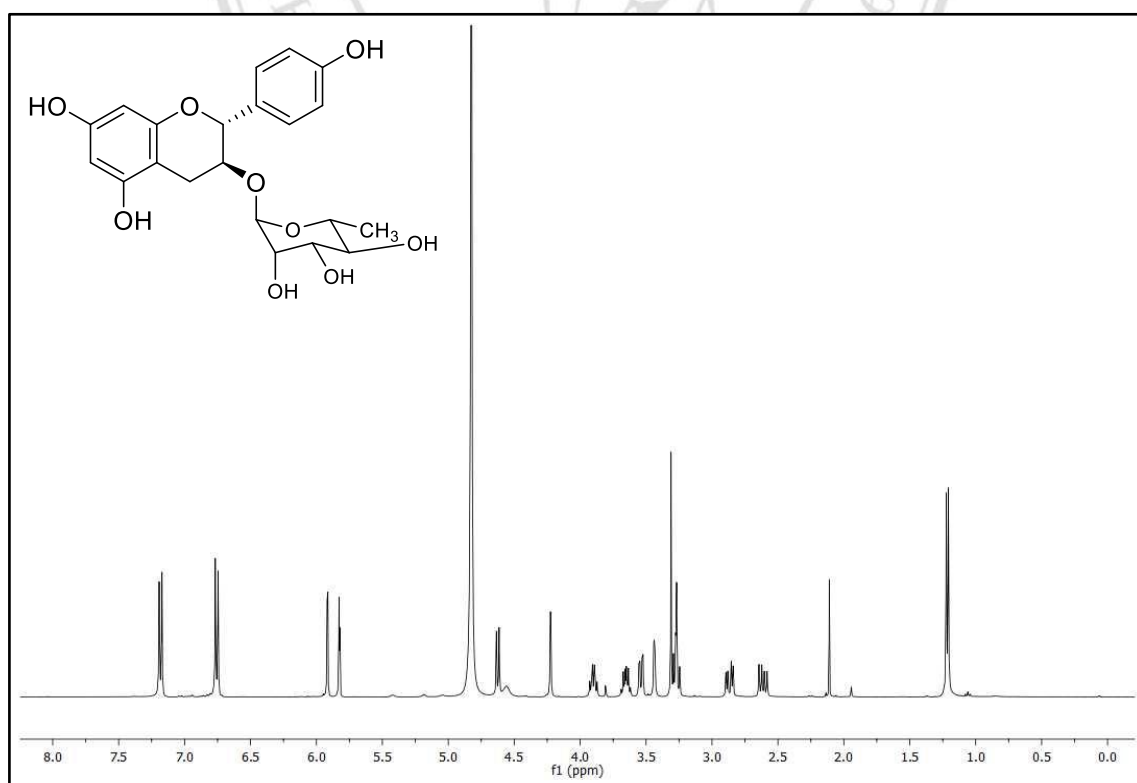


**Figure 41** The  $^1\text{H}$ -NMR (400 MHz,  $\text{MeOD-}d_4$ ) spectrum of compound **A28**

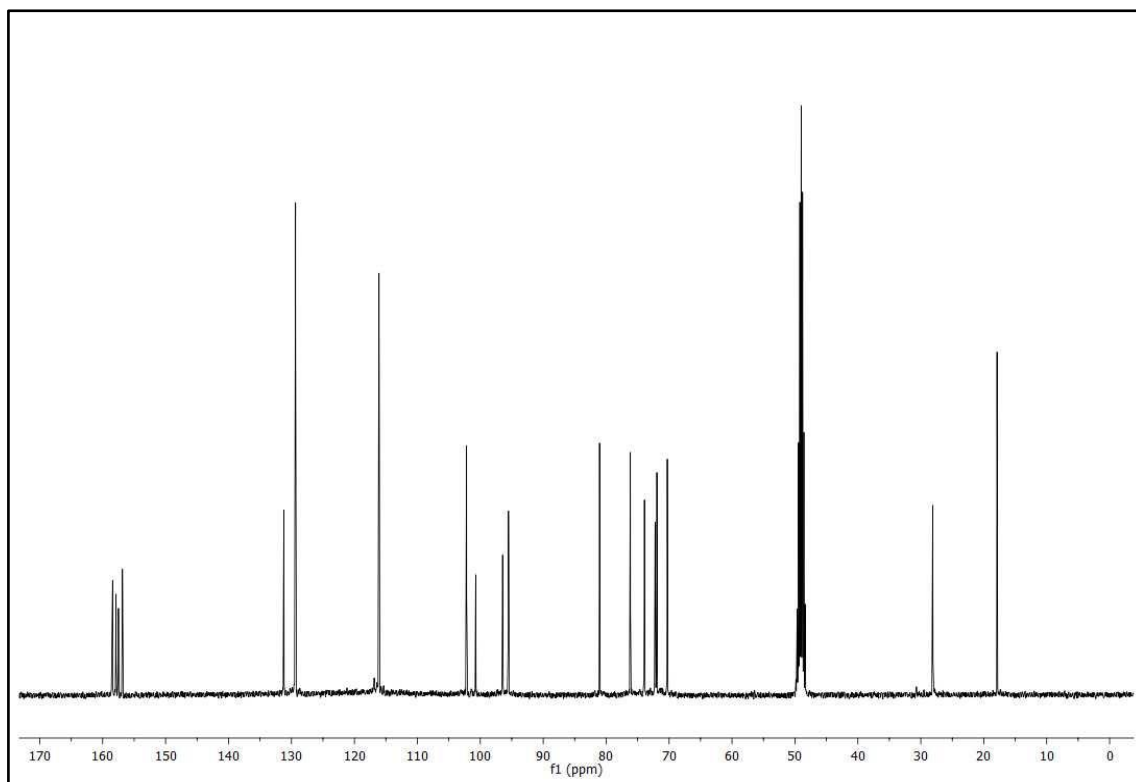


**Figure 42** The  $^{13}\text{C}$ -NMR (100 MHz,  $\text{MeOD-}d_4$ ) spectrum of compound **A28**

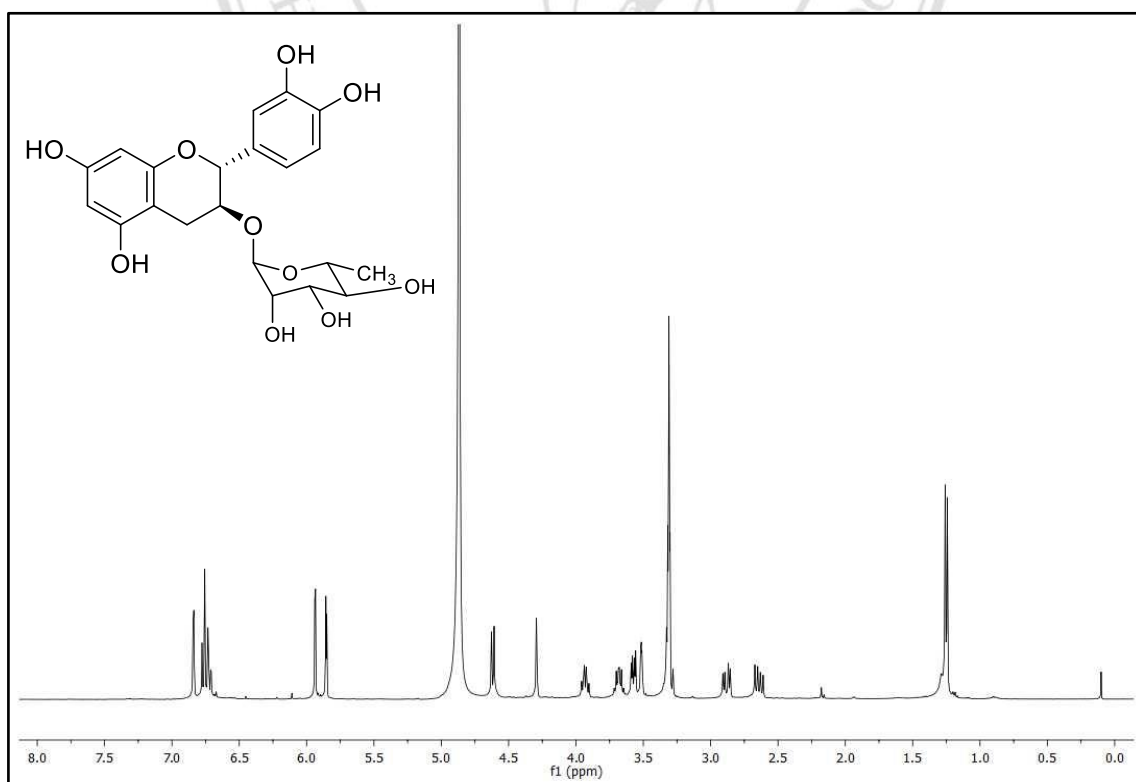


**Figure 43** The  $^1\text{H}$ -NMR (400 MHz,  $\text{MeOD-}d_4$ ) spectrum of compound **A29**

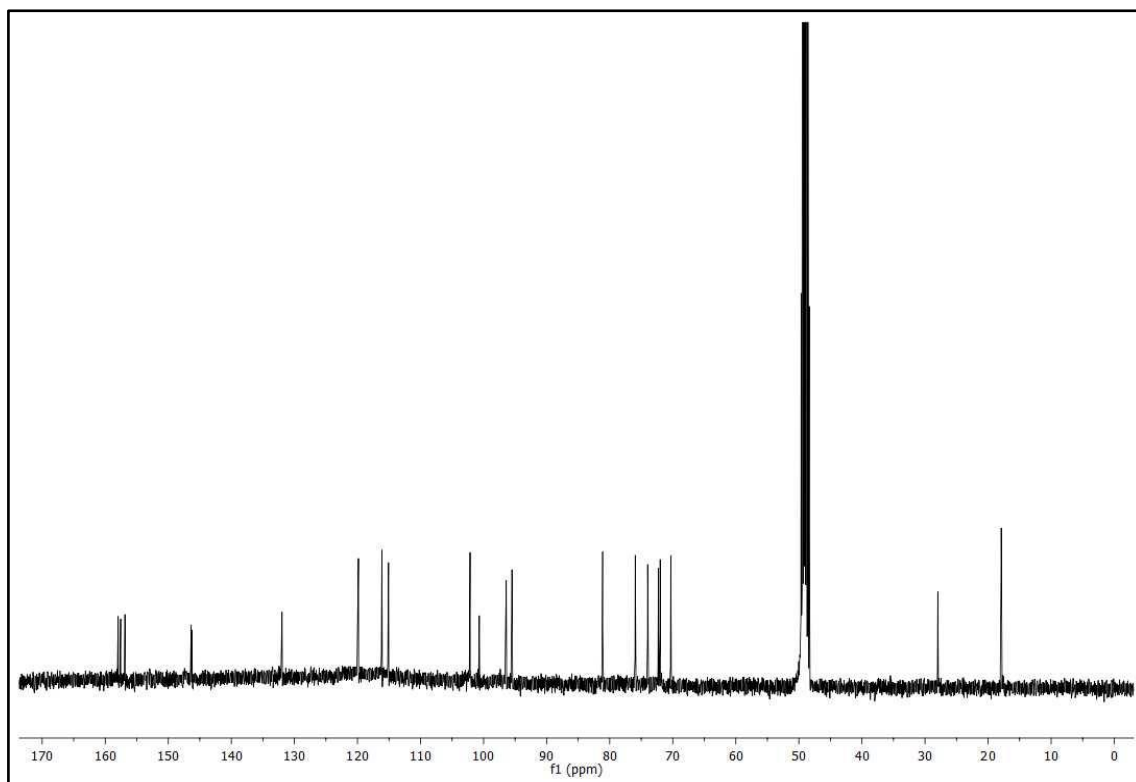


**Figure 44** The  $^{13}\text{C}$ -NMR (100 MHz,  $\text{MeOD-}d_4$ ) spectrum of compound A29

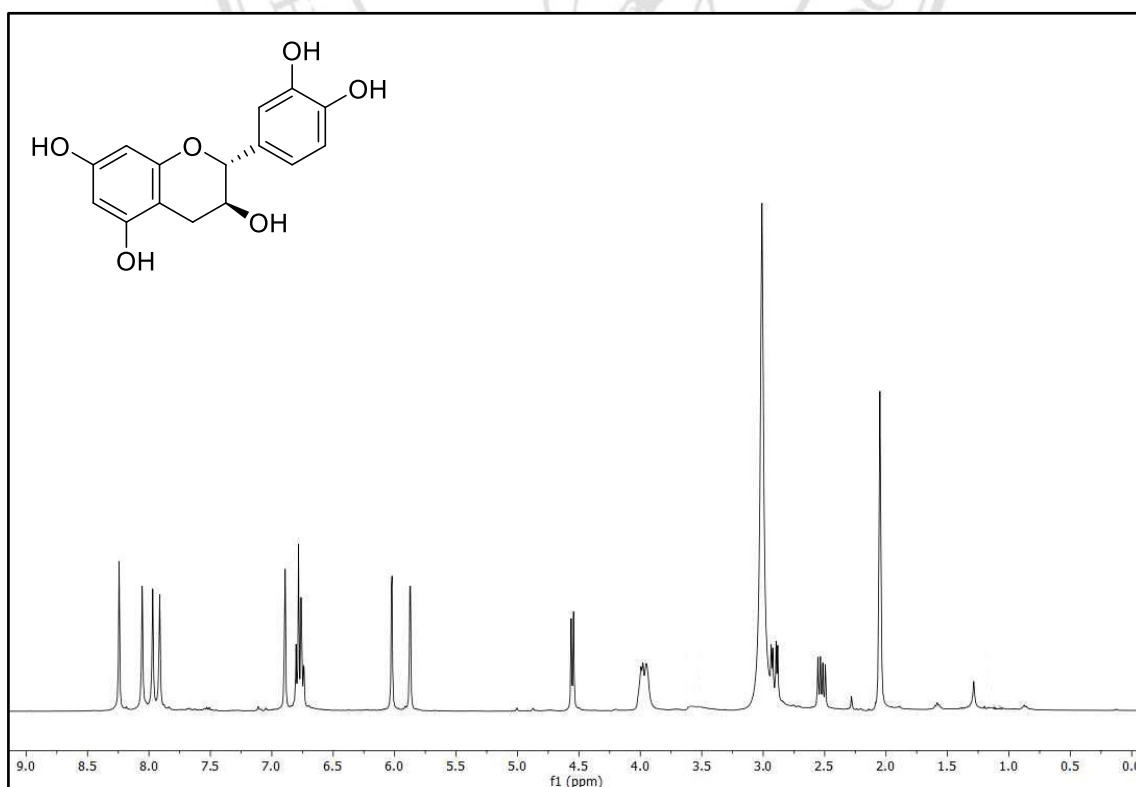


**Figure 45** The  $^1\text{H}$ -NMR (400 MHz,  $\text{acetone-}d_6$ ) spectrum of compound A30

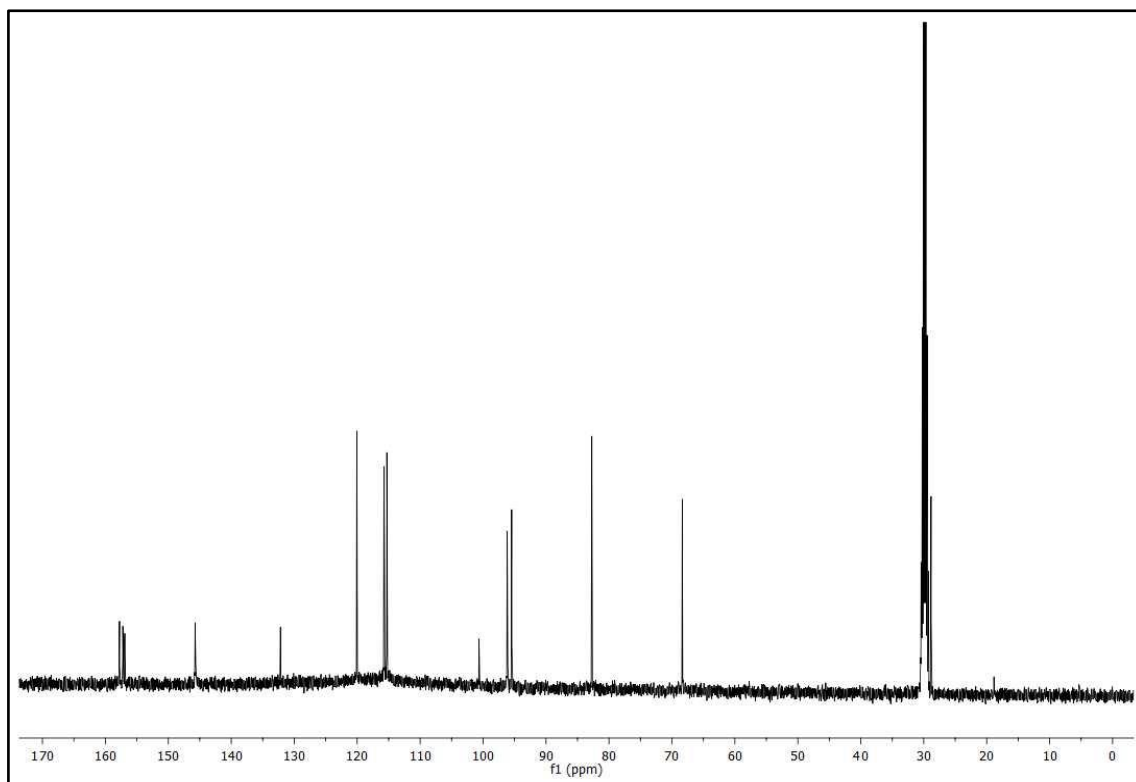


**Figure 46** The  $^{13}\text{C}$ -NMR (100 MHz, acetone- $d_6$ ) spectrum of compound **A30**

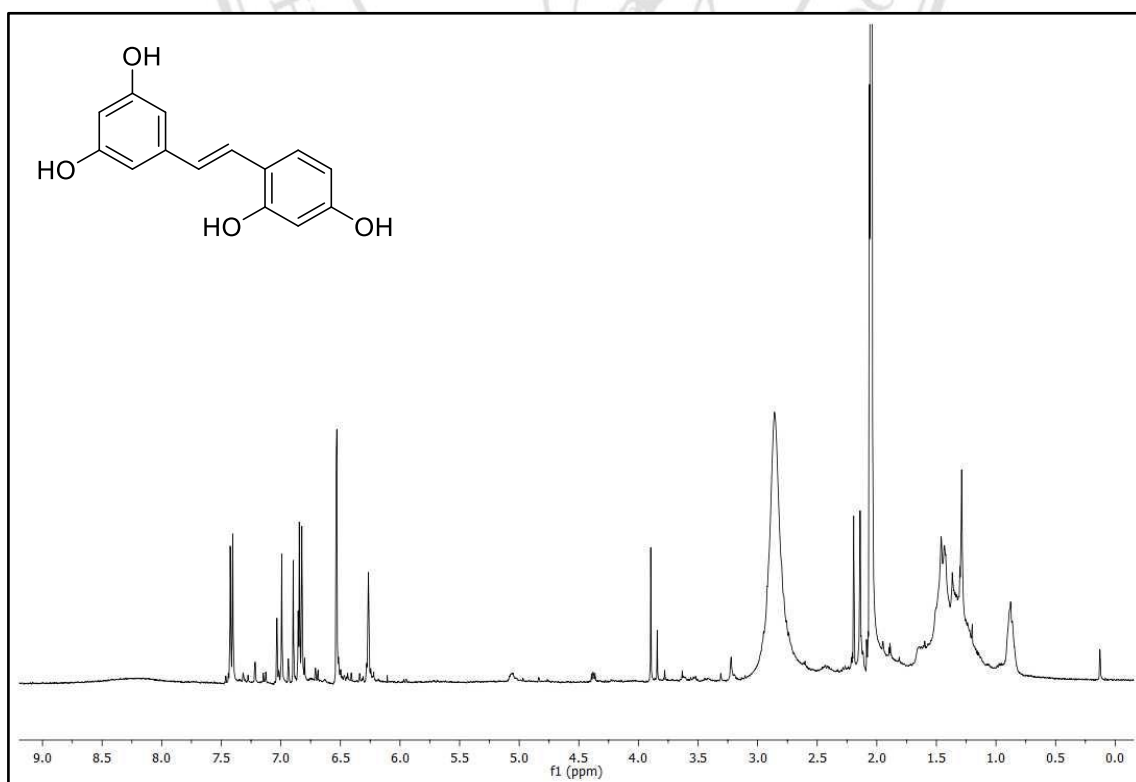


**Figure 47** The  $^1\text{H}$ -NMR (400 MHz, acetone- $d_6$ ) spectrum of compound **A31**

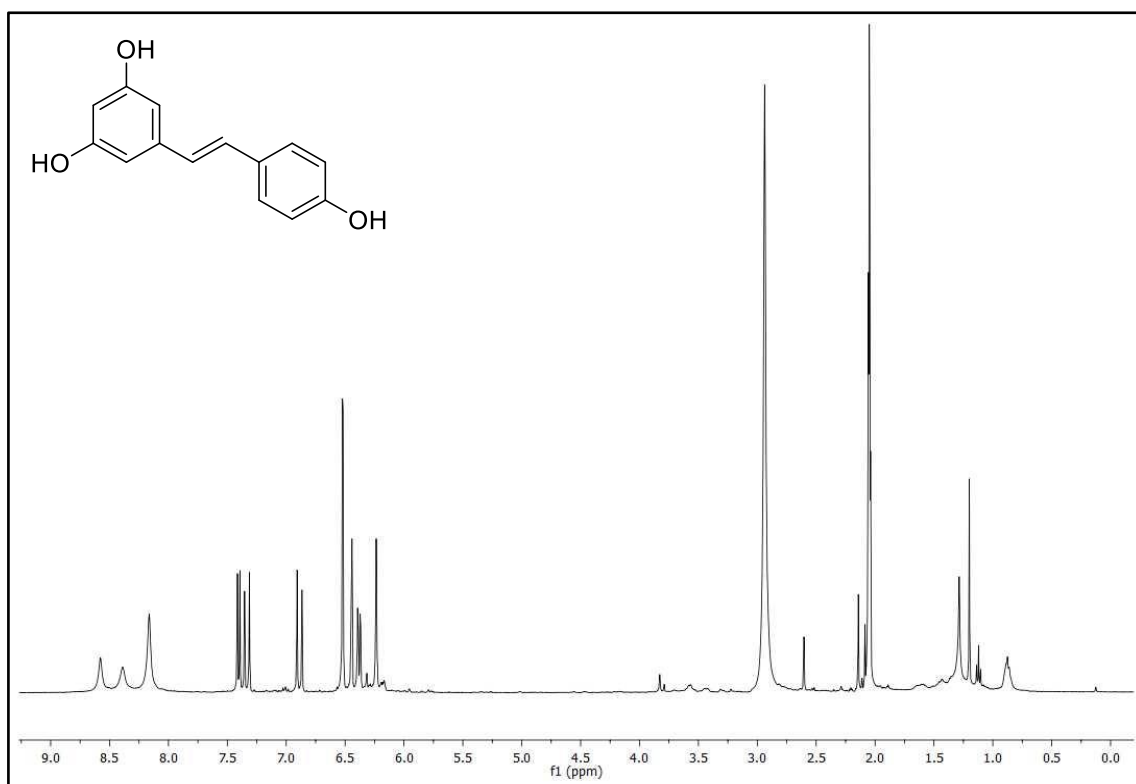


**Figure 48** The  $^1\text{H}$ -NMR (400 MHz, acetone- $d_6$ ) spectrum of compound **A32**

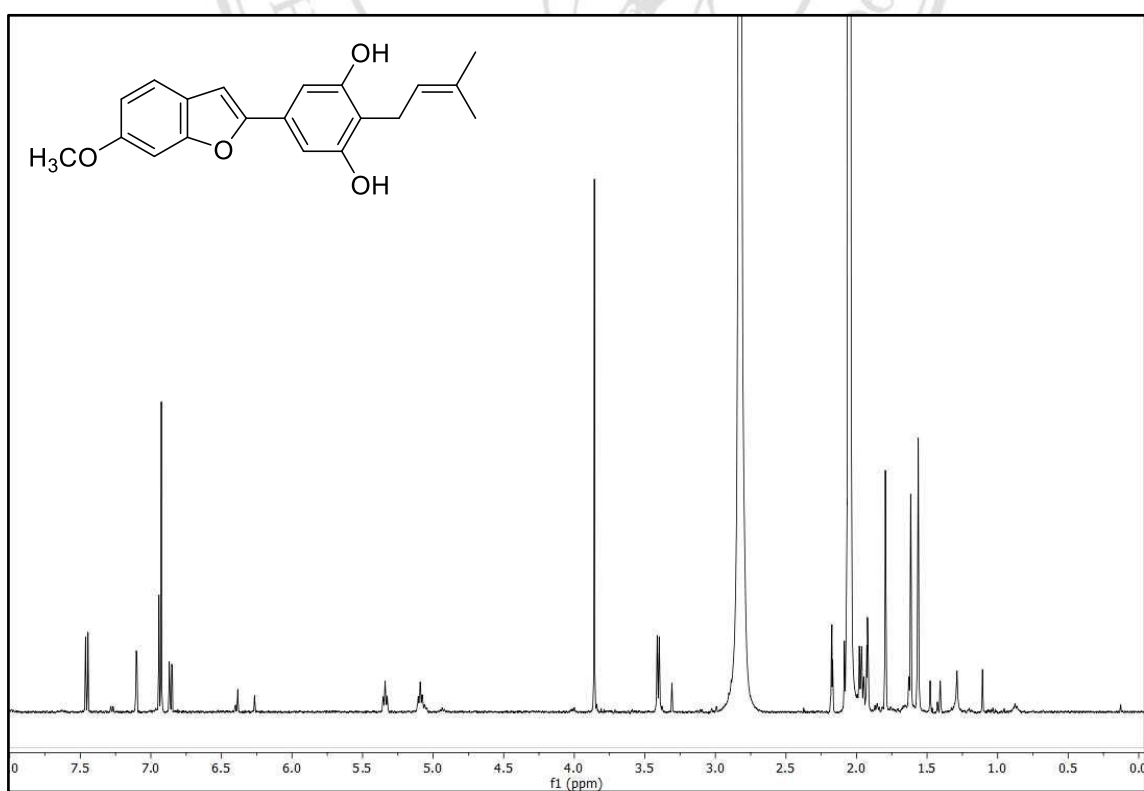


**Figure 49** The  $^1\text{H}$ -NMR (500 MHz, acetone- $d_6$ ) spectrum of compound **A33**

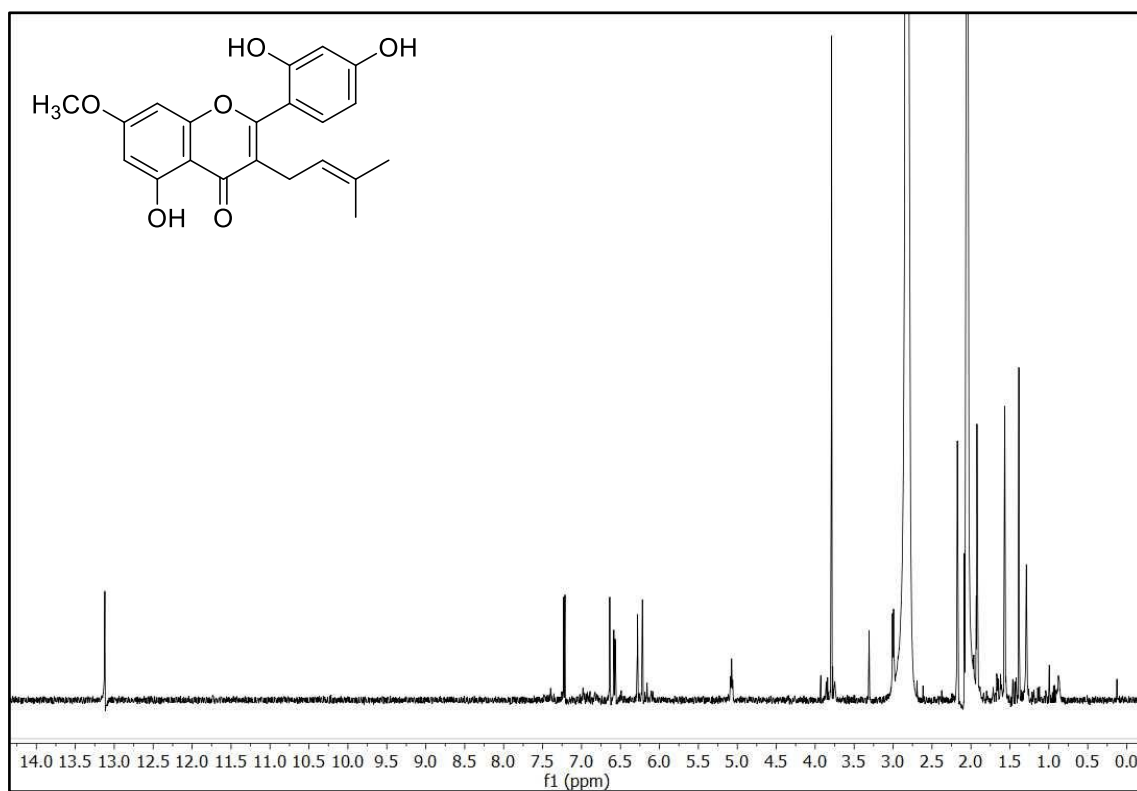


**Figure 50** The <sup>1</sup>H-NMR (500 MHz, acetone-*d*<sub>6</sub>) spectrum of compound A34

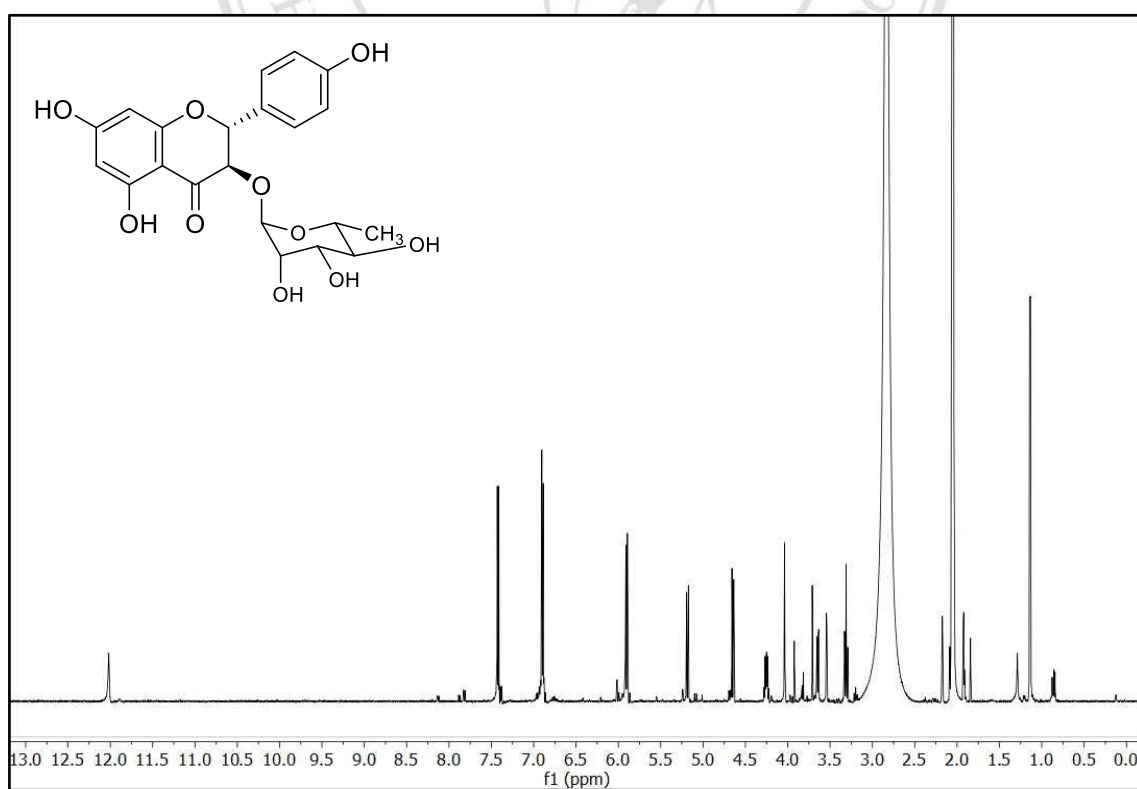


**Figure 51** The <sup>1</sup>H-NMR (500 MHz, acetone-*d*<sub>6</sub>) spectrum of compound A35

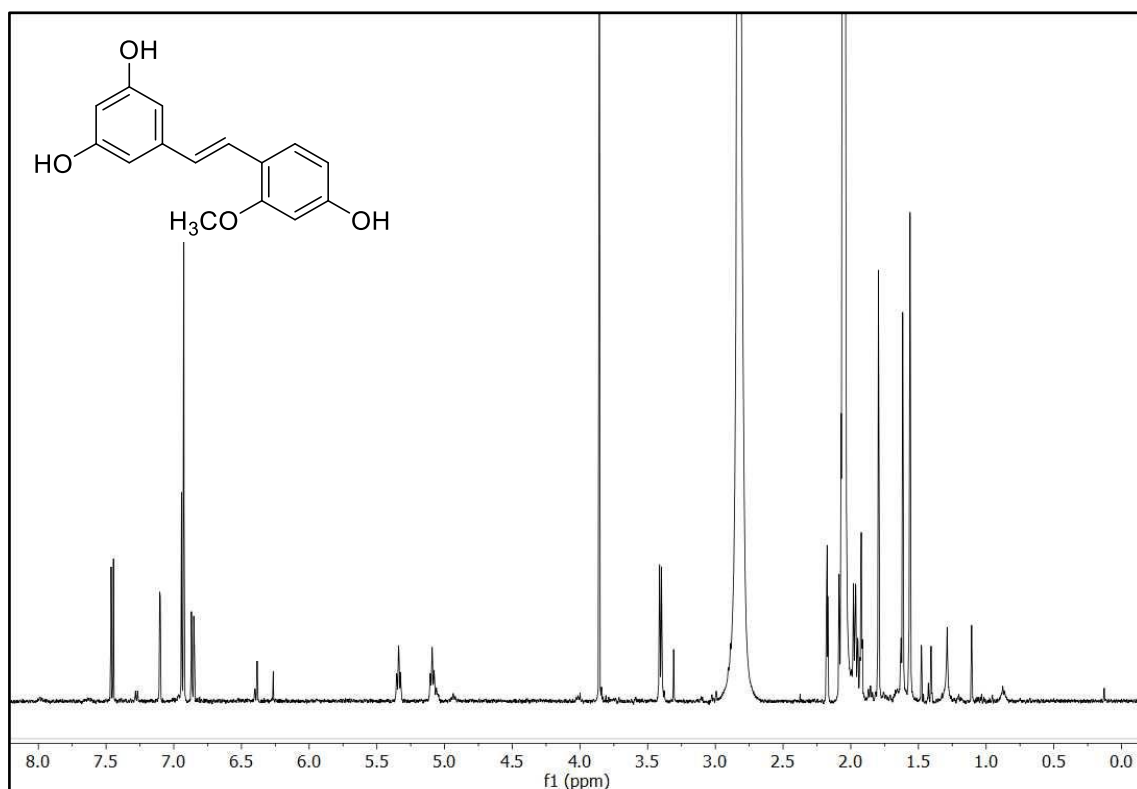


**Figure 52** The <sup>1</sup>H-NMR (500 MHz, acetone-*d*<sub>6</sub>) spectrum of compound A36

ลิขสิทธิ์มหาวิทยาลัยเชียงใหม่  
Copyright© by Chiang Mai University  
All rights reserved



## CIRRICULUM VITAE

Author's name	Miss Sirada Boonyaketgoson
Date of birth	5 October, 1991
Education	2016 Master of Science (Chemistry) Chiang Mai University  2014 Bachelor of Science (Chemistry) Chiang Mai University
Scholarship	Science Achievement Scholarship of Thailand
Publications	1. Boonyaketgoson, S., Rukachaisirikul, V., Phongpaichit, S., Trisuwan, K. 2017. Cytotoxic arylbenzofuran and stilbene derivatives from the twigs of <i>Artocarpus heterophyllus</i> . <i>Tetrahedron Letters</i> 58, 1585-1589.  2. Boonyaketgoson, S., Rukachaisirikul, V., Phongpaichit, S., Trisuwan, K. 2019. Deoxybenzoin and flavan derivatives from the twigs of <i>Artocarpus lakoocha</i> . <i>Phytochemistry Letters</i> 31, 96-100.
Presentation	Oral presentation at 2018 Pure and Applied Chemistry International Conference (PACCON 2018) 7-9 February 2018 in the topic "Arylbenzofuran derivatives from the twigs of <i>Artocarpus heterophyllus</i> "

